universität wien

DISSERTATION

Titel der Dissertation

Jak/Stat-signaling in function and development of normal and malignant hematopoiesis with focus on leukemic stem cells

angestrebter akademischer Grad

Doktor der Naturwissenschaften (Dr. rer. nat.)

Verfasser	Mag.rer.nat. Boris Kovacic
Matrikelnummer	9703916
Dissertationsgebiet (lt. Studienblatt)	Genetik und Mikrobiologie
Betreuer	Univ. Prof. Dr. Hartmut Beug
	Wien, am 04.06.2009

Abstract

(i) One of the key questions of cancer biology is whether the tumor development is caused by rare cancer stem cells. Evidence for this model and for the model of clonal evolution of tumorogenic clones are currently conflicting against each other. We show that both hypotheses can be true if one takes into account that tumors could arise from cells that are distinct from those which maintain the tumor. We have compared acute lymphoid and chronic myeloid leukemia and could observe that whereas myeloid leukemia develop from the same CSCs initially and during progression, lymphoid leukemia change the identity of CSCs that initiate to a distinct CSC that maintains the leukemia. This finding is essential in understanding of the process underlying leukemia development and explains the lineage determination so often associated with particular tumors.

(ii) The BCR/ABL-oncogene activates many different pathways including Stat5-signaling. We show that Stat5 is required for the maintenance of leukemia progression. Deletion of Stat5 in growing leukemia could completely ablate myeloid and a lymphoid leukemia. Stat5 is involved in survival of leukemic cells, since its deletion leads to a G0/G1 cell cycle arrest and subsequent apoptosis induction in imatinib-sensitive and in imatinib-resistant cells. Therefore, Stat5 is a potential drug for treatment of leukemia.

(iii) We demonstrate an essential function of Stat5 in the EpoR/Jak2/Stat5 axis during erythropoietic development. We could show here that expression of Stat5 in Jak2- and EpoR-deficient erythroid cells could rescue the erythropoiesis in vitro. Introduction of an constitutively active Stat5 mutant (cS5F) into Jak2-/- fetal liver cells, could rescue erythropoiesis and myelopoiesis in vivo.

(iv) Contrary to the implicated role of Stat1 as tumor suppressor, we describe a tumor-promoting role for Stat1 in MPD and lymphoid leukemia. Stat1-/- tumor cells express low levels of MCH class I molecules on their surface and therefore exert a better recognition and more efficient killing by NK-cells. We could also describe that Stat1-/- tumor cells acquire increased levels of MHC class I proteins, which could be a general mechanism of immune-escape of hematopoietic tumors.

(v) Finally, we demonstrate an essential role of Stat5 in lymphopoiesis and lymphoid leukemia. Stat5 is essential for the development of CD8+ T-cells, B-cells and gdT-cells. Because the B-cell development was impaired at the pre-pro B-cell stage, the initial transformation by Abelson oncogenes was completely abrogated in vitro and in vivo. This is the first description of Stat5 as a major player in normal hematopoiesis and malignancy.

Zusammenfassung

(i) Eine der zentralsten Fragen der Krebsforschung lautet, ob die Entwicklung eines Tumors durch selten vorkommende Krebs-Stammzellen verursacht wird. Zurzeit herrscht Unklarheit darüber, ob dieses Modell oder das Modell der klonalen Evolution von Tumorzellen der Wahrheit entspricht. Hier zeigen wir, dass beide Hypothesen wahr sein können, wenn man in Betracht zieht, dass Tumorzellen, die den Tumor erhalten, unterschiedlich von denen sind, die ihn initiieren. Wir haben akute lymphoide und chronisch myeloide Leukämien verglichen und entdeckten, dass die Tumor-initiierende und die Tumor-erhaltende Krebs-Stammzelle in myeloiden Leukämien zur ein und derselben Zellart gehört. In lymphoiden Leukämien hingegen ändert sich die Identität der Tumor-initiierenden Zelle zu einer andreren Krebs-Stammzelle, die den Tumor erhält. Dieser Befund ist essentiell, um den Mechanismus der Leukämie-Entwicklung zu verstehen und erklärt die Prävalenz der Onkogene für bestimmte hämatopoietische Linien.

(ii) Das BCR/ABL Onkogen aktiviert viele verschiedene Signaltransduktionswege, u.a. auch den Stat5 Signalweg. Wir zeigen, dass Stat5 essentiell für die Erhaltung dieser Leukämie ist. Die Beseitigung von Stat5 in einer etablierten Leukämie konnte sowohl myeloide als auch lymphoide Leukämien heilen. Stat5 ist mitverantwortlich für das Überleben von leukämischen Zellen, da dessen Beseitigung zu einem G_0/G_1 Zellzyklus-Arrest und anschliessend zu Apoptose führt - sowohl in Imatinib-empfindlichen wie auch in Imatinib-resistenten Zellen. Daher ist Stat5 ein potentieller Kandidat für neue Therapien.

(iii) Wir zeigen eine essentielle Funktion von Stat5 in der EpoR/Jak2/Stat5-Achse in der erythroiden Entwicklung. Wir konnten zeigen, dass die Überexpression von Stat5 in Jak2- und EpoR-defizienten erythroiden Zellen die Erythropoiese *in vitro* retten kann. Das Einbringen einer konstitutiv-aktiven Stat5-Mutante (cS5F) in *Jak2*$^{-/-}$ foetalen Leberzellen konnte sowohl die Erythropoiese als auch die Myelopoiese retten.

(iv) Im Gegensatz zu der erwarteten Rolle von Stat1 als Tumor-Suppressor, beschreiben wir eine Tumor-fördernde Rolle für Stat1 in MPD und lymphoider Leukämie. *Stat1*$^{-/-}$ Zellen exprimieren geringe Mengen an MHC Klasse I Molekülen an der Zelloberfläche und werden daher von NK-Zellen besser erkannt und eliminiert. Wir konnten weiters zeigen, dass *Stat1*$^{-/-}$ Tumorzellen in der Lage waren, höhere MHC Klasse I Expression zu erlangen - was ein allgemeiner Mechanismus für das Entkommen hämatopoietischer Tumoren vor dem Immunsystem sein könnte.

(v) Wir zeigen eine essentielle Rolle für Stat5 in der lymphoiden Entwicklung und in lymphoider Leukämie. Stat5 ist erforderlich für die Entwicklung von $CD8^+$ T-Zellen, von B-Zellen und γδ T-Zellen. Aufgrund der Beeinträchtigung der B-Zell-Entwicklung im Pre-Pro-B-Zellstadium, war die initiale Transformation mit Abelson-Onkogenen *in vitro* und *in vivo* völlig verhindert. Dies ist die erste Beschreibung von Stat5 als bedeutender Faktor in normaler Hämatopoiese und Leukämie.

Table of contents

1 Introduction

1.1 Hematopoiesis and leukemia

The developmental process of formation of all blood cells is called hematopoiesis. The word hematopoiesis is derived from greek words “haima” (blood) and “poiesis” (to make). Blood or the hematopoietic system is normally considered as an organ because of its complex structure. According to this, mature blood cells can be subdivided into three major cellular subpopulations. Erythrocytes or red blood cells are quantitatively the largest group of the hematopoietic system (4-6x10^6 cells/µl of human peripheral blood). The function of erythrocytes is the transport of oxygen to as well as the transport of CO_2 from all organs in a body. The second largest population of the hematopoietic system is represented by thrombocytes or platelets (2-5x10^5 cells/µl), which are responsible for prevention of accidental, injury-induced blood-loss. The third category of blood cells is called leukocytes or white blood cells. Leukocytes are organized as distinct sub-populations, consisting of many different cell types, which are mainly involved in immune responses to viruses, bacterial pathogens and surveillance and eradication of evolving tumors.

1.1.1 Origins of hematopoietic cells

In all tissues, a cellular requirement for regeneration is needed, in order to supply the organ with all specific cells throughout lifetime. In the blood system, these cells are called hematopoietic stem cells (HSCs) and reside in the bone marrow (BM) of adult individuals (Weissman, 2000).

However, despite blood being one of the best-studied organs, our knowledge about the earliest origins of blood cells is rather complex than clear. The reason for this is that development, per se, is a hierarchical system and therefore it assumes the existence of an ancestral cell for the whole blood system. Until now, emergence of hematopoietic cells has been described in four spatially and temporarily different sites of the embryonic development (Choi et al., 1998; Gekas et al., 2005; Muller et al., 1994; Samokhvalov et al., 2007). This chapter focuses on the description and explanation of these four origins of hematopoietic cells.

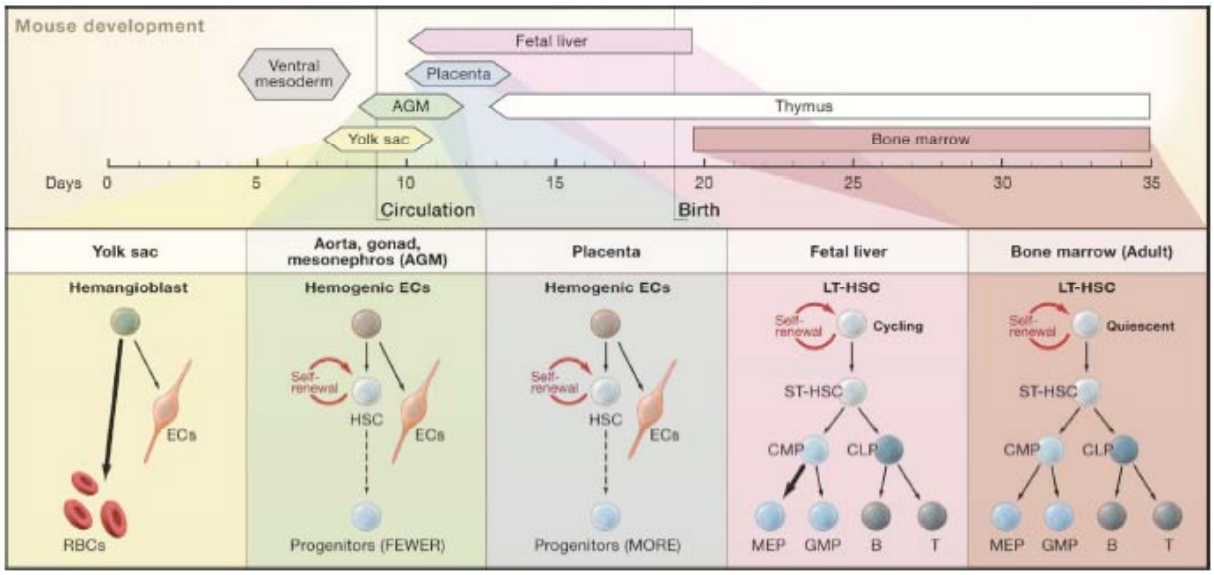

Figure 1: Spatial and temporal sites of origin of HSCs.

Upper panel: Developmental timewindows for shifting sites of hematopoiesis. Lower panel: Hematopoiesis in each location favors the production of specific blood lineages. Abbreviations: ECs, endothelial cells; RBCs, red blood cells; LTHSC, long-term hematopoietic stem cell; ST-HSC, short-term hematopoietic stem cell; CMP, common myeloid progenitor; CLP, common lymphoid progenitor; MEP, megakaryocyte/erythroid progenitor; GMP, granulocyte/macrophage progenitor (adapted from Orkin and Zon, 2008)

Interestingly, and common to all findings, one can conclude that the first commitment to the hematopoietic fate sets on in a part of the mesodermal germ layer called ventral mesoderm, right after the initiation of gastrulation (Murry and Keller, 2008). Temporarily, the development of blood cells can be subdivided in two major waves (Figure 1). In mice, the primitive erythropoiesis takes place from E7.25-E9.0 (Palis et al., 1999; Wong et al., 1986). The definitive erythropoiesis takes place from about E8.25-E10.5 and completely replaces the primitive erythropoiesis (Palis, 2008; Palis et al., 1999). Spatially, the onsets of primitive and definitive erythropoiesis are located in the yolk sac, but later on, the definitive erythropoiesis is relocated to the fetal liver. Upon the switch to fetal liver, the hematopoiesis converges to one organ in which the production of all mature lineages and amplification of hematopoietic cells takes place.

1.1.1.1 Hemangioblast hypothesis

Strikingly, during the stage of primitive erythropoiesis, primitive erythrocytes are present throughout the embryo proper already before the first emergence of HSCs. This finding

supports the (first of four) postulation of blood cell formation by a cell called hemangioblast. Due to the close spatial interaction between blood and endothelial cells in the yolk sac, it was hypothesized that a common ancestor (hemangioblast) could give rise to both, the hematopoietic and endothelial lineages during embryonic development (Figure 1, Ferkowicz and Yoder, 2005; Haar and Ackerman, 1971). Although, the experimental evidence for the existence of hemangioblast has been described *in vitro* (Choi et al., 1998) and *in vivo* (Huber et al., 2004), the formal proof of a single cell asymmetrically dividing into an erythroid and an endothelial cell, is still missing. The hemangioblast-hypothesis provides an explanation why primitive erythrocytes could be observed in embryos without the existence of a HSC, but does not explain how the emergence of HSCs is supported.

1.1.1.2 The AGM-region

The best established view of the place of origin of HSCs during embryonic development is the aorta-gonad-mesonephros (AGM) region. It consists of the dorsal aorta, the mesenchyme that engulfs the dorsal aorta and the urogenital ridges (Cumano et al., 1996; Ferkowicz and Yoder, 2005; Medvinsky and Dzierzak, 1996; Muller et al., 1994). It has been proposed that the cells residing in the ventral wall of dorsal aorta (hemogenic endothelial cells) are able to budd off HSCs (North et al., 1999; North et al., 2002). It should be mentioned here, that the identity of HSCs can only be assayed functionally and retrospectively by the observation of long-term engraftment and contribution to all hematopoietic lineages in animals transplanted with HSCs. Indeed, experimental evidence for AGM region as the source of HSCs was obtained by single cell transplantation studies of E11 AGM cell suspensions in primary and serially transplanted mice (Muller et al., 1994).

1.1.1.3 Yolk sac

In contrast to the AGM-region being the site of origin of HSCs, it has repeatedly been described that yolk sac might also be a place where HSCs are produced during embryonic development. Interestingly, early studies have shown that removal of yolk sac from E7.5 embryos and further cultivation *in vitro*, yielded an ablation of all hematopoietic cells (Moore and Metcalf, 1970). A more recent work strengthens the theory of yolk sac origin of HSCs (Samokhvalov et al., 2007). Here, the use of a transgenic mouse that was able to induce lacZ

expression only in Runx1-positive cells enabled the scientists to follow the fate of yolk sac cells *in vivo* (Runx1 is exclusively expressed in the yolk sac at E7.5). Activation of lacZ at the day 7.5 of pregnancy was sufficient to permanently stain all hematopoietic cells. Since the AGM-region could be stained as well, it was concluded that the yolk sac rather than the AGM-region is the site of origin of HSCs. However, the $Runx1^+$ cells described here could only constitute recipient mice if injected into the fetal liver of newborn mice - which indicated that further signals and maturation steps are required from the AGM-region or the fetal liver to obtain a full functioning HSC. This raises the possibility that these yolk sac cells might presumably be precursors of fetal HSCs.

1.1.1.4 Placenta

A very recent and intriguing observation suggests that HSC activity might also be initiated in the placenta of developing embryos (Rhodes et al., 2008). Interestingly, HSCs have been detected in placental tissue in several studies, but it has never been clear whether they are really generated there or whether placenta only provided the right microenvironmental cues for HSC expansion. To elucidate this, the authors have used mice which lack the heart beat and therefore no HSCs could be transported to placenta by the blood-circulation system (Koushik et al., 2001). Strikingly, mice lacking the $Na^+/Ca2^+$ transporter Ncx1 could develop $Runx1^+/CD41^+$ HSCs in the placenta. Additionally, $Runx1^+/CD41^+$ HSCs contributed to all hematopoietic lineages upon serial transplantation.

1.1.2 Fetal and adult (bone marrow) hematopoiesis

It is commonly accepted that the fetal liver is the site of expansion and differentiation of HSCs into all mature lineages. In addition, the fetal liver does not serve as the site of HSC-generation but provides a niche for amplification of hematopoietic cells, in order to produce enough cells to colonize all lymphoid organs after birth (Orkin and Zon, 2008). Compared to adult HSCs, fetal liver HSCs are different in their homeostatic properties. Accordingly, fetal liver HSCs enter the cell cycle more often than BM HSCs (Bowie et al., 2006; Kim et al., 2007).

Common to fetal and adult hematopoiesis is the hierarchy of developmental stages and the ability to differentiate into erythroid, myeloid and lymphoid cells from a common ancestor

(HSC). During the past two decades our view of the hematopoietic development has strengthened mainly through the discovery and purification of distinct hematopoietic subpopulations by FACS-sorting using a combination of unique surface markers. This powerful method has enabled researchers to test every single hematopoietic stem and precursor cell population for their ability to differentiate into mature cells *in vitro* and *in vivo*. Hence, a rare population in the BM could be identified that was negative for the expression of all tested lineage markers (lin-) and that expressed early developmental markers c-kit (CD117; Stem cell factor SCF-receptor) and Sca-1 (Ikuta and Weissman, 1992; Spangrude et al., 1988). This population, termed as LSK (for lin-/Sca-1+/c-kit+), turned out to be enriched for HSCs and could be serially transplanted into lethally irradiated recipient mice with successful engraftment (Ikuta and Weissman, 1992). Studies with additional cell surface markers have revealed a further heterogeneity among the HSC-population and have led to the discrimination between long-term repopulating hematopoietic stem cells (LT-HSCs), short-term repopulating hematopoietic stem cells (ST-HSCs) and multipotent progenitors (MPPs) (Osawa et al., 1996; Randall et al., 1996). However, the differences between the ST-HSCs and the MPPs turned out to be less prominent than expected. For instance, transplantation of ST-HSCs or MPPs into irradiated hosts has always led to a contribution to all three major blood lineages. The engraftment, however, was only temporarily and the differentiated cells have disappeared after 3-4 weeks - with ST-HSCs showing longer engraftment than MPPs (Morrison et al., 1997; Morrison and Weissman, 1994). Our classical view of the HSC-stages shows a linear connection between the LT-HSCs, ST-HSCs and MPPs. At the stage of MPPs, the hematopoietic development splits up for the first time into two branches - the common lymphoid progenitors (CLPs) (Kondo et al., 1997) and the common myeloid progenitors (CMPs) (Akashi et al., 2000). Both precursors are able to give arise to all downstream populations of the respective lineage, but they are not able to efficiently repopulate irradiated hosts. Interestingly, whereas CLPs can strictly differentiate into the lymphoid lineage (B-, T- and NK-cells), CMPs determine their fates into myeloid and erythroid lineages by first giving rise to either granulocyte-macrophage progenitors (GMPs) or erythrocyte-megakaryocyte progenitors (MEPs) (Traver et al., 2001).

It is exactly this rigid classical model that has been challenged over the last few years, for the reason of several findings showing an unexpected heterogeneity among different hematopoietic populations (Figure 2). According to the classical model, MPPs can give arise to all three hematopoietic lineages and a lineage commitment is established later at the stages of CMPs and CLPs. However, several groups have shown that some lineages are more

prominently, or even exclusively, chosen downstream of MPPs. For instance, about 25% of the MPP-population expressing high levels of fms-like tyrosine kinase 3 (Flt3 or Flk2) $Flt3^{high}$, has been shown to give arise to mere lymphoid and myeloid lineage (Adolfsson et al., 2005) and was termed lymphoid-primed multipotent progenitor (LMPP). Although another study has shown that LMPPs still possess a low (less than 3%) megakaryocyte-erythrocyte (MegE) potential, this issue remains a point of debate.

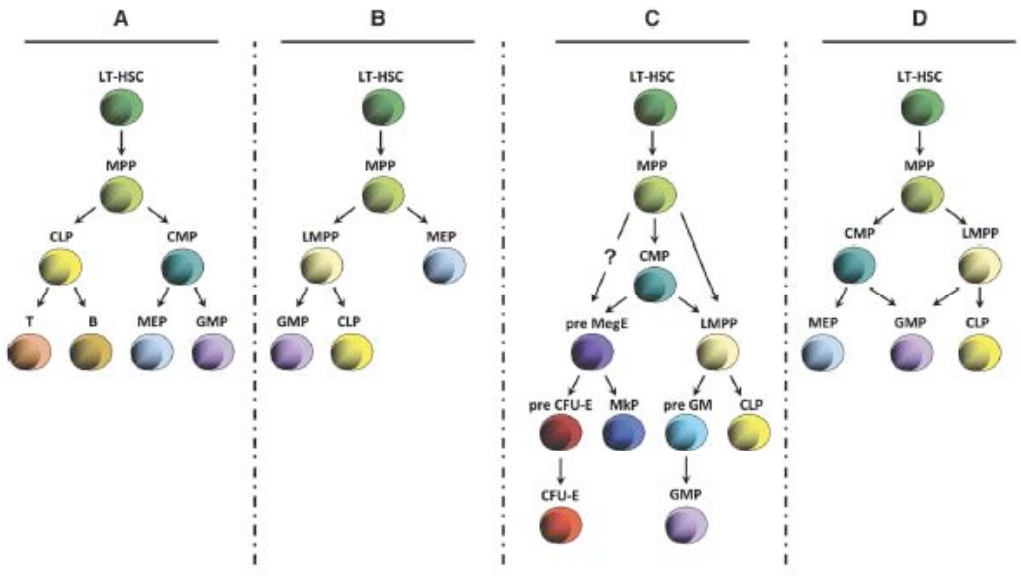

Figure 2: Road map of early hematopoiesis

A, Model proposed by Kondo et al (1997) & Akashi et al (2000)

B, Model proposed by Adolfsson et al (2005)

C, Model proposed by Pronk et al (2007)

D, Model proposed by Arinobu et al (2007)

(adapted from C.Murre – Cell Stem Cell 2007)

Another report also suggests a rather complex view of the hematopoietic development. Here, Pronk et al have assessed the differentiation potential of myeloid progenitors using CD150, CD105 (Endoglin) and CD41. Interestingly, they could show a novel hierarchy of progenitors with myeloid and erythroid potentials (Pronk et al., 2007).

A complete novel approach was undertaken by the group of Connie Eaves which re-evaluated the hematopoietic tree using functional markers (Hoechst and Rhodamine stainings for drug-resistance pumps expressed on HSCs) in order to define HSC-potential on a single cell level (Dykstra et al., 2007). By doing so, they could define four novel classes of HSCs according to their lineage determination ability (termed α, β, γ and δ). α cells had high self-renewal activity but were prone to differentiate into the myeloid lineage. β cells had similar self-

renewal activity and a multipotent potential. γ and δ cells, however lacked the ability to self-renew but γ cell displayed a robust myeloid and lymphoid potential, whereas δ cell only contributed to the lymphoid lineage.
Finally, the group of Koichi Akashi favors the view that multipotent cells like MPPs might be initially primed into the myeloid/erythroid or lymphoid lineage, depending on the expressing of GATA1 or PU.1, respectively (Arinobu et al., 2007). This, so called priming, determines the specific lineage and could be a hint for further plasticity of HSCs.

1.1.3 Leukemia

The word leukemia is derived from the ancient greek words "leukos" (white) and "aima" (blood). It is usually used to describe the cancer of the blood system. On their clinical etiology, the leukemias are simply subdivided in chronic and acute leukemias. Leukemias implicate real hematological malignancies and are therefore separated from the more benign hematological neoplasms like myeloproliferative disorders.

1.1.3.1 Myeloproliferative Disorders

Myeloproliferative disorders or, sometimes termed, diseases (MPD), is a classification of diseases that rely on a hyperproliferation of blood cells of the erythroid/myeloid lineage in general. Since this classification is based on historical and clinical/morphological discrimination of hematological neoplasms rather than on molecular pattern, the term MPDs still remains less well defined than that of classical hematological malignancies (leukemias) (Levine and Gilliland, 2008). The most prominent difference to classical leukemia is that MPDs are initially benign, but mostly develop into malignant forms. The first definition of MPDs dates back to 1951, when William Dameshek discovered that polycythemia vera (PV), essential thrombocytosis (ET) and primitive or idiopathic myelofibrosis (MF) were closely related (Kralovics et al., 2005; Levine and Gilliland, 2008). Today, the category of MPDs is further subdivided into two major subgroups consisting of Philadelphia Chromosome (Ph) positive and Ph-negative diseases. The initially defined PV, ET and MF are termed Ph-negative MPDs, whereas the chronic myelogenous (or myeloid) leukemia (CML) is viewed as Ph-positive MPDs (Kralovics et al., 2005; Levine and Gilliland, 2008). This is due to the fact

that CML normally exerts a milder phenotype than other “malignant” forms of leukemia, and has first to evolve into an acute phase disease.

The recent discovery of a dominant mutation in the pseudokinase domain of Jak2 has revolutionized our view of MPDs, especially of the Ph-negative origin (James et al., 2005; Kralovics et al., 2005; Levine et al., 2005). A point mutation leading to a mis-translation of one amino acid (valine 617 to phenylalanine) was discovered to be the cause of 80% of PV, 50% of MF and about 20% ET in human patients. Interestingly, all three forms lead to fibrosis of the BM and eventually cause death. The discovery of the Jak2V617F mutation was therefore a genetic or molecular proof for the common pathogenesis of PV, ET and MF.

Due to historical/clinical and genetic/molecular reasons, CML is treated in this chapter as both a leukemia, and a MPD. Therefore it will be discussed in more detail in the next chapter (chronic leukemia).

1.1.3.2 Chronic leukemia

Chronic leukemias are characterized by their clinical etiology, which is described as a year-long (=chronic) disease of the blood system. Normally, and inevitably, chronic leukemia, after an accelerated phase further proceeds into an acute phase. Chronic leukemia is characterized by extremely high numbers of relatively mature cells. It occurs predominantly in elder persons and is more easily treated due to reduced lethality rate. According to the cell lineage affected, chronic leukemia is further subdivided into a lymphoid and a myeloid form, CLL and CML, respectively.

Chronic lymphocytic or lymphoid leukemia (CLL) mostly affects adults over the age of 55 years and almost never occurs in children. CLL most often affects the B-lymphoid lineage and the survival rate is 77% after 5 years (Boelens et al., 2009; Chiorazzi et al., 2005).

Chronic myelogenous or myeloid leukemia (CML) also affects older persons and rarely children. CML progresses form the chronic phase to the accelerated phase over a period of several years. The accelerated phase further inevitably progresses to the acute phase, which completely resembles an acute leukemia. Due to the treatment with the tyrosine kinase inhibitor Imatinib-mesylate, the prognosis of about 56% survival after 5 years has changed to about 90% survival upon treatment (Druker, 2008; Faderl et al., 1999).

1.1.3.3 Acute Leukemia

Acute leukemias are generally considered to have a poor prognosis. Acute lymphoblastic/lymphoid leukemia (ALL) is the most common form of leukemia in children but it also occurs later in aged persons (Foon et al., 1980; Piccaluga et al., 2007).
Acute myelogenous/myeloid leukemia (AML) has a relatively complicated etiology, which is classified by the French-American-British (FAB) or the World Health Organization (WHO) systems. This is because AML seems to arise from, or secondarily acquire, a load of mutations (Bennett et al., 1976).
Both acute leukemia are associated rather poor prognosis, that is about zero percent survival without treatment and 20-50% survival upon treatment. The best prognosis is achieved in childhood ALL, because of bone marrow transplantation or stem cell transplantations have high rate of success in children.

1.1.3.4 Philadelphia Chromosome-positive leukemia

Philadelphia chromosome (Ph) was the first chromosomal translocation to be identified to encode a fusion-protein BCR/ABL, the major cause of several forms of leukemia. Leukemias characterized by a specific genetic abnormality, a t(9;22)(q34;q11) translocation, result from the formation of combined chromosome from chromosomes 9 and 22 (Groffen et al., 1984; Nowell and Hungerford, 1960). As a result of the translocation, a fusion gene product (BCR/ABL) is created, representing a constitutively active tyrosine kinase that lacks the regulatory domains of its full protein alias c-abl (Clark et al., 1988; Konopka and Witte, 1985; Rowley, 1973). The presence of the Ph is linked to three hematopoietic malignancies: CML, ALL and chronic neutrophilic leukemia (CNL) (Wong and Witte, 2001). Interestingly, whereas in CML, BCR/ABL is responsible for about 95% of all cases, only about 20-30% of adult ALL and 2-10% juvenile ALL patients possess the Ph-chromosome. CNL, however, is extremely rare and will not be discussed in more detail here.
The molecular basis for the three diseases is given through the identification of three different ways or breakpoints to form a BCR/ABL fusion protein (Wong and Witte, 2001). All different breakpoints are in the BCR-gene, whereas the breakpoint of the c-ABL gene remains the same. Therefore, three proteins with different weights exist in the already mentioned leukemias.

This thesis will focus on the two most prominent ones: the smallest BCR/ABLp185 (185kDa) protein occurring in about 20-40% of all ALLs and the medium BCR/ABLp210 (210kDa) predominantly arising almost all cases of CML (Wong and Witte, 2001).

1.2 Jak/Stat signaling and disease

1.2.1 Overview of Jak/Stat signaling

The Janus kinase (Jak) and signal transducer and activator of transcription (Stat) proteins are members of an evolutionary conserved signaling pathway. The Jak/Stat pathway is involved in the signal transduction of developmental, proliferative and survival signals from the environment to the nucleus of cells, where activation or repression of an appropriate repertoire of genes is initiated, leading to adequate responses to extracellular stimuli (Calo et al., 2003; Levy and Darnell, 2002; Murray, 1996).

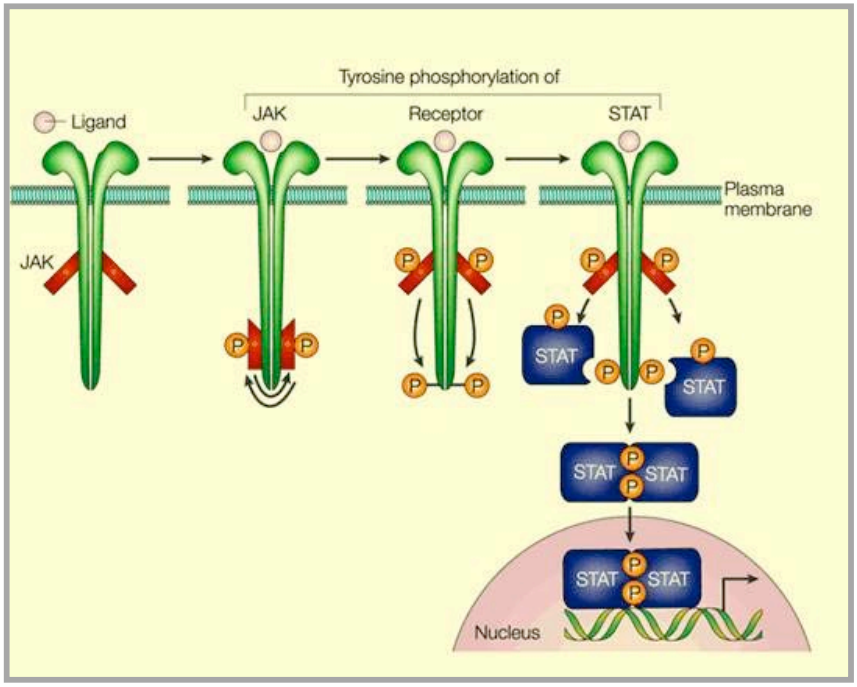

Figure 3: Jak/Stat signaling cascade

Upon ligand binding, receptor chains dimerize and activate Jaks. Jaks subsequently phosphorylate the receptor chain and thereafter, Stats, which bind to the receptor. Phosphorylated Stats dimerize and translocate to the nucleus. (adapted from Levy and Darnell, 2002)

The function of Jak/Stat pathway is mediated by the binding of an extracellular stimulating ligand to its cognate receptor which resides in the cytoplasmic membrane (Figure 3). The receptors of a non-classical tyrosine kinase family lack their own tyrosine kinase domain and are dependent on the physical interaction with Jak tyrosine kinases, bound to the intracellular domains of the receptor chains. Upon ligand binding, the receptor chains homo- and heterodimerize and bring the Jaks in a close vicinity to each other so that they can autophosphorylate themselves. The subsequent phosphorylation of tyrosine residues of the intracellular receptor domain is a prerequisite for binding of Stats to the receptors. In a similar way, Stats get phosphorylated and activated by Jaks, they homo- or heterodimerize and are translocated to the nucleus. Stats are genuine transcription factor and lead (in most cases) to an activation of specific target genes (Levy and Darnell, 2002).

1.2.2 Jaks

There have been four members of Jak proteins identified until now, termed Jak1, Jak2, Jak3 and Tyk2. All Jaks are expressed in a variety of tissues and it has been assumed that their function is mostly non-redundant. Analysis of knockout mice and identification of homozygous mutation in humans has implicated Jak proteins in many fundamental cellular processes. For instance, Jak1 and Jak2 knockout mice displayed the most severe phenotype, leading to an early embryonic lethality (Neubauer et al., 1998; Parganas et al., 1998; Rodig et al., 1998). It is thought that the function of Jak1 and Jak2 is therefore closely connected to either embryonic development per se, or to an essential role in hematopoietic development since the lethality of knockout embryos was shown to coincide with the onset of fetal hematopoiesis. Interestingly, the most receptors involved in the function of hematopoietic cells like proliferation, differentiation and homing - that are represented by the gp130-family, common gamma, common beta chains and interferon receptors - signal through Jak1 and Jak2. Deletion of Jak3 in mice has led to a severe combined immuno-deficiency (SCID) phenotype due to the lack of T- and NK-, but not B-cells (Nosaka et al., 1995; Thomis et al., 1995). Additionally, homozygous mutation in humans have been discovered in Jak3, that also led to a lack of T-cells, and Tyk2, which displayed a Hyper-IgE syndrome with increased susceptibility to different microorganisms (Minegishi et al., 2006; Notarangelo et al., 2001). Accordingly, Tyk2 knockout mice exhibited impaired interferon-response that affected the viral (Karaghiosoff et al., 2000) and bacterial (Karaghiosoff et al., 2003) response to pathogens.

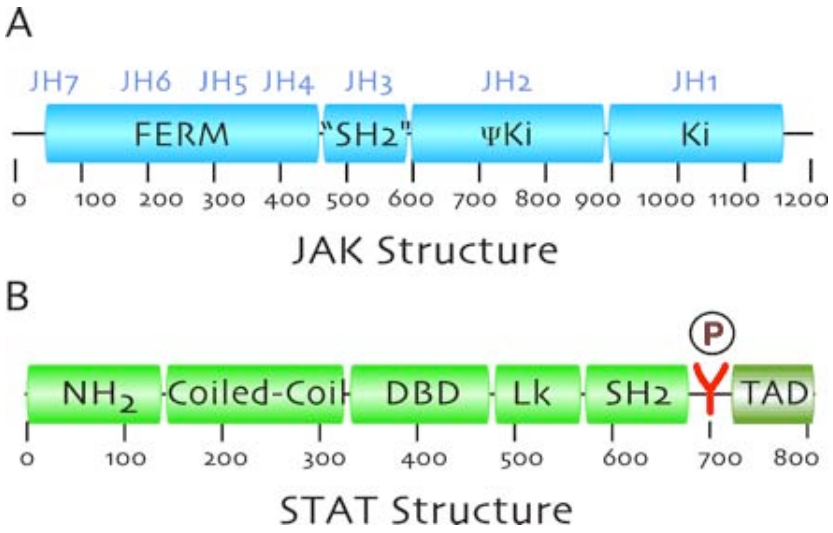

Figure 4: Common structure of Jaks (A) and Stats (B) (adapted from Schindler et al, 2007)

The structure of Jaks is comprised of seven unique domain structures, termed Jak-homology domains (Figure 4, JH1-7). Functionally, JH7-4 encode the FERM-domain, which is responsible for the binding to the cognate receptor chain and resides in the N-terminal part of Jak proteins. The SH2-like domain is adjacent to the FERM-domain and is followed by two unique Jak kinase domains. Interestingly, one the most C-terminal kinase domain is functional in Jaks and the prior kinase doman is therefore termed pseudo-kinase domain (Levy and Darnell, 2002). Recently, a mutation in this pseudo kinase domain was discovered in Jak2, that is involved in myeloproliferative disorders by possibly rendering the protein constitutively active (James et al., 2005; Kralovics et al., 2005; Levine et al., 2005).

1.2.3 Stats

Stat molecules consist of seven members - Stat1 to Stat6, whereas Stat5 is encoded by two different genes, Stat5A and Stat5B. In contrast to Jaks, studies on Stats have revealed a more redundant roles for Stat protein, with the exception of Stat3 and Stat5 (O'Shea et al., 2002). Knockouts for Stat1 and Stat2, for example, have led to an overall normal phenotype in mice, with defects becoming prominent only after pathogenic challenge - due to an impaired interferon response (Durbin et al., 1996; Meraz et al., 1996; Park et al., 2000). In case of Stat4 and Stat6, a role in T-cell polarity has become obvious that is responsible in the decision between the Th1 and Th2 differentiation and cytotoxic versus humoral immune responses. While Stat4 acts downstream of IL-12 signaling and therefore supports the differentiation into Th1 cells that mediate anti-pathogenic immunity (Wurster et al., 2000), Stat6 is responsible

for IL-4 and Il-13 signaling and Th2 polarity to viruses and helminthes (Wurster et al., 2000; Zhu et al., 2001), respectively. As elucidated by knockout studies in mice, the functions of Stat3 and Stat5 seem to be more redundant than of all other Stats. For instance, Stat3 deficient mice were embryonically lethal already at E6.5-7.5, probably due to a developmental defect leading to an impaired closure of the neural tube (Takeda et al., 1997). While mouse embryonic fibroblasts (MEFs) could be isolated and expanded *in vitro* form Stat3 deficient mice, it is still unclear whether Stat3 has an important role in other adult cells (O'Shea et al., 2002). Studies with dominant negative Stat3 or knockdown studies have however proposed an essential role in many adult cells and tissues (O'Shea et al., 2002). Similarly, Stat5 has been shown to exhibit an essential role in hematopoiesis (Hoelbl et al., 2006; Teglund et al., 1998; Yao et al., 2006). Stat5 knockout mice die mostly in utero and/or perinatally, and we and others have shown that Stat5 has an essential function in erythrocytes, T- and B-lymphocytes (Grebien et al., 2008; Hoelbl et al., 2006; Kerenyi et al., 2008).

The structure of Stats is well conserved throughout the seven members and evolutionary from D. melanoganster to humans (Figure 4). Presumably, Stats are derived from one Stat gene by gene duplication. The structure has been solved by christallography for Stat1, Stat3 and Stat4, except for their N-terminal parts and therefore mechanisms of DNA-binding and dimerization are quite well understood (Becker et al., 1998; Chen et al., 1998; Vinkemeier et al., 1998). The N-terminal part is thought to be involved in dimerization of inactive Stats and in nuclear import/export. At least for Stat5, this domain has also been shown to mediate oligomerization (tetramers) (Moriggl et al., 2005). The coiled-coil domain in its vicinity consists of several hydrophilic residues, probably implicated in binding of regulatory proteins. The DNA-binding domain (DBD) adjacent to the coiled-coil domain enables the binding of Stats to their consensus sequences (ISRE and/or GAS) in the promotor regions of many genes. Followed by a linker that assures the appropriate distance to DBD, the SH2-domain is the most conserved Stat-sequence and responsible for homo- and heterodimerization. Directly behind it, the tyrosine residue is situated to avoid intramolecular self-dimerization. At the C-terminal end of Stat proteins, the transactivating domain (TAD) is the least conserverd part among Stats. It induces promotor clearance and transcription of target genes (O'Shea et al., 2002; Schindler et al., 2007).

1.2.4 Jak/Stat signaling in normal hematopoiesis

Almost all processes involving two or more hematopoietic cells including development/differentiation, survival/cell death and homing/immunity are regulated by cytokines. Interestingly, cytokines like interleukins, interferons and other growth factors all signal through the Jak/Stat signaling pathway. Therefore Jaks and Stats have an indispensable role in hematopoiesis. As already mentioned, the knockout phenotypes in mice and other experiments have implicated Jaks and Stats in a variety of cellular functions.

1.2.5 Jak/Stat signaling in leukemia

The unique prevalence of Jak/Stat signaling pathway in hematopoiesis has implicated it in malignancies arising from blood cells. It is generally thought that aberrant signaling downstream of many cytokines important for self-renewal, proliferation or survival of blood cells might be involved in leukemia formation (O'Shea et al., 2002). Especially, hematopoietic stem cells, progenitors and other transit amplifying cells might harbor the potential to become malignant.

We and others have therefore focused on the elucidation of Jak/Stat signaling components that might be required for tumor initiation or tumor maintenance - and this is also one of the major focuses of this thesis.

Jak1 and Jak2, for example, have been implicated in leukemia development for a long period, not only because of their redundant roles in hematopoiesis. It has been proposed that Jak1 and Jak2 would promote leukemia formation (Vainchenker et al., 2008; Ward et al., 2000). Several groups have shown that Jak1 and Jak2 act downstream of fusion proteins and oncogenes (e.g. v-abl, BCR/ABL) that drive leukemia. Due to the lack of genetic models to address this issues (Jak1 and Jak2 knockouts are embryonically lethal), it has taken until the knockdown techniques have become available, to strengthen this hypothesis (Vainchenker et al., 2008). However, recently we could show that in case of Jak1 a tumor promoting role might not be correct at least for lymphoid leukemia (Sexl et al., 2003). Even on contrary, v-abl transformed Jak1 deficient fetal livers gave rise to an increased number of clones *in vitro* and have worsen the outcome of disease when transplanted *in vivo*.

Jak2's role in tumor promotion has been better substantiated. Tel/Jak2 is an occasionally occurring fusion protein due to a chromosomal translocation in childhood T-ALL (Schwaller et al., 1998). A recently identified point mutation in Jak2 has also been implicated in 50-90% of cases of polychythemia vera (PV) (James et al., 2005; Kralovics et al., 2005; Levine et al., 2005). In a study described in this thesis, we have addressed this question using Jak2-

deficient fetal livers (FL). Infection of Jak2$^{-/-}$ FL with a constitutively active mutant of the downstream player Stat5 (cS5F) has rescued erythropoiesis and myelopoiesis *in vivo*, but was not sufficient to induce leukemia formation, indicating that additional signaling was required for downstream of Jak2 for myeloid leukemia formation (Grebien et al., 2008).

Tyk2 has also been evaluated for its involvement in leukemia formation. Interestingly, we could show that loss of Tyk2 in a B-ALL model had no effect on the tumor cell per se, but nevertheless has accelerated tumor formation by impairing the NK-cell cytotoxicity and surveillance of tumors (Stoiber et al., 2004).

Stat1 has previously been shown to be a tumor suppressor in many tumors, although its role in leukemia formation has not been assessed (Shankaran et al., 2001). Very recently, we could show using a B-ALL and a MPD model, that Stat1 promoted leukemia development and its loss rendered the mice less tumor prone due to low MHC class I expression on the surface of tumor cells. Interestingly, Stat1-/- tumor cells could up-regulate MHC class I expression in order to escape the immunesurveillance by NK-cells (Kovacic et al., 2006).

In contrast to Stat1, Stat3 has initially been implicated in cancer formation as a proto-oncogene (Bromberg et al., 1999). Accordingly, active (phosphorylated) Stat3 has also been found in many leukemia and lymphoma (Yu and Jove, 2004). Stat3 is the major component downstream of gp130 receptor family and is therefore thought to be involved in differentiation and fate decision processes dependent on cytokines like LIF, IL-6, IL-11, G-CSF etc. and in inflammation processes (Yu and Jove, 2004). Although a genetic depletion of Stat3 has not yet been assessed in leukemia formation, experiments using RNA interference, antisense oligonucleotides or dominant negative versions of Stat3 have implicated this protein in tumorigenesis (Kisseleva et al., 2002; Levy and Darnell, 2002).

The role of Stat5 in leukemia formation has been assessed by several groups. For example, a constitutively active version of Stat5B was generated by substituting the histidine 299 and the serine 711 with arginine and phenylalanine, respectively (Burchill et al., 2003). A transgenic mouse bearing this mutant (Stat5B-CA) under the control of the μ-enhancer (Eμ) showed increased numbers of pro-B, mature α/β and γ/δT and NK/T, but no leukemia formation. Conversely, knockout strategy has initially been used to generate a hypomorphic version of Stat5 lacking the N-terminal part (Sexl et al., 2000; Teglund et al., 1998). Unfortunately, the rest of the protein was still expressed - leading to a somewhat mild phenotype in these knockout mice. For example, the mice were overall healthy, developed normally and showed only a reduced but not impaired transformation ability leading to lymphoid and myeloid leukemia formation. Interestingly, using a complete knockout of both Stat5 genes, we could

recently clarify the role of Stat5 in hematopoiesis and lymphoid leukemia (Hoelbl et al., 2006). Indeed, Stat5 knockout mice were embryonically and perinatally lethal, but fetal liver cells from rare survivors showed an impaired B and T-cell development and an inability of transformation with v-abl and BCR/ABLp185 *in vitro*, and impaired leukemia development *in vivo*.

1.3 Cancer stem cell hypothesis

1.3.1 Evidence for cancer stem cells

There has been emerging evidence over the last decade about the interrelationship between normal stem cells and tumor cells being capable of formation and development of novel tumors. Particularly, hematological malignancies have been shown to arise from rare or at least infrequent tumor cells that can be successfully transplanted into recipient mice (Al-Hajj et al., 2003; Bonnet and Dick, 1997; Lapidot et al., 1994; Ricci-Vitiani et al., 2007; Singh et al., 2004). The very first report states a successful transplantation of a rare cell fraction isolated by FASC-sorting from human AML-patients into non-obese diabetis (NOD)/severe combined immunodeficient (SCID) mice (Bonnet and Dick, 1997; Lapidot et al., 1994). These cells, forth on termed "cancer stem cells" (CSCs), have become the basis of the later postulated "cancer stem cell hypothesis". Importantly, it was not only frequency that has characterized a potential cancer stem cell. Moreover, on the top of the fact that CSC represented only 0.2-1% of all AML cells, it was the rest of the AML cells that were not able to grow in serial transplants (Bonnet and Dick, 1997). This experiment has clearly shown that the rare cells were somewhat superior to all other cells in their capacity to form novel tumors. Additionally, this finding has pointed out that cancers, like normal organs, could be hierarchically organized and possess stem cell-like cells within them. Most strikingly, the phenotype by which the presumable CSCs were isolated from AML-samples resembled the surface marker combinations used to identify and isolate HSCs previously ($Thy1^-$, $CD34^+$ and $CD38^-$) (Bonnet and Dick, 1997).

In recent years, CSCs have also been reported in the cancers of brain, breast and colon (Al-Hajj et al., 2003; Ricci-Vitiani et al., 2007; Singh et al., 2004). Interestingly, the marker expression on most if not all of these CSCs resembled closely the phenotype of HSCs. For instance, the prospective breast CSCs turned out to be lin-CD24- and CD44+ (Al-Hajj et al.,

2003). The presumable brain and colon CSCs, on the other hand, expressed a novel surface marker CD133 (prominin) which was found to be enriched in the CSC-fraction and also expressed of normal human HSCs (Ricci-Vitiani et al., 2007; Singh et al., 2004).

1.3.2 A paradigm cancer stem cell model

The hematopoietic system is one of the best studied and therefore best described organs in mammals. As mentioned previously, the blood system consists of a well-studied hierarchy of cells with largely known ancestors (like HSCs) and descendents. Moreover, a load of phenotypic markers, either as cell surface proteins or intracellular players are known that can distinguish between all the described subpopulations (Adams and Scadden, 2006). It is because of these hallmarks that the hematopoietic system is established as a paradigm model for studying the cancer stem cell hypothesis. Additionally, the blood system has also been a source of many mutations, chromosomal translocations and genetic aberrations that are associated with different diseases and malignancies (Caligiuri et al., 1997; Jordan, 2002). For that reason, it is thinkable that the CSC hypothesis will have to prove in all aspects of this model.
CSCs of the hematopoietic origin are also called leukemic stem cells (LSCs). In this thesis, the term CSC is used in order to achieve a general point of view.

1.3.3 The cell of origin of cancer

The quest for the cell of origin of cancer has turned out to be the most problematic part, right form the beginning of the cancer stem cell hypothesis. The reason for that is obvious from lessons with patients treated from leukemia. Normally, patients with cancer are treated by chemotherapy and, more recently with specific inhibitory drugs i.e.- like in case of CML - with imatinib-mesylate. However, a cure from cancer is only rarely achieved and in most cases the disease develops again, even after several years of successful treatment (Kantarjian et al., 2002; Ottmann et al., 2002; Sawyers et al., 2002). According to the cancer stem cell hypothesis these observations can be explained by the fact that CSCs share all abilities of normal stem cells like self-renewal, the ability the differentiate into more mature cells, quiescence, longevity and the ability to “pump out” drugs.

Unfortunately, there are two possibilities how this stem cell state of CSCs can be explained: First, it is possible that CSCs are normal stem cells that have acquired mutations over time and become aberrant. This is plausible if one thinks about stem cells needing less mutations, because the program of self-renewal is already active, or about the cells living long enough to acquire the mutation. Secondly, it is thinkable that CSCs are progenitors or even mature cells that have regained the ability to self-renew (Figure 5, Passegue et al., 2003).

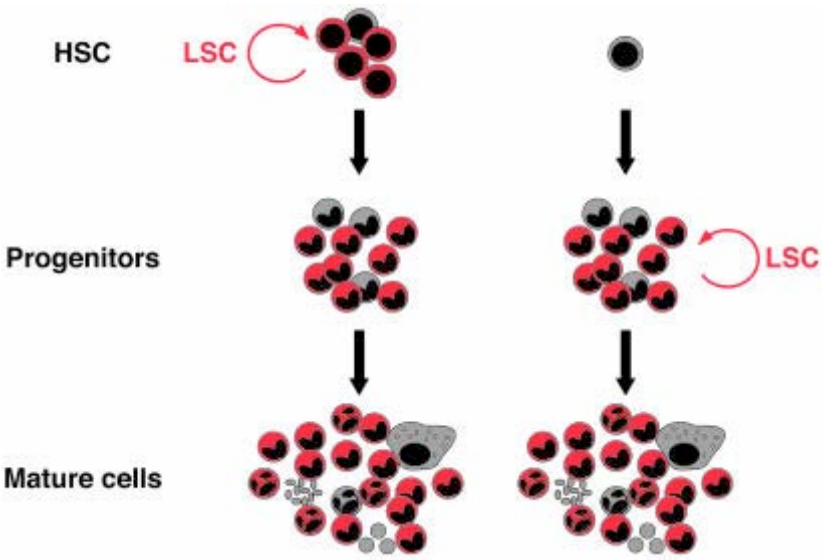

Figure 5: Leukemic stem cells (LSCs) could originate from normal HSCs or from progenitors (adapted from Passegue et al, 2003)

Several findings indicate that both scenarios are true and therefore the interpretation of the cancer stem cell model became even more complicated. As already mentioned, the studies on AML indicate that HSCs might have become aberrant and gave rise to CSCs. The same might be true for other tissues like colon, brain and the breast. However, numerous recent studies have implicated that leukemia-initiating cells from AML expressed either a predominantly mature myeloid phenotype or consisted of a myeloid progenitor population rather than of HSCs (Kelly et al., 2007; Krivtsov et al., 2006; Somervaille and Cleary, 2006).

Furthermore, it has been suggested that chronic phase CML is initiated in HSCs, or presumably LT-HSCs, because the characteristic Ph-translocation can be detected in several hematopoietic lineages of the same patient (Holyoake et al., 1999; Takahashi et al., 1998). Although in multiple studies BCR/ABL-positive CML (BCR/ABLp210) seemed to originate in the HSC-fraction during the chronic phase (Hu et al., 2004; Huntly et al., 2004; Krause et al., 2006), a different study placed the acute phase disease CSCs into the fraction of

progenitors (Jamieson et al., 2004). Another, perhaps aberrant, spontaneous JunB$^{-/-}$ CML-like leukemia was initiated from LT-HSCs (Passegue et al., 2004) and a BCR/ABLp210 Arf$^{-/-}$ leukemia was initiated from pre-B cells (Williams and Cancelas, 2006). Strikingly, one recent study has reported that 5-FU treatment of donor BM prior to infection with BCR/ABL induced CML in serial transplants, whereas direct infection with BCR/ABL without 5-FU treatment could redirect the disease into B-ALL lineage (Hu et al., 2004). Interestingly, all studies mentioned here using BCR/ABL BM transplantation used 5-FU treatment prior to infection. Therefore, it is possible that 5-FU treatment per se had an effect on the etiology of myeloid leukemia and may have pre-influenced its outcome.

1.3.4 The frequency of cancer stem cells and the generality of cancer stem cell hypothesis

Recently, several reports have raised the possibility that the frequency of CSCs in a tumor might actually be underscored (Kelly et al., 2007; Krivtsov et al., 2006; Quintana et al., 2008; Somervaille and Cleary, 2006). In transplantation experiments with different forms of leukemia and with solid cancers, it could be demonstrated that the number of CSCs relative to all other tumor cells is higher than initially suggested. Hence, the numbers were estimated between 15-50% of all cells and probably even extend to all tumor cells.

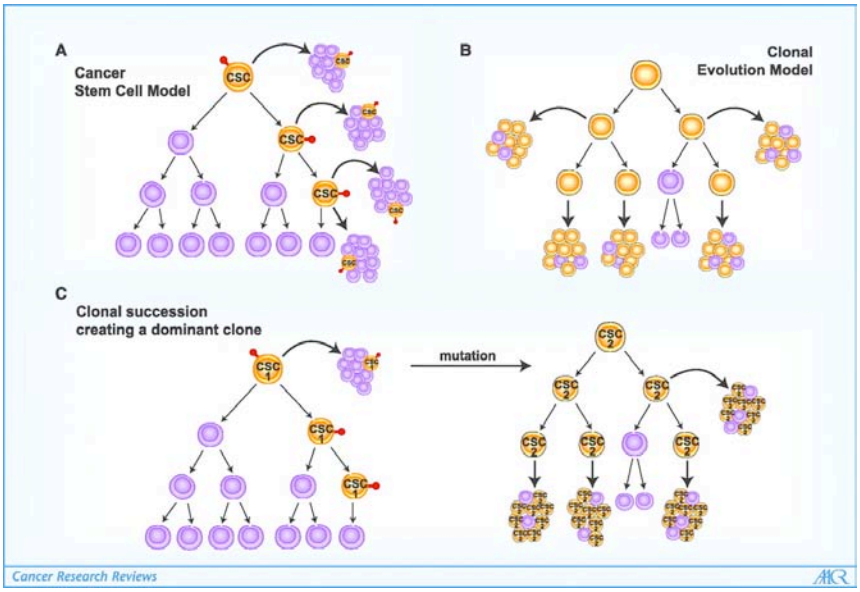

Figure 6: Tumors could arise either according to the cancer stem cell hypothesis (A) or by clonal evolution (B) or by a combination of both (C). (adapted from Adams et al, 2008)

The notion for these findings came from the consideration that the only ability of rare tumor cells to develop novel tumors might be a consequence of a lack of appropriate tumor microenvironment in NOD/SCID mice (Adams and Strasser, 2008; Kelly et al., 2007). In other words, the xenotransplantation experiments used to substantiate the cancer stem cell hypothesis seemed to have failed to provide all tumor cells with essential growth factors. These findings have challenged the cancer stem cell hypothesis insofar as they suggest that tumor growth might indeed be supported by clonally evolving cells - a model already proposed to exist for cancer cells (Figure 6).

1.4 Potential targets for treatment of hematopoietic malignancies

It is one of the major challenges in cancer biology to effectively treat cancers. As already mentioned before, current therapies mainly focus on the treatment of the bulk of cancer cells with diverse chemotherapeutical agents. Chemotherapy however is effective only on the majority of rapidly growing cells and has various side effects. Therefore, the patients are only exposed to chemotherapeutical agents for a relatively short period of time and the procedure has to be repeated several times. In recent years, many effective drugs were discovered that target mostly different tyrosine kinases, known to be expressed in cancers. One of this tyrosine kinase inhibitor, Imatinib-mesylate (Glivec, or STI571) was the first effective inhibitor used to combat CML and has revolutionized the therapy and the survival of patients with CML (Druker et al., 2001a; Druker et al., 2001b). However, the search for other inhibitors has turned out to be difficult and time-consuming, so that only few other tyrosine kinase inhibitors are in clinical use or in clinical trials. Another disadvantage of tyrosine kinase inhibitors like Imatinib-mesylate is that patients have to be treated a life-long, since Imatinib-mesylate only suppresses CML-progression, but does not completely eradicate the cells (Kantarjian et al., 2002; Ottmann et al., 2002; Sawyers et al., 2002).

1.4.1 Jak2 and Stat5

One focus of this thesis was to evaluate the possibility that Jak/Stat-signaling components may be potential targets for treatment of leukemia. As already mentioned, Jak/Stat proteins are implicated in essential hematopoietic processes and are therefore considered to be powerful new drug targets for treatment of leukemia. Jaks, for example, are already ideally

suited for drug development, because they are tyrosine kinases and many current strategies involve inhibition of this protein family by ATP-analogons, which specifically bind into the ATP-binding pocket of the kinase domain and thereby inhibits its function (Druker, 2008).
On the other side, Stats are transcription factors (TFs) and currently there is lack of knowledge how to effectively target transcription factor, although some approaches are quite promising. For example, one could design drugs that specifically bind to the DBD of a TF and inhibit its binding to DNA. Another approaches would be to specifically inhibit either the phosphorylation or the subsequent dimerization of Stat molecules. Probably, in future years, there will exist a strategy to cope these problems (Druker, 2008).
However, our very recent studies have implicated two Jak/Stat-siganaling molecules, namley Jak2 (Grebien et al., 2008) and Stat5 (Hoelbl et al., 2006) to be potential targets for the anti-tumor therapy.

1.4.2 Targeting of cancer stem cells

A completely different approach for complete eradication of cancers was established through the postulation of the cancer stem cell hypothesis. The cancer stem cell hypothesis implies that only a minority of cancer cells is able to progress the tumor thereby providing an explanation for unsuccessful outcomes of the conventional chemotherapy. The reason for the relapse of tumors is the inability to hit rare CSCs, so the hypothesis (Adams and Strasser, 2008; Passegue et al., 2003; Stubbs and Armstrong, 2007). However, the mechanistic reasons for this might be of various arts. Therefore, it is thinkable that the frequency of CSCs plays a major role in their targeting. On the other hand, it could also be the acquired or intrinsic ability of CSCs to self-renew or to overcome death signals induced by fate determinants. Additionally, it is possible that CSCs are more resistant to conventional drug therapy, because they could express “drug pumps”, similar to normal stem cells.
Nevertheless, it is obvious that if the cancer stem cell hypothesis is correct, it will be necessary to identify the molecular means, which underlie these processes in order to eradicate all CSCs. Additionally, it will also be required to discover differences between the normal and cancerous stem cells, so that a therapy can be designed that specifically impairs CSCs but keeps the normal stem cells alive.

2 Aims of this study

The main aim of this study was to elucidate the role of Jak/Stat-signaling components in normal hematopoiesis and leukemia. The immense importance of Jak/Stat signaling, as discussed in the introduction part of this thesis, and the availability of novel genetic tools (i.e. novel transgenic mouse models, discovery of new phenotypic markers and definition of more exact hematopoietic populations and new leukemia models) has made it necessary to newly address or to re-evaluate the function of Jak/Stat proteins in homeostasis and disease. The focus has been set on the evaluation of the janus kinase Jak2 and the transcription factors Stat1 and Stat5.

Beside the role in normal hematopoiesis, we have addressed the question of the impact of these proteins for the initiation and maintenance of leukemia. Therefore, several models covering MPDs, lymphoid and myeloid, as well as acute and chronic leukemia, have been tested during the thesis work. As can be depicted from the results part, the major focus within this work was made on the transcription factor Stat5, mostly because of the discovery of its striking phenotype and involvement in several lineage decisions as well as leukemia formation. Moreover, this thesis has contributed to some essential findings concerning the role of Stat1 in leukemia progression and immune surveillance.

Interestingly, while performing experiments in different leukemia models, we could also observe a link between the initiation and maintenance of leukemia, which had provided a foundation for a novel model about the development of leukemias in general.

This thesis consists of five major parts:

(i) Cancer stem cells of different developmental fates nourish acute and chronic leukemia.
(manuscript in preparation for submission)

(ii) Stat5 is a signaling bottleneck for the maintenance of *bcr/abl*-positive leukemia.
(under revision in Cancer Cell since 2009 March 2nd)

(iii) Stat5 activation enables erythropoiesis in the absence of EpoR and Jak2
(published in Blood. 2008 May 1;111(9):4511-22. Epub 2008 Jan 31)

(iv) STAT1 acts as a tumor promoter for leukemia development.

(published in Cancer Cell. 2006 Jul;10(1):77-87)

(v) Clarifying the role of Stat5 in lymphoid development and Abelson-induced transformation.

(published in Blood. 2006 Jun 15;107(12):4898-906)

Detailed aims and outcomes of the major thesis parts:

(i) Cancer stem cells of different developmental fates nourish acute and chronic leukemia.

Boris Kovacic, Andrea Hoelbl, Marc A. Kerenyi, Memetcan Alacakaptan, Gabriele Stengl and Hartmut Beug

This manuscript describes the key question of cancer biology, which is whether the tumor development is caused by rare cancer stem cells. Evidence for this model and for the model of clonal evolution of tumorogenic clones are currently conflicting against each other. We show that both hypotheses can be true if one takes into account that tumors could arise from cells that are distinct from those which maintain the tumor. We have compared acute lymphoid and chronic myeloid leukemia and could observe that whereas myeloid leukemia develop from the same CSCs initially and during progression, lymphoid leukemia change the identity of CSCs that initiate to a distinct CSC that progresses the leukemia. This finding is essential in understanding of the process that underlies leukemic development and explains the lineage determination so often associated with particular tumors.

(ii) Stat5 is a signaling bottleneck for the maintenance of *bcr/abl*-positive leukemia.

Andrea Hoelbl, Christian Schuster, Boris Kovacic, Maria A. Hoelzl, Sabine Fajmann, Florian Grebien, Wolfgang Warsch, Gabriele Stengl, Lothar Hennighausen, Hartmut Beug, Richard Moriggl, Veronika Sexl.

This study addresses for the first time the role of Stat5 protein in the maintenance of progressing leukemia. The BCR/ABL-oncogene was implicated in a plethora of different pathways and Stat5 has been suggested to mediate the most important downstream signals. Here we show that Stat5 is a suitable target for therapy because it is required for the

maintenance of leukemia progression. Deletion of Stat5 in growing leukemia in vivo could completely ablate the leukemic cells of a myeloid and a lymphoid leukemia. We further show that Stat5 seems to be involved in survival of leukemic cells, since its deletion leads to a G0/G1 cell cycle arrest and subsequent apoptosis induction in imatinib-sensitive and in imatinib-resistant cells. These results clearly demonstrate that Stat5 is a potential candidate for treatment of leukemia and could be used in addition to imatinib treatment.

(iii) Stat5 activation enables erythropoiesis in the absence of EpoR and Jak2

Florian Grebien, Marc A. Kerenyi, Boris Kovacic, Thomas Kolbe, Verena Becker, Helmut Dolznig, Klaus Pfeffer, Ursula Klingmüller, Mathias Müller, Hartmut Beug, Ernst W. Müllner and Richard Moriggl

This study demonstrates an essential function of Stat5 in the EpoR/Jak2/Stat5 axis for the induction and homeostasis of erythropoietic development. We could show here that expression of Stat5 in Jak2- and EpoR-deficient erythroid cells could rescue the erythropoiesis in vitro. By utilizing a constitutively active Stat5 mutant (cS5F) into Jak2-/- fetal liver cells, we could further show that cS5F could rescue erythropoiesis and myelopoiesis in vivo. Additionally, Jak2 was found to require c-kit-signaling through SCF and that SCF could induce Stat5 activity.

(iv) STAT1 acts as a tumor promoter for leukemia development.

Boris Kovacic, Dagmar Stoiber, Richard Moriggl, Eva Weisz, René G. Ott, Rita Kreibich, David E. Levy, Hartmut Beug, Michael Freissmuth and Veronika Sexl

Stat1 has been considered a tumor suppressor as an immune regulator of the surveillance of tumors. In contrast to this, this study describes a tumor-promoting role for Stat1 in MPD and lymphoid leukemia models. The explanation for this observation is that Stat1-/- tumor cells express low levels of MCH class I molecules on their surface and therefore exert a better recognition and more efficient killing by NK-cells. We could also describe that Stat1-/- tumor cells acquire increased levels of MHC class I proteins as the tumor progresses. These findings collectively indicate that Stat1 is a tumor promoter in leukemia development and that the

upregulation of MHC class I is a general mechanism of immune-escape of hematopoietic tumors.

(v) Clarifying the role of Stat5 in lymphoid development and Abelson-induced transformation.

Andrea Hoelbl, Boris Kovacic, Marc A. Kerenyi, Olivia Simma, Wolfgang Warsch,
Yongzhi Cui, Hartmut Beug, Lothar Hennighausen, Richard Moriggl, and Veronika Sexl

This study demonstrates an essential role of Stat5 in lymphopoiesis and lymphoid leukemia. By comparing lymphoid cells from wildtype, Stat5dN/dN and Stat5-/- mice, we could demonstrate that Stat5 is essential for the development of CD8+ T-cells, B-cells and gdT-cells. Interestingly, B-cell development was impaired at the pre-pro B-cell stage and therefore the initial transformation with the Abelson oncogenes was completely abrogated in vitro and in vivo. This publication is the first to implicate Stat5 as a major player in normal hematopoiesis and malignancy, because previous findings with Stat5dN/dN mice have exerted a rather mild phenotype.

3.1 Manuscripts

3.1.1 Cancer stem cells of different developmental fates nourish acute and chronic leukemia

Boris Kovacic[1], Andrea Hoelbl[1,2], Marc A. Kerenyi[3], Memetcan Alacakaptan[1], Gabriele Stengl[1] and Hartmut Beug[1]

[1]Research Institute of Molecular Pathology (IMP), 1030 Vienna, Austria
[2]Institute of Pharmacology, Centre of Biomolecular Medicine and Pharmacology, Medical University of Vienna (MUV), 1090 Vienna, Austria
[3]Max F. Perutz Laboratories, Department of Medical Biochemistry, Medical University of Vienna, 1030 Vienna, Austria

Cancer stem cells of different developmental fates nourish acute and chronic leukemia

Boris Kovacic[1], Andrea Hoelbl[1,2], Marc A. Kerenyi[3], Memetcan Alacakaptan[1], Gabriele Stengl[1] and Hartmut Beug[1]

[1]Research Institute of Molecular Pathology (IMP), 1030 Vienna, Austria
[2]Institute of Pharmacology, Centre of Biomolecular Medicine and Pharmacology, Medical University of Vienna (MUV), 1090 Vienna, Austria
[3]Max F. Perutz Laboratories, Department of Medical Biochemistry, Medical University of Vienna, 1030 Vienna, Austria

A key question in cancer biology is whether the processes of tumor-initiation and tumor-progression are caused by rare cancer stem cells (CSCs). One widely accepted evidence for this model is that rare human cancer cells are able to reseed tumors in non-obese diabetic/ severe combined immunodeficient (NOD/SCID) mice[1,2,3,4,5]. However, the generality of this 'cancer stem cell hypothesis' has recently been questioned by several observations showing that a more frequent amount of tumor cells might represent CSCs[6,7,8,9]. Here we show that both scenarios are true if CSCs of distinct developmental stages initiate and maintain cancers. Acute lymphoid BCR/ABLp185 leukemia is initiated, but not maintained by the rare long-term hematopoietic stem cell population. Initiating-CSCs change their fate, are lost and the progressing tumor is maintained through frequent precursor B-cells. In contrast, the chronic myeloid BCR/ABLp210 leukemia is both, initiated and maintained by rare malignant LT-HSCs. Our results indicate that lymphoid and myeloid tumors initially follow the cancer stem cell hypothesis, but lymphoid tumors progress by clonal evolution, whereas myeloid tumors progress according to the cancer stem cell model. This provides an explanation for the etiological discrepancy between the chronic and acute leukemia, and raises the question whether the mere targeting of rare CSCs might be successful for eradication of all tumors.

The most important assumption of the cancer stem cell hypothesis is that tumors are hierarchically organized and supported by a rare population of cancer stem cells[1,2,3,4,5]. However, many acute-type tumors do not seem to be hierarchically organized but rather

consist of a homogenous population of tumor cells[6,9,10,11,12]. Hence, emerging evidence suggests that in some malignancies, tumor growth is supported by the majority of tumor cells. Apart from the question if the cancer stem cell hypothesis can be generalized to all tumors, it is also not clear whether the cancer stem cell, which initiates the tumor, and the cancer stem cell, which maintains the tumor, are one and the same cell. One possible explanation is that tumors develop and progress through a sequence of steps from a stem cell to a population of more mature tumor cells and that in some tumors, the initial cancer stem cell population is lost, whereas in others, it remains a part of the tumor[13]. In this case, tumors might undergo a process similar to normal tissue development and the existence of cancer stem cells might depend on a specific developmental stage and on the acquired oncogenic mutation.

Whether some tumors are destined to develop into only one specific lineage, whereas others choose a distinct lineage or even multiple lineages, could therefore be dependent on both, the cell of origin and the oncogenic transformation event. A recent study, however, has implicated that 5-FU treatment of donor bone marrow prior to transplantation could influence the lineage decision of the normally CML-inducing BCR/ABLp210 protein. Without 5-FU pre-treatment, the transplanted mice developed a B-ALL[14]. However, most, if not all, studies of the cancer stem cell hypothesis involving BCR/ABL were performed using 5-FU pre-treated bone marrow. Therefore, the degree to which the potential cancer stem cells might have been biased by the 5-FU treatment is rather unclear.

In addition, the evidence that the genuine cancer stem cell population is uniquely responsible for the development of tumors and conversely, that eradication of cancer stem cells could destroy the tumor, is still lacking.

To clarify whether tumors arise from rare cancer stem cells, we have compared the tumor etiology of two closely related oncogenes, BCR/ABL p210 and BCR/ABL p185. The product of the fusion oncogene BCR/ABL - generated by a chromosomal translocation t(9:22)[15] and resulting in the Philadelphia chromosome (Ph)[16,17] - is a constitutively active tyrosine kinase[18], which empowers hematopoietic cells with proliferative and survival advantages. Interestingly, whereas exclusively in chronic myeloid leukemia (CML), the breakpoints of BCR and ABL generate a 210 kDa protein, a shorter version (185 kDa) exists in a fatal but rare childhood acute B-cell leukemia (B-ALL)[19,20]. Moreover, analysis of patients with CML has revealed that cells of all hematopoietic lineages are Ph^+, suggesting that these translocations may arise in the HSC-compartment[21,22].

Accordingly, we have assumed that if BCR/ABLp210- and BCR/ABLp185-translocations originated in the HSC-compartment, transformation of either whole bone marrow (BM) or

LT-HSCs alone would lead to comparable frequencies and etiologies of leukemia *in vivo*. In contrast, transformation of whole BM would induce more frequent leukemia formation compared to LT-HSCs, if the both oncogenes transformed progenitor cells (figure 1A). We have infected BM and LT-HSCs (isolated from 5-FU untreated donors; see supplementary methods) with both oncogenes and injected them into lethally irradiated wildtype syngeneic mice (in order to keep an intact tumor microenvironment) but to avoid an interaction with the host immune system. All mice transplanted with BCR/ABLp210 developed a CML-like disease, whereas all mice bearing BCR/ABLp185 succumbed to a B-ALL (figure 1B). Both oncogenes have led to severe infiltrations of bone marrow (BM), spleen and liver *in vivo* (supplementary figure 1). Interestingly, the same results in terms of frequency and etiology of leukemia formation were obtained irrespectively of the population (whole BM versus LT-HSCs) transformed by both oncogenes (figure 1B). These results clearly show that in both leukemias, the LT-HSC-population is capable of initiating tumor formation.

However, even if originated in the most primitive hematopoietic cell, the fates of the two leukemias seem to be diametrically opposed. GFP^+ BCR/ABLp210 leukemic cells were present throughout all lineages of the hematopoietic system (figure 2A and supplementary figure 2). In contrast, close analysis of GFP^+ BCR/ABLp185 leukemic cells has revealed that they were almost exclusively composed of $CD19^+/B220^+$ precursor-B cells, except for a - somewhat aberrant - $CD19^+/Gr\text{-}1^+$ population in the BM (3.02%) of diseased mice. In case of whole BM-transformation, the clear discrepancy between BCR/ABLp210 and BCR/ABLp185 leukemia could not be explained by the infection of different target cells, because in control mice, all mature hematopoietic lineages were GFP^+ (figure 2A). Moreover, the transformation of mere LT-HSCs yielded the same results for both leukemias. Hence, we hypothesized that the most privileged population of BCR/ABLp185 leukemia must have had its origin in the LT-HSC. One possible explanation for this would be that BCR/ABLp185-oncogene forces the differentiation of LT-HSCs into the B-cell lineage. To understand how this process takes place, we have compared the HSC-compartment of BCR/ABLp185 with BCR/ABLp210 terminally-diseased mice, both initially transplanted with transformed LT-HSCs. Strikingly, BCR/ABLp185 mice completely lacked leukemic GFP^+ cells in the LT-HSC population (Figure 2B, 0% GFP^+ cells) and also in more ST-HSC and MPP compartments (supplementary figure 2, 0% GFP^+ cells within ST-HSC and MPP). This effect was even more evident in respect to the total numbers of leukemic, GFP^+ HSCs in BCR/ABLp185 leukemia - which were found ~ 10 fold reduced as compared to control animals (Figure 2C). In contrast, the leukemic HSC population was ~ 20 fold increased in BCR/ABLp210

leukemia (figure 2C and supplementary figure 2, 69.1% GFP^+ cells in LT-HSC, 78.4% in ST-HSC and 29% in MPP compartments). These results indicate that, even if originating in rare LT-HSCs, BCR/ABLp210 and BCR/ABLp185 leukemia both distinctly influence their fate. While BCR/ABLp210 highly augments the number of LT-HSCs and thereby increases the number and contribution to all progeny-lineages, BCR/ABLp185 seems to determine LT-HSCs to one specific lineage and exhausts its pool.

To confirm that BCR/ABLp185 LT-HSC indeed directly differentiate into more committed $CD19^+$ cells *in vivo*, we have analyzed the fate of BCR/ABLp185- versus BCR/ABLp210-infected LT-HSCs *in vitro* (figure 2D). BCR/ABLp185 LT-HSCs have differentiated into $CD19^+/B220^+/IgM^-$ precursor-B cells within 11-15 days (figure 2D, upper panel). In contrast to BCR/ABLp210$^+$ LT-HSC, we could not detect any BCR/ABLp185 GFP^+ HSC after 18 days in culture (figure 2D, lower panel). Interestingly and in line with our findings, MOZ-TIF2, a fusion protein also causing an acute form of leukemia (AML), could similarly transform HSCs and induce a mature myeloid leukemia *in vivo*[23].

So far, our data suggest that particular oncogenes might change the fate of the initial cancer stem cell and thereby direct the fate of a developing tumor. The cell in which the cancer is initiated (initiating-CSC) and the cell which maintains the tumor (preserving-CSC) might therefore be two developmentally different cells. Therefore, we have speculated whether the low and the high frequencies of CSC in some tumors would be a consequence of the developmental stage of preserving-CSC. To investigate this, we have modeled three scenarios in which CSCs represent different stem or fate-determined cell-stage of leukemia (figure 3A): The first assumption is that all tumor cells have the capacity to induce a novel tumor (Model 1). The second possibility is that a rare stem cell population is exclusively capable to do so (Model 2). Conversly, the third possibility is that CSCs belong to a more mature progenitor cell pool (Model 3).

To address this issues, we have purified BCR/ABLp210 or BCR/ABLp185 GFP^+ LT-HSCs ($lin^-c^-kit^+Sca\text{-}1^+Thy1^{low}Flt3^-$) from terminally diseased primary transplants by FACS sorting, mixed them with HSC-depleted wildtype BM and injected into lethally irradiated secondary recipients. Conversely, wildtype LT-HSCs were mixed with BCR/ABLp210 or BCR/ABLp185 GFP^+ leukemic bone marrow cells which were devoid of all cells with HSC markers (see schemes in supplementary figure 3A and 3B). The expected results related to each one of the three models are summarized in figure 3A. Interestingly, when we transplanted GFP^+LT-HSCs from the BCR/ABLp210 leukemic pool, we observed a fast disease onset (15±2 days) in 100% of mice analyzed (n=9). The disease was phenotypically

identical to the primary transplant and consisted of GFP^+ cells in all hematopoietic lineages (figure 3B, upper panel). Moreover, leukemia development was not dependent on the cell dosage used for transplantation because injections of 100 - 70,000 cells did not significantly change the disease onset (data not shown). Strikingly, when we transplanted more mature BCR/ABLp210 leukemic cells (250,000 – 2,000.000) together with wildtype LT-HSC, we did not observe leukemia development in any transplanted animal over a period of 14 months (figure 3B, lower panel).

In a clear discrepancy to this, transplantation of BCR/ABLp185 HSC-depleted leukemic cells combined with wildtype LT-HSCs yielded a fatal precursor B-cell leukemia in all mice observed within 14 days (n=8). This leukemia again consisted of a homogeneous $CD19^+/B220^+/IgM^-$ cell population, which infiltrated the BM, spleen, liver and peripheral blood of diseased mice (Figure 3C, lower panel, and supplementary figure 3C). Since no GFP^+ BCR/ABLp185 LT-HSC were present at the time point of terminal disease (figure 2B), we decided to inject GFP^- LT-HSCs, in case that some cells have down-regulated GFP expression but still might induce leukemia upon transplantation. Nevertheless, those cells did not induce leukemia in secondary recipients over a period of 8 months (Figure 3C, upper panel).

These data clearly show that in progressing BCR/ABLp210 and BCR/ABLp185 leukemias, the diseases are maintained by CSCs that differ in their developmental fate - LT-HSCs and precursor B-cells, respectively. Normal precursor B-cells are lineage-restricted, whereas LT-HSCs possess the unique ability to self-renew and to differentiate into all mature hematopoietic cells. Lacking any cellular models to address the molecular mechanisms of leukemogenicity on stem cells, we have put in efforts to cultivate BCR/ABLp210 and BCR/ABLp185 CSCs *in vitro* and to examine whether they share any properties with normal LT-HSCs. Therefore, we have FACS sorted BCR/ABLp210 LT-HSCs and BCR/ABLp185 precursor B-cells from diseased mice and observed the outgrowth of leukemic cells under cell culture conditions. BCR/ABLp185 preserving-CSCs grew out rapidly *in vitro* using normal serum conditions (10% FCS). They were able to induce leukemia formation upon serial transplantation, but did not change their precursor B-cell phenotype nor did they express HSC-surface markers *in vivo* or *in vitro* (supplementary figure 4). BCR/ABLp210 CSCs, however, could not be grown under serum conditions (data not shown). This prompted us to cultivate the cells under serum-free conditions with defined growth factors enabling the proliferation of hematopoietic stem cells (SCF/Tpo/IGF-II and FGF-1). Interestingly, under these ‘self-renewal conditions’, proliferation of BCR/ABLp210 LT-HSCs was only achieved

if cells were seeded at very low density. On the morphological level, the colonies consisted of a population of more adherent and a population of more suspended cells, both compiling "cobblestone-like" structures on dishes (figure 4A). Interestingly, efficient replating required FACS-sorting of forward scatter (FSC) high (large) cells (Figure 4A), whereas FSC low (small) BCR/ABLp210 LT-HSCs were unable to give rise to any colonies *in vitro* (movie 1 and movie 2). In contrast to wildtype LT-HSC, which proliferated only for about 14 days, BCR/ABLp210 LT-HSCs could be expanded indefinitely (Figure 4B). In addition to this, we could observe expression of many classical HSC and HSC-niche markers (Table2).

Strikingly, when we injected BCR/ABLp210 LT-HSCs, grown under self-renewal conditions, into lethally irradiated mice, we could induce a CML-like leukemia formation. The disease accompanied with an increase in GFP^+ $GR\text{-}1^+/Mac\text{-}1^+$ cells and a contribution to $CD19^+$ and $CD3^+$ cells (figure 4C), indicating that these preserving-CSCs were able to differentiate *in vivo*.

These results indicate that BCR/ABLp210 LT-HSCs possess all hallmarks of hematopoietic stem cells - including HSC marker surface expression, infinite self-renewal and differentiation into all mature lineages of the hematopoietic system - and of CSCs - like recapitulation of the tumor phenotype upon serial transplantation. In contrast, BCR/ABLp185 CSCs are homogeneous precursor B-cells, do not express HSC surface markers and do not differentiate into mature B-cells *in vivo* or *in vitro*, but however they are able to reinitiate an acute leukemia in secondary transplants.

One prediction of the cancer stem cell hypothesis is that rare cancer stem cells might be more resistant to chemotherapy than frequent mature cancer cells, because of drug-resistance transporters, which are expressed on normal tissue stem cells. Therefore, we have analyzed the possibility that BCR/ABLp210 LT-HSC would be more resistant to Imatinib-mesylate treatment than BCR/ABLp185 precursor-B cells. As indicated in figure 3E, BCR/ABLp210 LT-HSC were indeed resistant to different concentrations of imatinib-mesylate, whereas BCR/ABLp185 precursor-B cells regressed in proliferation and cell number (figure 4D).

However, knowing that BCR/ABLp210 CSCs possess all characteristics of LT-HSCs, one possible strategy to eradicate CSCs - even if they are insensitive to imatinib-mesylate treatment - would be to force them into lineage-commitment. As depicted in Figure 4F (middle panel), addition for cytokines for terminal differentiation into erythroid, myeloid and lymphoid lineages has completely changed the phenotype of BCR/ABLp210 CSC *in vitro*. After 7 days, the cultures consisted of a mixture of $CD19^+$, $Mac\text{-}1^+$ and $CD71^+/TER119^{low}$ cells (figure 4F, upper panel and data not shown). To elucidate if those differentiated cells

were able to initiate leukemia in serial transplants, we have injected 250,000 cells together with 250,000 HSC-depleted BM cells into sub-lethally irradiated mice. None of the transplanted mice has developed leukemia or hyperplasia after a period of 12 months and close analysis of BM, spleens and blood has revealed that no GFP^+ cells have emerged during the observed period (figure 4F, lower panel).

The "cancer stem cell hypothesis" has been challenged by some observations showing a majority of tumor cells being responsible for tumor outgrowth. Our data unify and consolidate both theories by demonstrating that cancer stem cells have distinct developmental fates in terms of initiation and progression. In other words, these data suggest that oncogenes might endow cells with self-renewal and survival abilities only at specific commitment stages. In line with this are numerous studies showing that in acute leukemia, committed progenitors rather than HSCs could re-induce the disease upon serial transplantation[6,24,10,11,12,25,24]. Beside this, it might also be provocative to think that some CSCs are rare and others frequent as a consequence of abundance in the hematopoietic system. The goal of cancer therapy is the eradiction of all CSCs and therefore alternative targets are required for their efficient depletion. Interestingly, we found that BCR/ABLp210 CSCs were more drug-resistant to imatinib-mesylate treatment than BCR/ABLp185 CSCs. Therefore, the anti-cancer drug therapies in CML patients may be insufficient in eradication of chronic disease CSCs, but more efficient in killing of acute phase CSCs. However, the reason why chronic phase patients have unequally better prognosis than patients with acute form of leukemia might be due to the enormous total number of CSCs in acute leukemia.

Methods summary

Mice

All mice were kept under sterile conditions in individually ventilated IVC-cages at the IMP-animal facility. Animal experiments were preformed and protocoled according to the rules of the Austrain Tierversuchgesetz 1988, licence no. MA58/1253/03 and MA58/001489/2008/12. Since STAT5fl/fl and Mx-1Cre mice had a mixed (C57Bl/6J and 129/Sv) background, all wildtype donor and recipient mice were obtained from F1 crosses of C57Bl/6J x 129/Sv (B6/129 F1) mice.

Preparation of BM, spleens and PB

Femurs and tibiae were cut at the ends and the bone marrow cells flushed using a 22-gauche needle with 1x PBS. Spleens were crushed with a plunger of a syringe through a 70µm cell strainer. Peripheral blood erythrocytes were lyzed in 1xEry-Lysis buffer. All cells were collected by centrifugation and resuspended in 1xPBS.

Statistical analysis

Statistics have been performed using paired and unpaired student's t-test.

Methods

BM preparation and transplantation

Four-to-six-week wildtype or STAT5fl/fl Mx1Cre mice were used as donors for six-to-eight-week old recipient mice. No 5-FU treatments were performed in any of the transplant experiments to avoid a bias to the myeloid lineage or a depletion of the potential cell of origin of cancer. BM from donor mice was flushed from the femurs and tibiae, pooled and filtrated. Whole BM (2-2.5x10^6 cells/ml) was infected using stable producer lines carrying empty-IRES-GFP, BCR/ABLp210-IRES-GFP, BCR/ABLp185-IRES-GFP as described earlier[26].The stable producer cells (GP+E86 cell lines) were initially derived from mouse embryonic fibroblasts (MEFs) and display a supportive microenvironment/niche for hematopoietic cells and ES cells. 2-3x10^6 infected total BM cells were injected via tail-vein per lethally (10 Gy) irradiated B6/129F1 mouse. For LT-HSCs infections, the LT-HSCs were FACS-sorted as described later and infected with the mentioned producer cell lines on 96-well-plates in analogous way to whole BM[26]. For secondary transplantation, wildtype or GFP^+ leukemic

LT-HSCs and HSC-depleted wildtype or GFP^+ leukemic BM was FASC-sorted from sick primary transplanted mouse, mixed in the described manner (figure 3A) and injected into lethally irradiated secondary B6/129F1 recipients. To avoid differences in leukemogenicity of the sorted leukemic cells, we have waited until every single primary and secondary transplanted mouse has become terminally diseased. Similarly, mice that did not become sick in the expected latency time were observed over a period of at least 12 months before sacrificed.

FACS analysis and sorting

BM, spleen, liver and peripheral blood were isolated from every single transplanted mouse and the cells incubated with fluorescence-conjugated lineage antibodies (TER119, CD3, Mac-1, Gr-1 and CD19). BM and spleens were also stained with CD71 and Ter119 antibodies to determine erythroid precursor cells. In addition, BM was stained with (1) lineage markers, c-kit, Sca-1, Flt3 and Thy1.2 (or CD150) for detection of all HSC subpopulations, (2) with lineage markers, c-kit, Sca-1 and IL7Rα for detection of lymphoid precursors and (3) with lineage markers with IL7Rα, c-kit, Sca-1, CD16/CD32 and CD34 - for detection of myeloid precursor cells. Flow cytometric analysis of all organs was performed on 6-color BD FASC Canto (BD Biosciences) equipped with 488nm and 633nm lasers.

FACS-sorting of wildtype and leukemic LT-HSCs as well as wildtype and leukemic HSC-depleted BM was performed on 4°C immediately after biopsy of the diseased mouse and staining of BM cells with the mentioned HSC-markers using an 8-color BD FACS Aria equipped with 488nm, 633nm and 407nm lasers.

Antibodies

Lineage panel Kit containing biotinylated Ter119 (Ly-76, Ter119), CD3e (CD3ε, 145-2C11), CD45R/B220 (RA3-6B2), CD11b (Mac-1, M1/70) and Ly6G/Ly6C (Gr-1, RB6-8C5) were purchased from BD Pharmingen and eBioscience. Second step detection Streptavidin-APC-Cy7, Ter119 (Ly-76, Ter119)-PE and -APC, CD135 (Flk-2/Flt3/Ly-72, A2F10.1)-PE, Flk-1 (VEGF-R2/Ly-73, Avas12α1)-PE, CD3e (145-2C11)-PerCP, CD19 (1D3)-APC-Cy7, CD90.2 (Thy1.2, 53-2.1)-APC, Ly6G/Ly6C (Gr-1, RB6-8C5)-APC, CD62E (E-Selectin/ELAM-1, 10E9.6)-PE, CD44 (Pgp-1/Ly-24, IM7)-PE, CD34 (RAM34)-APC, IgM (II/41)-APC, Ly6A/E (Sca-1, D7)-PE-Cy7, CD71 (Transferrin receptor, C2)-PE, CD16/CD32 (FcgIII/IIR, 2.4G2)-PE, CD144 (VE-Cadherin, 11D4.1)-PE, CD162 (PSGL-1, 2PH1)-PE and CD31 (PECAM-1, MEC13.3)-PE were all obtained from BD Pharmingen. CD11b (Mac-1,

M1/70)-PE-Cy7, Tie-2 (Tek/CD202, TEK4)-PE, CD127 (IL7Ra, A7R34)-bio and CD117 (c-kit, 2B8)-PE-Cy5 were purchased from eBioscience. CD150 (SLAMf1, TC15-12F12.2)-APC and CD127 (IL7Ra, SB/199)-PE were purchased from Biolegend. Hamster anti-mouse Notch-1 (8G10) was purchased from AbD Serotec, rabbit anti-mouse Jagged-1 (H66) from Santa Cruz, APC-goat anti-rabbit IgG from Invitrogen and PE-goat anti hamster IgG from Acris.

In vitro cultivation and differentiation

Freshly sorted GFP^+ LT-HSC population from BCR/ABLp210 diseased mice was cultivated in 4-wells (1000 cells/well) in serum-free medium (StemPro-34 SFM, GIBCO) containing Nutrient supplement (GIBCO), 2mM L-glutamine, Pen/Strep and supplemented with 10ng/ml mSCF, 20ng/ml mTPO, 20ng/ml IGF-II, 10ng/ml hFGF-1 (acidic) and 10ng/ml Heparin. Confluent outgrowth of "cobblestone"-like structures (figure 4A and movie 1) was obtained after about 6-7 days. Thereafter, the smaller cells growing on top of the more adherent ones were removed from the 4-well, the adherent rest was washed with 1xPBS, trypsinized and pooled together with the smaller cells. The cells were sorted in a FSC^{high} and a FSC^{low} fraction and seeded at a density of 1000 cells per 6cm dish. This procedure of $FSC^{high/low}$ sorting was repeated when the cells were confluent again. The dish dimensions could be increased at every sorting/replating step.

Microscopy

Live cell imaging of leukemic LT-HSCs was performed using a ZEISS Axiovert 200M Life Cell Observer with incubator. Before and during live observation, the cells were grown on 4-well Lab-Tek Chamber Slides (Nunc). The data was analyzed using Metamorph software (Zeiss).

Confocal microscopy was performed on a LSM 510 Meta/Axiovert 200M system from Zeiss. The cells were grown on 4-well Lab-Tek Chamber Slides, fixed and stained according to a previously described protocol and mounted in Vecta Shield with DAPI.

Imatinib-mesylate treatment

BCR/ABLp210 LT-HSC and BCR/ABLp185 precursor-B cells were plated at a density of 30,000 cells on 96-wells in 100 µl medium supplemented with either no imatinib-mesylate, 100µM imatinib-mesylate or 200µM imatinib-mesylate. On day 16, the cells were taken from wells and counted.

Figure legends

Figure 1 | LT-HSCs are initiating-CSCs for BCR/ABLp210 and BCR/ABLp185 leukemia, but BCR/ABLp185 CSCs change their fate during disease progression.

A, Schematic overview of the hierarchical hematopoietic lineage. Potential initiating-CSCs are indicated by arrows. **B**, Either whole BM cells or FACS-sorted LT-HSCs alone were transduced with retroviruses encoding BCR/ABLp210, BCR/ABLp185 or an empty GFP-labeled vector. All (13/13) BCR/ABLp210-transplanted mice developed a CML and all (6/6) BCR/ABLp185-transplanted mice developed a B-ALL, irrespective whether whole BM or purified LT-HSCs alone were initially used for transformation (see also supplementary figure 1A).

Figure 2 | BCR/ABLp185 CSCs change their fate during disease progression and are lost.

A, FACS-analysis of peripheral blood cells isolated from control and terminally-diseased mice induced by transplantation of whole BM. Empty vector and BCR/ABLp210 leukemia prominently contribute to myeloid (Gr-1$^+$/Mac-1$^+$), lymphoid (CD19$^+$ and CD3$^+$) and erythroid (Ter119$^+$) lineages, whereas BCR/ABLp185 mainly contribute to the B-lymphoid lineage. The indicated percentages represent relative amounts of GFP+ cells from each population analyzed (**A** and **B**). **B**, FACS-analysis of BM cells from control and terminally-diseased mice induced by transplantation of LT-HSCs alone. In contrast to control or BCR/ABLp210 leukemic BM, BCR/ABLp185-diseased BM completely lacks GFP$^+$ LT-HSCs. **C**, Quantitative analysis of leukemic GFP$^+$ HSC cells in all diseased and control groups. The total numbers of GFP$^+$ cells per 100,000 BM cells and the fold-increase compared to empty vector-transplanted mice are indicated. The values for total GFP$^+$ cell numbers are represented as means ± SED. **D**, Analysis of *in vitro* cell outgrowth by the transformation of LT-HSCs with BCR/ABLp210 and BCR/ABLp185, respectively. Contour blots indicate the lineage into which the cells have differentiated (upper panel) and the presence of HSCs (lower panel). For detailed information on *in vitro* cultivation see supplementary method section.

Figure 3 | BCR/ABLp210 and BCR/ABLp185 preserving-CSCs are distinct in frequency and fate.

A, Models for disease-maintenance from differently committed preserving-CSCs. In model 1, all leukemic cell have the ability to re-initiate leukemia. Model 2 assumes that leukemia is maintained by frequent progenitor or lineage-restricted precursor cells and in model 3, the leukemia preserving cell is the rare LT-HSC. The predicted outcomes for transplantation of either the mixture of leukemic LT-HSCs with wildtype HSC-depleted BM or the mixture of wildtype LT-HSC with leukemic HSC-depleted BM, are indicated for every model. **B**, Preserving-CSCs from BCR/ABLp210 leukemia behave according to the model 3. Mixture of leukemic BCR/ABLp210 LT-HSCs with wildtype HSC-depleted BM induces a CML-like disease formation (upper panel) in 9/9 serially transplanted mice. Transplantation of the mixture of wildtype LT-HSCs with frequent, leukemic BCR/ABLp210 HSC-depleted BM leaves the mice disease-free for 14 months. No GFP+ cells are detectable after the observed period in the BM of 12/12 mice (lower panel). **C**, Preserving-CSCs from BCR/ABLp185 leukemia behave according to the model 2. Mixture of all BCR/ABLp185 LT-HSCs with wildtype HSC-depleted BM prevents B-ALL formation in 4/4 serially transplanted mice (upper panel). Transplantation of the mixture of wildtype LT-HSCs with frequent, leukemic BCR/ABLp185 HSC-depleted BM induces a B-ALL formation (lower panel) in 8/8 serially transplanted mice. GFP^+ leukemic cells in secondary transplanted mice exclusively comprise of precursor B-cells (lower panel).

Figure 4 | BCR/ABLp210 preserving-CSCs keep all properties of stem cells *in vitro*.

A, Scheme: Leukemic BCR/ABLp210 LT-HSCs were isolated from terminally-diseased primary transplanted mice and cultivated under conditions allowing for self-renewal of normal HSCs (see method section). The morphologically different cells were FACS-sorted in forward scatter high (FSC^{high}) and forward scatter low (FSC^{low}) cells. Only FSC^{high} cells give arise to new colonies *in vitro*. The cells are injected into recipient mice under self-renewing or fate-determining conditions (subfigures **C** and **F**). **B**, growth curves representing the cumulative cell number of BCR/ABLp210 LT-HSC and wildtype LT-HSCs. BCR/ABLp210 LT-HSCs grew continuously for at least 68 days. **C**, BCR/ABLp210 LT-HSCs under self-renewing conditions were injected into recipient mice. FACS-blots indicate the contribution of BCR/ABLp210 LT-HSC to myeloid and lymphoid lineages. Induction of leukemia was observed in 3/3 mice. **D** and **E**, Imatinib-mesylate treatment of BCR/ABLp185 precursor B-cells (**D**) and BCR/ABLp210 LT-HSCs (**E**). BCR/ABLp185 CSCs react with growth inhibition and decreased cell number whereas BCR/ABLp210 LT-HSCs do not. **F**, Enforced *in vitro* differentiation of BCR/ABLp210 LT-HSCs into mature cells and subsequent injection

into sublethally irradiated mice. FACS blots in upper panel show that the cells are already lineage-restricted at the time point of injection. Analysis of mice indicate no contribution to myeloid and lymphoid lineages (lower panel). No leukemia formation was observed.

References

1 Bonnet, D. and Dick, J. E., Human acute myeloid leukemia is organized as a hierarchy that originates from a primitive hematopoietic cell. *Nat Med* **3** (7), 730 (1997).

2 Al-Hajj, M. et al., Prospective identification of tumorigenic breast cancer cells. *Proc Natl Acad Sci U S A* **100** (7), 3983 (2003).

3 Singh, S. K. et al., Identification of human brain tumour initiating cells. *Nature* **432** (7015), 396 (2004).

4 Ricci-Vitiani, L. et al., Identification and expansion of human colon-cancer-initiating cells. *Nature* **445** (7123), 111 (2007).

5 Lapidot, T. et al., A cell initiating human acute myeloid leukaemia after transplantation into SCID mice. *Nature* **367** (6464), 645 (1994).

6 Kelly, P. N. et al., Tumor growth need not be driven by rare cancer stem cells. *Science* **317** (5836), 337 (2007).

7 Kennedy, J. A. et al., Comment on "Tumor growth need not be driven by rare cancer stem cells". *Science* **318** (5857), 1722; author reply 1722 (2007).

8 Quintana, E. et al., Efficient tumour formation by single human melanoma cells. *Nature* **456** (7222), 593 (2008).

9 Somervaille, T. C. and Cleary, M. L., Identification and characterization of leukemia stem cells in murine MLL-AF9 acute myeloid leukemia. *Cancer Cell* **10** (4), 257 (2006).

10 Krivtsov, A. V. et al., Transformation from committed progenitor to leukaemia stem cell initiated by MLL-AF9. *Nature* **442** (7104), 818 (2006).

11 Cozzio, A. et al., Similar MLL-associated leukemias arising from self-renewing stem cells and short-lived myeloid progenitors. *Genes Dev* **17** (24), 3029 (2003).

12 Jamieson, C. H. et al., Granulocyte-macrophage progenitors as candidate leukemic stem cells in blast-crisis CML. *N Engl J Med* **351** (7), 657 (2004).

13 Eaves, C. J., Cancer stem cells: Here, there, everywhere? *Nature* **456** (7222), 581 (2008).

14 Hu, Y. et al., Requirement of Src kinases Lyn, Hck and Fgr for BCR-ABL1-induced B-lymphoblastic leukemia but not chronic myeloid leukemia. *Nat Genet* **36** (5), 453 (2004).

15 Groffen, J. et al., Philadelphia chromosomal breakpoints are clustered within a limited region, bcr, on chromosome 22. *Cell* **36** (1), 93 (1984).

16 Nowell, P. C. and Hungerford, D. A., Chromosome studies on normal and leukemic human leukocytes. *J Natl Cancer Inst* **25**, 85 (1960).

17 Rowley, J. D., Letter: A new consistent chromosomal abnormality in chronic myelogenous leukaemia identified by quinacrine fluorescence and Giemsa staining. *Nature* **243** (5405), 290 (1973).

18 Konopka, J. B. and Witte, O. N., Detection of c-abl tyrosine kinase activity in vitro permits direct comparison of normal and altered abl gene products. *Mol Cell Biol* **5** (11), 3116 (1985).

19 Clark, S. S. et al., Expression of a distinctive BCR-ABL oncogene in Ph1-positive acute lymphocytic leukemia (ALL). *Science* **239** (4841 Pt 1), 775 (1988).

20 Westbrook, C. A. et al., Clinical significance of the BCR-ABL fusion gene in adult acute lymphoblastic leukemia: a Cancer and Leukemia Group B Study (8762). *Blood* **80** (12), 2983 (1992).

21 Takahashi, N., Miura, I., Saitoh, K., and Miura, A. B., Lineage involvement of stem cells bearing the philadelphia chromosome in chronic myeloid leukemia in the chronic

phase as shown by a combination of fluorescence-activated cell sorting and fluorescence in situ hybridization. *Blood* **92** (12), 4758 (1998).

[22] Holyoake, T., Jiang, X., Eaves, C., and Eaves, A., Isolation of a highly quiescent subpopulation of primitive leukemic cells in chronic myeloid leukemia. *Blood* **94** (6), 2056 (1999).

[23] Huntly, B. J. et al., MOZ-TIF2, but not BCR-ABL, confers properties of leukemic stem cells to committed murine hematopoietic progenitors. *Cancer Cell* **6** (6), 587 (2004).

[24] Jin, L. et al., Targeting of CD44 eradicates human acute myeloid leukemic stem cells. *Nat Med* **12** (10), 1167 (2006).

[25] Barabe, F., Kennedy, J. A., Hope, K. J., and Dick, J. E., Modeling the initiation and progression of human acute leukemia in mice. *Science* **316** (5824), 600 (2007).

[26] Moriggl, R. et al., Stat5 tetramer formation is associated with leukemogenesis. *Cancer Cell* **7** (1), 87 (2005).

Figure 1

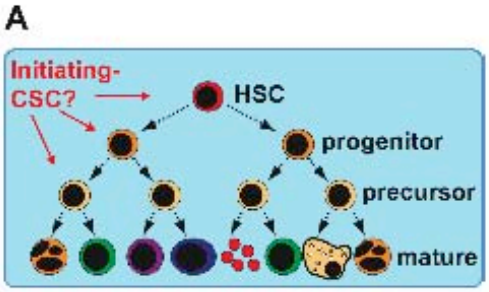

B

whole BM or *LT-HSCs* → +empty vector, +BCR/ABLp210, +BCR/ABLp185

	whole BM	LT-HSCs
bcr/abl p210	**9/9 (CML)**	**4/4 (CML)**
bcr/abl p185	**4/4 (B-ALL)**	**2/2 (B-ALL)**

Figure 2

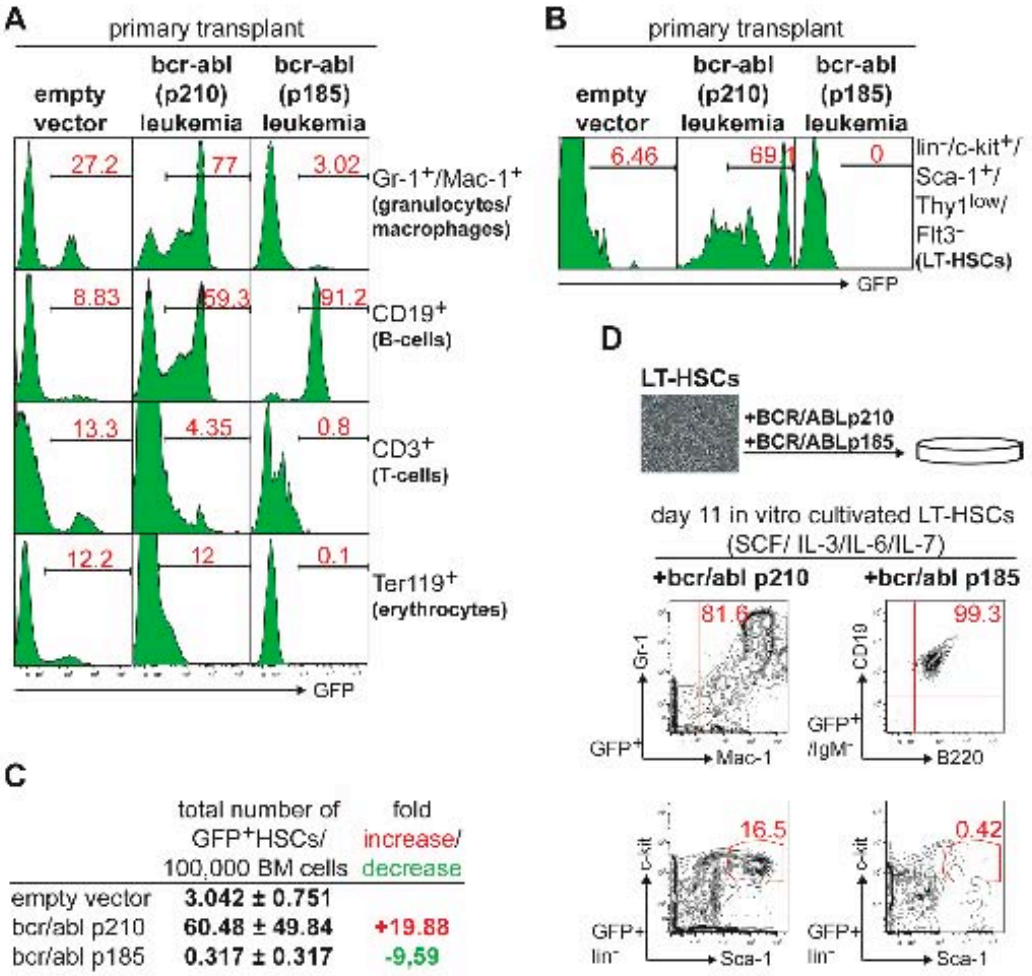
A
primary transplant
empty vector
bcr-abl (p210) leukemia
bcr-abl (p185) leukemia
27.2
77
3.02
Gr-1+/Mac-1+ (granulocytes/ macrophages)
8.83
59.3
91.2
CD19+ (B-cells)
13.3
4.35
0.8
CD3+ (T-cells)
12.2
12
0.1
Ter119+ (erythrocytes)
GFP
B
primary transplant
empty vector
bcr-abl (p210) leukemia
bcr-abl (p185) leukemia
6.46
69.1
0
lin-/c-kit+/ Sca-1+/ Thy1low/ Flt3- (LT-HSCs)
GFP
C
total number of GFP+HSCs/ 100,000 BM cells
fold increase/ decrease
empty vector 3.042 ± 0.751
bcr/abl p210 60.48 ± 49.84 +19.88
bcr/abl p185 0.317 ± 0.317 -9,59
D
LT-HSCs
+BCR/ABLp210
+BCR/ABLp185
day 11 in vitro cultivated LT-HSCs (SCF/ IL-3/IL-6/IL-7)
+bcr/abl p210
+bcr/abl p185
81.6
Gr-1
GFP+
Mac-1
99.3
CD19
GFP+ /IgM-
B220
16.5
c-kit
GFP+ lin-
Sca-1
0.42
c-kit
GFP+ lin-
Sca-1

Figure 3

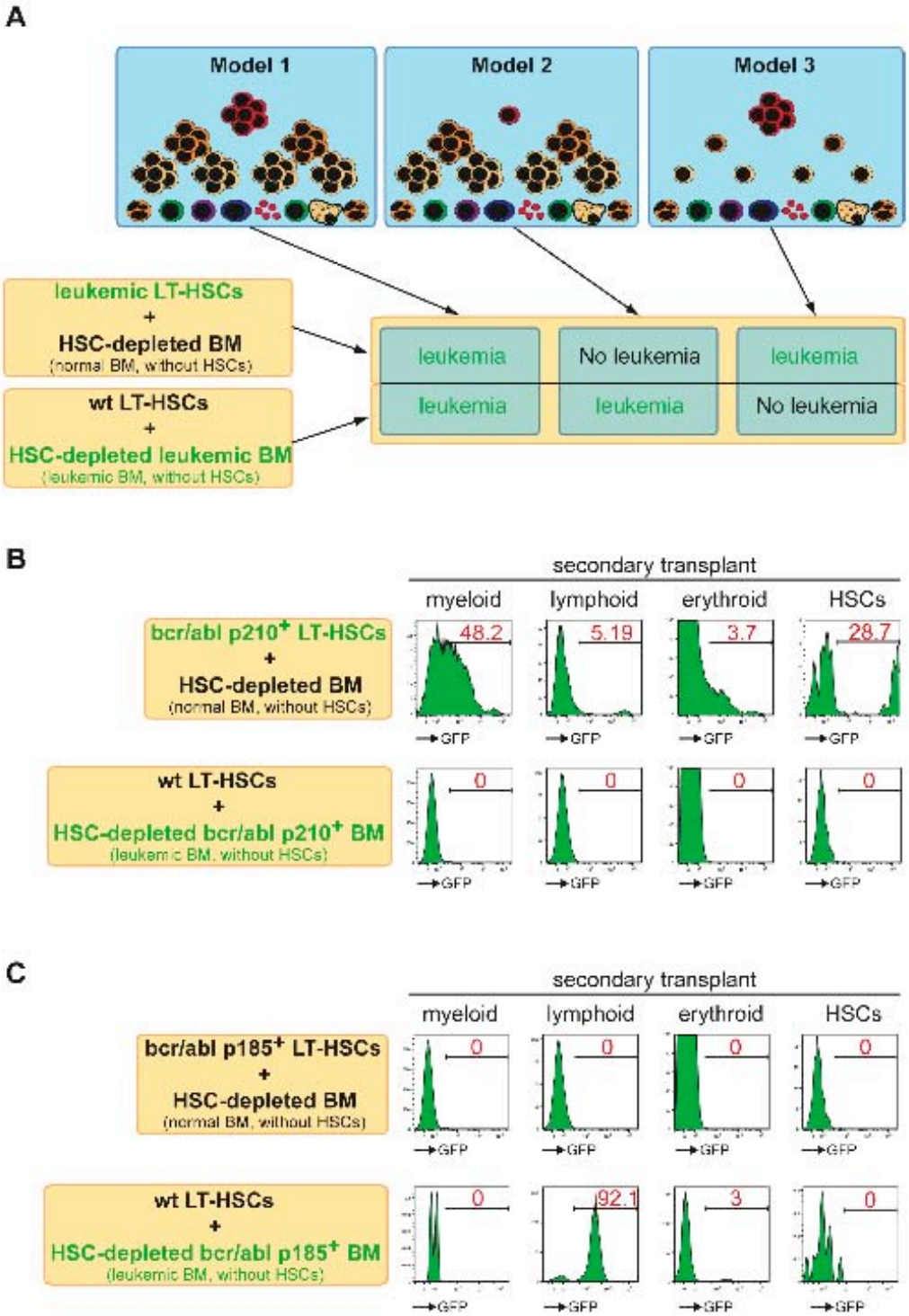
A
Model 1
Model 2
Model 3
leukemic LT-HSCs
+
HSC-depleted BM
(normal BM, without HSCs)
wt LT-HSCs
+
HSC-depleted leukemic BM
(leukemic BM, without HSCs)
leukemia
No leukemia
leukemia
leukemia
leukemia
No leukemia
B
secondary transplant
myeloid
lymphoid
erythroid
HSCs
bcr/abl p210+ LT-HSCs
+
HSC-depleted BM
(normal BM, without HSCs)
48.2
5.19
3.7
28.7
GFP
wt LT-HSCs
+
HSC-depleted bcr/abl p210+ BM
(leukemic BM, without HSCs)
0
C
secondary transplant
myeloid
lymphoid
erythroid
HSCs
bcr/abl p185+ LT-HSCs
+
HSC-depleted BM
(normal BM, without HSCs)
0
GFP
wt LT-HSCs
+
HSC-depleted bcr/abl p185+ BM
(leukemic BM, without HSCs)
92.1
3

Figure 4

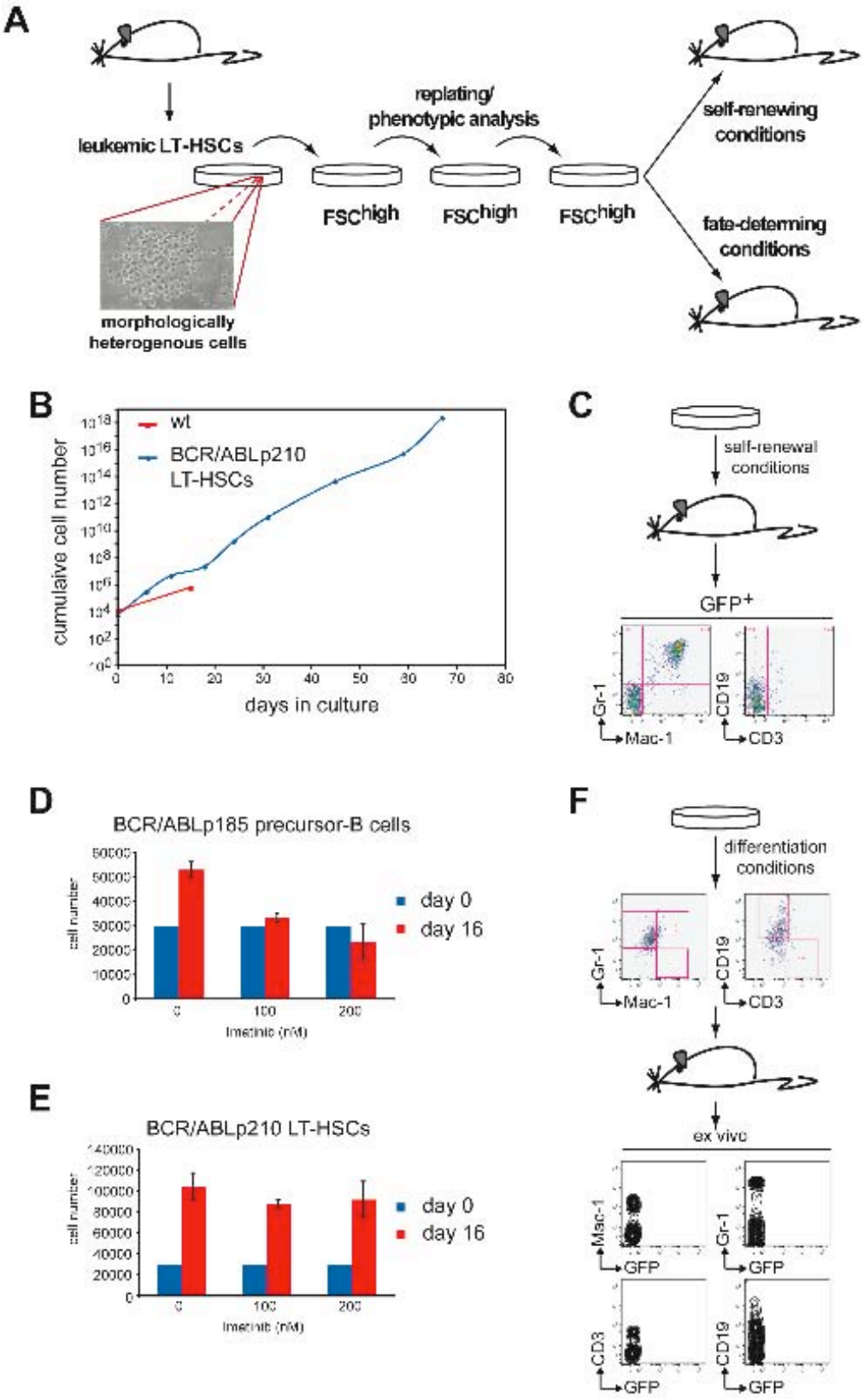
A
leukemic LT-HSCs
replating/
phenotypic analysis
self-renewing
conditions
FSChigh
FSChigh
FSChigh
fate-determing
conditions
morphologically
heterogenous cells
B
wt
BCR/ABLp210
LT-HSCs
cumulative cell number
days in culture
C
self-renewal
conditions
GFP+
Gr-1
Mac-1
CD19
CD3
D
BCR/ABLp185 precursor-B cells
cell number
day 0
day 16
Imatinib (nM)
E
BCR/ABLp210 LT-HSCs
cell number
day 0
day 16
Imatinib (nM)
F
differentiation
conditions
Gr-1
Mac-1
CD19
CD3
ex vivo
Mac-1
Gr-1
CD3
CD19
GFP

Supplementary figure 1

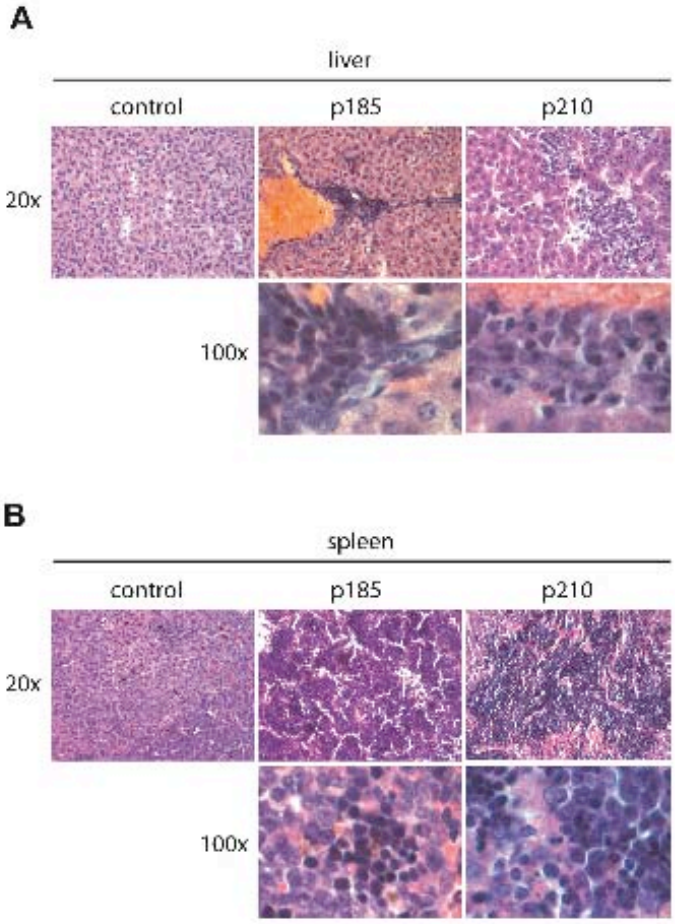

Supplementary figure 2

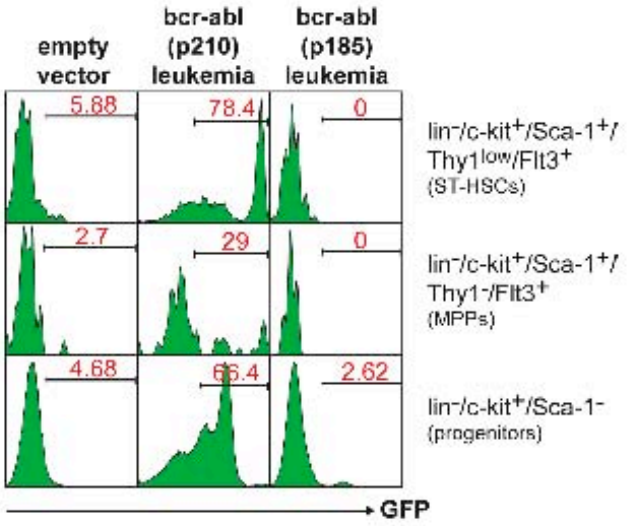

Supplementary figure 3

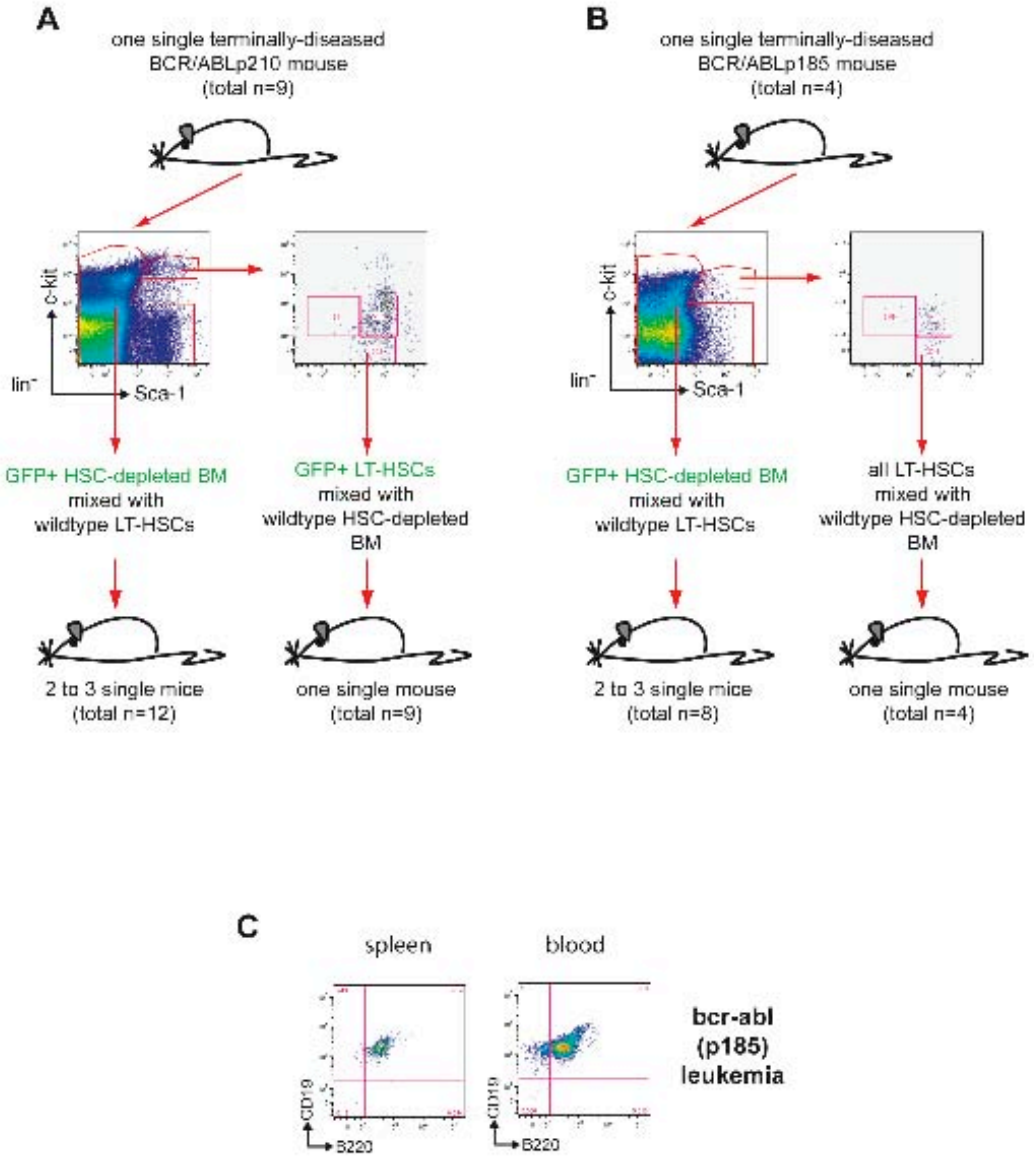

Supplementary figure 4

A

	Lineage / commitment markers						Stem cell markers				
	Gr-1	Mac-1	CD3	CD19	B220	Ter119	CD34	c-kit	Sca-1	Thy1	Flt3
wt HSC	-	-	-	-	-	-	+	+	+	+	+
Bcr-abl LSC	-	-	-	-	-	-	+	+	+	+	+

B

	VE-Cadherin	CD62L	CD62E	Flk-1	CD44	CD162	CD31	Notch-1	Jagged-1	Tie-2
LSC small	-	-	low	+	high	-	+	+	+	low
LSC big	-	-	low	+	-/low	-	+	+	+	low

Supplementary figure legends

Supplementary figure 1 | All mice transplanted with BCR/ABLp210 developed a CML-like disease, whereas all mice bearing BCR/ABLp185 succumbed to a B-ALL.

A and **B**, Hematoxilin/eosine (H&E) staining of livers (**A**) and spleens (**B**) from diseased BCR/ABLp210 and BCR/ABLp185 mice. BCR/ABLp210-induced leukemia is a CML disease defined by predominant infiltration of relatively large myeloid blast cells and monocytes. BCR/ABLp185-induced leukemia is enriched with lymphoid leukemic cells indicated by a stronger hematoxiline stain and less prominent cytoplasma.

Supplementary figure 2 | BCR/ABLp185 diseased mice completely lack leukemic cells in the ST-HSC and MPP-fractions.

FACS-analysis of the BM isolated from control and terminally-diseased mice induced by transplantation of LT-HSCs alone. In contrast to empty vector and BCR/ABLp210 leukemic BM, BCR/ABLp185-diseased BM completely lacks GFP^+ ST-HSCs and MPPs. One representative BM analysis from a control, a BCR/ABLp210 and a BCR/ABLp185-diseased mouse is shown.

Supplementary figure 3 | BCR/ABLp210 and BCR/ABLp185 preserving-CSCs are distinct in frequency and fate.

Scheme of all experiments performed with BCR/ABLp210 (**A**) and BCR/ABLp185 (**B**) preserving-CSCs. Presumable preserving-CSCs (either LT-HSCs or HSC-depleted leukemic pools) were FACS-sorted from every single primary diseased mouse and transplanted into secondary recipient mice The numbers of mice used for secondary transplantation per primary diseased mouse are indicated. Also, the total numbers of mice used per cell fraction are depicted below. C, BCR/ABLp185 leukemia consists of a homogeneous $CD19^+/B220^+/IgM^-$ cell population that infiltrates the spleen and peripheral blood of diseased mice. Representative FACS-plots are shown.

Supplementary figure 4 | BCR/ABLp210 preserving-CSCs keep all properties of stem cells *in vitro*.

A, Summary of FACS analysis of different surface proteins that are expressed in HSCs or in more mature cells. BCR/ABLp210 preserving-CSCs express all markers of HSCs and completely lack mature markers. B, Summary of FACS and confocal fluorescence

microscopy analysis of different surface proteins that are involved in HSC/niche interactions and homing to the bone marrow.

3.1.2 Stat5 is a signaling bottleneck for the maintenance of bcr/abl-positive leukemia

Andrea Hoelbl[1,7], Christian Schuster[1,7], Boris Kovacic[2], Maria A. Hoelzl[1], Sabine Fajmann[1], Florian Grebien[3,6], Wolfgang Warsch[1], Gabriele Stengl[2], Lothar Hennighausen[4], Hartmut Beug[2], Richard Moriggl[5], Veronika Sexl[1].

[1] Institute of Pharmacology, Centre of Biomolecular Medicine and Pharmacology, Medical University of Vienna (MUV), Vienna, 1090, Austria

[2] Research Institute of Molecular Pathology (IMP), Vienna, 1030, Austria

[3] Max F. Perutz Laboratories (MFPL), Medical University of Vienna (MUV), Vienna, 1030, Austria

[4] National Institute of Health (NIH), Bethesda, Maryland, 20892, USA

[5] Ludwig Boltzmann Institute for Cancer Research (LBI-CR), Vienna, 1090, Austria

[6] present address: Research Center for Molecular Medicine of the Austrian Academy of Sciences (CeMM), Lazarettgasse 19, Vienna, 1090, Austria

[7] These authors contributed equally to this work.

Stat5 is a signaling bottleneck for the maintenance of *bcr/abl*-positive leukemia

Andrea Hoelbl[1,7], Christian Schuster[1,7], Boris Kovacic[2], Maria A. Hoelzl[1], Sabine Fajmann[1], Florian Grebien[3,6], Wolfgang Warsch[1], Gabriele Stengl[2], Lothar Hennighausen[4], Hartmut Beug[2], Richard Moriggl[5], Veronika Sexl[1].

[1] Institute of Pharmacology, Centre of Biomolecular Medicine and Pharmacology, Medical University of Vienna (MUV), Vienna, 1090, Austria

[2] Research Institute of Molecular Pathology (IMP), Vienna, 1030, Austria

[3] Max F. Perutz Laboratories (MFPL), Medical University of Vienna (MUV), Vienna, 1030, Austria

[4] National Institute of Health (NIH), Bethesda, Maryland, 20892, USA

[5] Ludwig Boltzmann Institute for Cancer Research (LBI-CR), Vienna, 1090, Austria

[6] present address: Research Center for Molecular Medicine of the Austrian Academy of Sciences (CeMM), Lazarettgasse 19, Vienna, 1090, Austria

Contact information: Veronika Sexl

Email: veronika.sexl@meduniwien.ac.at

Phone: 0043-1-4277-64137

Fax: 0043-1-4277-9641

Running title: leukemia, Bcr/Abl, leukemic stem cells, Stat5

[7] These authors contributed equally to this work.

Summary

Signals initiated by the constitutively active Bcr/Abl oncoprotein reverberate through a complex network involving more than a dozen pathways. The transcription factors Stat5a/b have previously been implicated in the initial *bcr/abl*-induced transformation event. However, to be suitable for a targeted therapy, Stat5 must be required for maintenance of leukemia rather than its initiation. Accordingly, we examined the effects of *Stat5* deletion in either myeloid or lymphoid leukemia. Stat5 deletion was associated with effective elimination of both types of leukemic cells *in vivo* including leukemic stem cells. Lack of Stat5 induces G_0/G_1 cell cycle arrest and apoptosis in imatinib-sensitive and imatinib-resistant cells. Thus Stat5 is indispensable for the survival of a leukemic cell and a candidate alternative target for imatinib-resistant leukemia.

Significance

Deregulation of the Jak/Stat pathway is found in many tumors, including hematopoietic disorders associated with defined genetic alterations leading to the expression of oncoproteins (e.g. Bcr/Abl, Tel-Jak2, Jak2V617F, Flt3-ITD). Among all components of this pathway, in particular Stat5 was postulated a key regulator and prognostic marker. Here we used *bcr/abl*-induced leukemia as a model to validate the suitability of Stat5 as a new candidate for therapy. Given that its abrogation leads to tumor cell death in both, treatment-sensitive and treatment-insensitive leukemic cells - Stat5 is prefigured as a key player in tumor maintenance. Our data therefore qualify Stat5 as a suitable drug target in *bcr/abl*$^+$ leukemia. Importantly, this absolute dependency might expand to other hematopoietic malignancies associated with Stat5 deregulation.

Introduction

Jak (Janus kinase) and Stat (Signal transducer and activator of transcription) molecules are part of a highly conserved signaling pathway involved in cell fate decisions like differentiation, proliferation and apoptosis (Calo et al., 2003; Levy and Darnell, 2002; Murray, 1996). Seven members of the Stat family are known: Stat1, Stat2, Stat3, Stat4, Stat5a, Stat5b and Stat6 with a size ranging from 750 to 900 amino acids. Jak and Stat molecules are expressed in a variety of tissues mediating critical functions of cytokines and other signals (Levy and Darnell, 2002; Moriggl et al., 1999a; Moriggl et al., 1999b; O'Shea et al., 2002; Velazquez et al., 1992). The two closely related proteins Stat5a and Stat5b (here referred to as Stat5) have redundant functions in hematopoietic cells, and non-redundant functions in other tissues (Teglund et al., 1998).

Persistent Stat5 activation is found in various types of cancer: carcinoma of breast, head and neck as well as hematological disorders (Bromberg, 2002; Buettner et al., 2002; Kornfeld et al., 2008; Yu and Jove, 2004), allowing the tumor cells to overcome their dependence on cytokines and growth factors. Prominent examples are myeloid and lymphoid malignancies associated with constitutively active forms of Jak2 (Schwaller et al., 1998; Tefferi and Gilliland, 2005a; Tefferi and Gilliland, 2005b; Tefferi et al., 2005; Ward et al., 2000). In these tumors, the constitutive activation of Jak2 drives the phosphorylation and activation of Stat1, Stat3 and Stat5 (Ho et al., 1999; Schwaller et al., 2000). Moreover, constitutive activation of the Jak/Stat pathway was found in leukemic cells of patients suffering from *bcr/abl*-induced leukemia (Benekli et al., 2003; Bromberg, 2002; Lin et al., 2000; Steelman et al., 2004). *Bcr/abl*-induced leukemia are characterized by a t(9;22)(q34;q11) translocation leading to the expression of a chimeric fusion gene product (Bcr/Abl) representing a constitutively active tyrosine kinase. This translocation is mainly linked to two distinct hematopoietic disorders: acute lymphoid leukemia (ALL) and chronic myelogenous leukemia (CML) (Deininger et al., 2000). There is ample evidence that Stat5 is

activated in *bcr/abl*$^{+}$ cells (Carlesso et al., 1996; Chai et al., 1997; de Groot et al., 1999; Frank and Varticovski, 1996; Ilaria and Van Etten, 1996; Shuai et al., 1996; Spiekermann et al., 2002). Based on experiments using dominant negative mutants of Stat5, an important role for Stat5 in *bcr/abl*-induced survival was proposed (de Groot et al., 1999; Sillaber et al., 2000). The importance of Stat5 for transformation of hematopoitic cells and leukemogenesis is also evident from the fact that transduction of bone marrow (BM) cells with a constitutively active mutant of Stat5 induces multi-lineage leukemia in mice (Moriggl et al., 2005). Similar results were obtained when long-term HSC were retrovirally transduced with constitutively active Stat5 mutants and transplanted. Again, a fatal myeloproliferative disease (MPD) was observed in the recipient mice (Kato et al., 2005). Recent evidence elucidated a diagnostic and prognostic role of Stat5 in human myeloproliferative disorders. Single-cell profiling revealed that aberrant Stat5 activation correlates with advanced stages of disease (Kotecha et al., 2008).

However, initial experiments using mice expressing N-terminally deleted Stat5 (*Stat5*$^{\Delta N/\Delta N}$mice) underestimated the importance of Stat5 in *bcr/abl*-induced diseases since these animals still succumbed to leukemia (Sexl et al., 2000). Recently we clarified that Stat5 is indeed absolutely essential for the initial transformation process mediated by *v-abl* and *bcr/abl*^{p185} oncogenes *in vitro* and *in vivo* using a complete *Stat5* knockout model (*Stat5*^{null}) (Cui et al., 2004; Hoelbl et al., 2006).

Here, we examined whether Stat5 is also required for disease maintenance and qualifies as a potential alternative therapeutic target in leukemia. We show that Stat5 is a bottleneck in the signalling network downstream of Bcr/Abl and is unequivocally required for the maintenance of leukemia.

Results

Bcr/abl^{p210}- induced myeloid transformation requires Stat5

We have previously shown that initial lymphoid transformation by the *bcr/abl*^{p185} oncogene critically depends on Stat5 (Hoelbl et al., 2006). However the influence of Stat5 on chronic myeloid leukemia (CML) – associated with the *bcr/abl*^{p210} translocation form - has still not been unequivocally elucidated. Therefore, we transduced fetal liver (FL) cells derived from *Stat5*$^{+/+}$, *Stat5*$^{null/+}$ and *Stat5*$^{null/null}$ embryos with a retrovirus encoding *bcr/abl*^{p210} and plated the cells in growth factor free methylcellulose (numbers of *bcr/abl*$^{+}$/GFP^{+} cells before plating: 17%, 14.8% and 28,6% respectively). As depicted in **Figure 1** the number of factor-independent *Stat5*$^{null/+}$ colonies was drastically reduced compared to wild-type (wt) (5.4-fold). This reduction was even more evident for *Stat5*$^{null/null}$ FLs expressing *bcr/abl*^{p210}. Here, we hardly observed any outgrowth of colony-like structures (28.6- fold; $p< 0,0001$). These data indicate that Stat5 is required for the transforming capabilities of Bcr/Abl^{p210} in a dosage-dependent manner.

Next, we asked whether Stat5 is also required for the maintenance of leukemia progression. To induce deletion of *Stat5* at any given time point, we crossed *Stat5*$^{fl/fl}$ mice with *Mx1Cre* mice. In these animals the Cre recombinase is induced by type I interferons (IFNs) or p(I:C) treatment. In mice, a CML-like disease is driven by a *bcr/abl*$^{+}$c-kit^{+}Lin^{-} leukemic stem cell (LSC) population that is defined by their ability to carry on disease to a secondary recipient (Krause et al., 2006; Wang and Dick, 2005). B*cr/abl*^{p210} infected *Stat5*$^{fl/fl}$*Mx1Cre* BM was transplanted into lethally irradiated wt (B6129F1) recipient mice. After twelve weeks, first signs of disease evolved and significant numbers of *bcr/abl*$^{+}$/GFP^{+} cells in the peripheral blood were detected (data not shown). The mice were sacrificed and BMs were prepared. As depicted in **Figure 2A,** 13.4 $\pm$ 1.3% of the BM cells were *bcr/abl*$^{+}$/GFP^{+}. Further analysis revealed that this *bcr/abl*$^{+}$/GFP^{+} population consisted of

$Mac1^+Gr1^+$ (28.5 ± 8.9%) and Lin- (25.1 ± 15.3 %) cells being mainly stem/progenitor cells ($Lin^-c\text{-}kit^+Sca\text{-}1^-$; 86.7 ± 20.5%).

BM cells of three diseased animals were pooled and treated *ex vivo* with recombinant IFN-β (1000U/ml) to delete *Stat5* (see scheme depicted in **Figure 2A)**. We initially planned to transplant a pure $Stat5^{\Delta/\Delta}$ population and to monitor CML-like disease progression in the secondary recipient. However, despite several efforts using various concentrations of IFN-β we never obtained a pure $Stat5^{\Delta/\Delta}$ population by treating $bcr/abl^+/GFP^+$ $Stat5^{fl/fl}Mx1Cre$ cells **(Figure 2A middle panel)**. Thus, we reasoned that $Stat5^{\Delta/\Delta}$ cells might have a severe disadvantage *in vitro*. Hence, we decided to transplant an IFN-β treated "mixed" population of $Stat5^{fl/fl}Mx1Cre$ and $Stat5^{\Delta/\Delta}Mx1Cre$ cells to test whether $Stat5^{\Delta/\Delta}$ LSCs are capable to contribute to CML *in vivo* (n=9). The co-transplanted non-deleted LSCs served as internal control for successful transplantation.

Two weeks after the secondary transplant, recipient mice displayed clear signs of disease including decreased mobility and weight loss. All mice had developed leukemia with enlarged spleens and livers and significant numbers of $bcr/abl^+/GFP^+$ cells in the BM (**Figure 2A lower panel**). We found that 45.1 ± 31.5% of BM cells were $bcr/abl^+/GFP^+$. Further analysis revealed that these $bcr/abl^+/GFP^+$ populations were comprised of Lin^- cells (20.5 ± 7.5%) being mainly stem/progenitor cells ($Lin^-c\text{-}kit^+Sca\text{-}1^-$, 91 ± 5.5 %). $Mac1^+Gr1^+$ cells were only detected at low percentages (1.1 ± 1.7%) whereas 7.2 ± 4.1% of cells were $Mac1^+Gr1^-$. These findings indicated an accelerated stage of the disease. However, when we performed genotyping PCR analysis of the leukemic cells derived from BMs, we only detected a PCR product corresponding to the floxed *Stat5* allele. The $Stat5^{\Delta}$ allele was not found in any leukemic sample. Thus, the co-transplanted $Stat5^{\Delta/\Delta}$ LSCs did not contribute to leukemia (**Figure 2A lower panel**).

***Stat5*–heterozygous cells do not induce bcr/abl^+ myeloid leukemia progression**

As shown in Figure 1, *Stat5*-heterozygosity had a profound effect on *bcr/abl*^{p210}-induced myeloid colony formation. This indicates that lowering Stat5 levels already impedes myeloid transformation. To test the effects of reduced Stat5 in *bcr/abl*^{p210}-induced disease *in vivo,* we made use of *Stat5*$^{fl/+}$*Mx1Cre* BM cells. At the beginning of the experiment, these BM cells express *Stat5* from both, the wt and the floxed *Stat5* allele. Equally as described above, we infected these cells with *bcr/abl*^{p210} and transplanted them into primary recipients. When the numbers of *bcr/abl*$^{+}$/GFP^{+} cells in the peripheral blood increased (data not shown), the animals were sacrificed and BMs were prepared (n=3). The *bcr/abl*$^{+}$/GFP^{+} populations consisted of Mac1^{+}/Gr1^{+} (15.4 $\pm$ 11.8%) and Lin^{-} (22.8 ± 4.7%) cells being mainly stem/progenitor cells (Lin^{-}c-kit^{+}Sca-1^{-}; 82.6 $\pm$ 11.7%) (**Figure 2B, upper panel**). BM preparations from three mice were pooled and the floxed *Stat5* allele was deleted via IFN-ß treatment *in vitro*. In this setting a complete deletion of the remaining floxed *Stat5* allele was achieved as verified by PCR analysis (**Figure 2B, middle panel**). The resulting heterozygous *Stat5*$^{\Delta/+}$ population, comprised of leukemic and non-leukemic cells, was then transplanted into secondary, lethally irradiated, recipients (n=9).

Analysis of mice 30 days after transplantation revealed that *bcr/abl*$^{+}$/ GFP^{+} cells were entirely missing in the BM and all other organs investigated including lymph nodes, spleen and liver (**Figure 2B** and data not shown). However, the presence of the *Stat5*$^{\Delta}$ allele was confirmed in the BM of the recipient animals proving successful transplantation and reconstitution by non-leukemic *Stat5*$^{\Delta/+}$ cells (**Figure 2B, lower panel**). Thus, *Stat5* heterozygous cells contribute to hematopoietic reconstitution of lethally irradiated mice but do not allow the outgrowth of *bcr/abl*^{p210}-positive leukemic cells.

Since *Stat5*$^{\Delta/+}$ and *Stat5*$^{\Delta/\Delta}$ *bcr/abl*$^{+}$ cells did not contribute to leukemia, we next asked whether a p(I:C) induced loss or reduction of Stat5 would affect the survival of hematopoietic stem cells (HSCs) and progenitors *in vivo*. Therefore we induced deletion of *Stat5* in adult healthy *Stat5*$^{fl/fl}$*Mx1Cre* (n=3) and *Stat5*$^{fl/+}$*Mx1Cre* (n=3) by p(I:C) treatment. As a control we

included wt *Mx1Cre* mice (n=4). As shown in **Supplementary Figure 1** *Stat5* was effectively and completely deleted in both, progenitors and the HSC population without reducing the numbers of HSCs and progenitors.

Stat5 is required for lymphoid leukemia maintenance *in vivo*

Our experiments with *bcr/abl*^{p210} indicate that Stat5 is not only required for the initial transformation of myeloid cells but also for the maintenance and progression of the disease. However, primary myeloid *bcr/abl*^{p210} transformed cells are not suitable for long-term cultivation *in vitro*. Hence, we used the *v-abl*-induced lymphoid leukemia model to further study the underlying effects of Stat5 loss (Rosenberg and Baltimore, 1976; Rosenberg and Witte, 1988; Siegler and Zajdel, 1972). *V-abl*$^{+}$ lymphoid cell lines can be readily established *in vitro* and are applicable for long-term studies (Hoelbl et al., 2006; Kovacic et al., 2006; Sexl et al., 2000; Zebedin et al., 2008b). Moreover, *bcr/abl*-associated lymphoid disease represents a specific therapeutic challenge since it normally proceeds rapidly and is associated with a high mortality (Piccaluga et al., 2007; Pui and Jeha, 2007).

Stable *Stat5*$^{fl/fl}$*Mx1Cre* and *Stat5*$^{fl/fl}$ *v-abl*$^{+}$ lymphoid cell lines (CD19^{+}, B220^{+}, CD43^{+}) were established and controlled for comparable proliferation rates, clone sizes in methylcellulose, and homing to hematopoietic organs *in vivo* (**Supplementary Figure 2**).

To check whether cell survival of an already established lymphoid leukemia also depends on Stat5, we transplanted *Stat5*$^{fl/fl}$*Mx1Cre* and *Stat5*$^{fl/fl}$ *v-abl*$^{+}$ cell lines into *Rag2*$^{-/-}\gamma c^{-/-}$ mice (n=19 and 7, respectively; 1 x 10^5 cells/mouse). *Rag2*$^{-/-}\gamma c^{-/-}$ mice lack lymphoid cells and are therefore particularly suited to monitor lymphoid leukemia progression. Mice that had received *Stat5*$^{fl/fl}$*Mx1Cre* cells were divided into two groups (see scheme in **Figure 3A**). The first group received p(I:C) to induce type I IFN responses (n=13) to delete *Stat5* in the leukemic cells. The second group was mock-injected with PBS (n=6). To control for effects of p(I:C) mice that had received *Stat5*$^{fl/fl}$ cell lines were also p(I:C) treated (n=7). P(I:C)

treatment was initiated seven days after the transplantation of the cells and repeated every four days until mice displayed signs of sickness. Starting from day 16 post transplantation, animals harboring leukemic cells expressing Stat5 appeared sick with decreased mobility, scrubby hair and weight loss. In contrast, animals harboring *Stat5*$^{\Delta/\Delta}$ leukemic cells appeared healthy with normal mobility, fur and weight. Sick animals sacrificed on day 16 and 20 ("*Stat5*$^{fl/fl}$*Mx1Cre* + PBS" group) were compared to healthy appearing animals where deletion of *Stat5* was induced ("*Stat5*$^{fl/fl}$ + p(I:C)" group). In the diseased animals we found dense infiltrations of leukemic cells B220^{+}CD19^{+} cells in spleens and BMs (**Figure 3B, left panels**). In sharp contrast, leukemic cells were hardly detectable after 16 and 20 days in mice where *Stat5* had been deleted (**Figure 3B, middle and right panels**).

Mice, where *Stat5* had been deleted in the leukemic cells survived significantly longer (**Figure 3C**, mean survival of 49 days compared to 20 and 16 days in the "*Stat5*$^{fl/fl}$ + p(I:C)" and "*Stat5*$^{fl/fl}$*Mx1Cre* untreated" groups, respectively). Similar results were obtained when immuno-competent mice were used as recipient animals (**Supplementary Figure 3**). However, finally all mice succumbed to leukemia. Examination of the leukemic cells revealed protein expression of Stat5 and lack of the *Stat5*$^{\Delta}$ allele (**Figure 3D**). We reasoned that p(I:C) induced deletion was incomplete *in vivo* and that some cells escaped deletion. This scenario is supported by the fact that we still could induce cell cycle arrest and apoptosis in the *ex-vivo* derived leukemic cells by IFN-β treatment (**Figure 3E**). This rules out that the cells have acquired secondary mutations overcoming the Stat5-requirement. We reasoned that an effective cure of the affected animals was exclusively limited by the efficiency of Cre-recombinase-mediated gene deletion.

Stat5 is essential for both, proliferation and survival of *v-abl*-transformed cells

To be able to study the mechanisms how *Stat5* promotes leukemia maintenance *in vitro* we used recombinant IFN-β to activate Cre-mediated Stat5 deletion. A dose of

1000U/ml IFN-β was able to activate Cre-recombinase without blocking cell cycle progression (data not shown). In contrast to IFN-β treated *Stat5*$^{fl/fl}$ cells, the resulting *Stat5*$^{\Delta/\Delta}$ cells showed instantaneous proliferation arrest (**Figure 4A**) and no viable cells were detectable nine days after the initial IFN-β treatment. Genotyping PCR analysis confirmed efficient deletion of *Stat5* (**Figure 4B**). To characterize the effects of *Stat5* deletion, cell cycle profiles and apoptosis stains after IFN-β treatment were performed. As depicted in **Figure 4C** *Stat5*$^{\Delta/\Delta}$ cells underwent a G_0/G_1 cell cycle arrest two days after IFN-β treatment (67.7% $\pm$ 1.7% within G_0/G_1 phase). This cell cycle arrest was followed by apoptosis: nine days after the initiation of the experiment, 90.5% $\pm$ 0.7% of *Stat5*$^{\Delta/\Delta}$ but only 13.1% $\pm$ 2.1% of *Stat5*$^{fl/fl}$ cells treated with IFN-β were propidium iodide (PI)-positive (**Figure 4D**).

The re-expression of wt Stat5 rescues survival and proliferation

To verify that the observed effects are indeed solely provoked by the loss of Stat5 we introduced a retroviral construct encoding Stat5 into yet undeleted *Stat5*$^{fl/fl}$*Mx1Cre* cell lines. (Moriggl et al., 1999b). As depicted in **Figure 5A,** the expression of wt Stat5, but not of the empty vector was capable to prevent cell death after nine days upon deletion of endogenous *Stat5* via IFN-β *in vitro*. PCR analysis confirmed complete deletion of the endogenous *Stat5* alleles. Additionally, we examined two Stat5 variants. Stat5$^{\Delta 749}$ is described to exert dominant negative effects by blocking the DNA-binding site of Stat5 target genes (Moriggl et al., 1996). Stat5^{Y694F} was reported to prevent homodimerization – a prerequisite for nuclear translocation and transcriptional activity of Stat5 (Gouilleux et al., 1994; Stoecklin et al., 1997; Yamashita et al., 1998). Expression of both Stat5 mutants failed to rescue the apoptotic effect of endogenous Stat5 loss after IFN-β treatment (**Figure 5B**). Accordingly, 48 hours after IFN-β treatment, we observed down-regulations of several well-described Stat5 target genes such as *pim-1*, *cyclin D3*, *bcl-$_{XL}$*, *CIS*, *cyclin D2* and *c-myc* (**Figure 5C**) (Castro et al.,

1999; Dumon et al., 1999; Lord et al., 2000; Martino et al., 2001; Matsumoto et al., 1997; Moon et al., 2004; Peltola et al., 2004; Socolovsky et al., 1999; Stout et al., 2004; Yoshimura et al., 1995). To test whether a single target gene compensates for the loss of *Stat5* upon IFN-β administration, we over-expressed either *CIS*, *c-myc*, *cyclin D2*, *cyclin D3* or *bcl-$_{XL}$*. As depicted in **Figure 5D**, expression of neither of these Stat5 target genes was capable to compensate for the loss of Stat5. Therefore, not a single Stat5 target gene, but rather Stat5 as a superordinate molecule, maintains the leukemic capacity of *bcr/abl*$^{+}$ cells.

High Bcl_2 levels or deletion of Trp53 do not relieve Stat5-dependance

Tumor cells frequently acquire additional mutations after long term maintenance in culture. We therefore analyzed our *Stat5$^{fl/fl}$ Mx1Cre* cell lines after 14 months of continuous culture whether any spontaneously acquired mutation would be capable to release the necessity for Stat5. When we analyzed the cell lines for expressions of Trp53, Bcl_{XL} and Bcl_2, we found that two cell lines (#1 and #3) had completely lost the Trp53 protein (**Figure 6A**). Loss of Trp53 was reported to result in a decreased sensitivity towards imatinib (Wendel et al., 2006). Accordingly these cell lines displayed a 5.7-fold lesser sensitivity towards imatinib treatment (IC_{50} of 0.98 μM compared to IC_{50}=0.17 μM; data not shown). Cell line #1 additionally displayed a significant up-regulation of the Bcl_2 protein and a significant decrease in Stat5 protein expression. Bcl_2 is an anti-apoptotic protein, whose over-expression is found in many cancers contributing to tumor initiation, progression and resistance to therapies (Danial and Korsmeyer, 2004; Letai et al., 2004; Oltersdorf et al., 2005). However, when the residual Stat5 protein was removed by activation of Cre-recombinase, all cell lines still underwent complete apoptosis. Hence, even in the presence of elevated Bcl_2 protein the presence of Stat5 was indispensable for proliferation and survival of leukemic cells. This is in line with our observations that over-expression of Bcl_2 in *Stat5$^{fl/fl}$Mx1Cre* cell lines and subsequent deletion of endogenous Stat5 does not release Stat5 dependence. (**Figure 5D**).

Expression of an imatinib-resistant *bcr/abl* mutant (*bcr/abl*^{p210T315I}) does not relieve Stat5 dependance

Treatment of *bcr/abl*-induced CML has been significantly improved by the availability of imatinib (Druker et al., 2001a; Druker et al., 2001b). However, some patients acquire mutations in the Bcr/Abl oncoprotein which renders them insensitive to imatinib (Chu et al., 2005; Griswold et al., 2006). In this regard the *bcr/abl*^{p210T315I} mutation represents one of the biggest therapeutic challenges in CML therapy since it mediates complete resistance not only to imatinib but also to all of the next generation Abl kinase inhibitors (Quintas-Cardama et al., 2007; Skaggs et al., 2006). We therefore decided to test whether cells expressing *bcr/abl*^{p210T315I} require the presence of Stat5. *Stat5*$^{fl/fl}$*Mx1Cre* and *Stat5*$^{+/+}$*Mx1Cre* BM cells were infected with retrovirus encoding *bcr/abl*^{p210T315I} and treated either with imatinib or IFN-β-mediated *Stat5* deletion.

To ensure survival and proliferation of immature progenitors, cells were maintained in a medium supplemented with SCF, Flt3-ligand (Flt3-L), IgF-1, IL-3, IL-6 GM-SCF and dexamethasone as described previously (Kieslinger et al., 2000). As expected wt *Mx1Cre* and *Stat5*$^{fl/fl}$*Mx1Cre* cells expressing *bcr/abl*^{p210T315I} did not undergo apoptosis upon imatinib treatment (**Figure 6B**, **middle panels**). In contrast, *bcr/abl*^{p210T315I} expressing *Stat5*$^{fl/fl}$*Mx1Cre* cells showed substantial cell death upon loss of Stat5 after five days (**Figure 6B**, **right panels**).

Discussion

A major issue in cancer biology is to differentiate between initiating events and events that are required for cancer progression. While substantial progress has been made in understanding the evolution of solid tumors, the evolution of leukemic cells is less well understood (Albertson et al., 2003; Klein and Klein, 1985; Lengauer et al., 1998; Nowell, 1976; Visvader and Lindeman, 2008). In this regard, B*cr/abl*-induced leukemia is a good model system because the initiating event is a well-defined chromosomal translocation (Ren, 2005; Wong and Witte, 2001). Previously, we showed that Stat5 is required for the initiation of lymphoid leukemia (Hoelbl et al., 2006). In this manuscript we provide formal proof for an essential role of Stat5 in the maintenance of *bcr/abl*$^{+}$ leukemia. Deletion of *Stat5* in leukemic cells resulted in G_0/G_1 cell cycle arrest followed by apoptosis. To the best of our knowledge this is the first report where an indispensable and non-redundant function of a signaling component downstream of the Bcr/Abl tyrosine kinase is described to be necessary for leukemia progression *in vivo*. Several signaling pathways are activated downstream of the Bcr/Abl oncoprotein and are implied to contribute to leukemogenesis, e.g. the activation of the Phosphatidylinositol 3-kinase (PI3K) pathway or the mitogen-activated protein (MAP) kinase pathway (Cortez et al., 1997; Deininger et al., 2000; Ren, 2005; Wong and Witte, 2004; Zebedin et al., 2008a).

In this complex signaling network, controlled by Bcr/Abl, Stat5 appears to have a unique and privileged position: in fact, our experiments verify that Stat5 is the bottleneck for both, *bcr/abl*-induced disease initiation and progression. The unique role of Stat5 is conserved even in the absence of intact Trp53 signaling, as well as in imatinib-resistant cells and most importantly extends to the leukemic stem cell (LSC) compartment.

These findings single out Stat5 from other members of the family of Stat transcription factors that have been implicated in signaling downstream of Bcr/Abl. Stat3 is also involved in the initial transformation process which is severely impaired in the absence of Stat3.

However, Stat3 is dispensable for leukemia progression (V. Sexl, unpublished observations). Importantly, the requirement for Stat5 extends to the LSC compartment. LSCs have been characterized in myeloid *bcr/abl*^{p210}-induced leukemia by their ability to allow for serial transplantation of the disease (Krause et al., 2006; Wang and Dick, 2005). One of the big current therapeutic challenges is to find strategies how to target and eradicate such LSCs. The most frequently used drug in CML therapy - imatinib - induces apoptosis in *bcr/abl*$^{+}$ cells but fails to eradicate LSCs *in vivo* (Krause and Van Etten, 2007; Neering et al., 2007). Therefore, patients must be subjected to continuous treatment to keep them in remission. This situation fosters Darwinian evolution and the emergence of resistant clones. In this context, it is worth pointing out that even one of the most dreaded imatinib-resistant mutants of Bcr/Abl - Bcr/Abl^{p210T315I} – remains strictly dependent on Stat5. Taken together, these observations support the concept that targeting Stat5 provides new therapeutic opportunities. This conjecture is further supported by the observation that the mere lowering of Stat5 levels in *bcr/abl*$^{p210+}$ *Stat5*$^{fl/+}$*Mx1Cre* cells by IFN-β treatment was sufficient to prevent leukemia progression in secondary recipient animals - again pointing at the role of Stat5 in LSCs. In these animals, the non-leukemic *Stat5*$^{\Delta/+}$ cells contributed to normal hematopoiesis. This indicates that a reduced Stat5 protein level may be well tolerated in normal tissue but is deleterious for the *bcr/abl*$^{+}$ cell population. It also indicates that partial blockage of Stat5 may be tolerated, despite its described role in HSC functionality and hematopoiesis (Wierenga et al., 2008). While it is difficult to extrapolate these experiments in mice to patients, at the very least these observations justify the assumption that potential side effects of Stat5 blockage will not *a priori* preclude their use in clinics. This conjecture is further supported by the development of an inhibitor targeting Jak2. Jak2 is essential for erythropoiesis - but nevertheless, Jak2 inhibitors have successfully entered clinical trials (Hexner et al., 2008; Lasho et al., 2008; Wernig et al., 2008).

For the past decade, signal interceptor-based therapies have been the most promising new strategies in the treatment of cancer. Stat5 fulfills two important criteria as a drug target for a signal interceptor: (i) Stat5 is a valid target in *bcr/abl*-induced leukemia because it is essential for the disease; (ii) blockage of Stat5 can be anticipated to result in limited and tolerable side effects. (iii) Stat5 occupies a privileged position in the Bcr/Abl signaling network. This is also evident from microarray data showing that Stat5 target genes are prominently down-regulated in response to the Bcr/Abl kinase inhibitor dasatinib (O. Hantschel, paper in press).

However, we found that none of the downstream targets of Stat5 are capable of compensating for Stat5 loss in leukemic cells when over-expressed. Similarly, our observations are consistent with the interpretation that the function of Stat5 cannot be readily bypassed: down-regulation of Stat5 significantly impaired the expression of target genes that can also be addressed via alternative routes in the Bcr/Abl-controlled network: e.g. D-type cyclins or c-myc via the MAPK/ERK cascade (Marampon et al., 2006; Okabe et al., 2006; Serra et al., 2008; Vadiveloo et al., 1998). These findings again highlight that Stat5 is the Achilles' heel of the *bcr/abl*- transformed cell. Importantly, we observed that even the genetic instability associated with the abrogation of the Trp53 did not allow for the emergence of Stat5-independent leukemic clones.

Last but not least, we found that the requirement for Stat5 for cell survival was not relieved by forced expression of Bcl_2 or Bcl_{XL}. This data were confirmed by a spontaneous mutation occurring in one cell line that displayed high protein levels of Bcl_2. This cell line still underwent apoptosis upon *Stat5* abrogation.

Apart from regulating transcription, Tyr^{694}-phosphorylated Stat5 has recently been shown to function as a scaffold for Gab2/PI3K thereby promoting PI3K signaling (Nyga et al., 2005). Copious amounts of Stat5 are present in the cytoplasma of CML cells (Harir et al.,

2007). It is therefore attractive to speculate that this mechanism might also contribute to the effects of Stat5 within the Bcr/Abl signaling network.

Taken together our observations argue for a privileged position of Stat5 in the signaling network controlled by Bcr/Abl. Stat5 appears to be the bottleneck through which signals must be funneled in an obligatory and non-.redundant way.

Experimental procedures

Mice and genotyping

Stat5$^{fl/fl}$*Mx1Cre*, *Stat5*$^{fl/fl}$, *C57BL/6J* and *Rag2*$^{-/-}$*γc*$^{-/-}$ mice were maintained at the Biomedical Research Institute (Medical University of Vienna), C57BL/6J x Sv129 F1 (here referred to as B6129F1), at the Institute of Molecular Pathology (IMP, Vienna) under specifically pathogen-free sterile conditions. Genotyping of mice and cells was performed as described previously (Cui et al., 2004). All animal experiments were carried out in accordance with protocols approved by Austrian law.

BM transplants of *bcr/abl*^{p210} infected cells

BM cells from 6 weeks old *Stat5*$^{fl/fl}$*Mx1Cre* and *Stat5*$^{f/+}$*Mx1Cre* donor mice were co-cultivated on *bcr/abl*^{p210} retroviral producer cells for 48 hours in the presence of IL-3 (25 ng/ml), IL-6 (50 ng/ml), SCF (50 ng/ml) and 7 µg/ml polybrene. Then, cells were transplanted via tail vein injection into lethally irradiated (10 Gy) B6129F1 recipient mice. Peripheral blood was taken every week and upon detection of *bcr/abl*$^{+}$/GFP^{+} cells, mice were sacrificed. BM cells of three diseased animals were pooled and treated with recombinant IFN-ß (1000U/ml; Serotech) for 48 hours to delete *Stat5*. Thereafter cells were transplanted into lethally irradiated secondary recipients (B6129F1).

Deletion of Stat5 in leukemic cell lines

For *in vivo* deletion of *Stat5*, 1 x 10^5 or 1 x 10^6 *v-abl*$^{+}$ *Stat5*$^{fl/fl}$ and *Stat5*$^{fl/fl}$*Mx1Cre cells* were injected via the tail vein into *Rag2*$^{-/-}$*γc*$^{-/-}$ or C57BL/6J mice, respectively. From day seven on, mice received 400µg p(I:C) (Sigma) intraperitoneally (i.p.) every four days to induce *Stat5* deletion in the transplanted leukemic cells. Mice, injected with PBS served as controls. Upon signs of sickness (decreased mobility, weight loss and scrubby fur), mice were sacrificed and lymphatic organs were analyzed for leukemic cell (CD19^{+}, B220^{+}) infiltration by flow cytometry.

For *in vitro* deletion of *Stat5*, *Stat5*$^{fl/fl}$*MxCre v-abl*$^{+}$ cell lines were seeded at a density of 3 x 10^5 cells/ml and incubated for 48 hours in 1000U/ml recombinant (IFN-ß; Serotech) in complete RPMI. *Stat5*$^{fl/fl}$ cell lines treated with IFN-ß and *Stat5*$^{fl/fl}$*MxCre* without any treatment served as controls. Cells were analyzed by flow cytometric analysis for cell cycle progression and apoptosis every day.

Flow cytometry

For analysis of leukemic cell lines or *ex-vivo* derived cells, single cell suspensions were pre-incubated with αCD16/CD32 antibodies to prevent non-specific Fc-receptor-mediated binding. Subsequently, 5 x 10^5 cells were stained with monoclonal antibodies conjugated with fluorescent markers and analyzed by a FACSCantoII flow cytometer using FACSDiva software (Becton-Dickinson). The following antibodies, all purchased from BD Biosciences, were used: B220 (RA3-6B2), CD19 (1D3), CD43 (1B11), Mac-1 (M1/70), GR-1 (RB6-8C5), mouse-lineage panel and Sca-1 (D7). C-kit (2B8) was purchased from eBioscience.

Cell cycle and apoptosis analysis: 1 x 10^6 cells were stained with PI (50 µg/ml) in a hypotonic lysis solution (0.1% sodium citrate, 0.1% triton X-100, 100 µg/ml RNAse) and incubated at 37°C for 30 minutes. Analysis of dead/ late apoptotic cells was performed by re-suspending in PBS containing PI (1µg/ml).

Acknowledgments

We are deeply indebted to M. Freissmuth, M. Busslinger, P. Valent, O. Hantschel, G. Superti-Furga and T. Decker for continuous discussion and scientific input. We also thank M. Mayerhofer for providing the Bcr/Abl ^{p210T315I} mutant. This work was made possible by financial support from the Austrian Research fund (FWF-SFB-28), the Vienna Science and Technology Fund (WWTF-LS07-037) and the GEN-AU-program DRAGON.

References

Albertson, D. G., Collins, C., McCormick, F., and Gray, J. W. (2003). Chromosome aberrations in solid tumors. Nat Genet *34*, 369-376.

Benekli, M., Baer, M. R., Baumann, H., and Wetzler, M. (2003). Signal transducer and activator of transcription proteins in leukemias. Blood *101*, 2940-2954.

Bromberg, J. (2002). Stat proteins and oncogenesis. J Clin Invest *109*, 1139-1142.
Buettner, R., Mora, L. B., and Jove, R. (2002). Activated STAT signaling in human tumors provides novel molecular targets for therapeutic intervention. Clin Cancer Res *8*, 945-954.

Calo, V., Migliavacca, M., Bazan, V., Macaluso, M., Buscemi, M., Gebbia, N., and Russo, A. (2003). STAT proteins: from normal control of cellular events to tumorigenesis. J Cell Physiol *197*, 157-168.

Carlesso, N., Frank, D. A., and Griffin, J. D. (1996). Tyrosyl phosphorylation and DNA binding activity of signal transducers and activators of transcription (STAT) proteins in hematopoietic cell lines transformed by Bcr/Abl. J Exp Med *183*, 811-820.

Castro, A., Sengupta, T. K., Ruiz, D. C., Yang, E., and Ivashkiv, L. B. (1999). IL-4 selectively inhibits IL-2-triggered Stat5 activation, but not proliferation, in human T cells. J Immunol *162*, 1261-1269.

Chai, S. K., Nichols, G. L., and Rothman, P. (1997). Constitutive activation of JAKs and STATs in BCR-Abl-expressing cell lines and peripheral blood cells derived from leukemic patients. J Immunol *159*, 4720-4728.

Chu, S., Xu, H., Shah, N. P., Snyder, D. S., Forman, S. J., Sawyers, C. L., and Bhatia, R. (2005). Detection of BCR-ABL kinase mutations in CD34+ cells from chronic myelogenous leukemia patients in complete cytogenetic remission on imatinib mesylate treatment. Blood *105*, 2093-2098.

Cortez, D., Reuther, G., and Pendergast, A. M. (1997). The Bcr-Abl tyrosine kinase activates mitogenic signaling pathways and stimulates G1-to-S phase transition in hematopoietic cells. Oncogene *15*, 2333-2342.

Cui, Y., Riedlinger, G., Miyoshi, K., Tang, W., Li, C., Deng, C. X., Robinson, G. W., and Hennighausen, L. (2004). Inactivation of Stat5 in mouse mammary epithelium during pregnancy reveals distinct functions in cell proliferation, survival, and differentiation. Mol Cell Biol *24*, 8037-8047.

Danial, N. N., and Korsmeyer, S. J. (2004). Cell death: critical control points. Cell *116*, 205-219.

de Groot, R. P., Raaijmakers, J. A., Lammers, J. W., Jove, R., and Koenderman, L. (1999). STAT5 activation by BCR-Abl contributes to transformation of K562 leukemia cells. Blood *94*, 1108-1112.

Deininger, M. W., Goldman, J. M., and Melo, J. V. (2000). The molecular biology of chronic myeloid leukemia. Blood *96*, 3343-3356.

Druker, B. J., Sawyers, C. L., Kantarjian, H., Resta, D. J., Reese, S. F., Ford, J. M., Capdeville, R., and Talpaz, M. (2001a). Activity of a specific inhibitor of the BCR-ABL tyrosine kinase in the blast crisis of chronic myeloid leukemia and acute lymphoblastic leukemia with the Philadelphia chromosome. N Engl J Med *344*, 1038-1042.

Druker, B. J., Talpaz, M., Resta, D. J., Peng, B., Buchdunger, E., Ford, J. M., Lydon, N. B., Kantarjian, H., Capdeville, R., Ohno-Jones, S., and Sawyers, C. L. (2001b). Efficacy and safety of a specific inhibitor of the BCR-ABL tyrosine kinase in chronic myeloid leukemia. N Engl J Med *344*, 1031-1037.

Dumon, S., Santos, S. C., Debierre-Grockiego, F., Gouilleux-Gruart, V., Cocault, L., Boucheron, C., Mollat, P., Gisselbrecht, S., and Gouilleux, F. (1999). IL-3 dependent regulation of Bcl-xL gene expression by STAT5 in a bone marrow derived cell line. Oncogene *18*, 4191-4199.

Frank, D. A., and Varticovski, L. (1996). BCR/abl leads to the constitutive activation of Stat proteins, and shares an epitope with tyrosine phosphorylated Stats. Leukemia *10*, 1724-1730.
Gouilleux, F., Wakao, H., Mundt, M., and Groner, B. (1994). Prolactin induces phosphorylation of Tyr694 of Stat5 (MGF), a prerequisite for DNA binding and induction of transcription. EMBO J *13*, 4361-4369.

Griswold, I. J., MacPartlin, M., Bumm, T., Goss, V. L., O'Hare, T., Lee, K. A., Corbin, A. S., Stoffregen, E. P., Smith, C., Johnson, K.*, et al.* (2006). Kinase domain mutants of Bcr-Abl exhibit altered transformation potency, kinase activity, and substrate utilization, irrespective of sensitivity to imatinib. Mol Cell Biol *26*, 6082-6093.

Harir, N., Pecquet, C., Kerenyi, M., Sonneck, K., Kovacic, B., Nyga, R., Brevet, M., Dhennin, I., Gouilleux-Gruart, V., Beug, H.*, et al.* (2007). Constitutive activation of Stat5 promotes its cytoplasmic localization and association with PI3-kinase in myeloid leukemias. Blood *109*, 1678-1686.

Hexner, E. O., Serdikoff, C., Jan, M., Swider, C. R., Robinson, C., Yang, S., Angeles, T., Emerson, S. G., Carroll, M., Ruggeri, B., and Dobrzanski, P. (2008). Lestaurtinib (CEP701) is a JAK2 inhibitor that suppresses JAK2/STAT5 signaling and the proliferation of primary erythroid cells from patients with myeloproliferative disorders. Blood *111*, 5663-5671.

Ho, J. M., Beattie, B. K., Squire, J. A., Frank, D. A., and Barber, D. L. (1999). Fusion of the ets transcription factor TEL to Jak2 results in constitutive Jak-Stat signaling. Blood *93*, 4354-4364.

Hoelbl, A., Kovacic, B., Kerenyi, M. A., Simma, O., Warsch, W., Cui, Y., Beug, H., Hennighausen, L., Moriggl, R., and Sexl, V. (2006). Clarifying the role of Stat5 in lymphoid development and Abelson-induced transformation. Blood *107*, 4898-4906.

Ilaria, R. L., Jr., and Van Etten, R. A. (1996). P210 and P190(BCR/ABL) induce the tyrosine phosphorylation and DNA binding activity of multiple specific STAT family members. J Biol Chem *271*, 31704-31710.

Kato, Y., Iwama, A., Tadokoro, Y., Shimoda, K., Minoguchi, M., Akira, S., Tanaka, M., Miyajima, A., Kitamura, T., and Nakauchi, H. (2005). Selective activation of STAT5 unveils

its role in stem cell self-renewal in normal and leukemic hematopoiesis. J Exp Med *202*, 169-179.

Kieslinger, M., Woldman, I., Moriggl, R., Hofmann, J., Marine, J. C., Ihle, J. N., Beug, H., and Decker, T. (2000). Antiapoptotic activity of Stat5 required during terminal stages of myeloid differentiation. Genes Dev *14*, 232-244.

Klein, G., and Klein, E. (1985). Evolution of tumours and the impact of molecular oncology. Nature *315*, 190-195.

Kornfeld, J. W., Grebien, F., Kerenyi, M. A., Friedbichler, K., Kovacic, B., Zankl, B., Hoelbl, A., Nivarti, H., Beug, H., Sexl, V.*, et al.* (2008). The different functions of Stat5 and chromatin alteration through Stat5 proteins. Front Biosci *13*, 6237-6254.

Kotecha, N., Flores, N. J., Irish, J. M., Simonds, E. F., Sakai, D. S., Archambeault, S., Diaz-Flores, E., Coram, M., Shannon, K. M., Nolan, G. P., and Loh, M. L. (2008). Single-cell profiling identifies aberrant STAT5 activation in myeloid malignancies with specific clinical and biologic correlates. Cancer Cell *14*, 335-343.

Kovacic, B., Stoiber, D., Moriggl, R., Weisz, E., Ott, R. G., Kreibich, R., Levy, D. E., Beug, H., Freissmuth, M., and Sexl, V. (2006). STAT1 acts as a tumor promoter for leukemia development. Cancer Cell *10*, 77-87.

Krause, D. S., Lazarides, K., von Andrian, U. H., and Van Etten, R. A. (2006). Requirement for CD44 in homing and engraftment of BCR-ABL-expressing leukemic stem cells. Nat Med *12*, 1175-1180.

Krause, D. S., and Van Etten, R. A. (2007). Right on target: eradicating leukemic stem cells. Trends Mol Med *13*, 470-481.

Lasho, T. L., Tefferi, A., Hood, J. D., Verstovsek, S., Gilliland, D. G., and Pardanani, A. (2008). TG101348, a JAK2-selective antagonist, inhibits primary hematopoietic cells derived from myeloproliferative disorder patients with JAK2V617F, MPLW515K or JAK2 exon 12 mutations as well as mutation negative patients. Leukemia *22*, 1790-1792.

Lengauer, C., Kinzler, K. W., and Vogelstein, B. (1998). Genetic instabilities in human cancers. Nature *396*, 643-649.

Letai, A., Sorcinelli, M. D., Beard, C., and Korsmeyer, S. J. (2004). Antiapoptotic BCL-2 is required for maintenance of a model leukemia. Cancer Cell *6*, 241-249.

Levy, D. E., and Darnell, J. E., Jr. (2002). Stats: transcriptional control and biological impact. Nat Rev Mol Cell Biol *3*, 651-662.

Lin, T. S., Mahajan, S., and Frank, D. A. (2000). STAT signaling in the pathogenesis and treatment of leukemias. Oncogene *19*, 2496-2504.

Lord, J. D., McIntosh, B. C., Greenberg, P. D., and Nelson, B. H. (2000). The IL-2 receptor promotes lymphocyte proliferation and induction of the c-myc, bcl-2, and bcl-x genes through the trans-activation domain of Stat5. J Immunol *164*, 2533-2541.

Marampon, F., Ciccarelli, C., and Zani, B. M. (2006). Down-regulation of c-Myc following MEK/ERK inhibition halts the expression of malignant phenotype in rhabdomyosarcoma and in non muscle-derived human tumors. Mol Cancer *5*, 31.

Martino, A., Holmes, J. H. t., Lord, J. D., Moon, J. J., and Nelson, B. H. (2001). Stat5 and Sp1 regulate transcription of the cyclin D2 gene in response to IL-2. J Immunol *166*, 1723-1729.

Matsumoto, A., Masuhara, M., Mitsui, K., Yokouchi, M., Ohtsubo, M., Misawa, H., Miyajima, A., and Yoshimura, A. (1997). CIS, a cytokine inducible SH2 protein, is a target of the JAK-STAT5 pathway and modulates STAT5 activation. Blood *89*, 3148-3154.

Moon, J. J., Rubio, E. D., Martino, A., Krumm, A., and Nelson, B. H. (2004). A permissive role for phosphatidylinositol 3-kinase in the Stat5-mediated expression of cyclin D2 by the interleukin-2 receptor. J Biol Chem *279*, 5520-5527.

Moriggl, R., Gouilleux-Gruart, V., Jahne, R., Berchtold, S., Gartmann, C., Liu, X., Hennighausen, L., Sotiropoulos, A., Groner, B., and Gouilleux, F. (1996). Deletion of the carboxyl-terminal transactivation domain of MGF-Stat5 results in sustained DNA binding and a dominant negative phenotype. Mol Cell Biol *16*, 5691-5700.

Moriggl, R., Sexl, V., Kenner, L., Duntsch, C., Stangl, K., Gingras, S., Hoffmeyer, A., Bauer, A., Piekorz, R., Wang, D.*, et al.* (2005). Stat5 tetramer formation is associated with leukemogenesis. Cancer Cell *7*, 87-99.

Moriggl, R., Sexl, V., Piekorz, R., Topham, D., and Ihle, J. N. (1999a). Stat5 activation is uniquely associated with cytokine signaling in peripheral T cells. Immunity *11*, 225-230.

Moriggl, R., Topham, D. J., Teglund, S., Sexl, V., McKay, C., Wang, D., Hoffmeyer, A., van Deursen, J., Sangster, M. Y., Bunting, K. D.*, et al.* (1999b). Stat5 is required for IL-2-induced cell cycle progression of peripheral T cells. Immunity *10*, 249-259.

Murray, R. (1996). Physiologic roles of interleukin-2, interleukin-4, and interleukin-7. Curr Opin Hematol *3*, 230-234.

Neering, S. J., Bushnell, T., Sozer, S., Ashton, J., Rossi, R. M., Wang, P. Y., Bell, D. R., Heinrich, D., Bottaro, A., and Jordan, C. T. (2007). Leukemia stem cells in a genetically defined murine model of blast-crisis CML. Blood *110*, 2578-2585.

Nowell, P. C. (1976). The clonal evolution of tumor cell populations. Science *194*, 23-28.

Nyga, R., Pecquet, C., Harir, N., Gu, H., Dhennin-Duthille, I., Regnier, A., Gouilleux-Gruart, V., Lassoued, K., and Gouilleux, F. (2005). Activated STAT5 proteins induce activation of the PI 3-kinase/Akt and Ras/MAPK pathways via the Gab2 scaffolding adapter. Biochem J *390*, 359-366.

O'Shea, J. J., Gadina, M., and Schreiber, R. D. (2002). Cytokine signaling in 2002: new surprises in the Jak/Stat pathway. Cell *109 Suppl*, S121-131.

Okabe, H., Lee, S. H., Phuchareon, J., Albertson, D. G., McCormick, F., and Tetsu, O. (2006). A critical role for FBXW8 and MAPK in cyclin D1 degradation and cancer cell proliferation. PLoS ONE *1*, e128.

Oltersdorf, T., Elmore, S. W., Shoemaker, A. R., Armstrong, R. C., Augeri, D. J., Belli, B. A., Bruncko, M., Deckwerth, T. L., Dinges, J., Hajduk, P. J.*, et al.* (2005). An inhibitor of Bcl-2 family proteins induces regression of solid tumours. Nature *435*, 677-681.

Peltola, K. J., Paukku, K., Aho, T. L., Ruuska, M., Silvennoinen, O., and Koskinen, P. J. (2004). Pim-1 kinase inhibits STAT5-dependent transcription via its interactions with SOCS1 and SOCS3. Blood *103*, 3744-3750.

Piccaluga, P. P., Paolini, S., and Martinelli, G. (2007). Tyrosine kinase inhibitors for the treatment of Philadelphia chromosome-positive adult acute lymphoblastic leukemia. Cancer *110*, 1178-1186.

Pui, C. H., and Jeha, S. (2007). New therapeutic strategies for the treatment of acute lymphoblastic leukaemia. Nat Rev Drug Discov *6*, 149-165.

Quintas-Cardama, A., Kantarjian, H., and Cortes, J. (2007). Flying under the radar: the new wave of BCR-ABL inhibitors. Nat Rev Drug Discov *6*, 834-848.

Ren, R. (2005). Mechanisms of BCR-ABL in the pathogenesis of chronic myelogenous leukaemia. Nat Rev Cancer *5*, 172-183.

Rosenberg, N., and Baltimore, D. (1976). A quantitative assay for transformation of bone marrow cells by Abelson murine leukemia virus. J Exp Med *143*, 1453-1463.

Rosenberg, N., and Witte, O. N. (1988). The viral and cellular forms of the Abelson (abl) oncogene. Adv Virus Res *35*, 39-81.

Schwaller, J., Frantsve, J., Aster, J., Williams, I. R., Tomasson, M. H., Ross, T. S., Peeters, P., Van Rompaey, L., Van Etten, R. A., Ilaria, R., Jr.*, et al.* (1998). Transformation of hematopoietic cell lines to growth-factor independence and induction of a fatal myelo- and lymphoproliferative disease in mice by retrovirally transduced TEL/JAK2 fusion genes. Embo J *17*, 5321-5333.

Schwaller, J., Parganas, E., Wang, D., Cain, D., Aster, J. C., Williams, I. R., Lee, C. K., Gerthner, R., Kitamura, T., Frantsve, J.*, et al.* (2000). Stat5 is essential for the myelo- and lymphoproliferative disease induced by TEL/JAK2. Mol Cell *6*, 693-704.

Serra, J. M., Gutierrez, A., Alemany, R., Navarro, M., Ros, T., Saus, C., Gines, J., Sampol, A., Amat, J. C., Serra-Moises, L.*, et al.* (2008). Inhibition of c-Myc down-regulation by sustained extracellular signal-regulated kinase activation prevents the antimetabolite methotrexate- and gemcitabine-induced differentiation in non-small-cell lung cancer cells. Mol Pharmacol *73*, 1679-1687.

Sexl, V., Piekorz, R., Moriggl, R., Rohrer, J., Brown, M. P., Bunting, K. D., Rothammer, K., Roussel, M. F., and Ihle, J. N. (2000). Stat5a/b contribute to interleukin 7-induced B-cell precursor expansion, but abl- and bcr/abl-induced transformation are independent of stat5. Blood *96*, 2277-2283.

Shuai, K., Halpern, J., ten Hoeve, J., Rao, X., and Sawyers, C. L. (1996). Constitutive activation of STAT5 by the BCR-ABL oncogene in chronic myelogenous leukemia. Oncogene *13*, 247-254.

Siegler, R., and Zajdel, S. (1972). Pathogenesis of Abelson-virus-induced murine leukemia. J Natl Cancer Inst *48*, 189-218.

Sillaber, C., Gesbert, F., Frank, D. A., Sattler, M., and Griffin, J. D. (2000). STAT5 activation contributes to growth and viability in Bcr/Abl-transformed cells. Blood *95*, 2118-2125.

Skaggs, B. J., Gorre, M. E., Ryvkin, A., Burgess, M. R., Xie, Y., Han, Y., Komisopoulou, E., Brown, L. M., Loo, J. A., Landaw, E. M.*, et al.* (2006). Phosphorylation of the ATP-binding loop directs oncogenicity of drug-resistant BCR-ABL mutants. Proc Natl Acad Sci U S A *103*, 19466-19471.

Socolovsky, M., Fallon, A. E., Wang, S., Brugnara, C., and Lodish, H. F. (1999). Fetal anemia and apoptosis of red cell progenitors in Stat5a-/-5b-/- mice: a direct role for Stat5 in Bcl-X(L) induction. Cell *98*, 181-191.

Spiekermann, K., Pau, M., Schwab, R., Schmieja, K., Franzrahe, S., and Hiddemann, W. (2002). Constitutive activation of STAT3 and STAT5 is induced by leukemic fusion proteins with protein tyrosine kinase activity and is sufficient for transformation of hematopoietic precursor cells. Exp Hematol *30*, 262-271.

Steelman, L. S., Pohnert, S. C., Shelton, J. G., Franklin, R. A., Bertrand, F. E., and McCubrey, J. A. (2004). JAK/STAT, Raf/MEK/ERK, PI3K/Akt and BCR-ABL in cell cycle progression and leukemogenesis. Leukemia *18*, 189-218.

Stoecklin, E., Wissler, M., Moriggl, R., and Groner, B. (1997). Specific DNA binding of Stat5, but not of glucocorticoid receptor, is required for their functional cooperation in the regulation of gene transcription. Mol Cell Biol *17*, 6708-6716.

Stout, B. A., Bates, M. E., Liu, L. Y., Farrington, N. N., and Bertics, P. J. (2004). IL-5 and granulocyte-macrophage colony-stimulating factor activate STAT3 and STAT5 and promote Pim-1 and cyclin D3 protein expression in human eosinophils. J Immunol *173*, 6409-6417.

Tefferi, A., and Gilliland, D. G. (2005a). JAK2 in myeloproliferative disorders is not just another kinase. Cell Cycle *4*, 1053-1056.

Tefferi, A., and Gilliland, D. G. (2005b). The JAK2V617F tyrosine kinase mutation in myeloproliferative disorders: status report and immediate implications for disease classification and diagnosis. Mayo Clin Proc *80*, 947-958.

Tefferi, A., Lasho, T. L., and Gilliland, G. (2005). JAK2 mutations in myeloproliferative disorders. N Engl J Med *353*, 1416-1417; author reply 1416-1417.

Teglund, S., McKay, C., Schuetz, E., van Deursen, J. M., Stravopodis, D., Wang, D., Brown, M., Bodner, S., Grosveld, G., and Ihle, J. N. (1998). Stat5a and Stat5b proteins have essential and nonessential, or redundant, roles in cytokine responses. Cell *93*, 841-850.

Vadiveloo, P. K., Vairo, G., Royston, A. K., Novak, U., and Hamilton, J. A. (1998). Proliferation-independent induction of macrophage cyclin D2, and repression of cyclin D1, by lipopolysaccharide. J Biol Chem *273*, 23104-23109.

Velazquez, L., Fellous, M., Stark, G. R., and Pellegrini, S. (1992). A protein tyrosine kinase in the interferon alpha/beta signaling pathway. Cell *70*, 313-322.

Visvader, J. E., and Lindeman, G. J. (2008). Cancer stem cells in solid tumours: accumulating evidence and unresolved questions. Nat Rev Cancer *8*, 755-768.

Wang, J. C., and Dick, J. E. (2005). Cancer stem cells: lessons from leukemia. Trends Cell Biol *15*, 494-501.

Ward, A. C., Touw, I., and Yoshimura, A. (2000). The Jak-Stat pathway in normal and perturbed hematopoiesis. Blood *95*, 19-29.

Wendel, H. G., de Stanchina, E., Cepero, E., Ray, S., Emig, M., Fridman, J. S., Veach, D. R., Bornmann, W. G., Clarkson, B., McCombie, W. R.*, et al.* (2006). Loss of p53 impedes the antileukemic response to BCR-ABL inhibition. Proc Natl Acad Sci U S A *103*, 7444-7449.

Wernig, G., Kharas, M. G., Okabe, R., Moore, S. A., Leeman, D. S., Cullen, D. E., Gozo, M., McDowell, E. P., Levine, R. L., Doukas, J.*, et al.* (2008). Efficacy of TG101348, a selective JAK2 inhibitor, in treatment of a murine model of JAK2V617F-induced polycythemia vera. Cancer Cell *13*, 311-320.

Wierenga, A. T., Vellenga, E., and Schuringa, J. J. (2008). Maximal STAT5-induced proliferation and self-renewal at intermediate STAT5 activity levels. Mol Cell Biol *28*, 6668-6680.

Wong, S., and Witte, O. N. (2001). Modeling Philadelphia chromosome positive leukemias. Oncogene *20*, 5644-5659.

Wong, S., and Witte, O. N. (2004). The BCR-ABL story: bench to bedside and back. Annu Rev Immunol *22*, 247-306.

Yamashita, H., Xu, J., Erwin, R. A., Farrar, W. L., Kirken, R. A., and Rui, H. (1998). Differential control of the phosphorylation state of proline-juxtaposed serine residues Ser725 of Stat5a and Ser730 of Stat5b in prolactin-sensitive cells. J Biol Chem *273*, 30218-30224.

Yoshimura, A., Ohkubo, T., Kiguchi, T., Jenkins, N. A., Gilbert, D. J., Copeland, N. G., Hara, T., and Miyajima, A. (1995). A novel cytokine-inducible gene CIS encodes an SH2-containing protein that binds to tyrosine-phosphorylated interleukin 3 and erythropoietin receptors. EMBO J *14*, 2816-2826.

Yu, H., and Jove, R. (2004). The STATs of cancer--new molecular targets come of age. Nat Rev Cancer *4*, 97-105.

Zebedin, E., Freissmuth, M., and Sexl, V. (2008a). Signal interception-based therapies--a double-edged sword in Bcr/abl-induced malignancies? Leuk Lymphoma *49*, 620-624.

Zebedin, E., Simma, O., Schuster, C., Putz, E. M., Fajmann, S., Warsch, W., Eckelhart, E., Stoiber, D., Weisz, E., Schmid, J. A.*, et al.* (2008b). Leukemic challenge unmasks a requirement for PI3Kdelta in NK cell-mediated tumor surveillance. Blood *112*, 4655-4664.

Figure legends

Figure 1. *bcr/abl*^{p210}-induced transformation depends on Stat5 *in vitro*.

Bcr/abl^{p210}- induced colony formation of *Stat5*$^{+/+}$, *Stat5*$^{null/+}$ and *Stat5*$^{null/null}$ FL cells in growth-factor free methylcellulose (n=3 for each genotype). One representative set of data is depicted. Data are summarized in a bar graph (right panel).

Figure 2. *bcr/abl*^{p210}-induced disease progression depends on Stat5 *in vivo*.

Stat5$^{fl/fl}$*Mx1Cre* **(A)** or *Stat5*$^{fl/+}$*Mx1Cre* **(B)** were used as donor mice. As depicted in schemes (left panel each) BM cells were infected with *bcr/abl*^{p210}and transplanted into lethally irradiated recipient mice ("1st tp"). After 12 weeks, BM cells were isolated, pooled (n=3), treated with IFN-ß for 48h *in vitro* to induce deletion of the *Stat5* alleles and injected into secondary lethally irradiated recipients ("2nd tp"; n=9 per genotype). Middle panels in (A) and (B) show PCR analysis of BMs at indicated steps of the experiments. Right panels in (A) and (B) depict flow cytometric analysis of BMs cells after 1st tp and 2nd tp as indicated. **(A)** PCR analysis revealed that only leukemic cells harbouring the floxed (*fl*), but no deleted (*Δ*) *Stat5* alleles contributed to leukemia. (**B)** No *bcr/abl*$^{+}$/GFP^{+} cells were detected in BM cells of secondary recipients. PCR analysis of the non-leukemic BM verified successful transplantation (two representative samples are shown). One representative flow cytometric profile of BM cells is depicted for each experimental group. Numbers indicate percentages of cells belonging to individual sub-populations.

Figure 3. Lymphoid leukemia progression depends on Stat5 *in vivo*.

(A) *V-abl*$^{+}$ *Stat5*$^{fl/fl}$*Mx1Cre* cells were injected into *Rag2*$^{-/-}$*γc*$^{-/-}$ mice and divided in two groups: one receiving p(I:C)- the other receiving PBS-injections (control).

(B) BM and spleen of p(I:C) - treated and control mice were analyzed at indicated time points for the presence of transplanted leukemic B-cells (B220^{+}CD19^{+}). Representative flow cytometric profiles are depicted.

(C) Transplantation of *Stat5*$^{fl/fl}$*Mx1*Cre and *Stat5*$^{fl/fl}$ cell lines into *Rag2*$^{-/-}$*γc*$^{-/-}$ mice. 1 x 10^5 cells of *Stat5*$^{fl/fl}$*Mx1*Cre or *Stat5*$^{fl/fl}$ cell lines (n=3 each) were injected via tail vein. From day 7 on, 400µg p(I:C) was injected i.p. every 4 days till the mice diseased. Kaplan-Maier plots revealed a statistically significant difference in survival time of mice after *Stat5* deletion compared to the control groups ("*Stat5*$^{fl/fl}$*Mx1Cre* + p(I:C)" vs. "*Stat5*$^{fl/fl}$*Mx1Cre* untreated" p<0.001; "*Stat5*$^{fl/fl}$*Mx1Cre* untreated" vs. *Stat5*$^{fl/fl}$ + p(I:C)" n.s.). Vertical bars indicate mice opened as controls on day 16 and 20 (see (B)).

(D) Analysis of *ex vivo* derived BM cells from mice of the "*Stat5*$^{fl/fl}$*Mx1Cre* + p(I:C" group sacrificed on day 56 (#1-3) and 57 (#4). Western Blot for Stat5 (upper panel) and corresponding genotyping PCR analysis (lower panel). Four representative samples are shown.

(E) *Ex-vivo* derived cells are still sensitive to the loss of *Stat5*. 0.5 x 10^5 *ex-vivo*-derived *Stat5*$^{fl/fl}$*Mx1Cre* cells (n=3) were incubated with 1000U/ml IFN-ß. Cell concentrations were determined per trypane-blue exclusion on indicated time points.

Figure 4. Leukemic cell survival depends on Stat5 *in vitro*.

(A) 0.5x10^5 cells of indicated cell lines (n=3 each) were treated with 1000U IFN-β or mock treated. Cell concentrations were determined by trypane-blue exclusion assay on indicated time points.

(B) PCR analysis after IFN-β treatment: Deletion efficiency was determined by specific PCR reaction for the floxed (*fl*) and deleted (*Δ*) *Stat5* alleles 48 hours after IFN-ß treatment.

Cell cycle **(C)** and apoptosis **(D)** analysis of IFN-β treated *v-abl* transformed cell lines, 48hours and 9 days after IFN-β treatment, respectively. Loss of Stat5 induces cell cycle arrest and apoptosis. Numbers show percentages of cells in indicated cell cycle phases (C) or in late apoptosis (D) of one representative sample for each genotype.

Figure 5. Stat5 re-expression rescues effects of Stat5 deficiency

Stat5$^{fl/fl}$*Mx1Cre* cell lines were infected with retroviruses encoding either empty vector, wt Stat5 **(A)**, Stat5Y694F and Stat5Δ749 **(B)** or indicated Stat5 target genes **(D)**. **(A)** Percentages of late apoptotic/dead cells, were determined nine days after IFN-β administration by PI staining. PCR analysis revealed complete deletion of Stat5-re-expressing cells. Numbers indicate percentages of PI^+ cells.

(C) 48 hours after IFN-β administration, expression levels of Stat5 target genes were analyzed by real-time PCR and compared to levels measured in equally treated *Stat5*$^{fl/fl}$ cells. Down-regulations of indicated target genes are summarized in bar graphs. Data represent means ± SD. Asteriks indicate statistical significance as determined by a one-sample T-test (two-tailed; *** $p<0.001$).

(B, D) Endogenous *Stat5* was deleted via IFN-β and outgrowth of GFP^+ cells was monitored by flow cytometry every 48 hours for eight subsequent days.

Figure 6. Leukemic cells harbouring second hits are still sensitive to Stat5 loss.

(A) Long term cultured (14 months) *Stat5*$^{fl/fl}$*Mx1Cre v-abl*$^+$ cell lines were examined by Western blot analysis for Stat5, Trp53, Bcl_2 and Bcl_{XL} protein expressions. Two cell lines either over-expressing Bcl-2 and/or lacking Trp53 (# 1, #3) were subjected to *Stat5* deletion via IFN-β. Cell cycle progression was analyzed by PI staining and FACS analysis after 48 hours. Percentages of apoptotic cells were determined via PI staining nine days after IFN-β administration. Numbers show percentages of cells in indicated cell cycle phases (middle panel) or in late apoptosis (right panel).

(B) BMs of wt *Mx1Cre* and *Stat5*$^{fl/fl}$*Mx1Cre* mice were infected with an imatinib-resistant *bcr/abl*^{p210} mutant (*bcr/abl*^{p210T315I}) and treated with either imatinib (0.1μM) or IFN-β. After 5 days cells of the IFN-ß-treated, but not of the imatinib-treated group, showed increased numbers of apoptotic (sub-G_1) cells. Numbers show percentages of cells in indicated cell cycle phases.

FIGURE 1

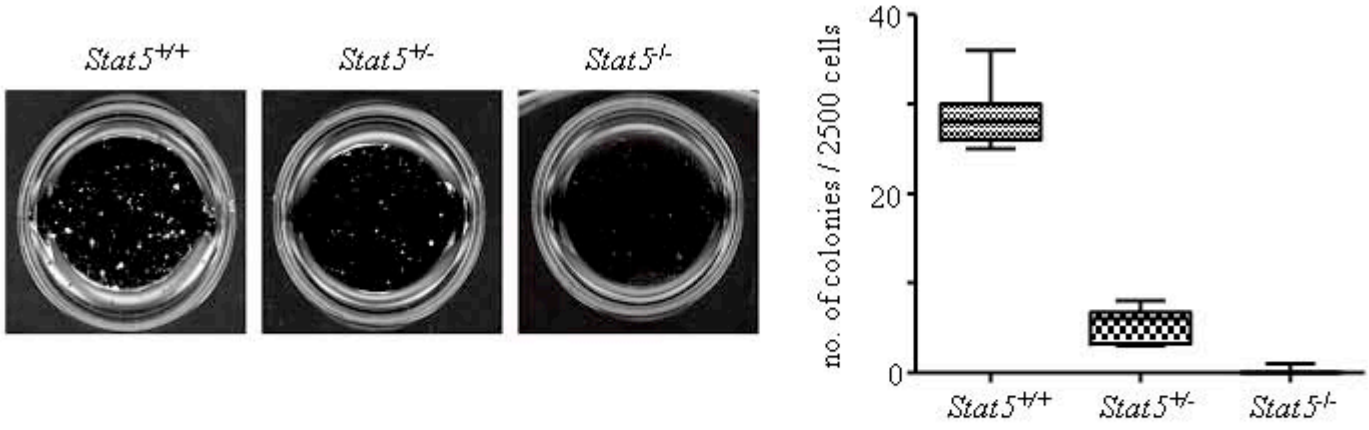
Stat5+/+
Stat5+/-
Stat5-/-
40
20
0
no. of colonies / 2500 cells
Stat5+/+
Stat5+/-
Stat5-/-

FIGURE 2

A

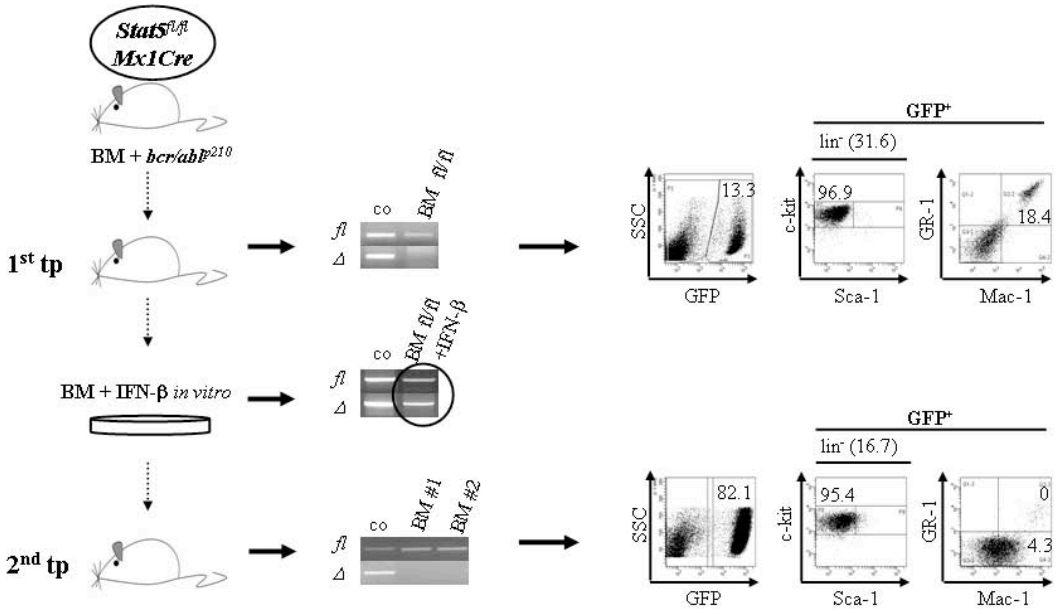
Stat5fl/fl
Mx1Cre
BM + bcr/ablp210
1st tp
BM + IFN-β in vitro
2nd tp
co
BM fl/fl
BM fl/fl +IFN-β
BM #1
BM #2
fl
Δ
GFP+
lin- (31.6)
13.3
96.9
18.4
SSC
GFP
c-kit
Sca-1
GR-1
Mac-1
lin- (16.7)
82.1
95.4
0
4.3

FIGURE 2

B

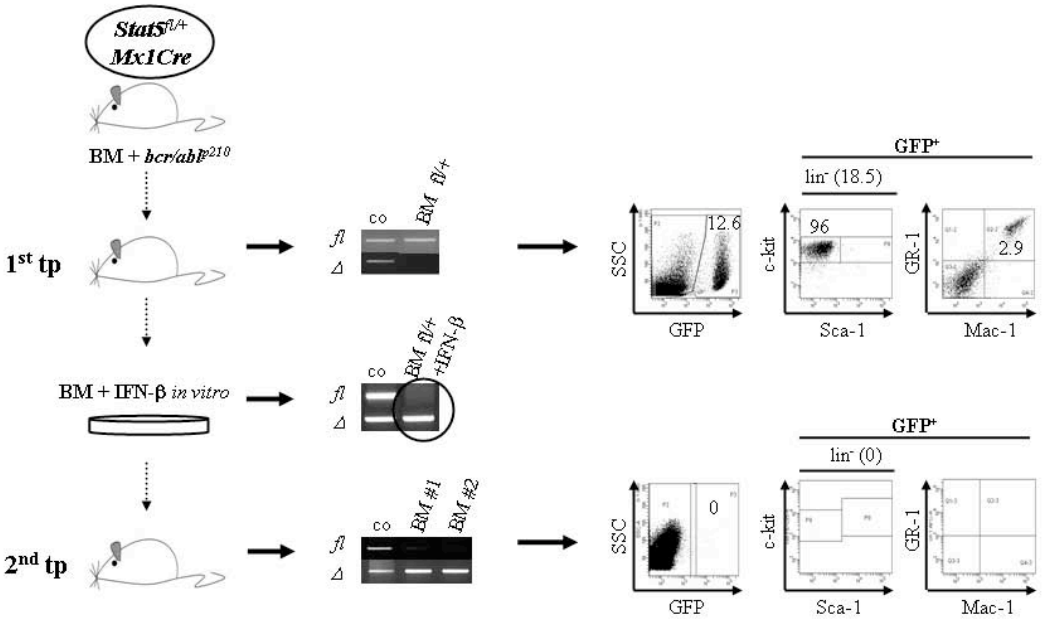
Stat5fl/+
Mx1Cre
BM + bcr/ablp210
1st tp
BM + IFN-β in vitro
2nd tp
co
BM fl/+
+IFN-β
BM #1
BM #2
fl
Δ
GFP+
lin- (18.5)
12.6
96
2.9
SSC
GFP
c-kit
Sca-1
GR-1
Mac-1
lin- (0)
0

FIGURE 3

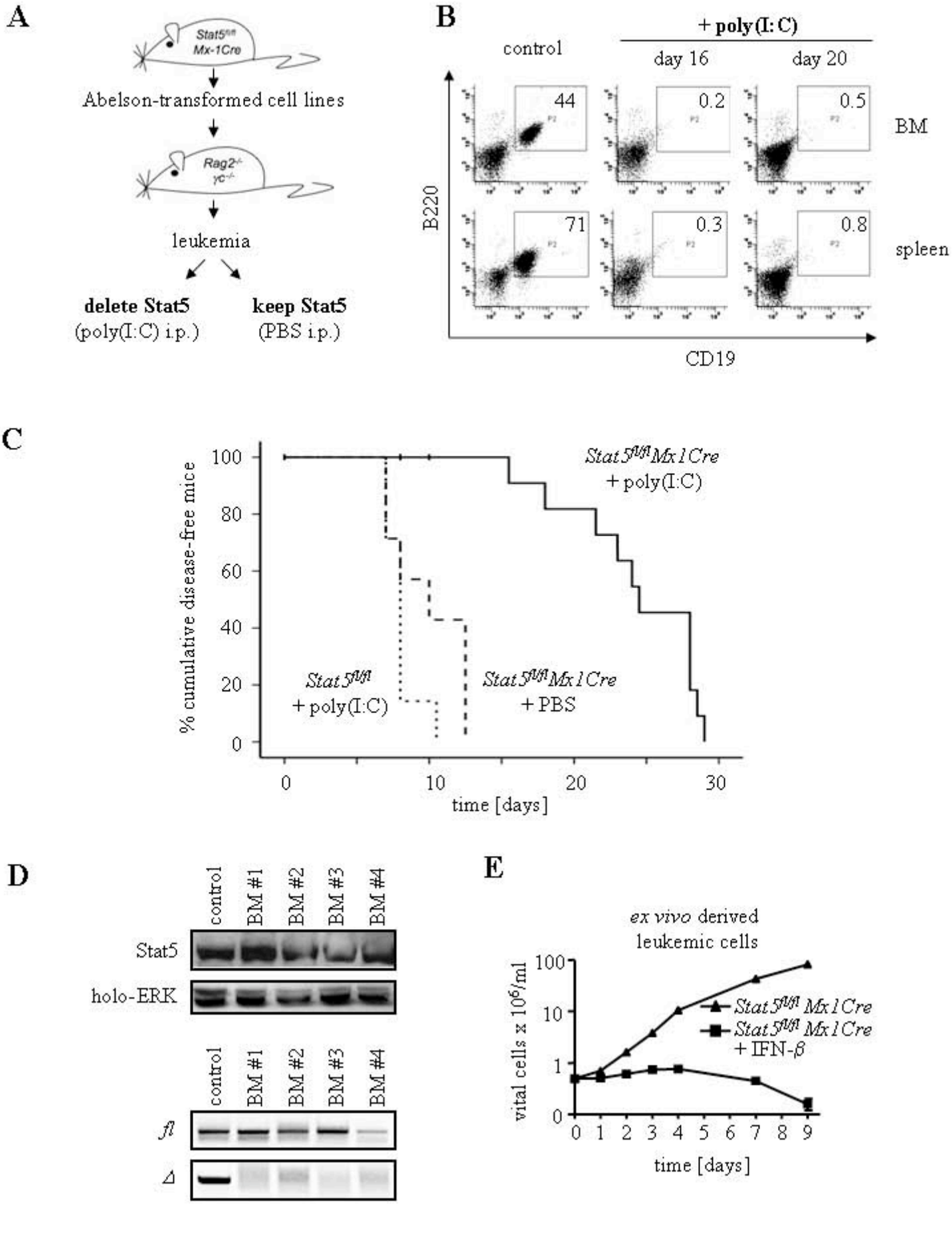
A
Stat5fl/fl Mx-1Cre
Abelson-transformed cell lines
Rag2-/- γc-/-
leukemia
delete Stat5
(poly(I:C) i.p.)
keep Stat5
(PBS i.p.)
B
control
+ poly(I:C)
day 16
day 20
44
0.2
0.5
BM
71
0.3
0.8
spleen
B220
CD19
C
% cumulative disease-free mice
100
80
60
40
20
0
Stat5fl/fl Mx1Cre
+ poly(I:C)
Stat5fl/fl
+ poly(I:C)
Stat5fl/fl Mx1Cre
+ PBS
0
10
20
30
time [days]
D
control
BM #1
BM #2
BM #3
BM #4
Stat5
holo-ERK
fl
Δ
E
ex vivo derived
leukemic cells
vital cells x 10^6/ml
100
10
1
0
Stat5fl/fl Mx1Cre
Stat5fl/fl Mx1Cre
+ IFN-β
0 1 2 3 4 5 6 7 8 9
time [days]

FIGURE 4

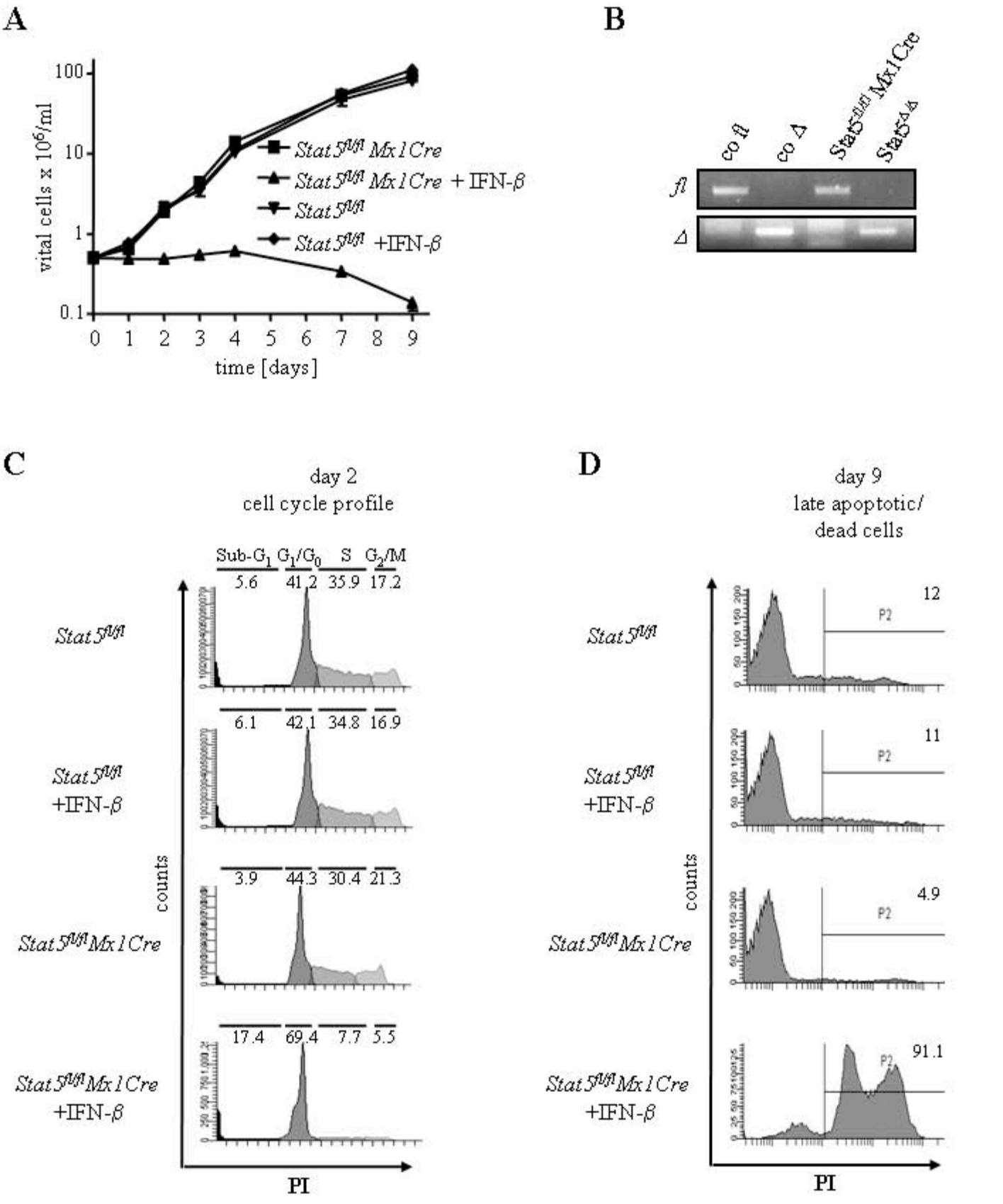
A
vital cells x 10^6/ml
100
10
1
0.1
0 1 2 3 4 5 6 7 8 9
time [days]
Stat5fl/fl Mx1Cre
Stat5fl/fl Mx1Cre + IFN-β
Stat5fl/fl
Stat5fl/fl +IFN-β
B
co fl
co Δ
Stat5fl/fl Mx1Cre
Stat5Δ/Δ
fl
Δ
C
day 2
cell cycle profile
Sub-G1 G1/G0 S G2/M
5.6 41.2 35.9 17.2
6.1 42.1 34.8 16.9
3.9 44.3 30.4 21.3
17.4 69.4 7.7 5.5
Stat5fl/fl
Stat5fl/fl +IFN-β
Stat5fl/fl Mx1Cre
Stat5fl/fl Mx1Cre +IFN-β
counts
PI
D
day 9
late apoptotic/
dead cells
12
11
4.9
91.1
P2
Stat5fl/fl
Stat5fl/fl +IFN-β
Stat5fl/fl Mx1Cre
Stat5fl/fl Mx1Cre +IFN-β
counts
PI

FIGURE 5

A

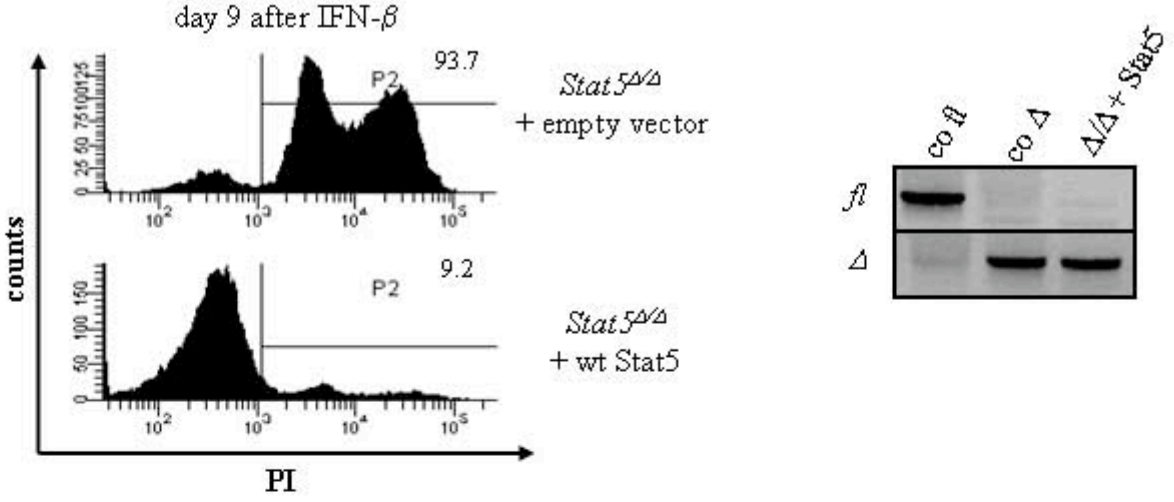

B

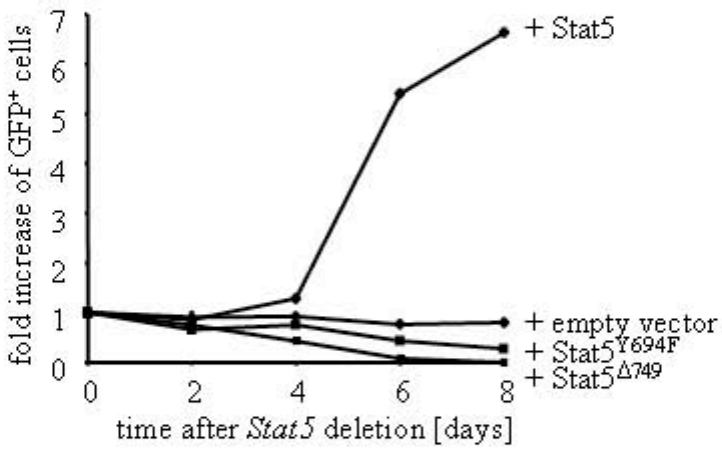

C

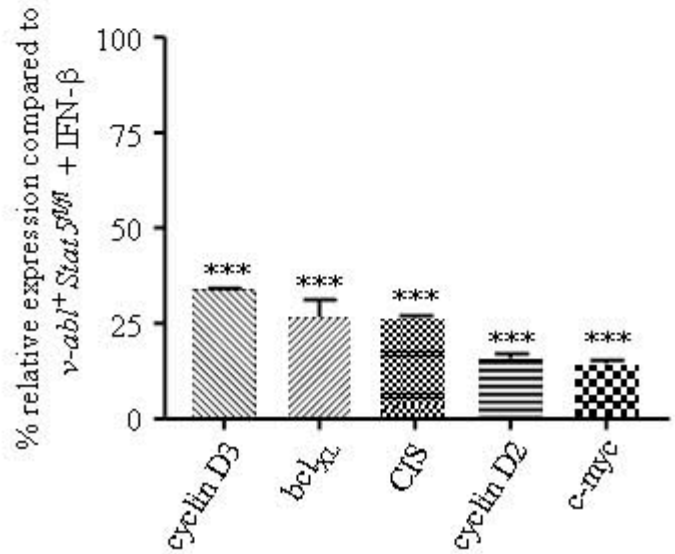

D

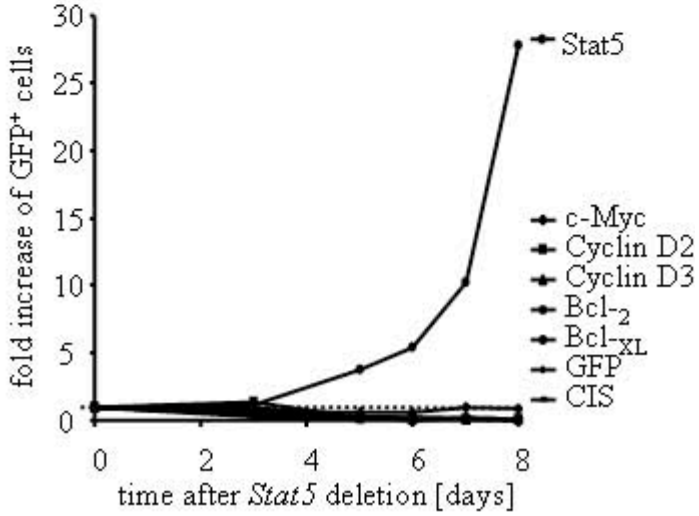

FIGURE 6

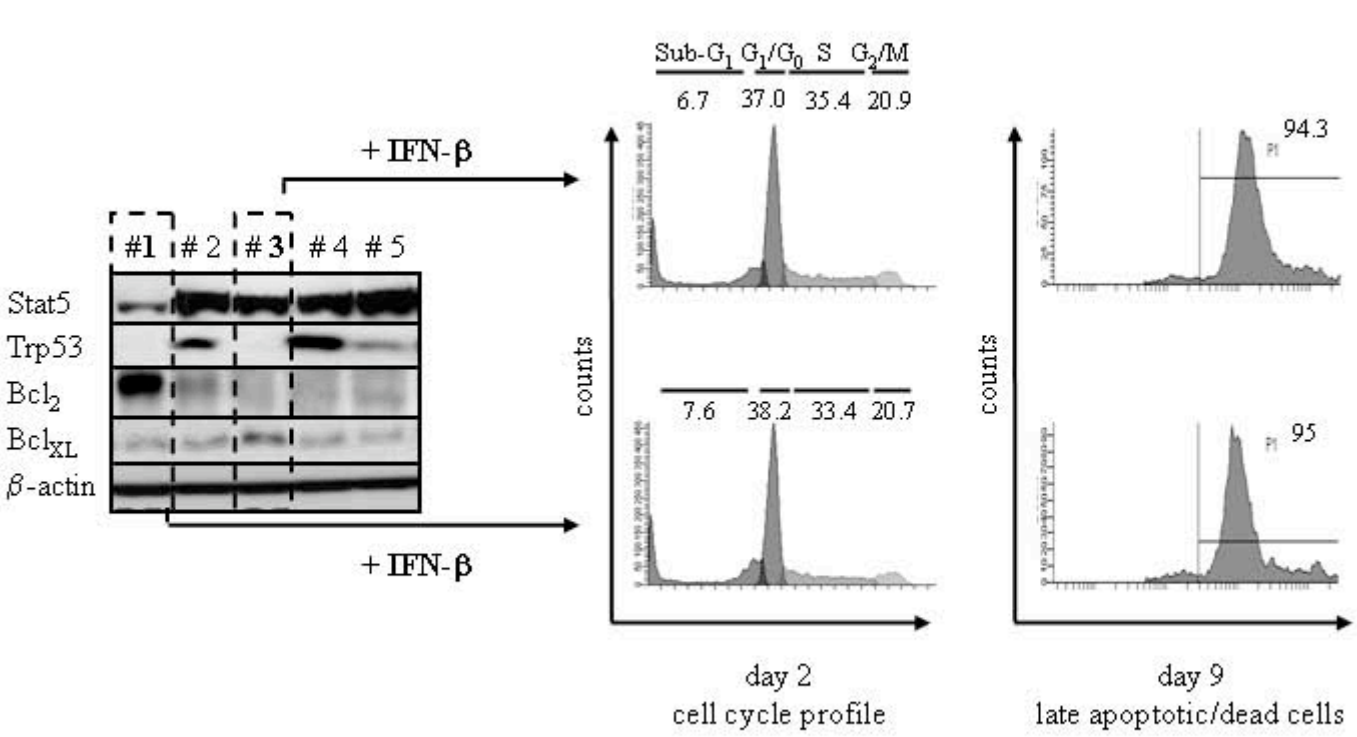
A
Sub-G1 G1/G0 S G2/M
6.7 37.0 35.4 20.9
+ IFN-β
#1 # 2 # 3 # 4 # 5
Stat5
Trp53
Bcl2
BclXL
β-actin
+ IFN-β
counts
7.6 38.2 33.4 20.7
94.3
95
counts
day 2
cell cycle profile
day 9
late apoptotic/dead cells

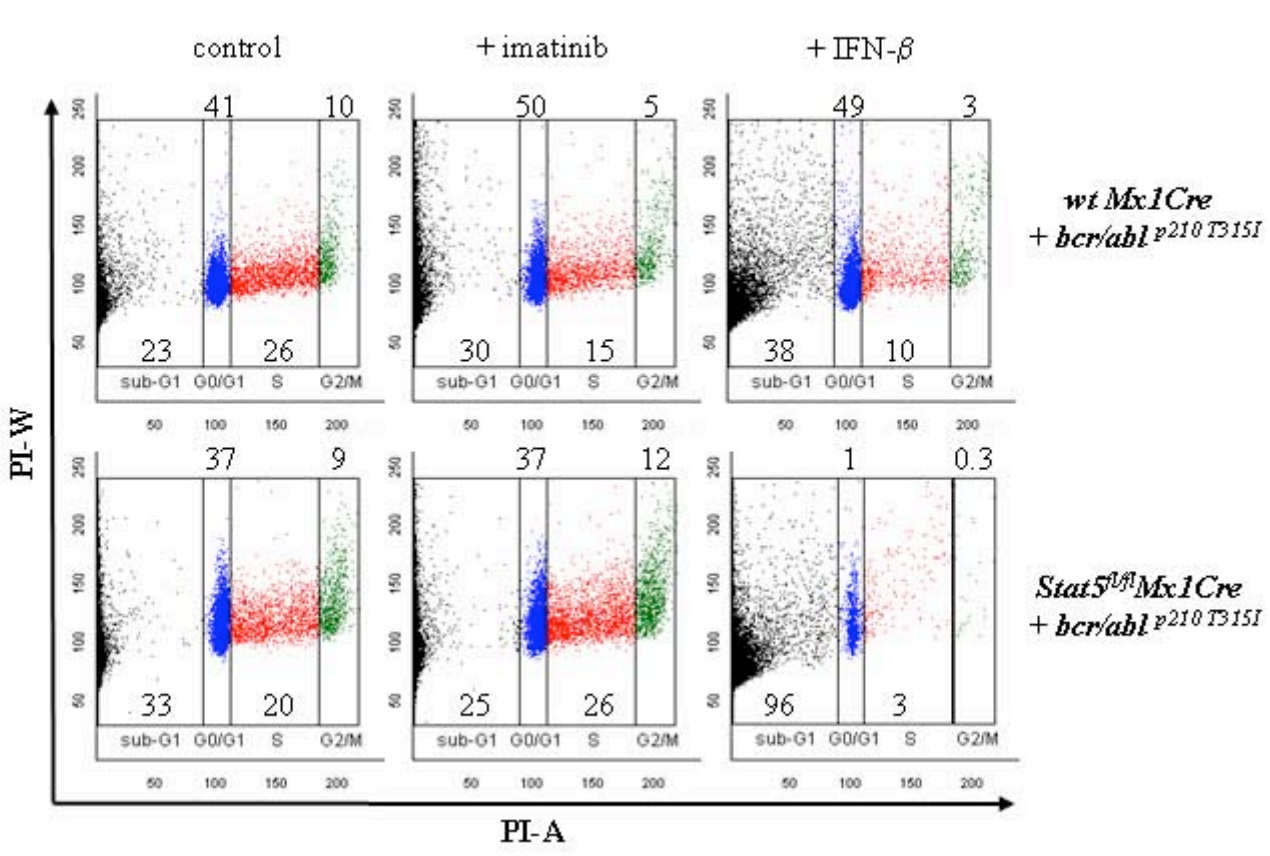
B
control
+ imatinib
+ IFN-β
41 10
23 26
50 5
30 15
49 3
38 10
37 9
33 20
37 12
25 26
1 0.3
96 3
sub-G1 G0/G1 S G2/M
PI-W
PI-A
wt Mx1Cre
+ bcr/abl p210 T315I
Stat5fl/fl Mx1Cre
+ bcr/abl p210 T315I

Supplemental Data

Stat5 is a signaling bottleneck for the maintenance of *bcr/abl*-positive leukemia

Andrea Hölbl, Christian Schuster, Boris Kovacic, Maria Hölzl, Sabine Fajmann, Florian Grebien, Wolfgang Warsch, Gabriele Stengl, Lothar Hennighausen, Hartmut Beug, Richard Moriggl, Veronika Sexl.

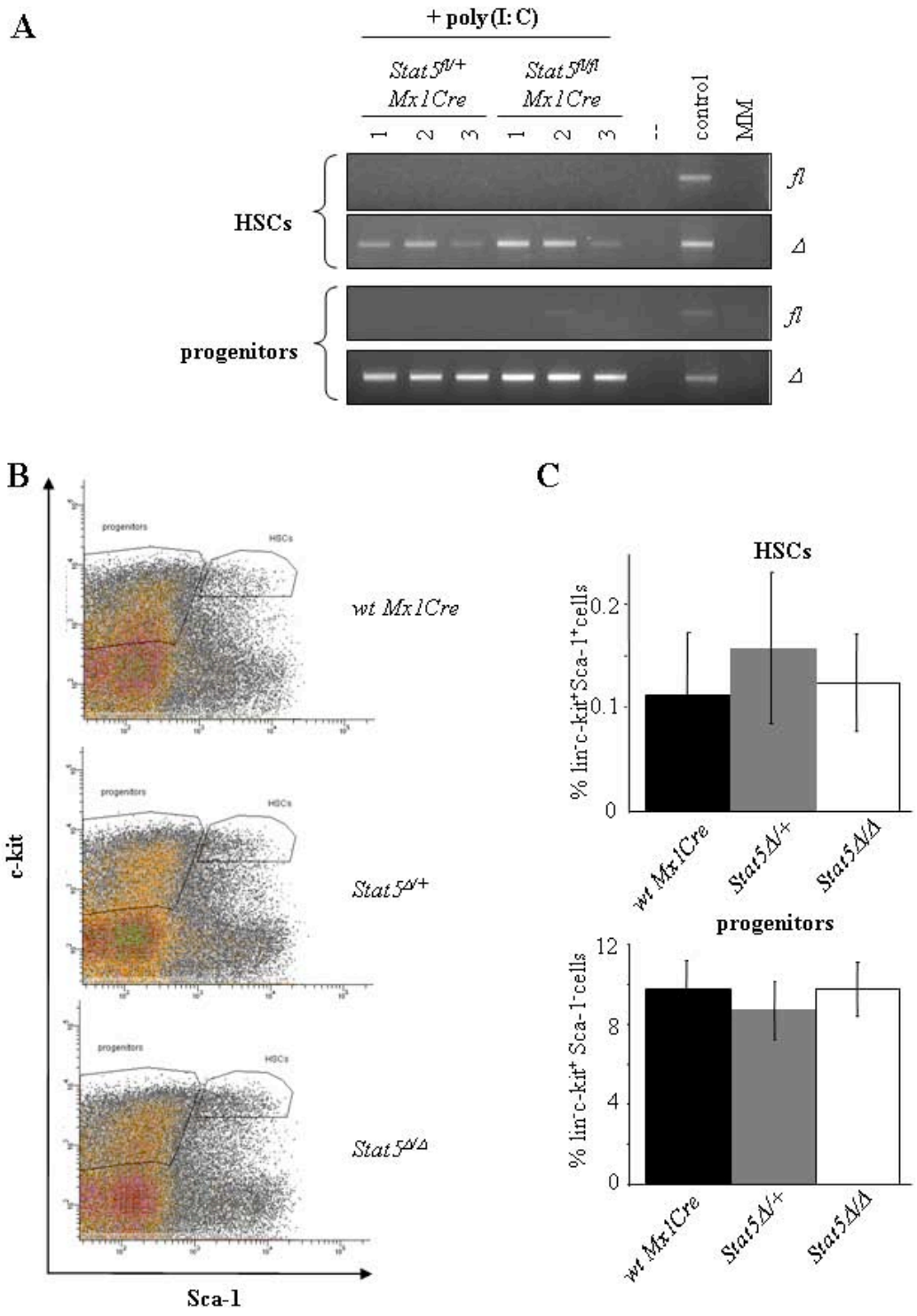

Figure S1. Effect of *Stat5* deletion on normal HSCs and progenitors.

(A) HSCs and progenitors from bone marrows of *Stat5*$^{fl/fl}$*Mx1*Cre and *Stat5*$^{fl/+}$*Mx1Cre* mice (6 weeks of age) were FACS-sorted after p(I:C) treatment (two times, 300µg i.p.). Deletion

efficiency was analyzed by PCR reactions specific for floxed (*fl*) or deleted (*Δ*) *Stat5* alleles. Numbers indicate samples from individual mice.

(B) FACS analysis of HSC and progenitor populations in wt *Mx1*Cre, *Stat5*$^{fl/fl}$*Mx1*Cre and *Stat5*$^{fl/+}$*Mx1Cre* mice after p(I:C) treatment. Lin$^-$ BM cells were gated and analyzed for c-kit and Sca-1 surface expression. Bar graphs summarize quantifications of Lin$^-$c-kit$^+$Sca-1$^+$ (HSCs) and Lin$^-$c-kit$^+$Sca-1$^-$ cells. Data represent means $\pm$ SD.

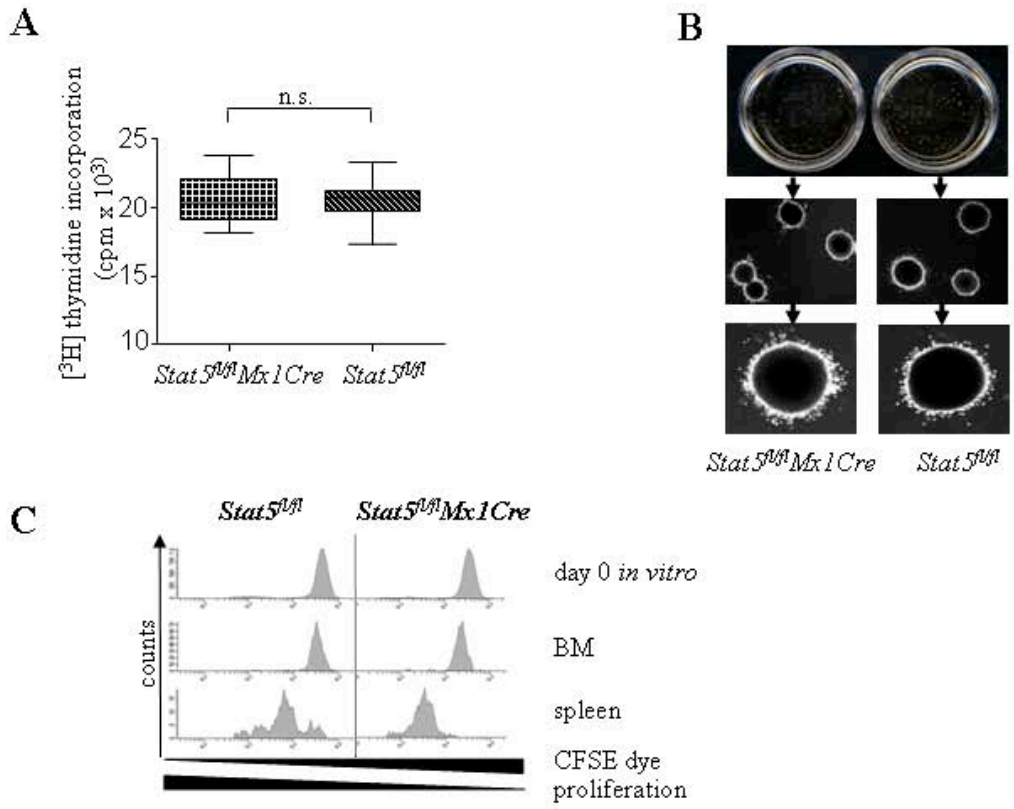

Figure S2. *Stat5$^{fl/fl}$Mx1Cre* and *Stat5$^{fl/fl}$ v-abl^{+}* cell lines proliferate comparably *in vitro* and *in vivo*.

(A) ^{3}[H] thymidine incorporation of *Stat5$^{fl/fl}$Mx1Cre* and *Stat5$^{fl/fl}$* cell lines. Data represent means of three individual cell lines per genotype ± SD. The experiment was performed in triplicates.

(B) Colony formation of stable *Stat5$^{fl/fl}$Mx1Cre* and *Stat5$^{fl/fl}$ v-abl^{+}* cell lines (n=3 each.) 1 x 10^{3} cells were plated in growth factor free methylcellulose. After seven days no differences in clone size were evident (magnification 4x, 40x). One representative data set is shown.

(C) Homing of *Stat5$^{fl/fl}$Mx1*Cre and *Stat5$^{fl/fl}$* cell lines *in vivo*. 1 x 10^{6} CSFE labelled cells were i.v. injected into *Rag2$^{-/-}\gamma c^{-/-}$* mice (n=3). After 24 hours the mice were sacrificed and BMs and spleens were analysed by FACS. One representative data set is shown.

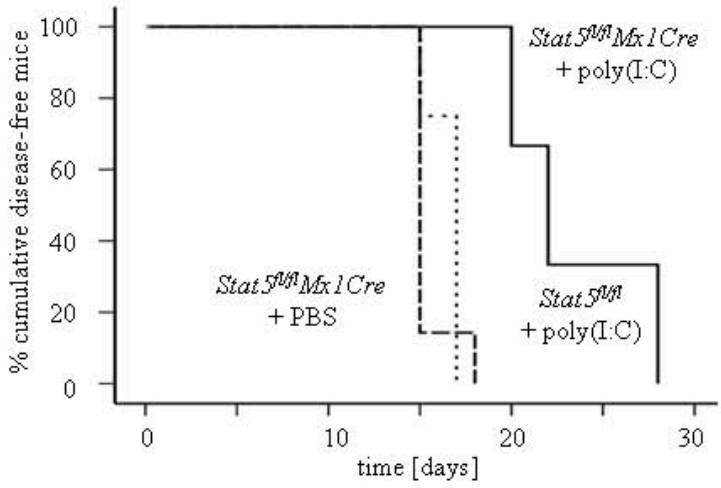

Figure S3. Transplantation of *Stat5$^{fl/fl}$Mx1*Cre and *Stat5$^{fl/fl}$ v-abl^{+}* cell lines into wt C57BL/6J mice.

1 x 10^6 cells of *Stat5$^{fl/fl}$Mx1Cre* or *Stat5$^{fl/fl}$* cell lines (n=3 each) were injected via the tail vein. From day seven on, 400µg p(I:C) was injected i.p. every four days until mice diseased. Kaplan-Meier analysis revealed a significant difference in survival time of mice after *Stat5* deletion compared to control group ("*Stat5$^{fl/fl}$Mx1Cre* + p(I:C)" vs. "*Stat5$^{fl/fl}$Mx1Cre* untreated" $p<0.001$; "*Stat5$^{fl/fl}$Mx1Cre* untreated" vs. *Stat5$^{fl/fl}$* + p(I:C)" n.s.). Mice of the ("*Stat5$^{fl/fl}$Mx1Cre* + p(I:C)" group displayed a mean survival of 23.3 days, whereas mice of "*Stat5$^{fl/fl}$Mx1Cre* untreated" and "*Stat5$^{fl/fl}$* + p(I:C)" groups survived on average 15.4 and 16.5 days, respectively.

Supplemental Experimental Procedures

Retroviral constructs

Stat5 target genes, Stat5 mutants and *bcr/abl*^{p210} were cloned into a pMSCV-IRES-GFP, *Bcr/Abl*^{p210T315I} into a pMSCV-IRES-dsRed backbone.

Tissue culture conditions and virus preparation

Transformed FL cells and tumor-derived cell lines were maintained in RPMI 1640 medium containing 10% fetal calf serum (FCS), 100U/ml penicillin/streptomycin, 50 μM β-mercaptoethanol and 2 mM L-glutamine ("RPMI complete"). A010 and gp+E86 cells were maintained in DMEM medium containing 10% fetal calf serum (FCS), 100U/ml penicillin/streptomycin, 50 μM β-mercaptoethanol and 2 mM L-glutamine ("DMEM complete"). Cell culture media were purchased from Sigma. Standard supplements were purchased from Gibco.

A010 cells produce an ecotropic replication deficient form of the Abelson murine leukemia virus (A-MuLV) encoding the *v-abl* oncogene and were a generous gift of Dr. Naomi Rosenberg. Gp+E86 retroviral packaging cell lines for Stat5 target genes, *bcr/abl*^{p210} as well as mutated version thereof (*bcr/abl*^{p210T315I}) were established by transfection (Lipofectamine Invitrogen®). Cells were sorted for expression of fluorescent proteins using BD FACS-Vantage device.

Bcr/abl^{p210} and *bcr/abl*^{p210T315I} infected BM cells were maintained in Stem Cell Pro medium supplemented with mSCF (50ng/ml), murine IL-3 (2ng/ml), Flt3-L (10ng/ml), murine GMCSF (3ng/ml), IGF-1 (40ng/ml), dexamethasone (1μg/ml) and mouse IL-6 (0,5 ng/ml) (all purchased from R&D Systems) ("stem cell medium") as described before (Kieslinger et al., 2000).

Infections and establishment of cell lines

For the preparation of lymphoid cell lines, *Stat5*$^{fl/fl}$ and *Stat5*$^{fl/fl}$*Mx1Cre* animals were set up for breeding. Fourteen days after conception pregnant animals were sacrificed and FLs

prepared. Single cell suspensions from FLs were infected for one hour with viral supernatant derived from A010 cells in the presence of 7 μg/ml polybrene as described previously (Sexl et al., 2000). The cells were then maintained in complete RPMI medium and observed for the outgrowth of stable transformed cell lines.

***In vitro* colony formation assay**

Single cell suspensions from FLs (ED 13.5) were co-cultivated on *bcr/abl* ^{p210} producer cells in the presence of IL-3 (25 ng/mL), IL-6 (50 ng/mL), SCF (50 ng/mL) and 7 μg/ml polybrene for 48 hours as described previously (Sexl et al., 2000). After infection, 1 x 10^4 GFP^+ cells were resuspended in 3 ml cytokine-free methylcellulose (Stem Cell Technologies) and plated in 35 mm dishes (1.5ml each). After five days, colonies were counted by light microscopy (Leica Fluovert microscope, 4 x magnification). Images of cell culture dishes were scanned using a standard on-desk scanner.

For comparison of growth capacity between *Stat5*$^{fl/fl}$*Mx1Cre* and *Stat5*$^{fl/fl}$ *v-abl*$^+$ stable lymphoid cell lines, 1 x 10^3 cells were plated in cytokine-free methylcellulose and evaluated as described above.

Re-expression of wt Stat5 and Stat5 target genes in stable *v-abl*$^+$ cell lines and rescue assays

Infections with indicated Stat5 target genes were performed using retroviral producer cell lines as described above. Thereafter GFP^+ cells were sorted using a FACSAria (Becton Dickinson) and pure GFP^+ cell lines were mixed with non-transfected ones of the same genotype at a ratio of 1:33. To determine rescue capacity of indicated target genes cells were treated with 1000U/ml recombinant IFN-β for 48 hours. Thereafter the percentage of GFP^+ cells was determined daily by flow cytometry.

CSFE *in vivo* proliferation assay

Cells were labelled with CFSE (carboxy-fluorescein diacetate, succinimidyl ester; Sigma) at a final concentration of 0,5 μM in PBS. Subsequently, 1 x 10^6 cells were injected via the tail vein into *Rag2*$^{-/-}\gamma c^{-/-}$ recipient mice. 24 hours after injection, mice were sacrificed and BMs and spleens were analyzed by flow cytometry for the presence of labelled cells. *In vitro* maintained cells served as control.

[^{3}H] thymidine incorporation

Cells were plated at a density of 2 x 10^5 cells in 96 round bottom wells. 0.1 μCi [^{3}H] thymidine/well (PerkinElmer). After 24 hours, cells were frozen at -80°C, re-thawn and then analyzed using a Skatron semi-automatic cell harvester. Incorporation of [^{3}H] thymidine was measured by a Packard scintillation counter upon addition of scintillation fluid (Rotiszint ECO plus, Roth GmbH & Co KG).

Cell extracts and Western blotting

Cells were lysed in a buffer containing protease and phosphatase inhibitors (50 mM Hepes, pH 7.5, 0.1% Tween-20, 150 mM NaCl, 1 mM EDTA, 20 mM β-glycero-phosphate, 0.1 mM sodium vanadate, 1 mM sodium fluoride, 10 μg/ml aprotinin, leupeptin and 1 mM PMSF, respectively). Protein concentrations were determined using a BCA-kit (Pierce, Rockford, IL).

Proteins (50-100 μg) were separated on an 8% SDS polyacrylamide gel and transferred onto Immobilon membranes. Membranes were probed with antibodies directed against Stat5, Trp53, Bcl_2, Bcl_{XL}, β-actin and holo-ERK (all purchased from Santa Cruz Biotechnologies). Immunoreactive bands were visualized by chemoluminiscent detection (ECL detection kit; Amersham, Arlington Heights, UK) using protein A-conjugated horseradish peroxidase (Amersham, Arlington Heights, UK).

Real-time PCR analysis

RNA was isolated using TriZol (Invitrogen). RNA integrity was checked with the Agilent Bioanalyzer (Agilent). 2.5 μg RNA was reverse transcribed using Superscript II

reverse transcriptase (Invitrogen). Real time PCR was performed on an Eppendorf RealPlex cycler using RealMasterMix (Eppendorf) and SYBR Green as described before (Kerenyi et al., 2008). The following primer pairs were used:

pim-1 5´ACGTGGAGAAGGACCCGATTTCC 3´ and 3´GATGTTTTCGTCCTTGATGTCGC 3´

cis 5´CTGCTGTGCATAGCCAAGACGTTC 3´ and 5´CAGAGTTGGAAGGGGTACTGTCGG 3´

cyclin D2, 5' AGA AGG GGC TAG CAG ATG A 3' and 5' AGG ATG ATG AAG TGA ACA CA-3'

cyclin D3 5´TGCATCTATACGGACCAGGCT 3´and 5´AGGAAGTCGTGCGCAATCA 3´

bcl_{XL} 5 TTGGATGGCCACCTATCTGAAT 3´and 5´TCTCGGCTGCTGCATTGTT 3´

hypoxanthine-guanine phosphoribosyltransferase (control)

hprt 5' TGA TTA GCG ATG ATG AAC CAG G 3' and 5' CCT TCA TGA CAT CTC GAG CAA G 3'

In vitro imatinib sensibility assay of bcr/abl^{p210T315I}- transformed cells

BM cells from 6 weeks old *Stat5$^{fl/fl}$Mx1Cre* and *Stat5$^{+/+}$ Mx1Cre* mice were co-cultivated with viral producer cells encoding a imatinib-resistant version of *bcr/abl^{p210}* (*bcr/abl^{p210T315I}*) as described above. After 48 hours of infection cells were maintained in stem cell medium as described above and treated either with 100 nM Imatinib or 1000U/ml recombinant IFN-ß. Cells were analyzed by flow cytometry for cell cycle distribution daily.

Statistical analysis

Statistics were carried out using Student´s t-test, Mann-Whitney-test or a one-way ANOVA test as appropriate. Differences in Kaplan-Meier plots were analyzed for statistical significance using the log-rank test. Data are presented as averages ± SD and were analyzed by Graph Pad® and SPSS software.

References (Supplemental Data)

Kerenyi, M. A., Grebien, F., Gehart, H., Schifrer, M., Artaker, M., Kovacic, B., Beug, H., Moriggl, R., and Mullner, E. W. (2008). Stat5 regulates cellular iron uptake of erythroid cells via IRP-2 and TfR-1. Blood *112*, 3878-3888.

Kieslinger, M., Woldman, I., Moriggl, R., Hofmann, J., Marine, J. C., Ihle, J. N., Beug, H., and Decker, T. (2000). Antiapoptotic activity of Stat5 required during terminal stages of myeloid differentiation. Genes Dev *14*, 232-244.

Sexl, V., Piekorz, R., Moriggl, R., Rohrer, J., Brown, M. P., Bunting, K. D., Rothammer, K., Roussel, M. F., and Ihle, J. N. (2000). Stat5a/b contribute to interleukin 7-induced B-cell precursor expansion, but abl- and bcr/abl-induced transformation are independent of stat5. Blood *96*, 2277-2283.

3.2 Original articles

3.2.1 Stat5 regulates cellular iron uptake of erythroid cells via IRP-2 and TfR-1

Marc A. Kerenyi[1#], Florian Grebien[1#], Helmuth Gehart[1], Manfred Schifrer[1], Matthias Artaker[1], Boris Kovacic[2], Hartmut Beug[2], Richard Moriggl[3] and Ernst W. Müllner[1&]

[1]Max F. Perutz Laboratories, Department of Medical Biochemistry, Medical University of Vienna, 1030 Vienna, Austria

[2]Research Institute of Molecular Pathology, 1030 Vienna, Austria

[3]Ludwig Boltzmann Institute for Cancer Research, 1090 Vienna, Austria

[#]equal contribution

[&]corresponding author

blood

2008 112: 3878-3888
Prepublished online Aug 11, 2008;
doi:10.1182/blood-2008-02-138339

Stat5 regulates cellular iron uptake of erythroid cells via IRP-2 and TfR-1

Marc A. Kerenyi, Florian Grebien, Helmuth Gehart, Manfred Schifrer, Matthias Artaker, Boris Kovacic, Hartmut Beug, Richard Moriggl and Ernst W. Müllner

Stat5 regulates cellular iron uptake of erythroid cells via IRP-2 and TfR-1

*Marc A. Kerenyi,[1] *Florian Grebien,[1] Helmuth Gehart,[1] Manfred Schifrer,[1] Matthias Artaker,[1] Boris Kovacic,[2] Hartmut Beug,[2] Richard Moriggl,[3] and Ernst W. Müllner[1]

[1]Max F. Perutz Laboratories, Department of Medical Biochemistry, Medical University of Vienna, Vienna; [2]Research Institute of Molecular Pathology, Vienna; and [3]Ludwig Boltzmann Institute for Cancer Research, Vienna, Austria

Erythropoiesis strictly depends on signal transduction through the erythropoietin receptor (EpoR)–Janus kinase 2 (Jak2)–signal transducer and activator of transcription 5 (Stat5) axis, regulating proliferation, differentiation, and survival. The exact role of the transcription factor Stat5 in erythropoiesis remained puzzling, however, since the first Stat5-deficient mice carried a hypomorphic *Stat5* allele, impeding full phenotypical analysis. Using mice completely lacking *Stat5*—displaying early lethality—we demonstrate that these animals suffer from microcytic anemia due to reduced expression of the antiapoptotic proteins Bcl-x_L and Mcl-1 followed by enhanced apoptosis. Moreover, transferrin receptor-1 (TfR-1) cell surface levels on erythroid cells were decreased more than 2-fold on erythroid cells of Stat5$^{-/-}$ animals. This reduction could be attributed to reduced transcription of TfR-1 mRNA and iron regulatory protein 2 (IRP-2), the major translational regulator of TfR-1 mRNA stability in erythroid cells. Both genes were demonstrated to be direct transcriptional targets of Stat5. This establishes an unexpected mechanistic link between EpoR/Jak/Stat signaling and iron metabolism, processes absolutely essential for erythropoiesis and life. (Blood. 2008;112:3878-3888)

Introduction

Erythroid cell formation needs to be tightly regulated to maintain proper tissue oxygenation. Although about 10^{11} red cells are produced every day in humans, total red cell numbers are kept within a narrow range in bone marrow, spleen, and fetal liver. While early erythroid lineage commitment is controlled by numerous transcription factors and their binding partners (like GATA-1, FOG-1, and EKLF),[1] later stage differentiation from erythroblasts to mature erythrocytes is strictly regulated by erythropoietin (Epo).[2]

Epo induces dimerization of erythropoietin receptor (EpoR), which results in juxtaposition and activation of the receptor-associated Janus kinase 2 (Jak2). Jak2 subsequently phosphorylates several tyrosine residues in the cytoplasmic tail of EpoR, which in turn acts as docking sites for signaling molecules such as PI3-K[3], MAPK,[4] PKC,[5] and PLC-γ.[6] A central pathway of EpoR signaling is the activation of the transcription factor signal transducer and activator of transcription 5 (Stat5).[7,8] Upon EpoR phosphorylation, Stat5 molecules are tyrosine-phosphorylated by Jak2 and translocate to the nucleus. This leads to activation of Stat5 target genes such as *Pim-1*, *c-myc*, *Bcl-x_L*, *D-type cyclins*, *oncostatin M*, and *SOCS* members that play important roles in differentiation, proliferation, apoptosis, and other processes.[9-15]

The importance of Epo signaling is evidenced by the phenotypes of Epo$^{-/-}$, EpoR$^{-/-}$, and Jak2$^{-/-}$ mice, which die in utero at embryonic day (E) 13.5 due to defects in erythropoiesis. Fetal livers of Jak2$^{-/-}$ animals completely lack BFU-E (burst forming unit–erythroid) and CFU-E (colony forming unit–erythroid) progenitors. In line with this, Epo- and EpoR-deficient embryos also fail to develop mature erythroid cells in vivo.[16-18] Interestingly, mice expressing a truncated form of EpoR (EpoR$_H$), which solely activates Stat5 and lacks all critical phosphotyrosine sites required to activate other signaling pathways, exhibited no strong erythroid phenotype,[15,19] suggesting Stat5 as a critical component of the EpoR signaling pathway. Unexpectedly, however, mice expressing an EpoR mutant additionally lacking the binding site for Stat5 (EpoR$_{HM}$) displayed no overt erythroid phenotype except under stress conditions.[15,19] Moreover, the mice initially reported to be deficient for Stat5a and Stat5b were viable and had a surprisingly mild erythroid phenotype.[7,20,21] Although showing fetal anemia, adult animals only displayed mild defects in recovery from phenylhydrazine-induced erythrolytic stress. This was explained by increased apoptosis in early erythroid progenitors, due to lack of Stat5-induced expression of the antiapoptotic gene *Bcl-x_L*.[21] Later, however, these initial Stat5 knockout animals—now referred to as Stat5$^{\Delta N/\Delta N}$—were found to express a N-terminally truncated protein able to bind DNA and to activate a subset of Stat5 target genes.[14,22-25] In contrast to Stat5$^{\Delta N/\Delta N}$, the recently described bona fide Stat5a/b null knockout mice (referred to as Stat5$^{-/-}$)[8] die during gestation or at latest (< 2%) shortly after birth. Complete ablation of Stat5 resulted in severe defects in generation of all lymphoid lineages.[23,24,26] However, an accurate analysis of the erythroid compartment from these mice is still missing.

Maturing erythroid progenitors depend on large amounts of bioavailable iron (humans require 20 mg iron complexed to transferrin per day) to enable efficient heme synthesis. Cellular uptake of iron-loaded transferrin is mediated by transferrin receptor-1 (TfR-1; also called CD71),[27] followed by receptor internalization. Accordingly, maturing erythroid cells express high

Submitted February 7, 2008; accepted July 24, 2008. Prepublished online as *Blood* First Edition paper, August 11, 2008; DOI 10.1182/blood-2008-02-138339.

*M.A.K. and F.G. contributed equally to this article.

The online version of this article contains a data supplement.

The publication costs of this article were defrayed in part by page charge payment. Therefore, and solely to indicate this fact, this article is hereby marked "advertisement" in accordance with 18 USC section 1734.

levels of TfR-1. However, as excess iron would lead to oxidative damage, expression of proteins involved in iron uptake, storage, and utilization is tightly controlled. In case of TfR-1, this occurs primarily at the level of TfR-1 mRNA stability[28] and to a lesser extent at the transcriptional level.[29] At low-iron conditions, *trans*-acting iron regulatory proteins (IRP1 + 2) bind to conserved hairpin structures (iron-responsive elements [IREs]) in the 3′-untranslated region (UTR) of TfR-1 mRNA, which selectively stabilizes this mRNA and ensures proper TfR-1 cell-surface expression and iron uptake.[30-32] Upon iron excess, IRP-1 is converted to a cytosolic aconitase catalyzing isomerization of citrate to isocitrate,[33] while IRP-2 is degraded by the proteasome.[34] Thus, both proteins no longer bind to IREs, resulting in strongly reduced TfR-1 mRNA stability, which leads to reduced TfR-1 cell-surface expression and iron uptake.[35-37] Recently generated knockout mouse models for IRP-1 and IRP-2 suggested IRP-2 as the master regulator of IRE-regulated mRNAs, as ablation of IRP-2 led to a decrease in TfR-1 expression and microcytic anemia, while IRP-1 knockout animals had no overt phenotype.[38,39]

Here we show that Stat5$^{-/-}$ embryos suffer from severe microcytic anemia, a disease mostly associated with iron deficiency and characterized by small-sized red blood cells. In Stat5-deficient animals this anemia had 2 causes: first, fetal livers were much smaller in knockout embryos due to a strong increase of apoptosis in the erythron. We demonstrate that the antiapoptotic proteins Mcl-1 and Bcl-x_L were largely absent in Stat5$^{-/-}$ cells, but ectopic expression of Mcl-1 complemented the survival defect of Stat5$^{-/-}$ erythroid cells. Second and more important, we demonstrate for the first time a direct link between Stat5 and iron metabolism. In the absence of Stat5, IRP-2 expression was strongly decreased, resulting in more than 2-fold lower cell-surface expression of TfR-1 and thus strongly reduced iron uptake in erythroid cells. Together, the high levels of apoptosis and impaired iron uptake caused severe microcytic anemia and probably contributed to the death of Stat5$^{-/-}$ embryos.

Methods

Cell culture and retroviral infections

Stat5$^{+/-}$ mice[8] were maintained under pathogen-free conditions and bred on a mixed background (C57Bl/6 × Sv129F1) to obtain Stat5$^{-/-}$ embryos. For the determination of blood indices, heparinized blood was measured in a Vet ABC Blood Counter (Scil Animal Care, Viernheim, Germany). Serum Epo levels were determined using a Quantikine mouse erythropoietin enzyme-linked immunosorbent assay (ELISA) kit (R&D Systems, Minneapolis, MN) according to the manufacturer's protocol, measured on a Victor^{3}V 1420 multilabel counter (PerkinElmer, Waltham, MA). All animal experiments described in our manuscript were performed in accordance with Austrian and European laws and under approval of the ethical and animal protection committees of the Veterinary University of Vienna.

Fetal livers of E13.5 mouse embryos (Stat5$^{-/-}$ and wild type [wt]) were resuspended in serum-free medium (StemPro-34; Invitrogen, Carlsbad, CA). In brief, for self-renewal,[40] cells were seeded into medium containing 2 U/mL human recombinant Epo (Erypo; Cilag AG, Sulzbach, Germany), murine recombinant stem cell factor (SCF; 100 ng/mL; R&D Systems), 10^{-6} M dexamethasone (Dex; Sigma-Aldrich, St Louis, MO), and insulin-like growth factor 1 (IGF-1; 40 ng/mL; Promega, Madison, WI). The resulting erythroblast cultures were expanded by daily partial medium changes and addition of fresh factors, keeping cell densities between 2 and 4×10^6 cells/mL. Proliferation kinetics and size distribution of cell populations were monitored daily in an electronic cell counter (Casy-1; Innovatis AG, Reutlingen, Germany).[40] For retroviral infections, fetal liver erythroblasts were cocultured for 72 hours with retrovirus-producing fibroblast cell lines selected for high virus production.[14] Infection efficiency was 75% to 95% as measured by flow cytometry for green fluorescent protein (GFP) expression. Cytospun cells were fixed in methanol, embedded in Entellan (Sigma-Aldrich), and stained with either Benzidine, May-Gruenwald Giemsa, or Wright-Giemsa solutions according to manufacturer's protocols (all Sigma-Aldrich). Photomicrographs were taken using an Axiovert 10 microscope (Zeiss, Jena, Germany) equipped with a 63× oil-immersion lens (numeric aperture 44-07-61), a Zeiss AxioCam MRc5, and Axiovision LE software, version 4.5. Images were processed with Adobe Photoship CS2 and are presented at ×630 magnification.

Flow cytometry

Cultured erythroblasts or single-cell suspensions of freshly isolated fetal livers were stained with fluorescence-conjugated antibodies (all from BD Biosciences, San Jose, CA) against Ter-119 (PE-conjugated) and TfR-1 (biotinylated) for in vivo erythroid development analyses. Annexin V (APC-conjugated) staining was performed according to the manufacturer's instructions. For in vivo proliferation assays, pregnant mice were injected with 80 mg BrdU per kilogram of body mass. After 1 hour, embryos were isolated, and fetal liver cells were fixed and stained with anti-BrdU–FITC plus Ter-119–PE following the manufacturer's protocol (BrdU flow kit; BD Biosciences). Samples were analyzed on a FACSCalibur flow cytometer (BD Biosciences). Where indicated, Ter-119$^+$ cells were isolated by magnetic cell sorting using Auto-MACS (Miltenyi Biotec, Auburn, CA).

Western blot analysis

The following antibodies were used for Western blotting: anti–mouse ERK1/2, anti–horse ferritin H, anti–mouse actin (all from Sigma-Aldrich), anti–mouse TfR-1 (BioSource, Camarillo, CA), anti–mouse Bcl-x_L, anti–mouse PCNA, anti–mouse Stat5 (all from BD Transduction Laboratories, Erembodegem, Belgium), anti–mouse Mcl-1 (Abcam, Cambridge, United Kingdom), anti–mouse eIF4E, anti–mouse eIF2-alpha, pSer-eIF2-alpha (all from Cell Signaling Technology, Danvers, MA), anti–rat IRP-1,[41] and anti IRP-2.[39]

Chromatin immunoprecipitation

Chromatin immunoprecipitation was performed as in LeBaron et al.[42] A total of 2×10^7 primary erythroblasts were stimulated with 10 U Epo/mL for 30 minutes. Cells were fixed with 1% formaldehyde for 30 minutes. DNA was sonicated using a Bandelin Sonoplus GM70 sonicator (cycle count, 30%; power, 45%; 6 × 30 seconds; Bandelin Electronic, Berlin, Germany). DNA fragments were recovered using anti–mouse Stat5ab (C20; Santa Cruz Biotechnology, Santa Cruz, CA) or anti–mouse Stat5 (N20; Santa Cruz Biotechnology). Recovered DNA fragments were directly used for polymerase chain reaction (PCR) analysis.

Quantitative real-time PCR

RNA was isolated using the RNeasy Mini Kit (QIAGEN, Valencia, CA). RNA integrity was checked with the Agilent Bioanalyzer (Agilent, Palo Alto, CA). A total of 2.5 μg RNA was reverse transcribed using Superscript II reverse transcriptase (Invitrogen). Real-time PCR was performed on an Eppendorf Master-cycler RealPlex using RealMasterMix (Eppendorf, Hamburg, Germany) and SYBR Green. Results were quantified using the Delta Delta C(T) method.[43]

Statistical analyses

Statistical analyses were performed using Excel 2004 (Microsoft, Redmond, WA). The Student *t* test was used to calculate *P* values (2-tailed). *P* values of .05 or less are indicated in the figures by one asterisk; *P* values of .01 or less are indicated in the figures by 2 asterisks. Data are presented as mean values plus or minus standard deviation (SD).

Results

Stat5$^{-/-}$ embryos are severely anemic

Embryos lacking the entire *Stat5* locus (ie, *Stat5a/b*) die during gestation or at latest perinatally (approximately 99%) with severe defects in diverse hematopoietic lineages.[23,24] The previously demonstrated pivotal role of Stat5 in Epo signaling[19-22] prompted us to analyze the function of Stat5 in erythropoiesis in detail. E13.5 Stat5$^{-/-}$ embryos and newborn Stat5$^{-/-}$ animals appeared paler than their wt littermates, particularly in the fetal liver region (Figure 1A). The relative abundance of erythroid cells in Stat5$^{-/-}$ fetal livers (approximately 80% of all cells) remained unchanged, as determined by staining for the panerythroid marker Ter-119, followed by flow cytometry (Figure 1B left). However, the size of Stat5$^{-/-}$ fetal livers in E13.5 embryos was visibly reduced and total fetal liver cellularity was decreased by 50% (n = 6), corresponding to a similar reduction in the total number of erythroid cells (Figure 1B right). Since anemia causes elevation of Epo levels[44] to counteract hypoxia, sera from E16.5 or newborn wt and Stat5$^{-/-}$ animals were analyzed for Epo levels. These were highly elevated in Stat5$^{-/-}$ versus wt embryos (3.8 ± 0.6-fold; n = 5); newborn animals showed an even higher elevation (35.2 ± 5.1-fold; n = 5; Figure 1C). This strongly suggested that Stat5-deficient animals

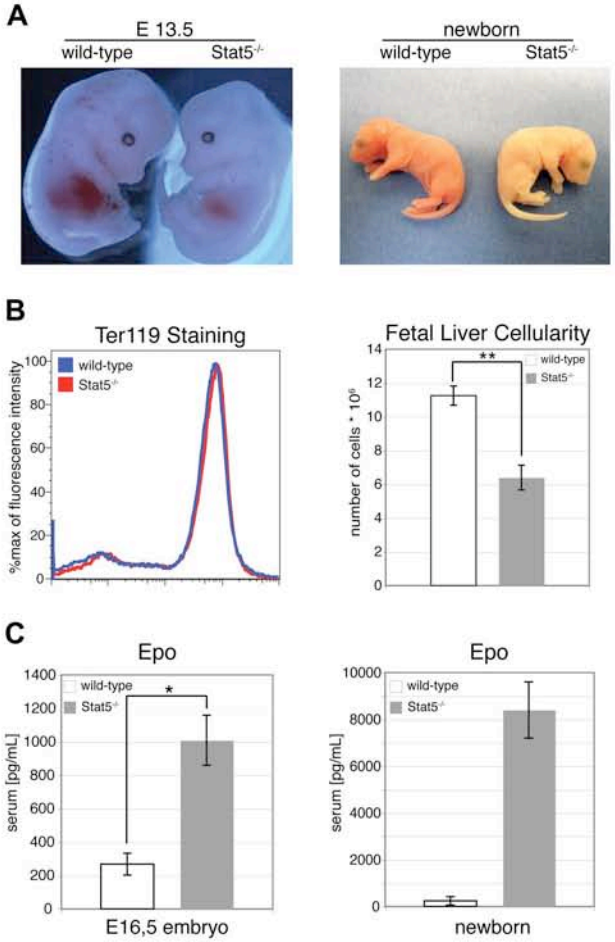

Figure 1. Stat5$^{-/-}$ embryos are severely anemic. (A) wt and Stat5$^{-/-}$ E13.5 embryos (left) and newborn animals (right). (B) Ter-119^{+} erythroid cells (left) and fetal liver cellularity (right; data are presented as mean ± SD; n = 6) of wt versus Stat5$^{-/-}$ fetal livers. (C) ELISA for Epo from serum of wt and knockout E16.5 embryos and newborns. Data are presented as means ± SD; n = 5. $^{*}P < .05$; $^{**}P < .01$.

Table 1. Stat5$^{-/-}$ embryos mice display severe microcytosis

E16.5 embryos	Wild-type	Stat5$^{-/-}$
RBC, 10^6/mm^3	2.4 ± 0.4	1.0 ± 0.3**
Hct, %	31.4 ± 1.8	9.8 ± 0.7**
Hgb, g/L	91 ± 12	23 ± 7**
MCV, μm^3	128.2 ± 3.7	95.9 ± 5.2**
MCH, pg	37.5 ± 0.3	23.1 ± 0.7**

Blood indices of E16.5 Stat5$^{-/-}$ embryos. Data are presented as mean ± SEM; n = 15 each genotype.

RBC indicates red blood cell count; Hct, hematocrit; Hgb, hemoglobin content; MCV, mean corpuscular volume; MCH, mean corpuscular hemoglobin.

$^{*}P < .05$; $^{**}P < .01$.

suffer from severe anemia. To determine the specific type of anemia, blood from E16.5 wt and Stat5$^{-/-}$ animals was analyzed (Table 1). Red blood cell counts of E16.5 Stat5$^{-/-}$ embryos were lowered to 1.0 plus or minus 0.3 × 10^6/mm^3, in contrast to 2.4 plus or minus 0.4 × 10^6/mm^3 in wt embryos. In line with this, hematocrit (Hct) of E16.5 Stat5$^{-/-}$ embryos was reduced to 9.8% plus or minus 0.7% compared with 31.4% plus or minus 1.8% in wt embryos. Likewise, mean corpuscular volume (MCV), hemoglobin content (Hgb), and mean corpuscular hemoglobin (MCH) of E16.5 Stat5$^{-/-}$ blood was strongly reduced. These effects also were clearly visible in blood smears, showing hypochromic microcytic erythrocytes (Figure S1A,B, available on the *Blood* website; see the Supporting Materials link at the top of the online article).

An additional cause for early lethality and high serum Epo levels could have been a lung defect leading to reduction in red cell oxygenation. Analysis of tissue sections from wt and Stat5$^{-/-}$ newborn animals, however, did not reveal any histologic differences (data not shown). Taken together, Stat5$^{-/-}$ mice suffer from microcytic anemia.

Loss of Stat5 causes enhanced apoptosis in the fetal liver

Hypomorphic Stat5$^{\Delta N/\Delta N}$ mice displayed enhanced erythroid cell death, which was attributed to reduced expression of the antiapoptotic protein Bcl-x_L.[20,21] To determine apoptosis in Stat5$^{-/-}$ mice, freshly isolated fetal liver cells were stained for Ter-119 and apoptosis assessed by annexin V staining. In Stat5$^{-/-}$ embryos, the frequency of annexin V^{+} cells was enhanced more than 2-fold, regardless of developmental stage (Figure 2A). In line with this, Stat5$^{-/-}$ fetal liver cells showed a greater than 6-fold reduction of erythroid colony numbers in CFU-E assays regardless of Epo concentrations, supporting the notion that lack of functional Stat5 reduces cell survival (Figure 2B). In contrast, no significant alterations were observed in BFU-E assays (Figure S1C).

To assess potential differences in viability of Stat5-deficient erythroid cells in an adult (bone marrow) versus an embryonic (fetal liver) microenvironment, short-term transplantation experiments were performed. Equal amounts of sorted GFP-expressing wt- or Stat5$^{-/-}$ proerythroblasts cultured from fetal livers (c-Kit^{+}/TfR-1^{high}/Ter-119^{-} cells[15]) were injected into lethally irradiated wt recipients (Figure 2C). This setup was chosen to circumvent any influence of the well-known repopulation defect of Stat5-deficient hematopoietic stem cells.[45-47] At 3 days after transplantation, bone marrow cells were harvested and scored for GFP^{+} mature Ter-119^{+} erythroid cells, as previously reported.[48] In line with the preceding experiments, a 5-fold reduction in abundance of transplanted mature Stat5$^{-/-}$ versus wt cells was determined in the adult microenvironment (bone marrow; Figure 2D). Moreover, these data indicated a cell-autonomous survival defect of Stat5$^{-/-}$ erythroid cells.

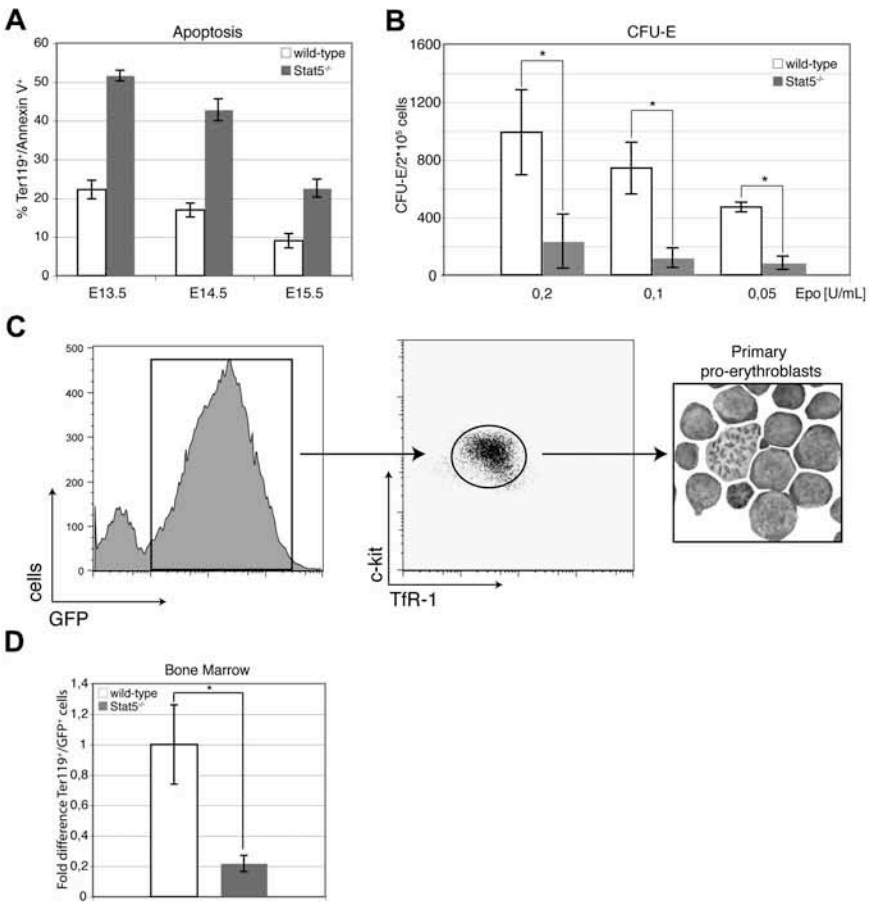

Figure 2. Loss of Stat5 results in increased levels of apoptosis in fetal liver cells. (A) Freshly isolated fetal livers from E13.5 to E15.5 were stained for Ter-119 and annexin V to determine rates of apoptosis (data are presented as means ± SD; n = 3) for each genotype and time point. (B) CFU-E colonies derived from wt or Stat5$^{-/-}$ fetal liver cells using the indicated Epo concentrations (data are presented as means ± SD; n = 4). (C) E13.5 fetal liver cells of wt and Stat5$^{-/-}$ embryos were infected with a retrovirus encoding GFP. TfR-1^{high}/c-Kit^{+}/GFP^{+} cells were isolated by FACS after 7 days under self-renewal conditions (cytospin; right panel). (D) A total of 1.5×10^7 TfR-1^{high}/c-Kit^{+}/GFP^{+} cells were injected into the tail vein of lethally irradiated mice (950 rad) and Ter-119^{+}/GFP^{+} bone marrow cells were scored 3 days later (mean ± SD; n = 4). *$P < .05$; **$P < .01$.

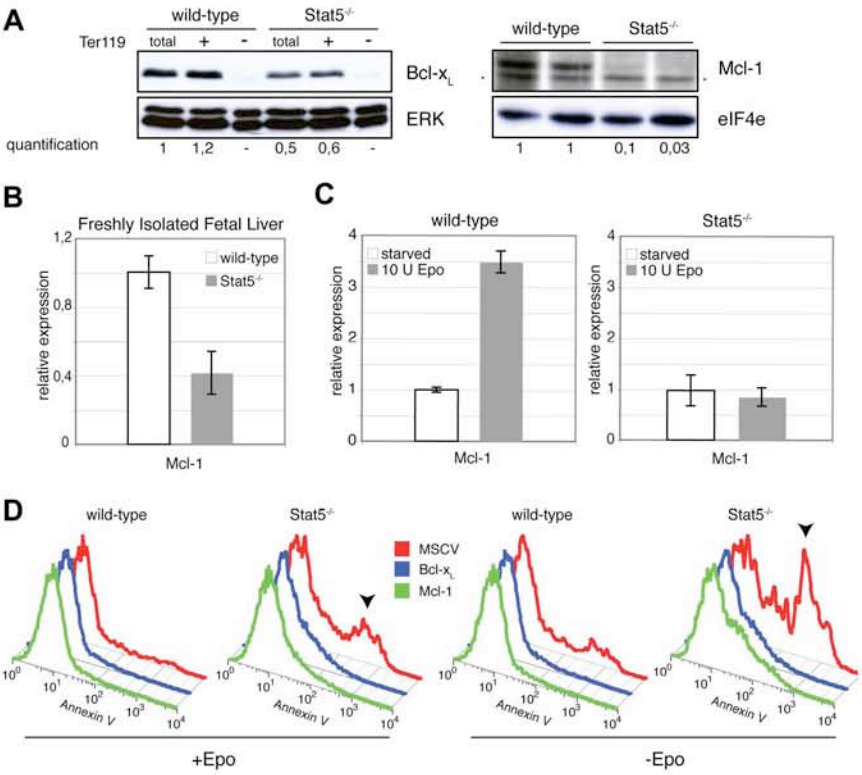

Figure 3. Loss of the antiapoptotic protein Mcl-1 in Stat5$^{-/-}$ fetal liver. (A) Western blot of lysates from freshly isolated fetal livers or Ter-119^{+} and Ter-119^{-} subfractions (separated using magnetic beads; "Methods") for Bcl-x$_L$ (left; ERK, loading control). Western blot for Mcl-1 of 2 individual freshly isolated fetal livers of each genotype (right; eIF4E, loading control). (B) Quantitative PCR analysis for Mcl-1 mRNA isolated from the Ter-119^{+} subfraction of freshly isolated fetal liver cells (data are presented as means ± SD; n = 3). (C) wt and Stat5$^{-/-}$ primary erythroblasts expanded for 5 days under self renewal conditions ("Methods") were deprived of factors for 3 hours, followed by a 30-minute restimulation with 10 U/mL Epo. qPCR analysis for Mcl-1 (representative experiment; error bars are SD of experimental triplicates). (D) wt or Stat5$^{-/-}$ fetal liver cells were infected with retroviruses encoding GFP alone (murine stem cell virus [MSCV]), or Bcl-x$_L$ plus GFP, or Mcl-1 plus GFP from bicistronic constructs. After retroviral infection (72 hours), primary erythroblasts were cultivated for another 48 hours under self-renewal conditions ("Methods") in the presence or absence of Epo. Rates of apoptosis were determined by flow cytometry for annexin V. One representative set of histograms from 3 independently performed experiments of GFP-gated annexin V^{+} cells at 48 hours of treatment is depicted. Arrowheads indicate increased levels of apoptosis. *$P < .05$; **$P < .01$.

Stat5 deficiency leads to reduced expression of antiapoptotic proteins

Consistent with the apoptotic phenotype described, Ter-119$^+$ cells from Stat5$^{-/-}$ fetal livers showed decreased levels of Bcl-x$_L$ as compared with wt cells (Figure 3A left). Nevertheless, Bcl-x$_L$ protein levels in Stat5$^{-/-}$ cells were still approximately 50% of that of wt. This prompted us to analyze the expression of other antiapoptotic *Bcl-2* family members. We focused on Mcl-1 for 3 reasons: (1) Mcl-1 is up-regulated during early erythroid commitment in human cells[49]; (2) its bone marrow–specific ablation reduces blood formation[50]; and (3) it appears to be regulated by Stat5.[51-53] Indeed, Mcl-1 protein and mRNA expression were drastically reduced in Stat5-deficient cells (Figure 3A right; Figure 3B). To assess whether *Mcl-1* is an Epo-inducible Stat5-regulated gene, primary wt and Stat5$^{-/-}$ erythroblasts were factor-deprived for 2 hours and subsequently restimulated with Epo for 30 minutes. Quantitative PCR (qPCR) revealed a 3.5-fold increase in Mcl-1 mRNA in Epo-stimulated cells, which was abrogated in Stat5-deficient cells (Figure 3C).

To test whether exogenous Mcl-1 provides protection against apoptosis to erythroid cells, primary wt or Stat5$^{-/-}$ fetal liver cells were transduced with retroviral constructs encoding *GFP*, *Bcl-x$_L$*, or *Mcl-1*. Erythroblasts were cultivated for 48 hours in the presence or absence of Epo, and apoptosis was determined by flow cytometry. Ectopic expression of either Mcl-1 or Bcl-x$_L$ completely prevented apoptosis of wt as well as Stat5 knockout erythroblasts upon Epo withdrawal (Figure 3D).

The decrease of fetal liver size and cellularity in Stat5$^{-/-}$ embryos could also have been due to reduced proliferation of erythroid cells, as suggested by the known ability of Stat5 to enhance expression of proliferation-promoting genes such as *c-Myc, Cyclin D2* and *D3*, or *oncostatin M*.[14,23,54,55] Cell division kinetics of erythroid cells in vivo and in vitro, however, were similar in Stat5$^{-/-}$ and wt cells (Figure S2; Document S1).

Taken together, Stat5-deficient fetal liver erythroid cells were massively apoptotic. This effect could be attributed to reduction of Bcl-x$_L$ levels together with complete loss of Mcl-1, translating into massive decrease of fetal liver cellularity.

TfR-1 expression is strongly reduced in Stat5$^{-/-}$ erythroid cells

To analyze whether Stat5-deficient mice had a defect in erythroid lineage commitment, wt and Stat5$^{-/-}$ fetal livers were analyzed for the presence of megakaryocytic-erythroid progenitors[56,57] (MEPs), the first erythroid-committed progenitor detectable by flow cytometry. Interestingly, we observed a 2-fold increase of the MEP compartment in Stat5-deficient fetal livers (Figure S3), suggesting a compensatory attempt to counteract the increased erythroid cell death during definitive erythropoiesis.

To determine whether the anemia in Stat5$^{-/-}$ embryos was due to a defect in erythroid differentiation, fetal liver cells were analyzed for erythroid markers Ter-119 and TfR-1. This combination allows staging of maturing erythroid cells from immature progenitors (TfR-1^{low} Ter-119^{low}) over an intermediate stage (TfR-1^{high} Ter-119^{high}) to late orthochromatophilic erythroblasts (TfR-1^{neg} Ter-119^{high}; Figure 4A left; gates R1 to R5, increasing maturity[58]). Stat5-deficient and wt fetal livers contained cells of all differentiation stages at indistinguishable frequencies (Figure 4A). For detailed morphologic analysis, wt and Stat5$^{-/-}$ fetal liver cells were sorted according to their cell-surface marker phenotype (R2-R5), spun onto glass slides, and subsequently stained with either May-Grunwald Giemsa or Benzidine-Wright Giemsa (Figure S4). No apparent morphologic differences in maturity between wt and Stat5$^{-/-}$ cells were observed. Thus, the reduction in fetal liver cellularity (Figure 1B) was probably not due to differentiation arrest at a distinct step of maturation. We did, however, observe a reproducible decrease in TfR-1 cell-surface expression, which prompted us to align the gating strategy accordingly.

Accumulation of hemoglobin is the hallmark of terminal erythropoiesis, requiring an enormous up-regulation of iron intake via increased expression of TfR-1. Quantification of TfR-1 levels in Stat5-deficicient versus wt cells by flow cytometry revealed a greater than 2-fold reduction in knockout cells (Figure 4B). This was confirmed at the mRNA level (Figure 4C) and further corroborated by Western blot analysis of wt, Stat5$^{+/-}$, and Stat5$^{-/-}$ fetal liver cell lysates (Figure 4D,E). A recent report described functional Stat5-binding sites (interferon-gamma–activated sequence [GAS] elements) in the first intron of the TfR-1 gene, using an erythroleukemic cell line expressing a constitutively active Stat5 variant.[59] To corroborate these data, we decided to analyze DNA binding of endogenous Stat5 to these elements in primary fetal liver erythroblasts after Epo stimulation by chromatin immunoprecipitation (Figure 4F). Indeed, DNA binding of Stat5 to all 3 sites analyzed was confirmed and apparently resulted in an Epo-induced increase of TfR-1 mRNA as quantified by qPCR (Figure 4G). As expected from the well-known inverse relation in expression of TfR-1 to the iron-storage protein ferritin,[30] Stat5$^{-/-}$ cells showed elevated levels of ferritin protein (Figure S5).

As a direct consequence of reduced TfR-1 cell-surface expression, we observed a significant reduction of intracellular iron (approximately 40%) in freshly isolated Stat5$^{-/-}$ fetal livers as measured by atomic absorption spectrometry (Figure 4H), further supporting the idea of altered iron metabolism in Stat5$^{-/-}$ cells. Reduced iron availability leads to a drop in heme synthesis,[60] known to result in activation of heme-regulated inhibitor (HRI).[61] This kinase, via inactivation of translation initiation factor eIF2-alpha, throttles expression of globins to ensure that heme, alpha-globin, and beta-globin are always synthesized at the appropriate ratio of 4:2:2.[61] To test whether this regulatory circuit was disturbed in Stat5$^{-/-}$ erythroid cells, an abundance of globin mRNAs in lysates from erythroid cells sorted out of wt or Stat5$^{-/-}$ fetal livers were analyzed by qPCR. Indeed, relative levels of both globin mRNAs were significantly reduced in Stat5$^{-/-}$ cells; moreover, eIF2-alpha showed the expected increase in phosphorylation (Figure S6). In summary, these data demonstrated that Stat5$^{-/-}$ erythroid cells were severely iron-deficient.

IRP-2 expression and mRNA-binding activity is reduced in Stat5-deficient cells

Stabilization of TfR-1 mRNA by binding of IRP-1 and IRP-2 is considered the predominant mechanism to satisfy the iron demand of proliferating cells.[30,31] A possible activation of IRPs by Epo has been discussed.[62,63] Accordingly, Western blot analyses for IRP-1 and IRP-2 from lysates of wt and Stat5$^{-/-}$ primary erythroblasts revealed a striking, 5-fold down-regulation of IRP-2 in Stat5 knockout cells (Figure 5A,B right), accompanied by a 2-fold up-regulation in IRP-1 expression. IRP-1 and IRP-2 mRNA levels were similarly changed in Stat5-deficent cells (data not shown). Determination of IRP-2 RNA binding in Stat5$^{-/-}$ cells using in vitro–transcribed, radioactively labeled IRE probes in electrophoretic mobility shift assays (EMSAs; Figure 5C) showed a similar decrease of IRP-2 activity (Figure 5D). Given the important role of IRP-2 in TfR-1 expression in erythroid cells,[38,39] these data

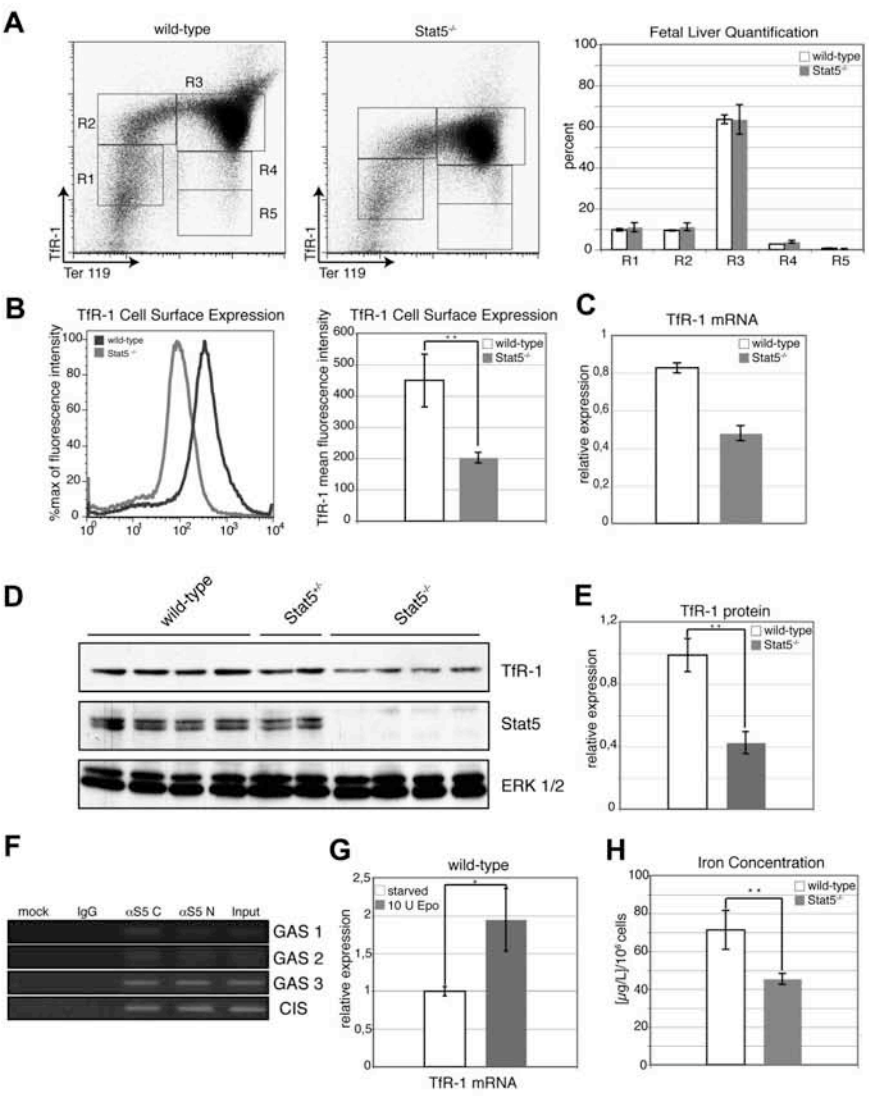

Figure 4. Cell-surface expression of TfR-1 is strongly reduced in Stat5$^{-/-}$ erythroid progenitors. (A) Representative flow cytometry histograms of E13.5 wt and Stat5$^{-/-}$ fetal liver cells stained for the erythroid markers TfR-1 and Ter-119 (left). The sequence from gate R1 (TfR-1^{low} Ter-119^{low}) to gate R5 (TfR-1^{-} Ter-119^{high}) represents development from the most immature erythroid progenitors (late BFU-E; CFU-E) to mature erythroid cells (orthochromatic erythroblasts; reticulocytes).[58] Quantification of gates R1 to R5 (data are presented as means ± SD; n = 4) (right). (B) Cell-surface expression of TfR-1 of Ter-119^{high} gated wt (dark gray line) or Stat5$^{-/-}$ (light gray line) fetal liver cells (left). Quantification of TfR-1 cell-surface expression of wt and Stat5$^{-/-}$ fetal livers (right; data are presented as means ± SD; n = 4). (C) Expression of TfR-1 mRNA from lysates of freshly isolated wt or Stat5$^{-/-}$ fetal liver cells (data are presented as means ± SD; n = 3). Expression was normalized on hypoxanthine-guanine phosphoribosyltransferase (HPRT) levels. (D) Western blot analysis of freshly isolated wt and Stat5$^{-/-}$ fetal liver cell lysates for TfR-1. ERK was used as loading control. (E) Densitometric quantification of TfR-1 Western blot in 3D (data are presented as means ± SD; n = 4). (F) Primary wt fetal liver erythroblasts were stimulated with Epo for 30 minutes and ChIP for Stat5 was performed. DNA from Epo-stimulated primary wt erythroblasts was recovered using 2 different antisera directed against N- or C-terminal epitopes (αS5 C, αS5 N). Specific PCR products from Stat5-binding sites GAS 1, GAS 2, and GAS 3 in *TfR-1* intron 1[59] were only obtained with Stat5-specific antibodies but not with control IgGs. PCR for the genuine Stat5 site in the *CIS* promoter was used as positive control. (G) Primary wt fetal liver–derived erythroblasts were factor depleted for 2.5 hours, followed by 1.5 hours of Epo stimulation (10 U/mL). TfR-1 mRNA expression was scored by qPCR normalized on HPRT (data are presented as means ± SD; n = 4). (H) Iron concentration in freshly isolated fetal liver lysates determined via atomic absorption spectrometry (data are presented as means ± SD; n = 4; for experimental details, see Document S1). *$P < .05$; **$P < .01$.

strongly suggested that the decrease of IRP-2 was an additional cause for reduction of TfR-1 cell-surface expression.

IRP-2 is a direct transcriptional target of Stat5

To test a possible direct role of Stat5 in regulating *IRP-2* expression, we analyzed the *IRP-2* promoter in detail. A region 1030 to 1100 bp upstream of the transcriptional start site contained one perfect Stat5 DNA-binding site (TTCN$_3$GAA)[65] plus 2 adjacent low-affinity Stat5 response elements with a mismatch in one half-site of the inverted repeat (Figure 6A). Annotated Stat5 sites[24,65] together with the IRP-2 sequence I suggested that the latter fulfilled bioinformatic criteria for perfect Stat5 binding (Figure 6B).

To test whether there was a direct transcriptional induction of *IRP-2* by Stat5, the 2 kb fragment of the *IRP-2* promoter upstream of the predicted transcription start site, comprising all 3 putative Stat5 response elements (REs), was inserted into a firefly-luciferase reporter gene construct. 293T cells were cotransfected with Stat5a and EpoR cDNAs together with the respective reporter construct. Transfected cells were stimulated with Epo or left untreated. Epo-treated cells displayed a significant increase of luminescence over untreated controls (Figure 6C). Direct Epo-induced expression of endogenous *IRP-2* and *oncostatin M* (a bona fide Stat5 target gene) was demonstrated in murine erythroid leukemia cells: following 3 hours of factor deprivation, cells were restimulated for 1 hour with Epo and mRNA expression levels determined by qPCR. Epo stimulation induced expression of IRP-2 as well as oncostatin M about 3-fold (Figure 6D).

To further substantiate that IRP-2 is a direct target of Stat5, EMSAs were performed. 293T cells were cotransfected with constructs encoding EpoR and murine Stat5a. Transfected cells were Epo-stimulated or left untreated. Extracts were subsequently subjected to EMSAs using radiolabeled oligonucleotides encompassing either the newly identified Stat5-RE I of the IRP-2 promoter or a well-described Stat5-RE probe from the bovine β-casein promoter as positive control. For supershifts, a serum directed against the C-terminus of Stat5 was added to the oligonucleotide/lysate mixture. Stat5-DNA complexes were clearly evident in Epo-stimulated extracts, using both the IRP-2-I or the β-casein probe, as these complexes were readily super-shifted upon addition of anti-Stat5 serum (Figure 6E). Similar results were obtained using Epo-stimulated cells transfected with murine Stat5b (data not shown).

To test whether Stat5 recognizes one of these putative DNA-binding sites in vivo, we finally performed chromatin-immunoprecipitation (ChIP) experiments using 2 different antisera directed

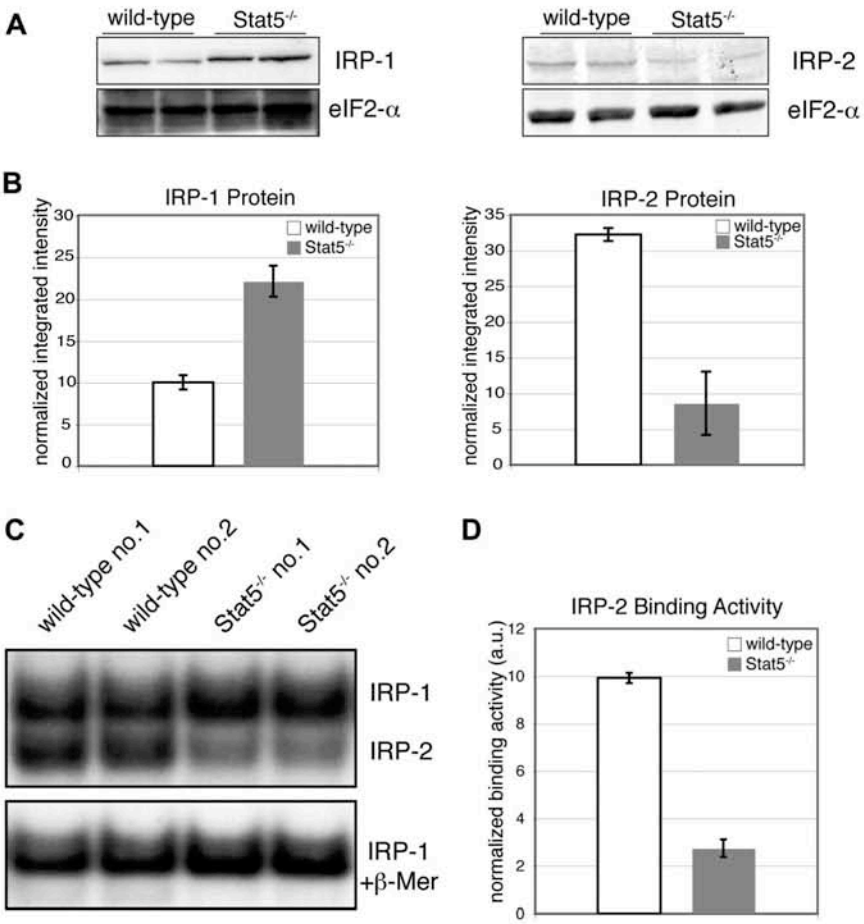

Figure 5. Stat5-deficient erythroid cells display reduced *IRP-2* expression and mRNA-binding activity. (A) Western blot analysis of primary wt and Stat5$^{-/-}$ erythroblast lysates for IRP-1 (left panel) and IRP-2 (right panel). (B) Quantification of Western blot analysis from panel A (data are presented as means ± SD). Samples were normalized on eIF4E as levels and quantified using the Odyssey infrared imaging system. (C) Two representative lysates each of wt and Stat5$^{-/-}$ erythroblasts were subjected to RNA-EMSAs for IRP-1 and IRP-2 using an IRE-RNA probe corresponding to the IRE of mouse ferritin heavy chain[64] (for experimental details, see Document S1). (D) Quantification of IRP-2–binding activity (data are presented as means ± SD; n = 4). *$P < .05$; **$P < .01$.

against N- or C-terminal epitopes in Stat5. PCR analysis of immunoprecipitated Stat5-DNA complexes from Epo-stimulated primary wt erythroblasts yielded a PCR product representing Stat5-binding sites in the *IRP-2* promoter in both specific Stat5 ChIPs, but not in control IgG ChIP experiments (Figure 6F).

Together, these results indicated that Stat5 is directly involved in the control of *TfR-1* transcription as well as in the modulation of its mRNA stability by regulating expression of *IRP-2*.

Discussion

In this paper cooperating mechanisms underlying the erythroid defect leading to microcytic anemia in Stat5$^{-/-}$ mice were uncovered, demonstrating a novel direct link between the EpoR-Stat5 axis and regulation of iron metabolism in vivo. First, Stat5$^{-/-}$ fetal livers showed reduced cellularity due to massively enhanced apoptosis of maturing erythroid cells, apparently caused by defective expression of the antiapoptotic genes *Mcl-1* and *Bcl-x$_L$*. Second, Stat5$^{-/-}$ erythroid cells exhibited reduced expression of IRP-2 and TfR-1, resulting in a large decrease of TfR-1 cell surface expression, iron uptake, and globin synthesis. Together, these mechanisms appear to be sufficient to explain the severe anemia of Stat5$^{-/-}$ animals.

Complete ablation of Stat5 leads to early lethality

None of the conditional Stat5 knockout models created so far in multiple cell types such as hemangioblasts (Stat5fl/fl Tie2-Cre),[59] B cells (CD19-Cre),[66] T cells (CD4-Cre, Lck-Cre),[23,24] hepatocytes (albumin-Cre, albumin-alpha-fetoprotein-Cre),[25,67] pancreatic β cells/hypothalamus (Rip-Cre),[68] endocrine/exocrine pancreas progenitors (Pdx1-Cre),[68] or skeletal muscle (Myf5-Cre)[69] die during fetal development. In contrast, ablation of Stat5 in the entire organism resulted in mortality[8] during gestation or at latest shortly after birth. Since Epo$^{-/-}$, EpoR$^{-/-}$, and Jak2$^{-/-}$ mice all die in utero at E13.5 due to defects in definitive erythropoiesis and given the prominent role of Stat5 in EpoR signaling, it was unexpected that a few Stat5$^{-/-}$ embryos developed to term.

There are several possible explanations for the discrepancy in phenotypes. First, we detected high levels of pY-Stat1 and pY-Stat3 in Stat5-deficient cultivated primary erythroblasts as well as in lysates from freshly isolated fetal livers but not in wt counterparts (M.A.K., F.G., unpublished data). This is in line with increased pY-Stat1 and pY-Stat3 levels found upon liver-specific Stat5 deletion.[67,70,71] Since Stat3 and Stat5 response elements are similar,[65] increased activation of Stat3 might partially compensate for loss of Stat5. Second, the anemia of Stat5$^{-/-}$ embryos led to a compensatory elevation of Epo levels in the serum, which was most pronounced in the few newborn animals. This might contribute to prolonged survival mediated by hyperactivation of Stat5-independent EpoR signaling. Third, Stat5-deficient erythroid cells exhibited elevated levels of phosphorylated eIF2-alpha, indicative for an active "integrated stress response" (ISR), presumably via the kinase HRI.[72] In mouse models for the red blood cell disorders erythropoietic protoporphyria and β-thalassemia, ablation of HRI exacerbated the phenotype of these diseases.[72] Thus, the modulation

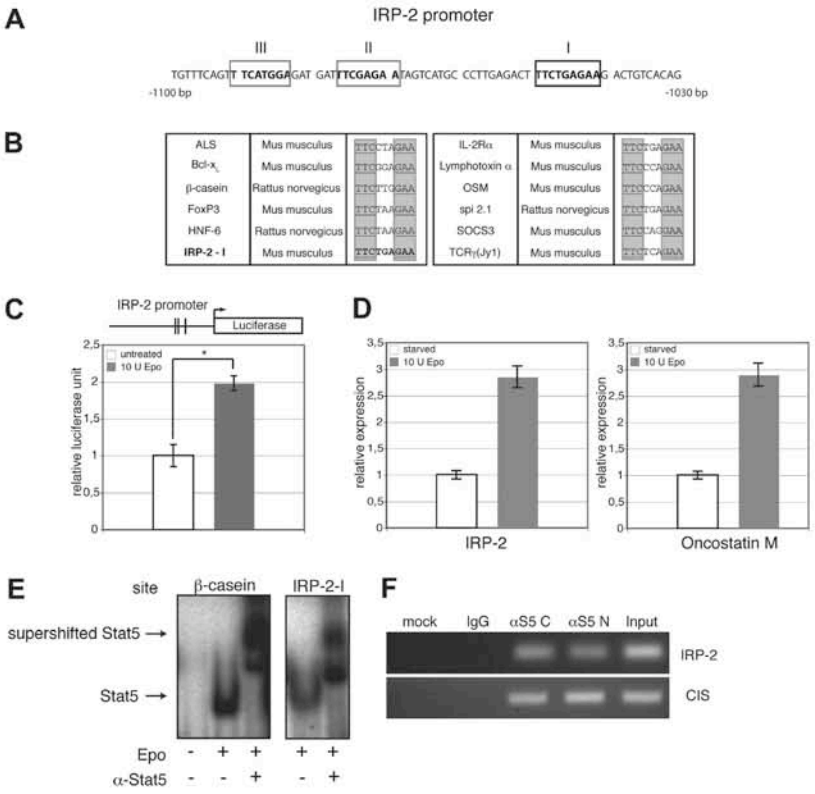

Figure 6. Loss of Stat5 directly decreases IRP-2 gene expression. (A) Sequence of the IRP-2 promoter −1030 bp to −1100 bp upstream of the transcription start, showing one perfect GAS site (boxed in black) and 2 GAS sites with one mismatch (boxed in gray). (B) Multiple perfect Stat5 sites taken from Yao et al[26] and Ehret et al[65] together with the IRP-2-I. (C) Luciferase reporter assay using a DNA fragment ranging from 2 kb immediately upstream of the predicted IRP-2 transcription start site. Vertical lines indicate the approximate positions of the putative Stat5 response elements. 293T cells were cotransfected with constructs encoding IRP-2-firefly-luciferase, renilla-luciferase, Stat5a, and EpoR. Cells were treated with 10 U/mL Epo or left untreated, and luminescence was scored 3 hours later. Transfection efficiencies were normalized to renilla-luciferase activity (representative experiment; error bars are SD of experimental triplicates). (D) Epo-dependent induction of endogenous *IRP-2* and *oncostatin M* analyzed via quantitative PCR in murine erythroid leukemia cells serum deprived for 3 hours, followed by stimulation with 10 U/mL Epo (1 hour). Quantitative PCR was normalized on HPRT (data are presented as means ± SD; n = 4). (E) 293T cells were cotransfected with constructs for EpoR and wt Stat5a, followed by 30 minutes of stimulation with 10 U Epo/mL. Whole-cell extracts of these cells were subjected to EMSAs using either the IRP-2-I oligonucleotide (left) or β-casein oligonucleotide as positive control (right). Respective arrows indicate Stat5 DNA complexes and Stat5 DNA complex supershifts. (F) Primary wt fetal liver erythroblasts were stimulated with Epo for 30 minutes, and ChIP for Stat5 was performed. Recovered DNA was analyzed for the presence of promoters of IRP-2 and CIS (positive control) by PCR. $^*P < .05$; $^{**}P < .01$.

of translational efficiency to balance heme and globin production could represent another protective mechanism accounting for the "mild" erythroid phenotype of Stat5$^{-/-}$ animals. Nevertheless, the ultimate reason for the early death of the animals remains to be determined.

Stat5 is not essential for erythroid differentiation

Earlier studies addressing the role of Stat5 (ie, Stat5a and Statb) in erythropoiesis were performed with *Stat5*$^{\Delta N/\Delta N}$ animals. These mice are born, viable, and show only a mild erythroid phenotype.[20,21] *Stat5*$^{\Delta N/\Delta N}$ animals express a N-terminally truncated Stat5, which still activates target genes.[22] Here, we used Stat5$^{-/-}$ mice lacking the entire *Stat5a/b* locus.[8] Animals lacking other components of Epo signaling upstream of Stat5 (Epo, EpoR, or Jak2),[2] all die in utero around E13.5 due to a block in definitive erythropoiesis. If Stat5 was the only crucial target of this pathway, full Stat5 knockout animals should show a similarly severe phenotype. Indeed, Stat5-deficient animals display erythroid defects and die at latest after birth. Although Stat5 is essential for differentiation of other hematopoietic lineages like maturation of pre-pro– to pro-B cells,[23,24] or in formation of FoxP3$^+$ regulatory T cells,[26] the observed block in erythroid maturation in vivo was not complete. The presence of erythroid cells at all developmental stages in Stat5$^{-/-}$ embryos strongly argued against an absolutely essential function of Stat5 in erythroid development. Nevertheless, there were defects in hemoglobinization of Stat5$^{-/-}$ erythroid cells, which may have several causes. For instance, it could decrease through direct defects in the erythroid differentiation program and/or through a secondary response to iron deficiency.

Involvement of Stat5 in iron metabolism

The most striking observation in the peripheral blood morphology of Stat5$^{-/-}$ animals was an apparent microcytic hypochromic anemia. This type of anemia, characterized by decreased mean corpuscular volume and reduced mean cell hemoglobin, is frequently associated with iron deficiency. Thus, it was tempting to investigate the molecular players involved.

The normal adaptive response to low iron is the well-characterized feedback regulation that increases TfR-1 mRNA stability upon binding of IRPs to its 3′-UTR (Figure 7). In Stat5$^{-/-}$ cells, this response apparently was impeded as delineated from the reduced expression of TfR-1, which in turn was the direct result of decreased IRP-2 protein levels. This mechanistic link was further substantiated by the measured reduction in total intracellular iron in Stat5$^{-/-}$ fetal livers, finally resulting in decreased globin mRNA expression. It remained unclear, however, whether a connection between Stat5 and IRP-2 expression existed. The promoter region of the *IRP-2* gene contains 3 adjacent potential binding sites for Stat5, which indeed turned out to be functional. Moreover, qPCR showed reduced IRP-2 mRNA abundance in the absence of Stat5. Thus, one could envision a chain of events in Stat5-deficient erythroid cells, starting with decreased IRP-2 and TfR-1 expression, resulting in a net decrease of TfR-1 mRNA stability and abundance, followed by diminished TfR-1 surface expression. The consequence would be insufficient iron uptake (even in iron-depleted cells), ultimately leading to decreased heme synthesis, activation of the integrated stress response pathway and reduced globin mRNA translation. Interestingly, no functional compensation for low IRP-2 levels by the highly homologous IRP-1 protein was observed. This is in line with in vivo

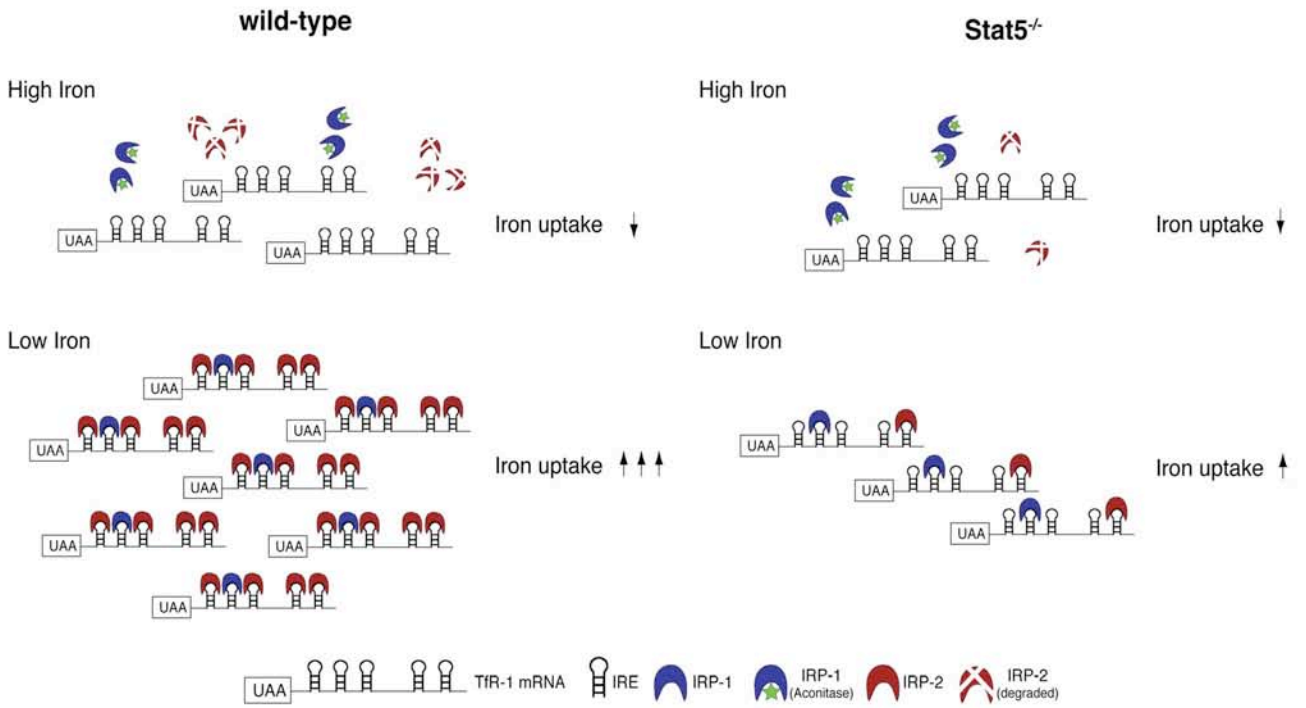

Figure 7. Model for involvement of Stat5 in iron uptake. Left side shows that in iron-replete cells, IRP-1 is converted into cytosolic aconitase (catalyzes isomerization of citrate to isocitrate in the citric acid cycle and exhibits no mRNA-binding affinity; green asterisk) and IRP-2 is degraded. Therefore, both cannot bind to IREs in the 3′UTR of TfR-1 mRNA. Free unprotected IREs in turn enhance degradation rates of TfR-1 mRNA, resulting in reduced iron uptake. In iron-depleted cells, IRP-1 and IRP-2 bind to the respective IREs, thereby stabilizing TfR-1 mRNA, resulting in increased iron uptake. The right side shows Stat5$^{-/-}$. Due to lack of Stat5, basal TfR-1 transcript abundance is reduced in comparison to wt cells. In addition, Stat5 deficiency further results in decreased levels of IRP-2 and, in consequence, a reduction of binding to IREs in the 3′UTR of TfR-1 mRNA and decreased transcript stabilization. Together, this constitutes a double-negative effect on erythroid iron uptake even in a situation of high iron demand, as in iron-deficiency anemia. $^{*}P < .05$; $^{**}P < .01$.

data from corresponding IRP-1 or IRP-2 knockout animals,[38,39] which indicated that IRP-2 is the predominant regulatory factor modulating TfR-1 mRNA stability. While ablation of *IRP-1* produced no overt phenotype, loss of *IRP-2* resulted in hypochromic microcytic anemia due to reduced TfR-1 expression, a phenotype reminiscent to the one of Stat5 knockout animals described here. Accordingly, lowering the expression of TfR-1 by 50% led to a similar phenotype, as TfR-1$^{+/-}$ mice also displayed the same type of anemia.[73] It should be mentioned, however, also other conditions are known to result in microcytosis, including ablation of the genuine Stat5 target Pim-1.[9]

Involvement of Stats in iron metabolism might even be a more general mechanism. Hepcidin,[74,75] the dominant regulator of dietary iron absorption in enterocytes and iron release from macrophages, is a direct Stat3 target gene[74,75]: upon infection, the inflammatory cytokine IL-6 promotes hepcidin expression via Stat3, trapping iron in macrophages, resulting in decreased plasma iron concentrations. Hepcidin expression is decreased by hypoxia and anemia, directly responding to increased Epo levels.[74-76] Thus, its regulation in the anemia resulting from Stat5 deficiency may be of interest in future studies.

Stat5$^{-/-}$ fetal liver cells exhibit high levels of apoptosis

In erythropoiesis, up-regulation of Bcl-x_L was found to be defective in Stat5$^{\Delta N/\Delta N}$ erythroid cells.[20,21] Other studies, however, suggested that Bcl-x_L prevents apoptosis only of late-stage erythroblasts,[11,77] but not directly via EpoR.[77] Upon readdressing this question in mice that are fully devoid of Stat5, we observed a reduction in Bcl-x_L levels of about 50% in fetal liver erythroid cells. Furthermore, Mcl-1 expression in Stat5$^{-/-}$ erythroid cells was analyzed, based on the finding that this *Bcl-2* gene family member could be a Stat5 target gene.[52,53,78] Indeed, Mcl-1 was completely absent in Stat5$^{-/-}$ fetal liver cells, whereas Epo stimulation of wt primary erythroblasts led to a 3.5-fold increase of Mcl-1 mRNA. Furthermore, reintroduction of Mcl-1 or Bcl-x_L completely prevented apoptosis of wt as well as Stat5 knockout erythroblasts upon Epo withdrawal.

Besides the finding that Mcl-1 is a Stat5-dependent Epo target gene, down-regulation of Mcl-1 in Stat5$^{-/-}$ erythroid cells could also occur through an additional mechanism, which is induced through iron deficiency in Stat5 knockout animals. Recently, it was suggested that Mcl-1 levels decrease after activation of the phospho-eIF2-alpha–mediated ISR pathway already mentioned.[79-81] eIF2-alpha phosphorylation can be induced by different kinases in response to several stress stimuli,[82] including HRI. Iron deficiency activates HRI, which in turn phosphorylates eIF2-alpha on its inhibitory Ser51, resulting in global reduction of mRNA translation,[61] which immediately affects Mcl-1, as it is a highly unstable protein.[83] The observed reduced iron levels, together with elevated eIF2-alpha phosphorylation in Stat5$^{-/-}$ primary erythroblasts, suggested an active ISR in Stat5$^{-/-}$ cells. Hence, loss of Stat5 could lead to a direct decrease of Mcl-1 mRNA, but alternatively also to a down-regulation of Mcl-1 protein due to iron deficiency–induced ISR. Taken together, the apoptosis in Stat5$^{-/-}$ fetal livers most probably reflects a composite effect of reduced levels of Bcl-x_L and loss of Mcl-1.

This contribution should help to clarify the long-discussed role of Stat5 in erythropoiesis in vivo: We identify Stat5 as a key factor

regulating erythroid iron metabolism in vivo and, additionally, link the antiapoptotic machinery of erythroid cells with their iron uptake system.

Acknowledgments

We thank L. Hennighausen for providing Stat5$^{-/-}$ mice, G. Stengl for FACS sorting, G. Litos for technical assistance, and M. von Lindern for critical reading of the manuscript. We are grateful to R. S. Eisenstein and T. Roault for antibodies against IRP-1 and IRP-2, respectively.

This work was supported by grants WK-001 (to F.G. and M.A.K.) and SFB F028 (to H.B., R.M., and E.W.M.) from the Austrian Research Foundation, Fonds zur Föderung der wissenschaftlichen Forschung (FWF), and the Herzfelder Family Foundation (to E.W.M.).

Authorship

Contribution: M.A.K., F.G., H.G., M.S., M.A., and B.K. conducted experiments; M.A.K. and E.W.M. designed experiments and interpreted results; H.B. contributed essential reagents and worked on the draft of the manuscript; and M.A.K., R.M., and E.W.M. wrote the paper.

Conflict-of-interest disclosure: The authors declare no competing financial interests.

Correspondence: Ernst W. Müllner, Max F. Perutz Laboratories, Department of Medical Biochemistry, Medical University of Vienna, Dr. Bohr-Gasse 9, A-1030 Vienna, Austria; e-mail: ernst.muellner@meduniwien.ac.at.

References

1. Cantor AB, Orkin SH. Transcriptional regulation of erythropoiesis: an affair involving multiple partners. Oncogene. 2002;21:3368-3376.
2. Richmond TD, Chohan M, Barber DL. Turning cells red: signal transduction mediated by erythropoietin. Trends Cell Biol. 2005;15:146-155.
3. Klingmuller U, Wu H, Hsiao JG, et al. Identification of a novel pathway important for proliferation and differentiation of primary erythroid progenitors. Proc Natl Acad Sci U S A. 1997;94:3016-3021.
4. Chen C, Sytkowski AJ. Erythropoietin regulation of Raf-1 and MEK: evidence for a Ras-independent mechanism. Blood. 2004;104:73-80.
5. von Lindern M, Parren-van Amelsvoort M, van Dijk T, et al. Protein kinase C alpha controls erythropoietin receptor signaling. J Biol Chem. 2000; 275:34719-34727.
6. Tong Q, Chu X, Cheung JY, et al. Erythropoietin-modulated calcium influx through TRPC2 is mediated by phospholipase Cgamma and IP3R. Am J Physiol Cell Physiol. 2004;287:C1667-C1678.
7. Teglund S, McKay C, Schuetz E, et al. Stat5a and Stat5b proteins have essential and nonessential, or redundant, roles in cytokine responses. Cell. 1998;93:841-850.
8. Cui Y, Riedlinger G, Miyoshi K, et al. Inactivation of Stat5 in mouse mammary epithelium during pregnancy reveals distinct functions in cell proliferation, survival, and differentiation. Mol Cell Biol. 2004;24:8037-8047.
9. Laird PW, van der Lugt NM, Clarke A, et al. In vivo analysis of Pim-1 deficiency. Nucleic Acids Res. 1993;21:4750-4755.
10. Wilson A, Murphy MJ, Oskarsson T, et al. c-Myc controls the balance between hematopoietic stem cell self-renewal and differentiation. Genes Dev. 2004;18:2747-2763.
11. Wagner KU, Claudio E, Rucker EB 3rd, et al. Conditional deletion of the Bcl-x gene from erythroid cells results in hemolytic anemia and profound splenomegaly. Development. 2000;127: 4949-4958.
12. Sasaki A, Yasukawa H, Shouda T, Kitamura T, Dikic I, Yoshimura A. CIS3/SOCS-3 suppresses erythropoietin (EPO) signaling by binding the EPO receptor and JAK2. J Biol Chem. 2000;275: 29338-29347.
13. Kozar K, Ciemerych MA, Rebel VI, et al. Mouse development and cell proliferation in the absence of D-cyclins. Cell. 2004;118:477-491.
14. Moriggl R, Sexl V, Kenner L, et al. Stat5 tetramer formation is associated with leukemogenesis. Cancer Cell. 2005;7:87-99.
15. Menon MP, Karur V, Bogacheva O, Bogachev O, Cuetara B, Wojchowski DM. Signals for stress erythropoiesis are integrated via an erythropoietin receptor-phosphotyrosine-343-Stat5 axis. J Clin Invest. 2006;116:683-694.
16. Wu H, Liu X, Jaenisch R, Lodish HF. Generation of committed erythroid BFU-E and CFU-E progenitors does not require erythropoietin or the erythropoietin receptor. Cell. 1995;83:59-67.
17. Parganas E, Wang D, Stravopodis D, et al. Jak2 is essential for signaling through a variety of cytokine receptors. Cell. 1998;93:385-395.
18. Neubauer H, Cumano A, Muller M, Wu H, Huffstadt U, Pfeffer K. Jak2 deficiency defines an essential developmental checkpoint in definitive hematopoiesis. Cell. 1998;93:397-409.
19. Menon MP, Fang J, Wojchowski DM. Core erythropoietin receptor signals for late erythroblast development. Blood. 2006;107:2662-2672.
20. Socolovsky M, Fallon AE, Wang S, Brugnara C, Lodish HF. Fetal anemia and apoptosis of red cell progenitors in Stat5a-/-5b-/- mice: a direct role for Stat5 in Bcl-X(L) in-duction. Cell. 1999;98:181-191.
21. Socolovsky M, Nam H, Fleming MD, Haase VH, Brugnara C, Lodish HF. Ineffective erythropoiesis in Stat5a(-/-)5b(-/-) mice due to decreased survival of early erythro-blasts. Blood. 2001;98: 3261-3273.
22. Dolznig H, Grebien F, Deiner EM, et al. Erythroid progenitor renewal versus differentiation: genetic evidence for cell autonomous, essential functions of EpoR, Stat5 and the GR. Oncogene. 2006;25: 2890-2900.
23. Hoelbl A, Kovacic B, Kerenyi MA, et al. Clarifying the role of Stat5 in lymphoid development and Abelson-induced transformation. Blood. 2006; 107:4898-4906.
24. Yao Z, Cui Y, Watford WT, et al. Stat5a/b are essential for normal lymphoid development and differentiation. Proc Natl Acad Sci U S A. 2006;103: 1000-1005.
25. Engblom D, Kornfeld JW, Schwake L, et al. Direct glucocorticoid receptor-Stat5 interaction in hepatocytes controls body size and maturation-related gene expression. Genes Dev. 2007;21:1157-1162.
26. Yao Z, Kanno Y, Kerenyi M, et al. Nonredundant roles for Stat5a/b in directly regulating Foxp3. Blood. 2007;109:4368-4375.
27. Aisen P. Transferrin receptor 1. Int J Biochem Cell Biol. 2004;36:2137-2143.
28. Mullner EW, Kuhn LC. A stem-loop in the 3′ untranslated region mediates iron-dependent regulation of transferrin receptor mRNA stability in the cytoplasm. Cell. 1988;53:815-825.
29. Chan RY, Seiser C, Schulman HM, Kuhn LC, Ponka P. Regulation of transferrin receptor mRNA expression. Distinct regulatory features in erythroid cells. Eur J Biochem. 1994;220:683-692.
30. Hentze MW, Muckenthaler MU, Andrews NC. Balancing acts: molecular control of mammalian iron metabolism. Cell. 2004;117:285-297.
31. Rouault TA. The role of iron regulatory proteins in mammalian iron homeostasis and disease. Nat Chem Biol. 2006;2:406-414.
32. Pantopoulos K. Iron metabolism and the IRE/IRP regulatory system: an update. Ann N Y Acad Sci. 2004;1012:1-13.
33. Haile DJ, Rouault TA, Harford JB, et al. Cellular regulation of the iron-responsive element binding protein: disassembly of the cubane iron-sulfur cluster results in high-affinity RNA binding. Proc Natl Acad Sci U S A. 1992;89:11735-11739.
34. Guo B, Phillips JD, Yu Y, Leibold EA. Iron regulates the intracellular degradation of iron regulatory protein 2 by the proteasome. J Biol Chem. 1995;270:21645-21651.
35. Koeller DM, Casey JL, Hentze MW, et al. A cytosolic protein binds to structural elements within the iron regulatory region of the transferrin receptor mRNA. Proc Natl Acad Sci U S A. 1989;86: 3574-3578.
36. Binder R, Horowitz JA, Basilion JP, Koeller DM, Klausner RD, Harford JB. Evidence that the pathway of transferrin receptor mRNA degradation involves an endonucleolytic cleavage within the 3′ UTR and does not involve poly(A) tail shortening. EMBO J. 1994;13:1969-1980.
37. Mullner EW, Neupert B, Kuhn LC. A specific mRNA binding factor regulates the iron-dependent stability of cytoplasmic transferrin receptor mRNA. Cell. 1989;58:373-382.
38. Galy B, Ferring D, Minana B, et al. Altered body iron distribution and microcytosis in mice deficient in iron regulatory protein 2 (IRP2). Blood. 2005; 106:2580-2589.
39. Cooperman SS, Meyron-Holtz EG, Olivierre-Wilson H, Ghosh MC, McConnell JP, Rouault TA. Microcytic anemia, erythropoietic protoporphyria, and neurodegeneration in mice with targeted deletion of iron-regulatory protein 2. Blood. 2005; 106:1084-1091.
40. Grebien F, Kerenyi MA, Kovacic B, et al. Stat5 activation enables erythropoiesis in the absence of EpoR and Jak2. Blood. 2008;111:4511-4522.
41. Eisenstein RS, Tuazon PT, Schalinske KL, Anderson SA, Traugh JA. Iron-responsive element-binding protein. Phosphorylation by protein kinase C. J Biol Chem. 1993;268:27363-27370.

42. LeBaron MJ, Xie J, Rui H. Evaluation of genome-wide chromatin library of Stat5 binding sites in human breast cancer. Mol Cancer. 2005;4:6.
43. Livak KJ, Schmittgen TD. Analysis of relative gene expression data using real-time quantitative PCR and the 2(-Delta Delta C(T)) method. Methods. 2001;25:402-408.
44. Gruber M, Hu CJ, Johnson RS, Brown EJ, Keith B, Simon MC. Acute postnatal ablation of Hif-2alpha results in anemia. Proc Natl Acad Sci U S A. 2007;104:2301-2306.
45. Snow JW, Abraham N, Ma MC, Abbey NW, Herndier B, Goldsmith MA. STAT5 promotes multilineage hematolymphoid development in vivo through effects on early hematopoietic progenitor cells. Blood. 2002;99:95-101.
46. Bunting KD, Bradley HL, Hawley TS, Moriggl R, Sorrentino BP, Ihle JN. Reduced lymphomyeloid repopulating activity from adult bone marrow and fetal liver of mice lacking expression of STAT5. Blood. 2002;99:479-487.
47. Bakker WJ, van Dijk TB, Parren-van Amelsvoort M, et al. Differential regulation of Foxo3a target genes in erythropoiesis. Mol Cell Biol. 2007;27:3839-3854.
48. Carotta S, Pilat S, Mairhofer A, et al. Directed differentiation and mass cultivation of pure erythroid progenitors from mouse embryonic stem cells. Blood. 2004;104:1873-1880.
49. Josefsen D, Myklebust JH, Lomo J, Sioud M, Blomhoff HK, Smeland EB. Differential expression of bcl-2 homologs in human CD34(+) hematopoietic progenitor cells induced to differentiate into erythroid or granulocytic cells. Stem Cells. 2000;18:261-272.
50. Opferman JT, Iwasaki H, Ong CC, et al. Obligate role of anti-apoptotic MCL-1 in the survival of hematopoietic stem cells. Science. 2005;307:1101-1104.
51. Huang M, Dorsey JF, Epling-Burnette PK, et al. Inhibition of Bcr-Abl kinase activity by PD180970 blocks constitutive activation of Stat5 and growth of CML cells. Oncogene. 2002;21:8804-8816.
52. Opferman JT, Letai A, Beard C, Sorcinelli MD, Ong CC, Korsmeyer SJ. Development and maintenance of B and T lymphocytes requires antiapoptotic MCL-1. Nature. 2003;426:671-676.
53. Aichberger KJ, Mayerhofer M, Krauth MT, et al. Identification of mcl-1 as a BCR/ABL-dependent target in chronic myeloid leukemia (CML): evidence for cooperative antileukemic effects of imatinib and mcl-1 antisense oligonucleotides. Blood. 2005;105:3303-3311.
54. Moriggl R, Topham DJ, Teglund S, et al. Stat5 is required for IL-2-induced cell cycle progression of peripheral T cells. Immunity. 1999;10:249-259.
55. Fang J, Menon M, Kapelle W, et al. EPO modulation of cell cycle regulatory genes, and cell division, in primary bone marrow erythroblasts. Blood. 2007;110:2361-2370.
56. Akashi K, Traver D, Miyamoto T, Weissman IL. A clonogenic common myeloid progenitor that gives rise to all myeloid lineages. Nature. 2000;404:193-197.
57. Traver D, Miyamoto T, Christensen J, Iwasaki-Arai J, Akashi K, Weissman IL. Fetal liver myelopoiesis occurs through distinct, prospectively isolatable progenitor subsets. Blood. 2001;98:627-635.
58. Zhang J, Socolovsky M, Gross AW, Lodish HF. Role of Ras signaling in erythroid differentiation of mouse fetal liver cells: functional analysis by a flow cytometry-based novel culture system. Blood. 2003;102:3938-3946.
59. Zhu BM, McLaughlin SK, Na R, et al. Hematopoietic-specific Stat5-null mice display microcytic hypochromic anemia associated with reduced transferrin receptor gene expression. Blood. 2008;112:2071-2080.
60. Lange H, Muhlenhoff U, Denzel M, Kispal G, Lill R. The heme synthesis defect of mutants impaired in mitochondrial iron-sulfur protein biogenesis is caused by reversible inhibition of ferrochelatase. J Biol Chem. 2004;279:29101-29108.
61. Chen JJ. Regulation of protein synthesis by the heme-regulated eIF2alpha kinase: relevance to anemias. Blood. 2007;109:2693-2699.
62. Weiss G, Houston T, Kastner S, Johrer K, Grunewald K, Brock JH. Regulation of cellular iron metabolism by erythropoietin: activation of iron-regulatory protein and upregulation of transferrin receptor expression in erythroid cells. Blood. 1997;89:680-687.
63. Sposi NM, Cianetti L, Tritarelli E, et al. Mechanisms of differential transferrin receptor expression in normal hematopoiesis. Eur J Biochem. 2000;267:6762-6774.
64. Schranzhofer M, Schifrer M, Cabrera JA, et al. Remodeling the regulation of iron metabolism during erythroid differentiation to ensure efficient heme biosynthesis. Blood. 2006;107:4159-4167.
65. Ehret GB, Reichenbach P, Schindler U, et al. DNA binding specificity of different STAT proteins: comparison of in vitro specificity with natural target sites. J Biol Chem. 2001;276:6675-6688.
66. Dai X, Chen Y, Di L, et al. Stat5 is essential for early B cell development but not for B cell maturation and function. J Immunol. 2007;179:1068-1079.
67. Cui Y, Hosui A, Sun R, et al. Loss of signal transducer and activator of transcription 5 leads to hepatosteatosis and impaired liver regeneration. Hepatology. 2007;46:504-513.
68. Lee JY, Gavrilova O, Davani B, Na R, Robinson GW, Hennighausen L. The transcription factors Stat5a/b are not required for islet development but modulate pancreatic beta-cell physiology upon aging. Biochim Biophys Acta. 2007;1773:1455-1461.
69. Klover P, Hennighausen L. Postnatal body growth is dependent on the transcription factors signal transducers and activators of transcription 5a/b in muscle: a role for autocrine/paracrine insulin-like growth factor I. Endocrinology. 2007;148:1489-1497.
70. Hosui A, Hennighausen L. Genomic dissection of the cytokine controlled STAT5 signaling network in liver. Physiol Genomics. 2008;34:135-143.
71. Hennighausen L, Robinson GW. Interpretation of cytokine signaling through the transcription factors STAT5A and STAT5B. Genes Dev. 2008;22:711-721.
72. Han AP, Fleming MD, Chen JJ. Heme-regulated eIF2alpha kinase modifies the phenotypic severity of murine models of erythropoietic protoporphyria and beta-thalassemia. J Clin Invest. 2005;115:1562-1570.
73. Levy JE, Jin O, Fujiwara Y, Kuo F, Andrews NC. Transferrin receptor is necessary for development of erythrocytes and the nervous system. Nat Genet. 1999;21:396-399.
74. Ganz T. Hepcidin and its role in regulating systemic iron metabolism. Hematology Am Soc Hematol Educ Program. 2006:29-35, 507.
75. Wrighting DM, Andrews NC. Interleukin-6 induces hepcidin expression through STAT3. Blood. 2006;108:3204-3209.
76. Pinto JP, Ribeiro S, Pontes H, et al. Erythropoietin mediates hepcidin expression in hepatocytes through EPOR signaling and regulation of C/EBP-Palpha. Blood. 2008;111:5727-5733.
77. Rhodes MM, Kopsombut P, Bondurant MC, Price JO, Koury MJ. Bcl-x(L) prevents apoptosis of late-stage erythroblasts but does not mediate the antiapoptotic effect of erythropoietin. Blood. 2005;106:1857-1863.
78. Buettner R, Mora LB, Jove R. Activated STAT signaling in human tumors provides novel molecular targets for therapeutic intervention. Clin Cancer Res. 2002;8:945-954.
79. Fritsch RM, Schneider G, Saur D, Scheibel M, Schmid RM. Translational repression of MCL-1 couples stress-induced eIF2alpha phosphorylation to mitochondrial apoptosis initiation. J Biol Chem. 2007;282:22551-22562.
80. Rahmani M, Davis EM, Crabtree TR, et al. The kinase inhibitor sorafenib induces cell death through a process involving induction of endoplasmic reticulum stress. Mol Cell Biol. 2007;27:5499-5513.
81. Iglesias-Serret D, Pique M, Gil J, Pons G, Lopez JM. Transcriptional and translational control of Mcl-1 during apoptosis. Arch Biochem Biophys. 2003;417:141-152.
82. Rutkowski DT, Kaufman RJ. All roads lead to ATF4. Dev Cell. 2003;4:442-444.
83. Michels J, Johnson PW, Packham G. Mcl-1. Int J Biochem Cell Biol. 2005;37:267-271.

3.2.2 Stat5 enables erythropoiesis in the absence of EpoR and Jak2

Florian Grebien[1], Marc A. Kernyi[1], Boris Kovacic[2], Thomas Kolbe[3,4], Verena Becker[5], Helmut Dolznig[6], Klaus Pfeffer[7], Ursula Klingmüller[5], Mathias Müller[3,8], Hartmut Beug[2], Ernst W. Müllner[1,10] und Richard Moriggl[9,10]

[1]Max F. Perutz Laboratories, Department of Medical Biochemistry, Medical University of Vienna, 1030 Vienna, Austria
[2]Research Institute of Molecular Pathology, 1030 Vienna, Austria
[3]Biomodels Austria, Veterinary University Vienna, 1210 Vienna, Austria
[4]Dept. Agrobiotechnology, IFA-Tulln, Biotechnology in Animal Production, University of Natural Resources and Applied Life Sciences, 1180 Vienna, Austria
[5]German Cancer Research Center, 69120 Heidelberg, Germany
[6]Institute of Pathology, Medical University of Vienna, Waehringer Guertel 18-20, 1090 Vienna, Austria
[7]Institute of Medical Microbiology, Heinrich-Heine University, 40225 Duesseldorf, Germany
[8]Institute of Animal Breeding and Genetics, Veterinary University Vienna, 1210 Vienna, Austria
[9]Ludwig Boltzmann Institute for Cancer Research, 1090 Vienna, Austria
[10]corresponding authors. These authors contributed equally to this work

blood

2008 111: 4511-4522
Prepublished online Jan 31, 2008;
doi:10.1182/blood-2007-07-102848

Stat5 activation enables erythropoiesis in the absence of EpoR and Jak2

Florian Grebien, Marc A. Kerenyi, Boris Kovacic, Thomas Kolbe, Verena Becker, Helmut Dolznig, Klaus Pfeffer, Ursula Klingmüller, Mathias Müller, Hartmut Beug, Ernst W. Müllner and Richard Moriggl

Stat5 activation enables erythropoiesis in the absence of EpoR and Jak2

Florian Grebien,[1] Marc A. Kerenyi,[1] Boris Kovacic,[2] Thomas Kolbe,[3,4] Verena Becker,[5] Helmut Dolznig,[6] Klaus Pfeffer,[7] Ursula Klingmüller,[5] Mathias Müller,[3,8] Hartmut Beug,[2] *Ernst W. Müllner,[1] and *Richard Moriggl[9]

[1]Max F. Perutz Laboratories, Department of Medical Biochemistry, Medical University of Vienna, Vienna, Austria; [2]Research Institute of Molecular Pathology, Vienna, Austria; [3]Biomodels Austria, Veterinary University Vienna, Vienna, Austria; [4]Department of Agrobiotechnology, IFA (Interuniversitären Forschungsinstitutes für Agrarbiotechnologie)–Tulln, Biotechnology in Animal Production, University of Natural Resources and Applied Life Sciences, Vienna, Austria; [5]German Cancer Research Center, Heidelberg, Germany; [6]Institute of Pathology, Medical University of Vienna, Vienna, Austria; [7]Institute of Medical Microbiology, Heinrich-Heine University, Duesseldorf, Germany; [8]Institute of Animal Breeding and Genetics, Veterinary University Vienna, Vienna, Austria; and [9]Ludwig Boltzmann Institute for Cancer Research, Vienna, Austria

Erythropoiesis requires erythropoietin (Epo) and stem cell factor (SCF) signaling via their receptors EpoR and c-Kit. EpoR, like many other receptors involved in hematopoiesis, acts via the kinase Jak2. Deletion of EpoR or Janus kinase 2 (Jak2) causes embryonic lethality as a result of defective erythropoiesis. The contribution of distinct EpoR/Jak2-induced signaling pathways (mitogen-activated protein kinase, phosphatidylinositol 3-kinase, signal transducer and activator of transcription 5 [Stat5]) to functional erythropoiesis is incompletely understood. Here we demonstrate that expression of a constitutively activated Stat5a mutant (cS5) was sufficient to relieve the proliferation defect of Jak2$^{-/-}$ and EpoR$^{-/-}$ cells in an Epo-independent manner. In addition, tamoxifen-induced DNA binding of a Stat5a–estrogen receptor (ER)* fusion construct enabled erythropoiesis in the absence of Epo. Furthermore, c-Kit was able to enhance signaling through the Jak2-Stat5 axis, particularly in lymphoid and myeloid progenitors. Although abundance of hematopoietic stem cells was 2.5-fold reduced in Jak2$^{-/-}$ fetal livers, transplantation of Jak2$^{-/-}$-cS5 fetal liver cells into irradiated mice gave rise to mature erythroid and myeloid cells of donor origin up to 6 months after transplantation. Cytokine- and c-Kit pathways do not function independently of each other in hematopoiesis but cooperate to attain full Jak2/Stat5 activation. In conclusion, activated Stat5 is a critical downstream effector of Jak2 in erythropoiesis/myelopoiesis, and Jak2 functionally links cytokine- with c-Kit-receptor tyrosine kinase signaling. (Blood. 2008;111:4511-4522)

Introduction

Erythropoiesis is a tightly controlled process in bone marrow and spleen of adult mammals and in the fetal liver of embryos that produces highly variable erythrocyte numbers during fetal development and in diseases such as anemia, induced by, for example, hypoxia or blood loss. Erythroid maturation proceeds through burst-forming unit-erythroid (BFU-E) and colony-forming unit-erythroid (CFU-E) stages, the latter cell type dividing 4 to 5 times while maturing into erythrocytes in response to erythropoietin (Epo).

Epo is strictly required for erythropoiesis, promoting survival and late maturation stages.[1] Ligand-induced Epo-receptor (EpoR) dimerization triggers activation of the pre-associated kinase Jak2, which then phosphorylates tyrosine residues in the cytoplasmic tail of EpoR. These phosphotyrosines serve as docking sites for SH2-domain containing proteins, leading to activation of various signaling pathways, including phosphatidylinositol 3-kinase (PI3-K),[2] mitogen-activated protein kinase,[3] protein kinase C,[4] and phospholipase C-γ.[5] A central pathway in EpoR signaling, however, is the activation of the transcription factor known as signal transducer and activator of transcription 5 (Stat5).[6-8] Upon phosphorylation, Stat5 dimers translocate to the nucleus, bind to cognate elements in various promoters, and activate transcription. Stat5-mediated functions regulate cell proliferation, differentiation, apoptosis, and other processes. Several important Stat5 target genes, such as *Pim*, *c-Myc*, *OncostatinM*, *Bcl-xL*, *SOCS*, or *D-type cyclins* are required for functional erythropoiesis.[9-14]

The requirement of Epo signaling pathway components for erythropoiesis is evident from mice deficient for Epo, EpoR, or Jak2. All mutant animals die in utero at embryonic day 13.5 (E13.5) because of a failure of erythropoiesis; BFU-E and CFU-E progenitors are completely absent from the fetal liver.[15-17] The absolute requirement for Jak2 to transduce EpoR signals was recently substantiated by mutational analyses of EpoR domains: all EpoR mutants unable to bind Jak2 were nonfunctional.[18]

Knowledge about signaling downstream of Epo is still limited. Exogenous Bcr-Abl rescued the erythroid defect of Jak2$^{-/-}$ fetal liver cells in vitro.[19] Likewise, a dominant-active mutant of Akt restored erythroid differentiation in Jak2-deficient erythroid progenitors.[20]

At first, Stat5 seemed to be nonessential for erythropoiesis, in that original Stat5ab$^{-/-}$ mice were viable and showed no overt erythroid defects.[8] Later, these mice were found to display fetal anemia and elevated rates of apoptosis of erythroid cells as a result of a failure in Bcl-xL up-regulation.[21,22] A recently generated complete knockout of Stat5ab, however, is perinatally lethal and

Submitted July 23, 2007; accepted January 16, 2008. Prepublished online as *Blood* First Edition paper, January 31, 2008; DOI 10.1182/blood-2007-07-102848.

*E.W.M. and R.M. contributed equally to this work.

The online version of this article contains a data supplement.

The publication costs of this article were defrayed in part by page charge payment. Therefore, and solely to indicate this fact, this article is hereby marked "advertisement" in accordance with 18 USC section 1734.

highly anemic in utero.[6] Conversely, mice expressing truncated EpoR-mutants that retain solely the ability to activate Stat5 but lack all other tyrosines critical for activation of other signaling pathways live normally.[23] These animals display only mild phenotypes in recovery from erythropoietic stress. Additional mutation of Tyr343 (required for Stat5 activation), however, strongly affected stress erythropoiesis.[24]

This wide range of erythroid phenotypes of mice mutated in the EpoR/Jak2/Stat5 axis prompted us to clarify the role of Stat5 in erythropoiesis. To this purpose, we introduced a hyperactivatable mutant of Stat5a (cS5, S711F[25]) into EpoR$^{-/-}$ and Jak2$^{-/-}$ hematopoietic cells. Tyrosine-phosphorylated, DNA-bound cS5 complemented the proliferation defect of the mutant cells, enabling self-renewal and erythroid differentiation in the absence of Epo signals. Likewise, 4-hydroxy-tamoxifen (4-OH-T)-induced activation of a Stat5a–estrogen receptor (ER)* fusion construct was sufficient to replace Epo in erythropoiesis. Jak2-deficient fetal liver cells also showed defects in myelopoiesis and massively decreased responses to SCF, SCF + IL-3, or SCF + IL-7. Expression of cS5 in Jak2$^{-/-}$ cells partially corrected these proliferation defects in vitro. Moreover, Jak2$^{-/-}$-cS5 cells efficiently contributed to the erythroid and myeloid lineages in vivo upon transplantation. cS5-mediated rescue of myeloid and erythroid lineages was strictly dependent on c-Kit signaling and Jak2.

Methods

All animal experiments were performed in accordance with Austrian and European laws and under approval of the ethical and animal protection committees.

Cell culture and retroviral infections

E12.5 fetal liver cells from Jak2$^{-/-}$, EpoR$^{-/-}$, and wild-type (WT) embryos were isolated and cultivated as described previously.[26] For a detailed description of isolation, retroviral infection, and culture of primary erythroblasts; see Document S1 (available on the *Blood* website; see the Supplemental Materials link at the top of the online article) 293T cells were maintained in Dulbecco modified Eagle medium (DMEM) with 10% fetal calf serum (FCS; Invitrogen, Carlsbad, CA). Transient transfections were done with Lipofectamine 2000 (Invitrogen). Colony assays of retrovirally transduced cells were performed in triplicate as described[17] using MethoCult M3234 (StemCell Technologies, Vancouver, BC). The Bcr-Abl-inhibitor imatinib (Gleevec; inhibiting also c-Kit) was used at 10 μmol/L.

Plasmids

The cS5 mutant of mouse Stat5a (S711F) was used.[27] In the murine Stat5a cDNA, however, the serine residue lies at amino acid position 710 instead of 711 as initially reported by Onishi et al.[25] For clarity, the initial nomenclature was retained here. For the generation of Stat5-ER* constructs, a point-mutated ligand binding domain of the estrogen receptor[28] was fused in frame to the C terminus of Stat5a, or cS5 or Stat5aΔ749,[7] after digestion with SacII. The Stat5a-EE/AA and Stat5a-Y_{694}F mutants were described by Wang et al.[29] Both mutations were introduced into cS5 by polymerase chain reaction (PCR) mutagenesis or cassette exchange.

All constructs were cloned into the retroviral vector pMSCV-IRES-GFP (Clontech, Mountain View, CA) and verified by sequencing. Ecotropic, replication incompetent gp + E86 producers were generated as described previously[27] and selected for high virus titer production by fluorescence-activated cell sorting (FACS).

Transplantation of fetal liver-derived hematopoietic progenitors

Freshly isolated E12.5 WT and Jak2$^{-/-}$ fetal liver cells (C57Bl/6, CD45.2) were cocultured with retrovirus-producing cells in DMEM, 15% FCS, stem cell factor (SCF; 200 ng/mL), interleukin-6 (IL-6, 50ng/mL; R&D Systems, Minneapolis, MN) and IL-3 (25 ng/mL; R&D Systems) for 72 hours. Hematopoietic cells (1-2 × 10^6) were injected into 4- to 6-week-old mice (B6.SJL-*Ptprc^{a}Pep3^b*/BoyJ; Ly-5.1; CD45.1) after sublethal irradiation (750 rad) via the tail vein. Engraftment of injected cells was monitored by FACS analysis of peripheral blood starting 4 weeks after transplantation at regular intervals.

Flow cytometry

Cultured erythroblasts or single cell suspensions of spleen and bone marrow cells from mice 6 months after transplantation were stained with fluorescence-conjugated antibodies against Ter-119, CD71, GR-1, Mac-1, c-Kit, Sca-1, CD19, B220, CD4, and CD8 (all from BD Biosciences, San Jose, CA). Annexin V staining was performed according to the manufacturer's instructions (BD Biosciences). Samples were analyzed on a FACScalibur flow cytometer (BD Biosciences).

Cytokine stimulation, Western blot analysis, and DNA binding assays

Cultured erythroblasts were starved for 3 hours in plain DMEM and subsequently stimulated for 10 minutes with Epo (10 U/mL) or SCF (100 ng/mL) or with SCF plus imatinib (10 μmol/L). 293T cells transiently transfected with the murine pXM-EpoR expression vector and different Stat5 constructs were stimulated with Epo (50 U/mL) and/or 4-OH-T (50 nM) for 30 minutes. Sample preparation and Western blotting was performed according to standard techniques. Antibodies used for Western blotting were anti-phospho-Stat5ab (Millipore, Billerica, MA), anti-Stat5ab (BD Biosciences), anti-Jak2 (Cell Signaling Technology, Danvers, MA), anti-EpoR (Santa Cruz Biotechnology, Santa Cruz, CA), anti-extracellular signal-regulated kinase 1/2 (Sigma-Aldrich, St Louis, MO), and anti-Actin (Sigma-Aldrich). Stat5-EMSAs were performed as described previously.[7]

Reporter gene assays

Self-renewing primary WT and Jak2$^{-/-}$ erythroblasts were transfected in triplicate with 2.5 μg of luciferase reporter constructs containing the β-casein-promoter (β-casein-luc)[30] or the promoter of the IL-2R-α gene (IL-2R-α-luc)[31] along with 0.5 μg of pRL-TK2 (Promega, Madison, WI) using the Nucleofector technology (program U-08; Amaxa Biosystems, Gaithersburg, MD). Cells were stimulated with Epo (50 U/mL) for 6 hours after transfection or left untreated. Luciferase activity was measured 12 hours after transfection.

Quantitative PCR

RNA was isolated using TRIzol (Invitrogen). RNA integrity was checked with a Bioanalyzer (Agilent Technologies, Palo Alto, CA). RNA (2.5 μg) was reverse-transcribed using SuperScript II reverse transcriptase (Invitrogen). Real-time PCR was performed on an Eppendorf RealPlex cycler using RealMasterMix (Eppendorf North America, New York, NY) and SYBR Green. The sequences of primers used can be found in Document S1.

Results

Persistent Stat5 activation complemented the proliferation defect of EpoR$^{-/-}$ and Jak2$^{-/-}$ erythroid cells

Primary WT erythroblasts cultivated in vitro undergo limited self-renewal in response to SCF, Epo, and dexamethasone (Dex).[26] Such expanding progenitors behave like primary erythroid cells from young mice, expressing only adult hemoglobins.[32] Fetal liver-derived cells from WT, EpoR$^{-/-}$, or Jak2$^{-/-}$ E12.5 embryos were tested for outgrowth of immature erythroblasts in the presence of SCF, Epo, and Dex (hence termed "self-renewal conditions"). WT fetal liver erythroblasts proliferated exponentially for 15 days (Figure 1A left), whereas EpoR$^{-/-}$ and Jak2$^{-/-}$

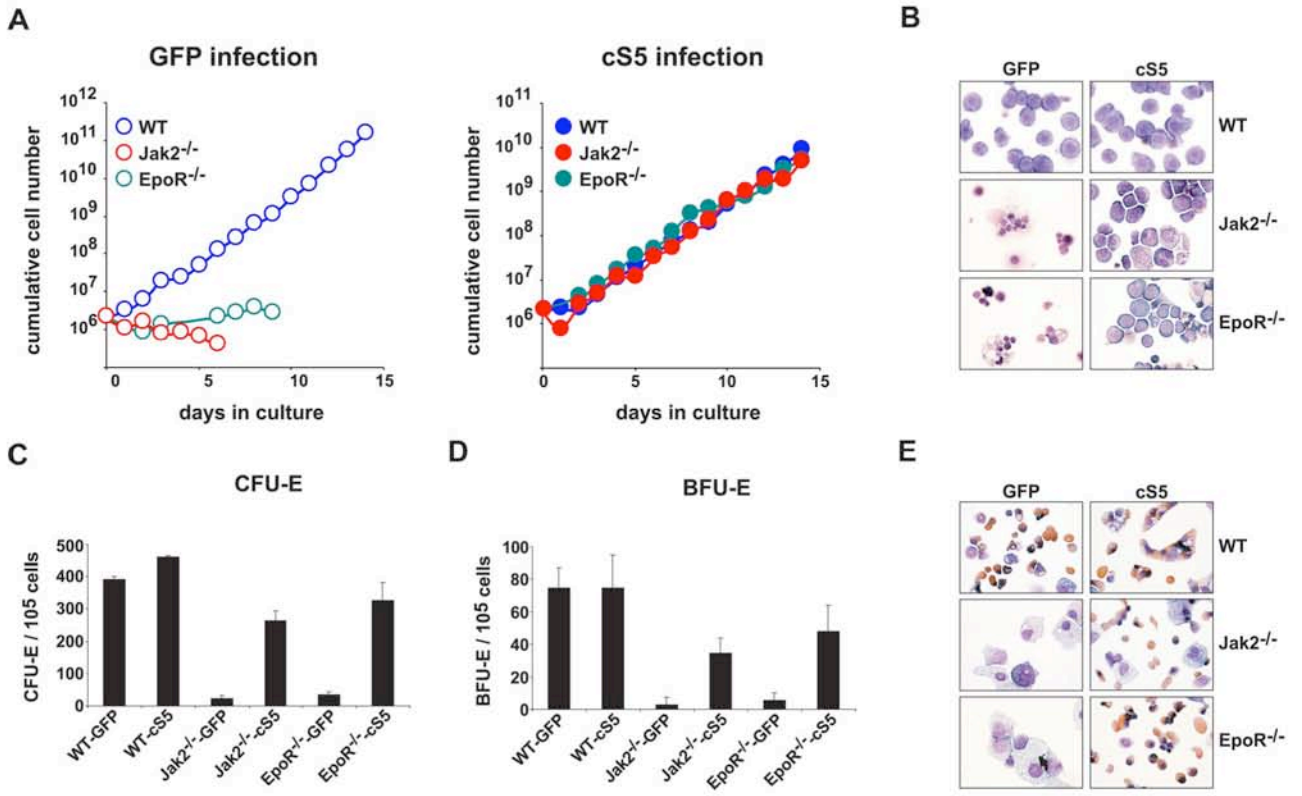

Figure 1. Expression of cS5 rescues proliferation and differentiation of EpoR$^{-/-}$ and Jak2$^{-/-}$ erythroid cells. (A) E12.5 WT, EpoR$^{-/-}$, and Jak2$^{-/-}$ fetal liver cells infected with retroviruses encoding GFP (left panel) or cS5 (right panel) were cultivated in proliferation medium and cumulative cell numbers calculated after daily determination of growth rates. Data plotted for 1 typical experiment of 4. (B) Cytospins were prepared at day 6 from erythroid cultures shown in (A) and stained for hemoglobin (brownish color) plus histologic dyes. WT, Jak2$^{-/-}$, and EpoR$^{-/-}$ fetal liver cells expressing cS5 or GFP were subjected to CFU-E- (C) or BFU-E assays (D), and acid benzidine–positive colonies were scored at day 2 (CFU-E) or day 8 (BFU-E), respectively. (E) Cytospins of cells retrieved from the CFU-E assays in (C), stained with hematoxylin/eosin and for hemoglobin (brownish color).

fetal liver cells failed to do so and disintegrated (Figure 1B). To clarify the role of Stat5 in Epo signaling, we used the Stat5a mutant S711F (cS5), which is persistently tyrosine-phosphorylated and exhibits enhanced chromatin binding activity.[27] Retroviral transduction of EpoR$^{-/-}$ and Jak2$^{-/-}$ cells with cS5 rescued the severe proliferation defect of mutant cells. All cS5-transduced cell types could be expanded for more than 2 weeks with identical proliferation kinetics (Figure 1A right). WT and cS5-transduced mutant cells showed a typical pro-erythroblast phenotype after 6 days of expansion in cytospins (Figure 1B), whereas uninfected control cells disintegrated. Complementation was confirmed by surface marker analysis after 9 days, which showed coexpression of c-Kit and CD71 together with low levels of Ter119. All cultures contained low numbers of immature progenitors (c-Kit$^+$Sca-1$^+$), whereas T- and B-lymphoid cells were absent (Table S1). Although after 3 days, approximately 65% of immature progenitors were retrovirally infected under the conditions used (data not shown), cS5 did not induce proliferation of multipotent cells, because these would have contributed to both erythroid and other myeloid lineages.

To confirm cS5-dependent erythropoiesis of EpoR$^{-/-}$ and Jak2$^{-/-}$ cells, colony-forming assays for committed erythroid progenitors (BFU-E, CFU-E) were performed. In WT cells, cS5 expression did not alter the numbers of benzidine-positive BFU-E or CFU-E colonies compared with green fluorescent protein (GFP)–vector infected controls (Figure 1C,D). Conversely, the low incidence of CFU-E and BFU-E colonies in EpoR$^{-/-}$ and Jak2$^{-/-}$ cells transduced with a GFP vector control could be raised approximately 10-fold upon expression of cS5, reaching levels comparable with those of WT cultures. Remarkably, Jak2$^{-/-}$-cS5 and EpoR$^{-/-}$-cS5 colonies showed the same, typical morphology as WT colonies (Figure S1) and contained mature, enucleated, highly hemoglobinated erythrocytes, similar to WT samples (Figure 1E).

In contrast to cS5, retrovirally transduced WT Stat5a or Bcl-xL failed to induce efficient erythroid colony formation in EpoR$^{-/-}$ and Jak2$^{-/-}$ cells (Figure S2). Thus, activated Stat5 was required and sufficient to overcome the proliferation defect and erythroid colony formation potential of EpoR- and Jak2-deficient cells.

cS5 expression allowed Epo-independent erythropoiesis

Next we sought to determine whether cS5 activity was sufficient to substitute for Epo signaling in erythropoiesis. WT, EpoR$^{-/-}$, and Jak2$^{-/-}$ cells expressing cS5 were kept in Epo-free medium for 6 days. cS5-expressing WT, EpoR$^{-/-}$, or Jak2$^{-/-}$ cells continued to proliferate in the absence of Epo (Figure 2A) without detectable cell disintegration (Figure 2B). WT controls expressing GFP ceased to proliferate after 3 to 4 days (Figure 2A). Dead cells (Figure 2B arrows) and pyknotic nuclei (Figure 2B arrowheads) became visible in cytospins after 4 days without Epo. Withdrawal of SCF rapidly induced terminal differentiation and/or apoptosis in all cell types, indicating that cS5 could not substitute for SCF-signaling (data not shown).

In CFU-E assays, Epo withdrawal prevented colony formation of WT cells. In contrast, cS5-expressing WT, EpoR$^{-/-}$, and Jak2$^{-/-}$ cells formed erythroid colonies at more than 100-fold

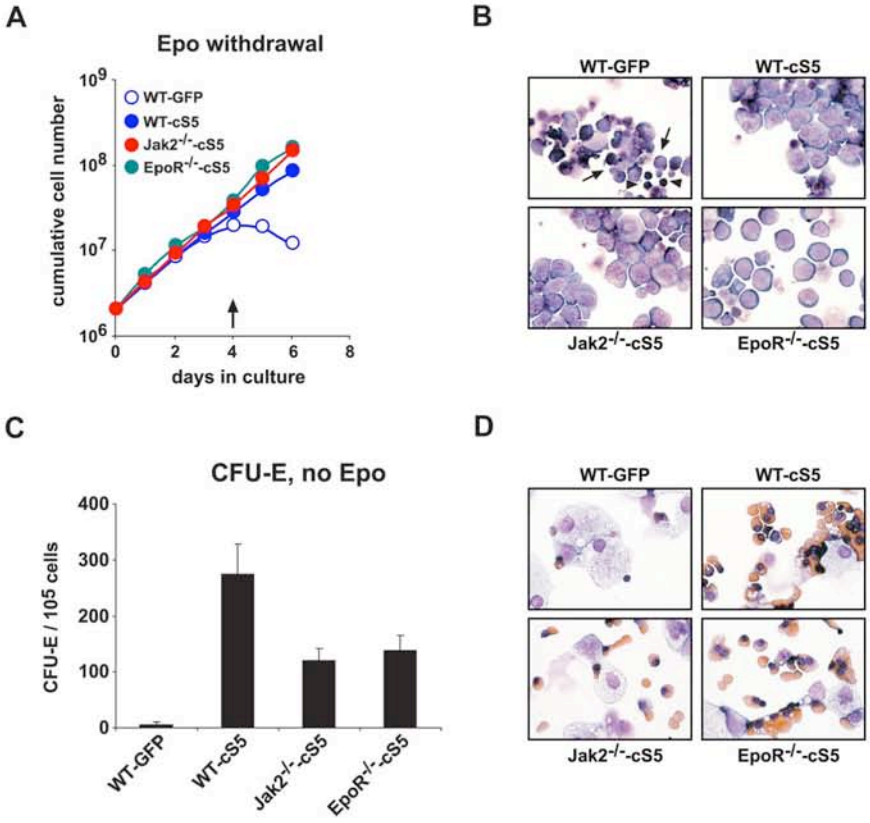

Figure 2. cS5 expression allows erythroid development in the absence of Epo. (A) E12.5 WT, EpoR$^{-/-}$, and Jak2$^{-/-}$ fetal liver cells were infected with retroviruses encoding GFP or cS5 and cultivated in proliferation medium without Epo for 6 days. Cumulative cell numbers are shown for one representative experiments of 3. (B) Cytospins were prepared from cultures shown in panel A at day 4 (→ in A) and stained with hematoxylin/eosin and benzidine. → indicates apoptotic cells; ▶, pyknotic nuclei. (C) WT fetal liver cells expressing cS5 or GFP, or Jak2$^{-/-}$ and EpoR$^{-/-}$ cells expressing cS5, were subjected to CFU-E assays in the absence of Epo and acid benzidine–positive colonies scored at day 2. (D) Cytospins of cells retrieved from the CFU-E assays in (C), stained with hematoxylin/eosin and for hemoglobin (brownish).

higher frequency under the same conditions (Figure 2C). Epo-independent CFU-E formation was more efficient in WT cS5 cells than EpoR$^{-/-}$-cS5 or Jak2$^{-/-}$-cS5 cells. Cytospins of cells retrieved from the CFU-E assays revealed the presence of normoblasts and enucleating erythrocytes in cS5 expressing WT, Jak2$^{-/-}$, and EpoR$^{-/-}$ cells but not in WT GFP cultures (Figure 2D). Apparently, Stat5 activity via cS5 can partially but effectively substitute for Epo signals in WT, EpoR$^{-/-}$, and Jak2$^{-/-}$ cells during both erythroid progenitor proliferation and terminal differentiation.

cS5 induced Epo-independent Stat5 reporter gene expression but its activity was dependent on tyrosine phosphorylation and DNA-binding

To test whether Epo-independent erythropoiesis in cS5-expressing cells was really due to transcriptional activity of cS5, we performed promoter reporter experiments, using a previously described construct containing a Stat5-responsive part of the IL-2Rα gene enhancer[31] (Figure 3A, right). Primary WT GFP, WT cS5, and Jak2$^{-/-}$-cS5 erythroblasts were transfected with IL-2Rα-luc, and the cells were stimulated with Epo 5 hours before harvest or left untreated. WT GFP cells showed a modest induction of reporter gene expression upon stimulation with Epo (Figure 3A). However, in cS5-expressing WT and Jak2$^{-/-}$ erythroblasts, we observed a much higher induction of the reporter gene expression, even in the absence of Epo stimulation (Figure 3A). Similar results were obtained using a different reporter construct, containing the Stat5-responsive part of the β-casein promoter[30] (data not shown). This indicates that cS5 indeed was able to activate gene expression in WT and Jak2$^{-/-}$ erythroid cells.

To prove that the cS5-mediated rescue of erythropoiesis in Jak2$^{-/-}$ and EpoR$^{-/-}$ cells was indeed dependent on transcriptional activation of DNA-bound, tyrosine-phosphorylated Stat5 complexes, 2 additional cS5-derived constructs were generated (Figure 3B). In the mutant cS5-EE/AA, 2 glutamic acid residues (Glu437/Glu438) in the DNA-binding domain of cS5 are mutated to alanine, resulting in a tyrosine-phosphorylated cS5 molecule unable to bind to DNA (Figure 3C,D). Conversely, the Y694F mutation in cS5 prevented phosphorylation of the critical tyrosine required for dimerization and DNA binding in transient transfections of 293T cells (Figure 3C,D). Expression of cS5-EE/AA and cS5-Y694F in primary WT fetal liver erythroblasts did not significantly alter CFU-E formation compared with expression of cS5 or GFP (data not shown). In CFU-E assays of Jak2$^{-/-}$ cells expressing GFP, cS5, or the mutants cS5-EE/AA and cS5-Y694F, however, only expression of cS5 resulted in a significant increase in erythroid colony formation (Figure 3E). The same results were obtained using EpoR$^{-/-}$ cells (Figure 3F). Thus, tyrosine-phosphorylation and DNA-binding functions of cS5 are required to allow erythropoiesis of Jak2$^{-/-}$ and EpoR$^{-/-}$ cells.

Induced activation of Stat5 could replace Epo in erythropoiesis

Because cS5 is a leukemogenic protein with enhanced signaling capacity, we generated constructs consisting of Stat5a or cS5 fused to ER*, a point-mutated ligand-binding domain of the estrogen receptor.[33] In the respective fusion proteins (Stat5a-ER*, cS5-ER*; Figure 4A), dimerization, nuclear translocation, DNA binding, and transcriptional activity can be triggered by 4-hydroxy-tamoxifen (4-OH-T).[28] It is noteworthy that the cS5-dependent hyperactivation of PI3-K signaling[34] was not induced by cS5-ER* compared with Stat5a-ER* (Figure S3A). 4-OH-T or Epo induced specific binding of Stat5a-ER* as well as cS5-ER* to a β-casein Stat5 DNA response element, whereas 4-OH-T + Epo strongly enhanced Stat5a-ER* DNA binding (Figure S3B). Retrovirally transduced Stat5a-ER*

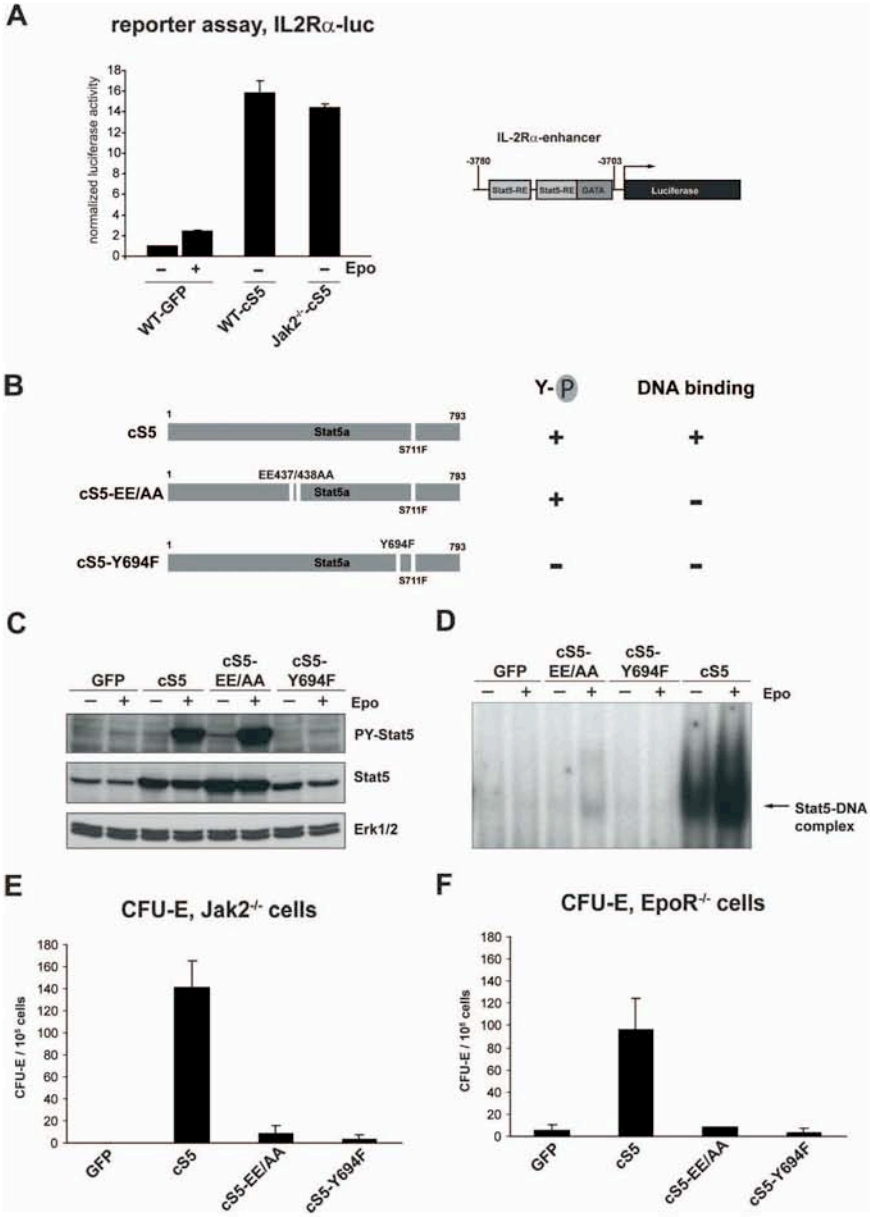

Figure 3. cS5 allows Epo-independent induction of a Stat5-responsive reporter construct but requires tyrosine phosphorylation and DNA-binding for activity. (A) Self renewing WT GFP and cS5-expressing WT and Jak2$^{-/-}$ erythroblasts were transfected with IL-2R-α-Luc. Before harvesting, cells were stimulated with Epo for 5 hours (+) or left untreated (−). Luciferase expression was measured 12 hours after transfection. Right, schematic representation of the promoter enhancer element from the IL-2R-α gene containing 2 Stat5 response elements (Stat5-RE) fused to the luciferase gene (IL-2R-α-Luc). (B) Schematic representation of the mutants used. 293T cells were transiently transfected with different cS5 constructs, together with a murine EpoR cDNA. Twenty-four hours later, cells were left untreated or treated for 30 minutes with Epo. Extracts were analyzed for tyrosine-phosphorylated Stat5 and total Stat5 by Western blot (C) and DNA-binding of transfected Stat5 constructs by EMSAs on a β-casein-specific promoter sequence (D). Jak2$^{-/-}$ (E) and EpoR$^{-/-}$ (F) fetal liver cells were infected with retroviruses encoding GFP, cS5, cS5-EE/AA, or cS5-Y694F and subjected to CFU-E assays. Acid benzidine–positive colonies were scored at day 2.

underwent Epo-induced tyrosine phosphorylation in primary WT fetal liver erythroblasts, as shown by Western blot analysis (Figure 4B). An inducible dominant-negative Stat5-ER* fusion protein (Stat5aΔ749-ER*, Figure 4A[7]) was not tolerated in primary erythroid cells, resulting in strong negative selection against cells expressing this construct (data not shown).

Using primary erythroblasts expressing Stat5a-ER* or GFP, we tested whether 4-OH-T–induced activation of WT Stat5 could substitute for Epo in erythroid progenitor expansion. Under self-renewal conditions, both Stat5a-ER*- and GFP-expressing cells proliferated with identical kinetics (Figure 4C left) and equally low rates of apoptosis (annexin V staining, day 6, Figure 4D left). Replacement of Epo with 4-OH-T under the same conditions allowed sustained proliferation of Stat5a-ER* expressing cells, but not of GFP-control cells (Figure 4C middle), consistent with corresponding apoptotic indices (~10% vs > 50% annexin V–positive cells; Figure 4D middle). In the absence of Epo and 4-OH-T, both cell types gradually ceased to proliferate and underwent cell death (Figure 4C,D right). Cultures of fetal liver cells expressing cS5-ER* instead of Stat5a-ER* behaved similar in these experiments (data not shown).

Induction of terminal erythroid differentiation by 4-OH-T-activated Stat5a-ER* was analyzed in CFU-E assays in the presence of 4-OH-T instead of Epo. Stat5a-ER*– but not GFP-expressing cells formed CFU-E colonies (Figure 4E), which in both cases mainly consisted of mature normoblasts and erythrocytes as seen in cytospins of cells recovered from CFU-E assays and stained for hemoglobin (Figure 4F).

Taken together, 4-OH-T–induced activation of Stat5a-ER* was able to significantly substitute for Epo signaling in erythropoiesis.

A role for Jak2 in c-Kit signaling in hematopoietic progenitors

In addition to EpoR, Jak2 interacts with a variety of other cytokine receptors. Thus, we tested whether cS5 would alleviate Jak2 deficiency also in other lineages. cS5- or GFP-expressing WT or Jak2$^{-/-}$ fetal liver cells were subjected to colony-forming assays in the presence of granulocyte macrophage–colony-stimulating factor

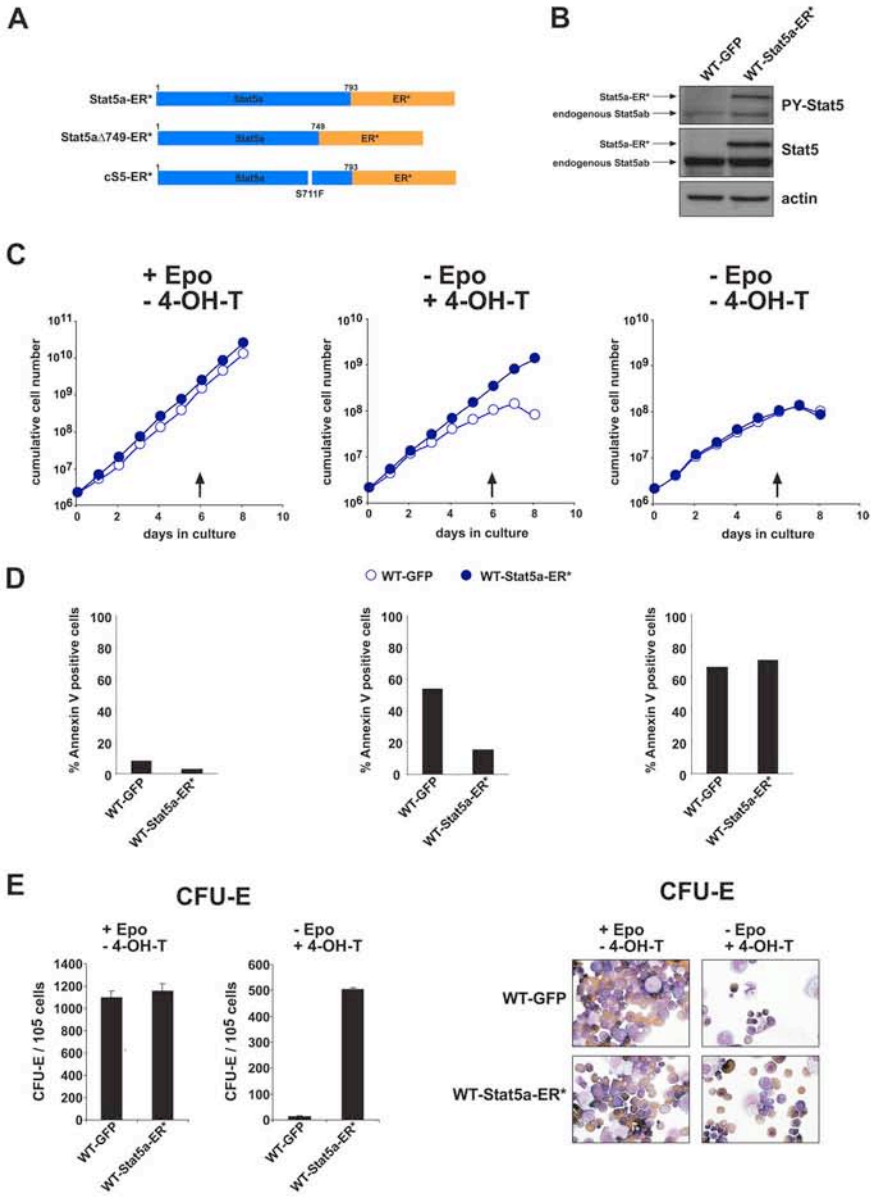

Figure 4. 4-Hydroxy-tamoxifen-induced Stat5a-ER* activation replaced Epo in erythropoiesis. (A) Scheme of the 4-OH-T-inducible Stat5-ER* constructs used, encoding fusion proteins of WT Stat5a, cS5, or Stat5aΔ749 with ER* (see "Methods"). (B) Western blot analysis of phosphorylated Stat5 (P-Y-Stat5), and total Stat5 protein in WT fetal liver erythroblasts expressing GFP or Stat5a-ER*. The larger protein recognized by P-Y-Stat5 and Stat5 antibodies corresponds to Stat5a-ER*. Actin, loading control. (C) Cumulative cell numbers (1 representative experiment of 3) of proliferating primary erythroblast cultures expressing Stat5a-ER* or GFP determined in the presence of Epo (+ EPO, −4-OH-T, left, normal self-renewal conditions), the presence of 4-OH-T (5 nM) instead of Epo (−Epo, + 4-OH-T, middle) and without Epo and 4-OH-T (right). (D) Percentage of apoptotic cells of cultures in panel C at day 6 (arrows in panel C) as analyzed by annexin V staining. (E) WT fetal liver cells expressing Stat5a-ER* or GFP were subjected to CFU-E assays in the presence of Epo (left panels) or 4-OH-T (50 nM) instead of Epo (right panels). Acid benzidine–positive colonies were scored at day 2. (F) Cytospins of cells retrieved from the CFU-E assays in panel E and stained with hematoxylin/eosin and for hemoglobin (brownish color).

(GM-CSF). Jak2$^{-/-}$-GFP cells yielded 5.2-fold lower colony numbers than WT GFP cells, whereas expression of cS5 increased colony numbers 2.6-fold in Jak2$^{-/-}$ cells (Table 1). Therefore, activation of Stat5 may be sufficient to augment myeloid differentiation in absence of Jak2.

Immature blood cells of all lineages require c-Kit signaling for proliferation and/or differentiation, mainly visible in cooperation with other hematopoietic cytokines.[35-37] We therefore analyzed whether loss of Jak2 would affect colony formation induced by SCF alone or in combination with other cytokines. Jak2-deficient

Table 1. Colony formation ability of fetal liver hematopoietic cells in response to various cytokines and growth factors is dependent on Jak2 and Stat5

Cytokine	WT GFP	WT cS5	Jak2$^{-/-}$-GFP	Jak2$^{-/-}$-cS5	EpoR$^{-/-}$-GFP	EpoR$^{-/-}$-cS5
Epo	392 ± 8	461 ± 5†	24 ± 8	264 ± 29†	35 ± 9	325 ± 57†
Epo + IL-3	75 ± 12	75 ± 20‡	3 ± 5	35 ± 9†	5 ± 5	48 ± 16†
GM-CSF	293 ± 26	432 ± 32†	56 ± 8	144 ± 29†	nd	nd
SCF	304 ± 8	352 ± 21*	109 ± 12	173 ± 20†	nd	nd
SCF + IL-3	448 ± 8	528 ± 28†	139 ± 12	219 ± 28†	nd	nd
SCF + IL-7	360 ± 14	408 ± 32‡	149 ± 20	216 ± 16†	nd	nd
None	0	0 ± 1	1	1 ± 1	1	0 ± 1

SCF-induced colonies represent immature progenitors and mast cells, SCF + IL-3 and SCF + IL-7 induce colony formation of myeloid and lymphoid progenitors (data not shown).

nd indicates not determined.

*$P < .05$.

†$P < .01$.

‡Not significant.

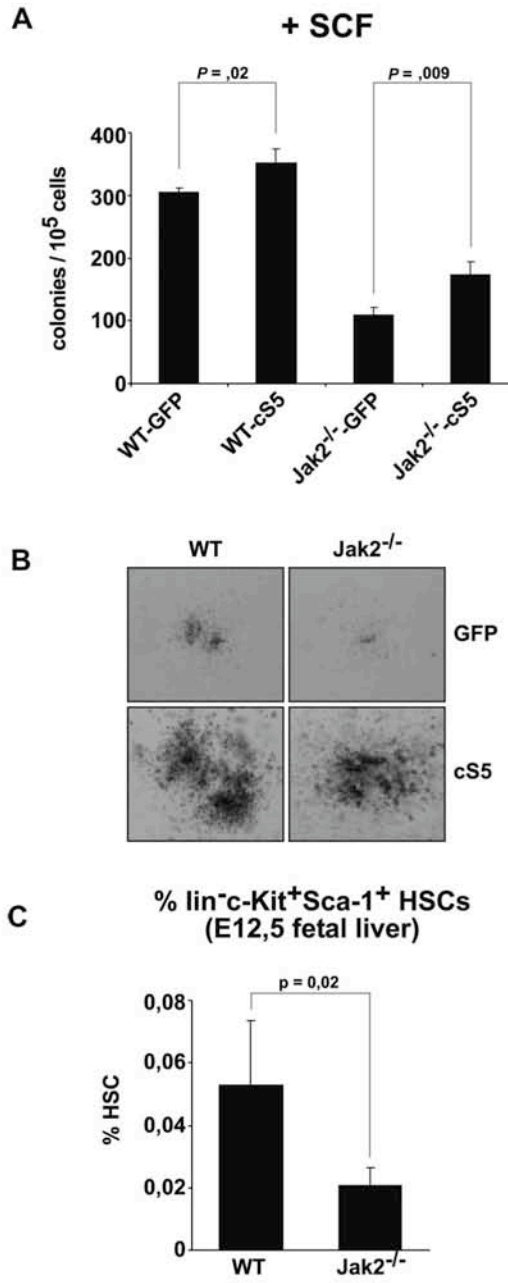

Figure 5. c-Kit signaling depends on Jak2 and is modulated by Stat5. (A) WT and Jak2$^{-/-}$ fetal liver cells transduced with GFP or cS5 were subjected to colony assays supplemented with SCF (50 ng/mL). Colonies were scored at day 8. (B) Photographs of colonies from (A). Representative pictures of 4 for each condition are shown. (C) E12.5 WT and Jak2$^{-/-}$ fetal livers analyzed for HSC content (lin$^-$c-Kit$^+$Sca-1$^+$ cells) by flow cytometry. The percentage of HSCs is depicted (n = 4).

fetal liver cells indeed showed a 2.8-fold reduction in SCF-dependent colony formation compared with WT cells (Figure 5A), in line with previous findings.[17,38] Jak2$^{-/-}$-cS5 cells generated significantly more colonies than Jak2$^{-/-}$-GFP cells (1.6 fold; Figure 5A). The size of SCF-dependent colonies was strongly reduced in Jak2$^{-/-}$-GFP cells but massively increased by cS5 in both WT and Jak2 mutant cells (Figure 5B). Colony formation of early myeloid and lymphoid progenitors induced by SCF + IL-3 and SCF + IL-7, respectively, was 3.2- and 2.5-fold reduced in Jak2-deficient cells (Table 1). Again, cS5 expression led to more than 1.6-fold increased colony numbers when expressed in Jak2$^{-/-}$ cells, whereas WT cells showed a similar but weaker increase (Table 1).

Hematopoietic stem cells (HSCs; lin$^-$c-Kit$^+$ Sca-1$^+$ cells) also depend on SCF for proliferation.[39] Because c-Kit function might be linked with Jak2, we tested whether Jak2 deficiency would affect HSC numbers. Indeed, HSC numbers were approximately 70% lower in Jak2$^{-/-}$ fetal livers than in WT fetal livers (n = 4; Figure 5C) as determined by flow cytometry in freshly prepared fetal livers of E12.5 embryos. These observations argue that Jak2 has an essential function in hematopoietic stem cells.

Complementation of Jak2 deficiency in vivo

The finding that Jak2 is not only necessary for erythropoiesis but also important for expansion of c-Kit–responsive immature hematopoietic progenitors and HSCs prompted us to analyze whether Jak2$^{-/-}$ cells expressing cS5 were capable of long-term repopulation of erythromyeloid lineages in vivo. Freshly isolated fetal liver cells from WT and Jak2$^{-/-}$ embryos were transduced with cS5. Equal cell numbers were injected into irradiated recipient mice 72 hours later. To rule out that Jak2$^{-/-}$ fetal livers generated lower numbers of HSCs during the retroviral infection period, we determined the amounts of GFP-positive, long-term (LT) HSCs 72 hours after retroviral infection. Thy1.1^{low}/Flt3$^-$ LT-HSCs are the sole cells capable of long-term reconstitution of transplanted mice.[40] We found that LT HSCs were efficiently infected by the retrovirus, leading to an equal presence of GFP$^+$ LT HSCs in WT cS5 and Jak2$^{-/-}$-cS5 cultures (1667 ± 451 GFP$^+$ LT HSC per 10^6 WT cS5 cells; 1967 ± 351 GFP$^+$ LT HSC per 10^6 Jak2$^{-/-}$-cS5 cells; n = 3, data not shown).

Use of congenic mice expressing CD45.1 allowed detection of CD45.2$^+$ donor cells among the host cells.[41] Because cS5-expressing fetal liver cells cause leukemia,[27] onset of the disease was strongly delayed by transplanting reduced numbers of cS5-transduced fetal liver cells into sublethally rather than lethally irradiated mice. Indeed, all mice in which the transplanted Jak2$^{-/-}$-cS5 cells were engrafted (n = 6) remained disease-free for more than 6 months and did not develop leukemia.

Transplanted mice were regularly monitored for transplant-derived, GFP-CD45.2 double-positive cells in peripheral blood. Animals were killed 6 months after transplantation and assayed for the presence of GFP$^+$Ter119$^+$ erythroid cells in bone marrow and spleen and for GFP$^+$GR-1$^+$ and/or GFP$^+$Mac-1$^+$ myeloid cells in peripheral blood and bone marrow. Significant numbers of transplant-derived, GFP$^+$Ter119$^+$ double-positive cells were observed in spleen and bone marrow of mice receiving WT cS5 cells

Table 2. Hematopoietic repopulation is influenced by Jak2

Transplant	Mice engrafted	Engraftment of GFP$^+$CD45.2$^+$ cells in peripheral blood % (range)	Erythroid (mice with GFP$^+$Ter119$^+$ cells)	Granulocytic (mice with GFP$^+$GR-1$^+$ cells)	Macrophage (mice with GFP$^+$Mac-1$^+$ cells)
WT-cS5	10 (10)	14.8 (4-40)	9 (10)	10 (10)	5 (10)
Jak2$^{-/-}$-cS5	6 (8)	8.6 (1-23)	4 (6)	6 (6)	2 (6)

GFP$^+$CD45.2$^+$ cells correspond to transplant-derived, cS5-expressing cells. Transplant-derived erythroid cells were scored in spleen and bone marrow, and GFP$^+$ myeloid (GR-1$^+$ and Mac-1$^+$) cells were measured in peripheral blood and bone marrow.

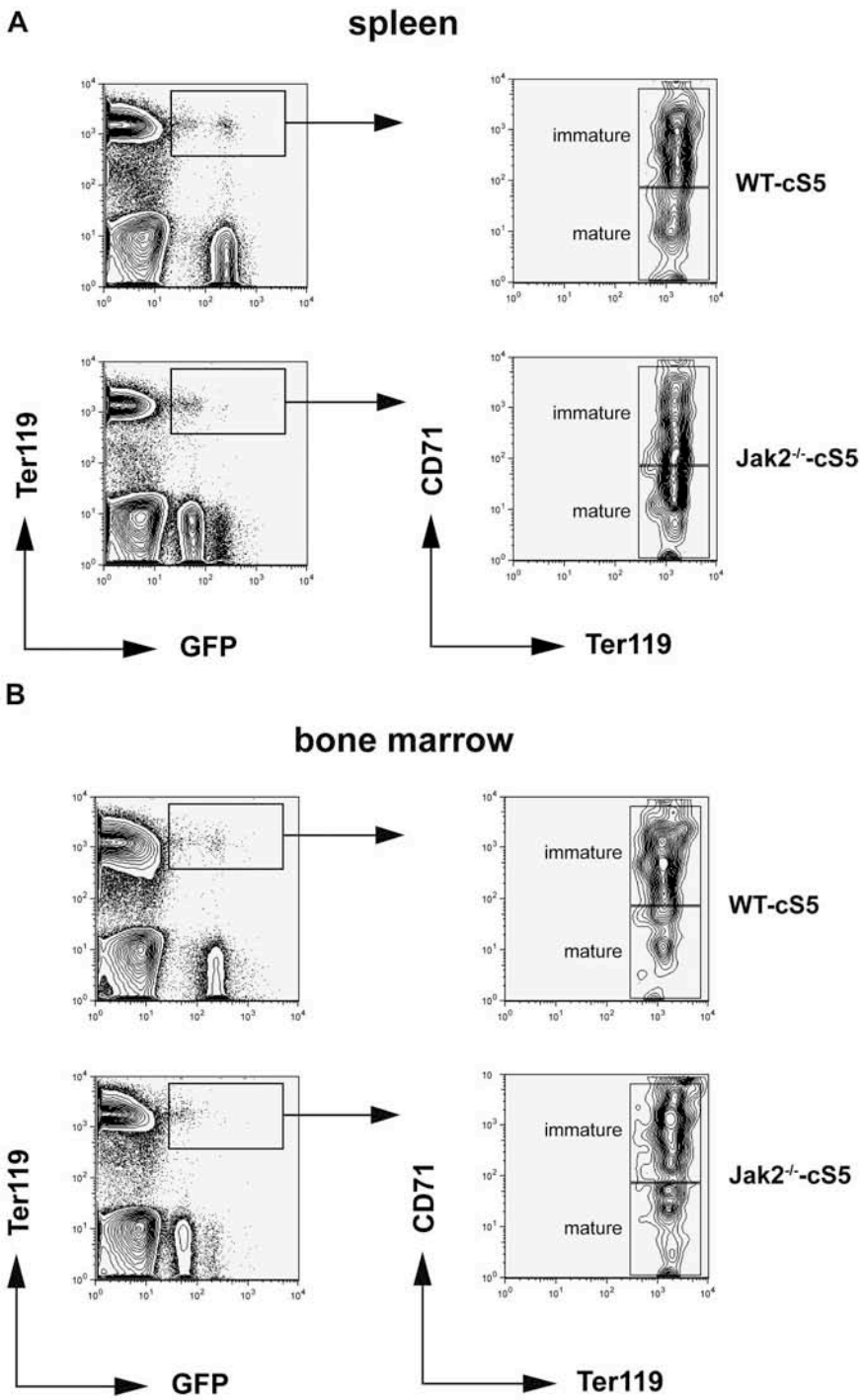

Figure 6. Jak2$^{-/-}$ cells expressing cS5 undergo erythroid differentiation in vivo. Equal numbers of cS5-transduced E12.5 WT and Jak2$^{-/-}$ fetal liver cells were injected into sublethally irradiated mice. Six months after transplantation, spleen (A) and bone marrow (B) of engrafted animals were monitored for GFP-positive erythroid cells. FACS plots for Ter119 and GFP (left) indicate transplant-derived double-positive erythroid cells. Gated cells (boxed) were further analyzed for CD71 and Ter119 (right) to discriminate between immature (CD71^{high}Ter119^{pos}) and mature (CD71^{low}Ter119^{pos}) erythroid cells.

(9 of 10 animals) as well as Jak2$^{-/-}$-cS5 (4 of 6 mice, Table 2, Figure 6A,B top and bottom left panels). This indicated that cS5 could partially but efficiently substitute for Jak2 in erythroid differentiation in vivo. To characterize transplant-derived erythroid cells for different stages of maturation, GFP$^+$Ter119$^+$ cells were gated for high versus low CD71 expression, allowing us to distinguish mature (Ter119$^+$CD71^{low}) from more immature erythroid progenitors (Ter119$^+$CD71$^+$). In both spleen and bone marrow, transplanted Jak2$^{-/-}$-cS5 as well as WT cS5 cells gave rise to multiple stages of erythroid cells in vivo, ranging from CD71$^+$Ter119$^+$ immature, basophilic erythroblasts to almost mature CD71$^-$Ter119$^+$ orthochromatophilic erythroblasts[22] (Figure 6A,B right panels).

Likewise, animals successfully engrafted with WT cS5 cells displayed robust contribution of GFP$^+$ cells to mature myeloid lineages (GFP$^+$GR-1$^+$ granulocytes, 10 of 10 mice; GFP$^+$Mac-1$^+$ monocytes/macrophages, 5 of 10 mice; Table 2) in peripheral blood and bone marrow (Figure S4 right panels and data not shown). It is noteworthy that Jak2$^{-/-}$-cS5 transplanted mice showed a significant contribution to the Mac-1$^+$- (2 of 6 animals with GFP$^+$ cells) and GR-1$^+$-compartments (6 of 6, Table 2; Figure S4 right panels), both in peripheral blood and bone marrow (Table 2 and data not shown). Thus, in GM-CSF-dependent myelopoiesis in vivo, cS5 can substitute for the lack of Jak2 to a significant extent.

It should be noted that overall engraftment was clearly lower in Jak2$^{-/-}$-cS5 transplanted mice (6 of 8, 8.6% engraftment) than in

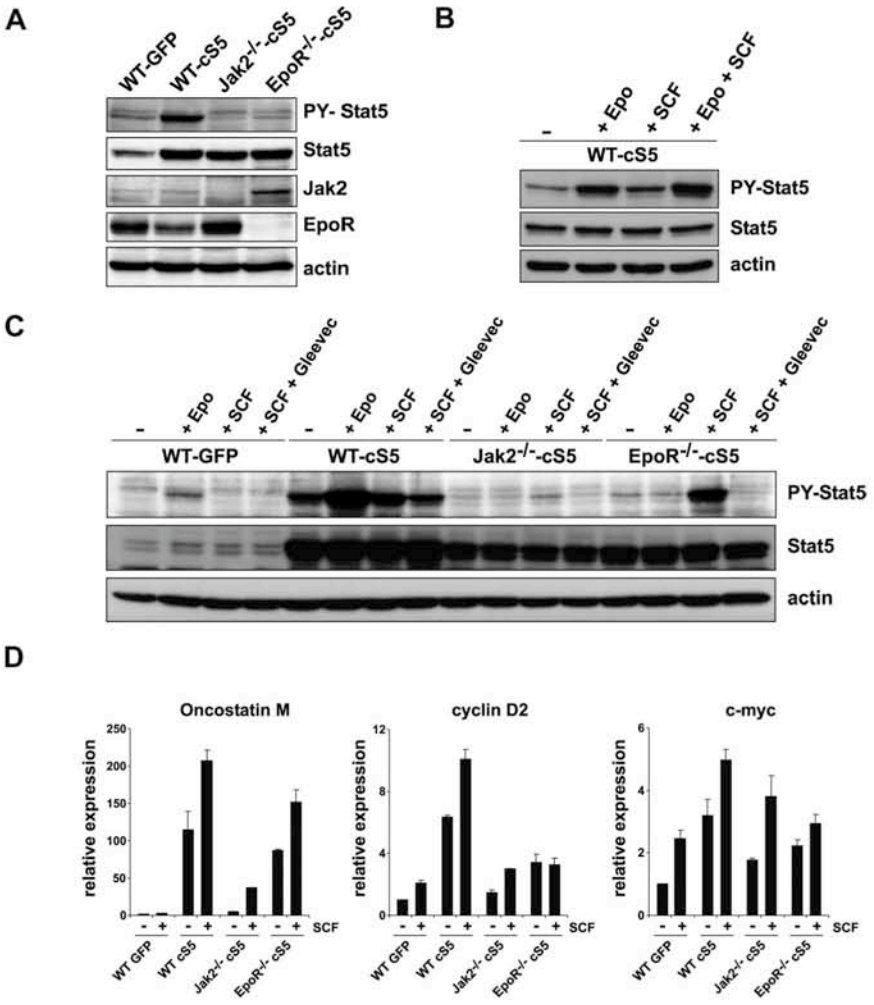

Figure 7. Jak kinase(s) and c-Kit cooperate in cS5 activation. (A) Lysates from self-renewing WT GFP, WT cS5, Jak2$^{-/-}$-cS5, and EpoR$^{-/-}$-cS5 cultures were analyzed for P-Y-Stat5, total Stat5, Jak2, and EpoR protein levels. Actin, loading control. (B) cS5-expressing WT erythroblasts were starved for 3 hours (−) and subsequently stimulated with Epo, SCF, or Epo + SCF for 10 minutes. Lysates were analyzed for P-Y-Stat5 and total Stat5 protein. Erk1/2, loading control. (C) WT erythroblasts expressing GFP or cS5, and Jak2$^{-/-}$ and EpoR$^{-/-}$ cells expressing cS5 were starved for 3 hours (−) and subsequently stimulated with Epo, SCF, or SCF + imatinib (10 μmol/L) for 10 minutes. Lysates were analyzed for P-Y-Stat5 and total Stat5 protein. Erk1/2, loading control. (D) WT GFP, WT cS5, Jak2$^{-/-}$-cS5, and EpoR$^{-/-}$-cS5 cultures were starved for 3 hours (−) and subsequently restimulated with SCF for 2 hours (+). Expression of the Stat5 target genes *oncostatinM*, *cyclin D2*, and c-*myc* was assessed by real-time PCR.

respective WT cS5 controls (10 of 10, 14.8% engraftment, Table 2). Likewise, contribution to erythroid (4 of 6) and macrophage lineages (2 of 6) was clearly reduced in Jak2$^{-/-}$-cS5 transplanted animals than in control WT cS5 mice (9 of 10 and 5 of 10, Table 2).

In summary, Jak2$^{-/-}$ cells expressing cS5 contribute to both erythroid and myeloid lineages upon transplantation, albeit with lower efficiency than WT cS5 cells. Furthermore, Jak2$^{-/-}$-cS5 cells were able to generate mature CD71^{-}Ter119^{+} erythroid cells. Thus, the severe defects resulting from Jak2 deficiency in erythro- and myelopoiesis can be efficiently but not completely corrected upon expression of cS5 in vivo.

cS5 phosphorylation required Jak2 or c-Kit kinase activity

We next tested the tyrosine phosphorylation status of WT Stat5 in self-renewing primary erythroblasts. WT cells expressing GFP exhibited low P-Y-Stat5 levels under self-renewal conditions[42] (Figure 7A). As expected, proliferating WT cells expressing cS5 displayed strongly increased P-Y-Stat5 abundance. It is noteworthy that Jak2$^{-/-}$-cS5 and EpoR$^{-/-}$-cS5 cells showed only modest P-Y-Stat5 levels, similar to those of WT GFP cells, although cS5 protein was similarly overexpressed in WT, Jak2$^{-/-}$, and EpoR$^{-/-}$ cells.

Thus, although the EpoR-Jak2 axis is the main pathway leading to Stat5 activation, the clearly detectable basal P-Y-Stat5 levels and, more importantly, the resulting strongly Stat5 activation in cells devoid of EpoR or Jak2, must originate from another tyrosine kinase. Because we found a role for Jak2 in c-Kit signaling, we reasoned that c-Kit might be critical for cS5 phosphorylation. cS5-expressing erythroblasts were stimulated with Epo, SCF, or Epo + SCF (see Document S1). Epo induced high P-Y-Stat5 levels, but SCF stimulation was also able to induce significant Stat5 phosphorylation (Figure 7B). Strikingly, the combination of Epo and SCF induced the highest P-Y-Stat5 levels, indicating that both c-Kit and EpoR could contribute to Stat5 activation. To elucidate the molecules involved in SCF-induced Stat5 activation, the previous experiment was repeated with WT GFP, WT cS5, EpoR$^{-/-}$-cS5, and Jak2$^{-/-}$-cS5 cells in the presence or absence of the Bcr-Abl inhibitor imatinib, which also inhibits c-Kit kinase activity. Analysis of P-Y-Stat5 levels revealed that Epo but not SCF stimulation induced significant levels of P-Y-Stat5 in WT GFP cells (Figure 7C). In contrast, WT cS5 cells showed high levels of P-Y-Stat5 after starvation, further increased by Epo. Jak2$^{-/-}$-cS5 cells showed lower expression levels of cS5 protein than WT cS5 or EpoR$^{-/-}$-cS5 cells. As expected, no significant P-Y-Stat5 was found after starvation or Epo stimulation. SCF stimulation induced significant Stat5-phosphorylation that could be blocked by imatinib treatment. In EpoR$^{-/-}$-cS5 cells, basal P-Y-Stat5 levels were unexpectedly high (similar to that in Jak2$^{-/-}$-cS5 cells after SCF stimulation) and did not disappear upon starvation. SCF strongly increased P-Y Stat5 levels, which were reduced back to basal levels by imatinib, whereas, as expected, Epo had no effect. Thus, SCF-activated c-Kit was able to induce strong tyrosine-phosphorylation of cS5 in the absence of EpoR, suggesting that

Jak2 contributed to both basal and c-Kit-enhanced cS5 phosphorylation in EpoR$^{-/-}$-cS5 cells.

To confirm that c-Kit could functionally activate cS5, we determined SCF-dependent gene expression of known Stat5 target genes. Self-renewing WT GFP, WT cS5, EpoR$^{-/-}$-cS5, and Jak2$^{-/-}$-cS5 cells were starved for 3 hours and subsequently restimulated with SCF or left untreated. In the absence of SCF, oncostatin M (OSM), cyclin D2, and c-myc mRNAs were already expressed at significantly elevated levels in WT cS5, EpoR$^{-/-}$-cS5, and Jak2$^{-/-}$-cS5 cells compared with WT GFP cells. It is noteworthy that all cS5-expressing cell types showed a further upregulation of Stat5 target genes in response to SCF (Figure 7D).

These data provide direct molecular evidence that the SCF-activated c-Kit tyrosine kinase was able to cause cS5 phosphorylation and target gene transcription, which to a large extent depends on the presence of Jak2.

Discussion

Activated Stat5 modulates diverse cellular processes, including induction of proliferation, suppression of apoptosis, and promotion or inhibition of differentiation, particularly in cells of the hematopoietic lineage. This output can vary extensively, depending on cell type and stages of maturity. Here, we showed that expression of activated Stat5 was sufficient to allow erythropoiesis in vitro and in vivo, both upon ablation of the EpoR or Jak2 or in the absence of Epo-signaling (Figure S5A). Moreover, our data clearly implicate the c-Kit pathway in Jak2/Stat5 activation in immature hematopoietic cells (Figure S5B).

Activated Stat5 was an essential target of Epo signaling in erythroid cells

The role of Stat5 in promoting erythropoiesis is well recognized but remained controversial because of different phenotypes of Stat5-deficient mouse models, either retaining a hypomorphic Stat5 allele[21,22,42] or representing a complete knockout.[6] Until now, however, it remained unclear whether or not Stat5 would be an essential downstream target of EpoR and Jak2 in erythropoiesis.

To test this possibility, we expressed cS5, a persistently activated Stat5a mutant (S711F,[27]), in primary fetal liver–derived hematopoietic progenitors of WT, Jak2$^{-/-}$, and EpoR$^{-/-}$ embryos. cS5 allowed proliferation and terminal differentiation of erythroid cells from Jak2- and EpoR-deficient embryos in vitro. Both EpoR$^{-/-}$-cS5 and Jak2$^{-/-}$-cS5 cells were able to produce mature CFU-E and BFU-E colonies of normal appearance. The observed effect of cS5 was completely dependent on tyrosine-phosphorylation and DNA-binding ability. cS5 did not require endogenous Stat5 proteins for constitutive activity, because cS5 readily transformed Stat5 mutant cells (Moriggl et al[27] and data not shown). In line, only the cS5 protein was persistently tyrosine-phosphorylated in the absence of cytokines in cS5-expressing WT cells, whereas stimulation with IL-3 induced activation of both endogenous WT Stat5 as well as exogenous cS5 proteins.[34]

Remarkably, cS5 was reported to cause activation of PI3-K signaling via binding to the adaptor protein Gab2.[34] PI3-K signaling, in turn, is required for erythroid renewal.[43] To rule out such possible indirect effects of cS5 on erythropoiesis, we used a 4-OH-T–inducible WT Stat5a-ER* construct, which has little effect on PI3-K activation. Consistent with a direct role for Stat5 proteins in promoting erythropoiesis, primary erythroblasts expressing WT Stat5a-ER* were able to proliferate and terminally differentiate upon replacement of Epo with 4-OH-T. Thereby it could be excluded that the observed genetic complementation of Jak2$^{-/-}$ and EpoR$^{-/-}$ cells with cS5 was due to effects caused by the particular mutation in cS5. We therefore concluded that tyrosine-phosphorylated, transcriptionally active Stat5 was essential and sufficient to enable terminal erythropoiesis.

The initially reported Stat5a/b double-knockout mice (Stat5$^{\Delta N}$) showed surprisingly mild hematopoietic phenotypes, especially with respect to Epo-signaling.[8] These mice still expressed a hypomorphic, N-terminally truncated Stat5 allele.[42,44] In contrast, complete ablation of Stat5a/b (Stat5^{null}) resulted in embryonic lethality.[6] On a mixed Sv129 × C57Bl/6 genetic background, however, approximately 1% of animals survived up to 6 weeks.[45] Thus, even the complete lack of Stat5 proteins resulted in a less severe erythroid phenotype than shown by EpoR$^{-/-}$ or Jak2$^{-/-}$ mice.[6] This could be due to additional signaling pathways, activated by Epo-EpoR-Jak2 besides Stat5 activation. Alternatively, other Stat protein family members might compensate for the absence of Stat5.[46] In Stat5^{null} but not WT erythroblasts, we indeed observed strong Stat1- and Stat3 tyrosine phosphorylation and DNA-binding (F.G. and M.A.K., unpublished observations). A final proof for redundancy among Stat family members will have to await additional experiments, including erythroid-specific Stat1/3/5 knockout mouse models.

One important Stat5 target in erythroid cells is the antiapoptotic protein Bcl-xL.[21,22] Bcl-xL–deficient mice display severe erythroid defects,[12] whereas Bcl-xL overexpression in erythroid cells allows Epo-independent maturation.[47,48] It is likely, however, that there are additional functions of the EpoR/Jak2/Stat5 axis in erythropoiesis. Recently, roles for Epo regulation of cell cycle progression[49] and cell adhesion[50] were indeed proposed. In line with these findings, cS5 but not Bcl-xL rescued renewal and alleviated Epo-dependence of primary erythroid cells of WT as well as EpoR$^{-/-}$ or Jak2$^{-/-}$ fetal livers. Likewise, expression of another hyperactive Stat5 variant was sufficient to allow Epo-independent colony formation of human erythroid cells,[48] and human CD34^{+} cells expressing a constitutive active Stat5 mutant showed enhanced self-renewal with increased erythroid commitment of transduced cells.[51] Besides their requirement for Epo-signaling in erythropoiesis, Jak2 and Stat5 are similarly essential in other hematopoietic lineages. Constitutive activation of Stat5 was recently shown to abrogate cytokine dependence for proliferation of several hematopoietic lineages.[34,52] Here, we show that GM-CSF–dependent myelopoiesis decreased more than 5-fold in Jak2-deficient versus WT fetal liver cells in vitro, whereas cS5 expression in Jak2$^{-/-}$ fetal liver cells robustly increased GM-CSF–dependent colony formation. This suggests that P-Y-Stat5 is necessary to allow functional myeloid differentiation in absence of Jak2. Together with the ability of activated Stat5 to promote renewal and differentiation of erythroid cells in the absence of Epo/EpoR/Jak2 signaling, this suggests a considerable amount of conservation among distinct cytokine receptor/Jak/Stat5 signaling pathways.

Jak2 was required for efficient c-Kit signaling during hematopoietic development

Hematopoietic progenitors and HSCs depend on SCF/c-Kit signaling for proliferation. In addition, erythropoiesis depends on both Epo/EpoR/Jak2- and SCF/c-Kit signals. This raised the question whether or not Jak2 participated in c-Kit signaling. Direct activation of Jak kinases by the tyrosine kinase activity of c-Kit remains controversial,[53,54] although a direct connection between EpoR and

c-Kit signaling modules was demonstrated.[55-57] A role for Jak2 in SCF-dependent colony formation and differentiation was also described in mast cells.[17,38] We consistently observed that Jak2-deficient fetal liver cells were impaired for SCF-dependent colony formation in several immature hematopoietic lineages. Jak2$^{-/-}$ cells not only failed to efficiently respond to SCF alone (favoring immature hematopoietic and mast cells) but were also less responsive to SCF + IL-3 and SCF + IL-7, promoting myeloid and lymphoid progenitor development, respectively. Again, cS5 expression partially reversed these defects in cytokine-dependent colony formation of Jak2$^{-/-}$ cells. These data suggest that c-Kit–dependent Stat5 activation via Jak2 mainly occurs in immature, primary hematopoietic cells (Figure S5B). SCF alone induced robust Stat5 phosphorylation in WT cS5 cells, which was further enhanced by the combination of Epo and SCF. Furthermore, Stat5 activation was also induced upon SCF stimulation in EpoR$^{-/-}$-cS5 and Jak2$^{-/-}$-cS5 cells. SCF-dependent activation of cS5 was completely dependent on the kinase activity of c-Kit, because it was blocked by the c-Kit inhibitor imatinib. The contribution of (other) Jak kinases in this process is likely because EpoR$^{-/-}$-cS5- and Jak2$^{-/-}$-cS5 cells were clearly more susceptible to a pan-Jak inhibitor than WT GFP and WT cS5 cells (data not shown). Alternatively, the c-Kit-dependent cS5 activation could occur in a complex "EpoR-c-Kit-signalosome," harboring different scaffold proteins and signal transducers.

Together, these interpretations are consistent with a model in which EpoR and c-Kit cooperate to activate the Jak-Stat pathway (Figure S5B), perhaps by interaction of the respective signaling modules upon receptor activation.[55,56,58] Such interactions could reflect the in vivo situation more closely than anticipated.

The role of Jak2 in c-Kit signaling might also have mechanistic implications for the biology of the Jak2V617F mutation in patients with polycythemia vera.[59-62] Because cells from respective patients respond more strongly to SCF,[63] it is conceivable that Jak2V617F is more susceptible to SCF signaling and thus also to Stat5 activation.

cS5 compensated for loss of Jak2 in mouse hematopoiesis in vivo

It is noteworthy that Jak2$^{-/-}$-cS5 cells gave rise to mature erythroid and myeloid cells in vivo upon transplantation of freshly transduced fetal liver cells in mice. To avoid development of the aggressive leukemia induced by cS5,[27] we used competitive repopulation conditions (ie, low amounts of fetal liver cells injected into sublethally irradiated mice). Under those conditions, all mice stayed healthy for longer than 6 months. Transplantation of higher cell numbers into lethally irradiated mice failed, because Jak2$^{-/-}$-cS5 cells did not provide radioprotection, whereas transplanted WT cS5 cells induced the expected leukemia.

It is noteworthy that Jak2$^{-/-}$-cS5 cells differentiated into mature CD71^{-}Ter119^{+} erythroid cells in vivo. This is of particular interest because erythroid cells of this stage were undetectable in fetal livers of Jak2$^{-/-}$ embryos. Attempts of transplanting Jak2$^{-/-}$-GFP cells failed because of the inability of those mutant cells to proliferate in vitro. Thus, we never obtained sufficient numbers of viable cells for transplantation experiments after the retroviral infection period (data not shown).

Despite the observed functional erythropoiesis of Jak2$^{-/-}$-cS5 cells in vivo, we observed a profound long-term repopulation defect of the Jak2 mutant cells. In line with this, transplantation of equal numbers of GFP^{+}Jak2$^{-/-}$-cS5 versus WT cS5 LT HSCs always resulted in a lower degree of chimerism in animals receiving Jak2$^{-/-}$-cS5 cells. Although all animals infused with WT cS5 cells maintained abundant GFP^{+} cells in their peripheral blood, 75% of mice receiving Jak2$^{-/-}$-cS5 cells were successfully engrafted, yet showed lower degrees of chimerism; some even lacked erythroid and/or macrophage-like cells.

Here we demonstrated that activation of Stat5 allowed in vitro and in vivo erythropoiesis and myelopoiesis in the absence of EpoR or Jak2. Note that the receptor tyrosine kinase c-Kit exhibited a significant degree of cross-talk with the Jak2-Stat5 axis to promote hematopoiesis (Figure S5B). Our data suggest that contributions from cytokine and growth factor signaling pathways converge on Jak2-Stat5 activation. This may represent a principle shared by different hematopoietic lineages or even multipotent progenitors and HSCs, to ensure efficient hematopoiesis as well as its strict regulation under different physiologic or pathologic conditions.

Acknowledgments

We thank G. Stengl for FACS and M. von Lindern for critical reading of the manuscript.

This work was supported by grants WK-001 (F.G. and M.A.K.) and SFB F028 (M.M,. H.B., R.M., E.W.M.) from the Austrian Research Foundation (Fonds zur Förderung der wissenschaftlichen Forschung); the Herzfelder Family Foundation (E.W.M.); and BM_WFa GZ200.112/1-VI/1/2004 (M.M.) from the Austrian Federal Ministry for Science and Research.

Authorship

Contribution: F.G., R.M., and H.B. designed research. F.G., M.A.K., B.K., R.M., and H.D. performed research and collected and analyzed data. T.K., V.B., U.K., K.P., and M.M. provided mouse lines and fetal liver cells. F.G. wrote the manuscript with the help of E.W.M., H.B., and R.M.

Conflict-of-interest disclosure: The authors declare no competing financial interests.

Correspondence: Prof Ernst W. Müllner, Max F. Perutz Laboratories, Medical University of Vienna, Dr Bohr-Gasse 9, Vienna 1030, Austria; e-mail: ernst.muellner@univie.ac.at.

References

1. Richmond TD, Chohan M, Barber DL. Turning cells red: signal transduction mediated by erythropoietin. Trends Cell Biol. 2005;15:146-155.
2. Klingmüller U, Wu H, Hsiao JG, et al. Identification of a novel pathway important for proliferation and differentiation of primary erythroid progenitors. Proc Natl Acad Sci U S A. 1997;94:3016-3021.
3. Chen C, Sytkowski AJ. Erythropoietin regulation of Raf-1 and MEK: evidence for a Ras-independent mechanism. Blood. 2004;104:73-80.
4. von Lindern M, Parren-van Amelsvoort M, van Dijk T, et al. Protein kinase C alpha controls erythropoietin receptor signaling. J Biol Chem. 2000; 275:34719-34727.
5. Tong Q, Chu X, Cheung JY, et al. Erythropoietin-modulated calcium influx through TRPC2 is mediated by phospholipase Cgamma and IP3R. Am J Physiol Cell Physiol. 2004;287:C1667-1678.
6. Cui Y, Riedlinger G, Miyoshi K, et al. Inactivation of Stat5 in mouse mammary epithelium during pregnancy reveals distinct functions in cell proliferation, survival, and differentiation. Mol Cell Biol. 2004;24:8037-8047.
7. Moriggl R, Gouilleux-Gruart V, Jahne R, et al. Deletion of the carboxyl-terminal transactivation domain of MGF-Stat5 results in sustained DNA binding and a dominant negative phenotype. Mol Cell Biol. 1996;16:5691-5700.
8. Teglund S, McKay C, Schuetz E, et al. Stat5a and Stat5b proteins have essential and nonessential, or redundant, roles in cytokine responses. Cell. 1998;93:841-850.
9. Hammerman PS, Fox CJ, Birnbaum MJ, Thompson CB. Pim and Akt oncogenes are independent

regulators of hematopoietic cell growth and survival. Blood. 2005;105:4477-4483.

10. Wilson A, Murphy MJ, Oskarsson T, et al. c-Myc controls the balance between hematopoietic stem cell self-renewal and differentiation. Genes Dev. 2004;18:2747-2763.
11. Tanaka M, Hirabayashi Y, Sekiguchi T, Inoue T, Katsuki M, Miyajima A. Targeted disruption of oncostatin M receptor results in altered hematopoiesis. Blood. 2003;102:3154-3162.
12. Wagner KU, Claudio E, Rucker EB 3rd, et al. Conditional deletion of the Bcl-x gene from erythroid cells results in hemolytic anemia and profound splenomegaly. Development. 2000;127:4949-4958.
13. Starr R, Metcalf D, Elefanty AG, et al. Liver degeneration and lymphoid deficiencies in mice lacking suppressor of cytokine signaling-1. Proc Natl Acad Sci U S A. 1998;95:14395-14399.
14. Kozar K, Ciemerych MA, Rebel VI, et al. Mouse development and cell proliferation in the absence of D-cyclins. Cell. 2004;118:477-491.
15. Wu H, Liu X, Jaenisch R, Lodish HF. Generation of committed erythroid BFU-E and CFU-E progenitors does not require erythropoietin or the erythropoietin receptor. Cell. 1995;83:59-67.
16. Neubauer H, Cumano A, Muller M, Wu H, Huffstadt U, Pfeffer K. Jak2 deficiency defines an essential developmental checkpoint in definitive hematopoiesis. Cell. 1998;93:397-409.
17. Parganas E, Wang D, Stravopodis D, et al. Jak2 is essential for signaling through a variety of cytokine receptors. Cell. 1998;93:385-395.
18. Pelletier S, Gingras S, Funakoshi-Tago M, Howell S, Ihle JN. Two domains of the erythropoietin receptor are sufficient for Jak2 binding/activation and function. Mol Cell Biol. 2006;26:8527-8538.
19. Ghaffari S, Kitidis C, Fleming MD, Neubauer H, Pfeffer K, Lodish HF. Erythropoiesis in the absence of janus-kinase 2: BCR-ABL induces red cell formation in JAK2$^{-/-}$ hematopoietic progenitors. Blood. 2001;98:2948-2957.
20. Ghaffari S, Kitidis C, Zhao W, et al. AKT induces erythroid-cell maturation of JAK2-deficient fetal liver progenitor cells and is required for Epo regulation of erythroid-cell differentiation. Blood. 2006;107:1888-1891.
21. Socolovsky M, Fallon AE, Wang S, Brugnara C, Lodish HF. Fetal anemia and apoptosis of red cell progenitors in Stat5a$^{-/-}$5b$^{-/-}$ mice: a direct role for Stat5 in Bcl-X(L) induction. Cell. 1999;98:181-191.
22. Socolovsky M, Nam H, Fleming MD, Haase VH, Brugnara C, Lodish HF. Ineffective erythropoiesis in Stat5a$^{-/-}$5b$^{-/-}$ mice due to decreased survival of early erythroblasts. Blood. 2001;98:3261-3273.
23. Zang H, Sato K, Nakajima H, McKay C, Ney PA, Ihle JN. The distal region and receptor tyrosines of the Epo receptor are non-essential for in vivo erythropoiesis. EMBO J. 2001;20:3156-3166.
24. Menon MP, Karur V, Bogacheva O, Bogachev O, Cuetara B, Wojchowski DM. Signals for stress erythropoiesis are integrated via an erythropoietin receptor-phosphotyrosine-343-Stat5 axis. J Clin Invest. 2006;116:683-694.
25. Onishi M, Nosaka T, Misawa K, et al. Identification and characterization of a constitutively active STAT5 mutant that promotes cell proliferation. Mol Cell Biol. 1998;18:3871-3879.
26. Dolznig H, Kolbus A, Leberbauer C, et al. Expansion and differentiation of immature mouse and human hematopoietic progenitors. Methods Mol Med. 2005;105:323-344.
27. Moriggl R, Sexl V, Kenner L, et al. Stat5 tetramer formation is associated with leukemogenesis. Cancer Cell. 2005;7:87-99.
28. Kamogawa Y, Lee HJ, Johnston JA, McMahon M, O'Garra A, Arai N. A conditionally active form of STAT6 can mimic certain effects of IL-4. J Immunol. 1998;161:1074-1077.
29. Wang D, Moriggl R, Stravopodis D, et al. A small amphipathic alpha-helical region is required for transcriptional activities and proteasome-dependent turnover of the tyrosine-phosphorylated Stat5. EMBO J. 2000;19:392-399.
30. Moriggl R, Berchtold S, Friedrich K, et al. Comparison of the transactivation domains of Stat5 and Stat6 in lymphoid cells and mammary epithelial cells. Mol Cell Biol. 1997;17:3663-3678.
31. John S, Vinkemeier U, Soldaini E, Darnell JE, Jr., Leonard WJ. The significance of tetramerization in promoter recruitment by Stat5. Mol Cell Biol. 1999;19:1910-1918.
32. Dolznig H, Boulme F, Stangl K, et al. Establishment of normal, terminally differentiating mouse erythroid progenitors: molecular characterization by cDNA arrays. Faseb J. 2001;15:1442-1444.
33. Littlewood TD, Hancock DC, Danielian PS, Parker MG, Evan GI. A modified oestrogen receptor ligand-binding domain as an improved switch for the regulation of heterologous proteins. Nucleic Acids Res. 1995;23:1686-1690.
34. Harir N, Pecquet C, Kerenyi M, et al. Constitutive activation of Stat5 promotes its cytoplasmic localization and association with PI3-kinase in myeloid leukemias. Blood. 2007;109:1678-1686.
35. Muta K, Krantz SB, Bondurant MC, Dai CH. Stem cell factor retards differentiation of normal human erythroid progenitor cells while stimulating proliferation. Blood. 1995;86:572-580.
36. Nocka K, Majumder S, Chabot B, et al. Expression of c-kit gene products in known cellular targets of W mutations in normal and W mutant mice–evidence for an impaired c-kit kinase in mutant mice. Genes Dev. 1989;3:816-826.
37. Zhao S, Zoller K, Masuko M, et al. JAK2, complemented by a second signal from c-kit or flt-3, triggers extensive self-renewal of primary multipotential hemopoietic cells. EMBO J. 2002;21:2159-2167.
38. Radosevic N, Winterstein D, Keller JR, Neubauer H, Pfeffer K, Linnekin D. JAK2 contributes to the intrinsic capacity of primary hematopoietic cells to respond to stem cell factor. Exp Hematol. 2004;32:149-156.
39. Bowie MB, Kent DG, Copley MR, Eaves CJ. Steel factor responsiveness regulates the high self-renewal phenotype of fetal hematopoietic stem cells. Blood. 2007;109:5043-5048.
40. Bryder D, Rossi DJ, Weissman IL. Hematopoietic stem cells: the paradigmatic tissue-specific stem cell. Am J Pathol. 2006;169:338-346.
41. Bradley HL, Couldrey C, Bunting KD. Hematopoietic-repopulating defects from STAT5-deficient bone marrow are not fully accounted for by loss of thrombopoietin responsiveness. Blood. 2004;103:2965-2972.
42. Dolznig H, Grebien F, Deiner EM, et al. Erythroid progenitor renewal versus differentiation: genetic evidence for cell autonomous, essential functions of EpoR, Stat5 and the GR. Oncogene. 2006;25:2890-2900.
43. von Lindern M, Deiner EM, Dolznig H, et al. Leukemic transformation of normal murine erythroid progenitors: v- and c-ErbB act through signaling pathways activated by the EpoR and c-Kit in stress erythropoiesis. Oncogene. 2001;20:3651-3664.
44. Engblom D, Kornfeld JW, Schwake L, et al. Direct glucocorticoid receptor-Stat5 interaction in hepatocytes controls body size and maturation-related gene expression. Genes Dev. 2007;21:1157-1162.
45. Hoelbl A, Kovacic B, Kerenyi MA, et al. Clarifying the role of Stat5 in lymphoid development and Abelson-induced transformation. Blood. 2006;107:4898-4906.
46. Murray PJ. The JAK-STAT signaling pathway: input and output integration. J Immunol. 2007;178:2623-2629.
47. Dolznig H, Habermann B, Stangl K, et al. Apoptosis protection by the Epo target Bcl-X(L) allows factor-independent differentiation of primary erythroblasts. Curr Biol. 2002;12:1076-1085.
48. Garçon L, Rivat C, James C, et al. Constitutive activation of STAT5 and Bcl-xL overexpression can induce endogenous erythroid colony formation in human primary cells. Blood. 2006;108:1551-1554.
49. Fang J, Menon M, Kapelle W, et al. EPO modulation of cell cycle regulatory genes, and cell division, in primary bone marrow erythroblasts. Blood. 2007;110:2361-2370.
50. Sathyanarayana P, Menon MP, Bogacheva O, et al. Erythropoietin modulation of podocalyxin and a proposed erythroblast niche. Blood. 2007;110:509-518.
51. Schuringa JJ, Chung KY, Morrone G, Moore MA. Constitutive activation of STAT5A promotes human hematopoietic stem cell self-renewal and erythroid differentiation. J Exp Med. 2004;200:623-635.
52. Taylor DK, Walsh PT, LaRosa DF, et al. Constitutive activation of STAT5 supersedes the requirement for cytokine and TCR engagement of CD4+ T cells in steady-state homeostasis. J Immunol. 2006;177:2216-2223.
53. Huppertz C, Schwartz C, Becker W, Horn F, Heinrich PC, Joost HG. Comparison of the effects of insulin, PDGF, interleukin-6, and interferon-gamma on glucose transport in 3T3-L1 cells: lack of cross-talk between tyrosine kinase receptors and JAK/STAT pathways. Diabetologia. 1996;39:1432-1439.
54. Weiler SR, Mou S, DeBerry CS, et al. JAK2 is associated with the c-kit proto-oncogene product and is phosphorylated in response to stem cell factor. Blood. 1996;87:3688-3693.
55. Wu H, Klingmuller U, Besmer P, Lodish HF. Interaction of the erythropoietin and stem-cell-factor receptors. Nature. 1995;377:242-246.
56. Wu H, Klingmuller U, Acurio A, Hsiao JG, Lodish HF. Functional interaction of erythropoietin and stem cell factor receptors is essential for erythroid colony formation. Proc Natl Acad Sci U S A. 1997;94:1806-1810.
57. von Lindern M, Schmidt U, Beug H. Control of erythropoiesis by erythropoietin and stem cell factor: a novel role for Bruton's tyrosine kinase. Cell Cycle. 2004;3:876-879.
58. Wessely O, Bauer A, Quang CT, et al. A novel way to induce erythroid progenitor self renewal: cooperation of c-Kit with the erythropoietin receptor. Biol Chem. 1999;380:187-202.
59. Baxter EJ, Scott LM, Campbell PJ, et al. Acquired mutation of the tyrosine kinase JAK2 in human myeloproliferative disorders. Lancet. 2005;365:1054-1061.
60. James C, Ugo V, Le Couedic JP, et al. A unique clonal JAK2 mutation leading to constitutive signalling causes polycythaemia vera. Nature. 2005;434:1144-1148.
61. Kralovics R, Passamonti F, Buser AS, et al. A gain-of-function mutation of JAK2 in myeloproliferative disorders. N Engl J Med. 2005;352:1779-1790.
62. Levine RL, Wadleigh M, Cools J, et al. Activating mutation in the tyrosine kinase JAK2 in polycythemia vera, essential thrombocythemia, and myeloid metaplasia with myelofibrosis. Cancer Cell. 2005;7:387-397.
63. Kaushansky K. On the molecular origins of the chronic myeloproliferative disorders: it all makes sense. Blood. 2005;105:4187-4190.

3.2.3 Signal transducer and activator of transcription 3 activation promotes invasive growth of colon carcinomas through matrix metalloproteinase induction.

Svetlana A. Tsareva*,†, Richard Moriggl‡, Florian M. Corvinus*, Bernd Wiederanders*, Alexander Schütz§, Boris Kovacic¶ and Karlheinz Friedrich*

*Institute of Biochemistry I, Friedrich-Schiller University Jena Medical School, Jena, Germany

†Novosibirsk State Medical Academy, Novosibirsk, Russia

‡Ludwig Boltzmann Institute for Cancer Research, Vienna, Austria

§Institute of Pathology, University of Leipzig, Leipzig, Germany

¶Institute of Molecular Pathology (IMP), Vienna, Austria

Neoplasia • Vol. 9, No. 4, April 2007, pp. 279–291 279

www.neoplasia.com

Signal Transducer and Activator of Transcription 3 Activation Promotes Invasive Growth of Colon Carcinomas through Matrix Metalloproteinase Induction[1]

Svetlana A. Tsareva[*,†], Richard Moriggl[‡], Florian M. Corvinus*, Bernd Wiederanders*, Alexander Schütz[§], Boris Kovacic[¶] and Karlheinz Friedrich**

*Institute of Biochemistry I, Friedrich-Schiller University Jena Medical School, Jena, Germany; †Novosibirsk State Medical Academy, Novosibirsk, Russia; ‡Ludwig Boltzmann Institute for Cancer Research, Vienna, Austria; §Institute of Pathology, University of Leipzig, Leipzig, Germany; ¶Institute of Molecular Pathology (IMP), Vienna, Austria

Abstract

Signal transducer and activator of transcription 3 (STAT3) is aberrantly activated in colorectal carcinomas (CRCs). Here, we define the relationship between STAT3 function and the malignant properties of colon carcinoma cells. Elevated activation of STAT3 enhances invasive growth of the CRC cell lines. To address mechanisms through which STAT3 influences invasiveness, the protease mRNA expression pattern of CRC biopsies was analyzed and correlated with the STAT3 activity status. These studies revealed a striking coincidence of STAT3 activation and strong expression of matrix metalloproteinases MMP-1, -3, -7, and -9. Immunohistological examination of CRC tumor specimens showed a clear colocalization of MMP-1 and activated STAT3. Experimentally induced STAT3 activity in CRC cell lines enhanced both the level of MMP-1 mRNA and secreted MMP-1 enzymatic activity. A direct connection of STAT3 activity and transcription from the MMP-1 promoter was shown by reporter gene experiments. Moreover, high-affinity binding of STAT3 to STAT recognition elements in both the MMP-1 and MMP-3 promoter was demonstrated. Xenograft tumors arising from implantation of CRC cells into nude mice showed simultaneous appearance and colocalization of p-Y-STAT3 and MMP-1 expression. Our results link aberrant activity of STAT3 in CRC to malignant tumor progression through upregulated expression of MMPs.

Neoplasia (2007) **9**, 279–291

Keywords: Colorectal carcinoma, invasiveness, STAT3, matrix metalloproteinases, gene regulation.

Introduction

Carcinomas frequently show aberrant activity of signal transducers and activators of transcription (STATs). Increased STAT3 activity is mostly tumor promoting, whereas elevated STAT1 activity is tumor growth inhibiting [1]. Among the members of the STAT family, STAT3 mediates the most complex spectrum of cellular responses including differentiation, proliferation, survival, and apoptosis, depending on the tissue context [2]. Constitutive activity of STAT3 was observed in many malignant tumors of both hematopoietic and solid type [3]. In addition, an artificially dimerized variant of STAT3 was shown to act as a *bona fide* oncoprotein by eliciting cellular transformation of fibroblasts and tumorigenesis in nude mice [4]. We have recently investigated biopsies of colorectal carcinomas (CRCs) and analyzed the spectrum of STAT activity. Most significantly, we observed constitutive activation of STAT3α in carcinoma cells of more than 90% of the tumors [5].

Experimental inhibition of STAT3 activity in tumor cell lines and tumor tissue yielded promising results with regard to STAT3 as an interesting target for tumor therapy [6–8]. Although downstream events connecting aberrant STAT3 activity to malignant cell properties are insufficiently defined, they involve the upregulation of genes promoting cell cycle progression (cyclin D1, c-myc) and/or preventing apoptosis (bcl-x, mcl-1, survivin) [4,9,10].

Recent studies showed that STAT3 activation in tumors may be associated with metastasis and poor prognosis [8,11], indicating that inappropriate signaling by STAT3 coincides with invasive growth of cancer cells. Interestingly, blocking STAT3 activity reduced the motility of ovarian cancer cells whose aggressive clinical behavior showed a correlation with constitutively active STAT3 levels [12]. So far, how STAT3 promotes

Abbreviations: c.a., constitutively active; CRC, colorectal carcinoma; d.n., dominant negative; EMSA, electrophoretic mobility shift assay; IL, interleukin; MMP, matrix metalloproteinase; JAK, janus kinase; STAT, signal transducer and activator of transcription

Address all correspondence to: Karlheinz Friedrich, Friedrich-Schiller University Jena Medical School, Institute of Biochemistry I, Nonnenplan 2, D-07743 Jena, Germany.
E-mail: khf@mti.uni-jena.de

[1]Part of this work was funded by the Interdisziplinäres Zentrum für Klinische Forschung—IZKF Jena, Project B 307-01035.
Received 22 December 2006; Revised 28 February 2007; Accepted 2 March 2007.

DOI 10.1593/neo.06820

cancer development and whether it is able to control invasive cell properties are largely undefined.

Tumor invasion and metastasis require proteolytic degradation of the basement membrane and the extracellular matrix (ECM). Matrix metalloproteinases (MMPs) are chiefly involved in the dissemination of cancer cells by breaking down the ECM and creating an environment that supports the initiation and maintenance of tumor growth. The MMP family, consisting of roughly 20 members, displays a conserved structure and enzymatic mechanism [13]. MMP expression is low in most normal cells under regular physiological conditions; however, it is dramatically increased in a variety of cancer types, which is indicative of invasive disease with a poor clinical prognosis [14–16]. Interestingly, knocking out or inhibition of some MMPs results in the reduction of tumor growth. For instance, the spontaneous development of intestinal tumors in mice with adenomatous polyposis coli (Apc) gene mutations is slower in MMP-7–deficient animals [17]. Moreover, experimental metastasis is suppressed in MMP-9–deficient mice [18], and MMP-11 knockout mice show reduced chemically induced tumorigenesis [19]. Inhibitors acting on MMP-1, MMP-3, MMP-7, and MMP-9 behaved as potent antiangiogenic and antimetastatic agents in animal models [20,21].

The recognition of STAT proteins as being potential players in oncogenic cell transformation was paralleled by their involvement in the modulation of activity for both promoters of MMPs and tissue inhibitors of MMP (TIMPs) [22–26]. A recent report demonstrated that transcriptional upregulation of MMP-9 is directly involved in the oncogenic transformation of mammary epithelial cells via a constitutively active mutant of STAT3 [27]. Similar studies on other MMPs have not yet been published.

The interstitial collagenase MMP-1 degrades collagen types I, II, and III, which are the most abundant proteins of the ECM [28]. It is already well established that MMP-1 is required for invasive growth of tumor cells [29]. For instance, it plays a critical role in the development of malignancy in CRC. Levels of MMP-1 increase during CRC progression and higher levels of expression are associated with shorter disease-free survival times [30,31]. The particular importance of MMP-1 for increased invasiveness of colon carcinoma cells *in vitro* has recently been demonstrated [32].

Various stimuli such as cytokines, growth factors, cell–cell, and cell–matrix interactions influence MMP expression through transcriptional regulation [33]. Well-characterized intracellular signal transduction reactions leading to the modulation of MMP promoter activity are mostly centered around mitogen-activated protein kinases, which, upon activation, enter the nucleus and phosphorylate transcription factors such as AP-1 and Ets proteins [34,35]. The complex transcriptional regulation of MMP promoters also involves contributions from more specific transcription factors, including NFκB as a mediator of toll-like receptors [36] and Smads, which are effectors of receptors for transforming growth factor-β, activins, and related ligands [37].

Our finding that STAT3 is activated in most CRCs left us with the question as to how STAT3-driven transcription might contribute to the malignancy of CRC cells. Reports on the involvement of janus kinase (JAK)/STAT signaling in the regulation of invasion-associated proteases [23–25] prompted us to study the correlation of STAT3 activation and MMP protease expression in CRC. Here, we show for the first time a causal role of STAT3 for the elevated expression of MMP-1, MMP-3, MMP-7, and MMP-9 in CRC leading to increased invasiveness of tumor cells.

Materials and Methods

Tumor Biopsies

Surgical tumor specimens were obtained from patients with CRC after approval of the study by the local ethical committee. Biopsies were snap-frozen in liquid nitrogen immediately after resection. For protein and RNA analysis, frozen blocks were disintegrated mechanically by using a Micro Dismembranator (Braun, Melsungen, Germany). For Western blot studies, whole-cell extracts were prepared by suspending the material in a buffer containing 20 mmol/l Hepes (pH 7.9), 400 mmol/l NaCl, 1 mmol/l EDTA, 20% glycerol, 1 mmol/l dithiothreitol, 1 mmol/l phenylmethylsulfonyl fluoride, 5 μg/ml leupeptin, 0.2 U/ml aprotinin, 5 mmol/l sodium orthovanadate, 10 mmol/l NaF, and 5 mol/l β-glycerophosphate, followed by three to four freeze–thaw cycles in liquid nitrogen and on ice. Extracts were cleared at 20,000*g* for 30 minutes at 4°C. Supernatants were subjected to protein determination and SDS-PAGE. Total RNA was isolated from disintegrated biopsies by homogenization in TRIzol Reagent (Gibco BRL, Gaithersburg, MD) as described below.

Cell Lines and Cell Culture

Colon carcinoma cell line HT-29 was purchased from the American Type Culture Collection (Rockville, MD). Low passage number cell line CoGa-1 [38] was obtained from L.A. Huber, Innsbruck. All cell lines were cultured in RPMI 1640 medium containing 10% fetal calf serum, 200 mmol/l L-glutamine, 100 mmol/l sodium pyruvate, and 1 mg/ml gentamycin. Cells were grown in coated tissue culture plasticware (Greiner Labortechnik, Frickenhausen, Germany).

For cytokine stimulation, HT-29 or CoGa-1 cells were incubated with 20 ng/ml recombinant human interleukin (IL)-6 (R&D Systems GmbH, Wiesbaden, Germany) for 30 minutes (Western blotting), 18 hours (reporter gene assay) or 24 hours (expression analysis) at 37°C. Cells were harvested at 80% confluence after three PBS washes at 4°C. Whole-cell extracts were prepared from cell pellets as described above.

DNA Constructs

Construction of the retroviral expression plasmids for STAT3 mutants and generation of HT-29–derived cell lines by retrovirus infection has been described previously [5]. CoGa-1 clones stably expressing STAT3 wild type or the constitutively active STAT3 mutant (STAT3 c.a.) were generated similarly.

The MMP-1 promoter/luciferase reporter plasmid −4372 hMMP-luci (GenBank accession no. AF023338), obtained from C. E. Brinckerhoff (Dartmouth Medical School, Hanover, NH) was described previously [39].

Electrophoretic Mobility Shift Assay

Extracts from tumor biopsies and cultivated cells were prepared and subjected to band shift analysis as described [5]. Briefly, double-stranded, blunt-ended oligonucleotides corresponding to known and potential STAT binding sites were annealed and end-labeled using [^{32}P]γ-ATP and T4 polynucleotide kinase to a specific activity of 10,000 cpm/fmol as described [40,41]. Binding reactions were performed by incubating 10,000 cpm of radiolabeled probe with 20 μg of cell lysate for 30 minutes at room temperature. For supershift reactions of STAT3-containing complexes, 2 μg of anti-STAT3 antibody C-20 (Santa Cruz Biotechnology, Santa Cruz, CA) was added to the binding reactions. Samples were separated by electrophoresis through 6% native polyacrylamide gels and analyzed by autoradiography using BioMax sensitive films (Kodak, Stuttgart, Germany). For the determination of inducible STAT3 binding to potential binding sites, 293T cells were cotransfected with eukaryotic expression vectors for STAT3 and JAK2 by the lipofectamine transfection method and further treated as described [40,41]. Cells were optionally stimulated with human IL-6 (10 ng/ml; R&D Systems) for 30 minutes before harvesting. Extracts were prepared using unstimulated [plain DMEM containing 10% fetal calf serum (FCS)] versus IL-6–stimulated extracts. The mutated "m67" STAT-binding site from the human c-fos promoter 5′-GTCGACATTTCCCGTAAATCGTCGA-3′ [41] served as a positive control for high-affinity binding of STAT3.

Immunohistology

Immunohistological detection of MMP-1 expression in tumor biopsies was performed as described previously [42]. Briefly, formalin-fixed, paraffin-embedded sections (4 μm) were deparaffinized and subsequently treated with 0.3% H_2O_2 for 30 minutes to reduce endogenous peroxidase activity. Sections were incubated at 4°C overnight with a 1:50 dilution of anti–MMP-1 (Dako Diagnostik, Hamburg, Germany) in TBS buffer containing 20% goat serum to block unspecific binding sites, followed by incubation with goat anti-mouse biotin and streptavidin–horseradish peroxidase (BioGenex, San Ramon, CA) and development with diaminobenzidine. Finally, all specimens were coverslipped using Aquatex (Merck, Darmstadt, Germany). Negative controls were performed by omission of the primary antibody.

Soft Agar Assay for Anchorage-Independent Growth

Formation of colonies in soft agar as a parameter of cell transformation was determined as described [43]. Briefly, HT-29– or CoGa-1–derived cells were assayed by seeding 10,000 cells into 500 μl of 0.6% agar (Agarose nobile, Becton Dickinson, Bedford, MA) diluted in RPMI 1640 medium containing 10% FCS. The mixture was poured into six-well plates lined previously with 500 μl of 0.5% agar in medium. The plates were incubated for 2 to 3 weeks at 37°C; 250 μl of fresh medium was added every 3 days. After this period, colonies were stained with 3-(4,5-dimethylthiazol-2-yl)-2,5-diphenyl tetrazolium bromide (MTT, 500 μg/ml) at 37°C for 2 hours before photography and counting.

In Vitro *Cell Invasion Assay*

Cell invasiveness was quantified by a modified Boyden chamber method using polycarbonate transwells (Corning Costar Corp., Cambridge, MA) as described in detail previously [44]. Briefly, 2×10^5 exponentially growing cells were seeded onto membrane filters coated with Matrigel (Becton Dickinson) and transmigration through the Matrigel layer was monitored after incubation for 24 hours at 37°C. The percentage of invasive cells was expressed by relating the total number of migrated cells to the number of cells originally applied to the top of the transwell, which was set at 100%.

Protease Expression Analysis by cDNA Arrays

cDNA macroarrays on the basis of nylon membranes were prepared as described previously [44]. Information on the sequences and the arrangement of probes as well as experimental details are available upon request.

Polymerase chain reaction (PCR) primers used to generate the probes relevant in this study were the following: MMP1 sense, 5′-AGGGTCAAGCAGACATCATG-3′; MMP1 antisense, 5′-AGCATCGATATGCTTCACAGT-3′; MMP3 sense, 5′-TTGCAGTTAGTGAACATGGA-3′; MMP3 antisense, 5′-ATCCAGCTCGTACCTCA-3′; MMP7 sense, 5′-GGCATGAGTGAGCTACAGTG-3′; MMP7 antisense, 5′-CCAGCGTTCATCCTCATCGA-3′; MMP9 sense, 5′-CTTCTACGGCCACTACTGTG-3′; MMP9 antisense, 5′-CACTGCAGGATGTCATAGGT-3′; β-actin sense, 5′-ACCACGGCCGAGCGGGAAATC-3′; and β-actin antisense, 5′-GAGCCGCCGATCCACACGGAGTA-3′.

Hybridization pattern data were processed by use of the AIDA imaging software (Raytest, Straubenhardt, Germany). The average densitometry signals of the duplicate spots, minus background, were calculated. The signals were then normalized against an average of all signals from the respective membranes and expressed as relative densitometric units.

Quantification of Specific mRNAs by Real-Time PCR

Quantitation of cDNA from specific mRNA transcripts was accomplished by real-time reverse transcription-PCR (RT-PCR) using the TaqMan protocol and an ABI/Prism 7000 equipment (Applied Biosystems, Foster City, CA). Predesigned fluorogenic Assays-on-Demand TaqMan probes and primer pairs for MMP-1 (Hs00233958_m1) and 18S rRNA (Hs99999901_s1) were obtained from Applied Biosystems. The following 6-carboxy-fluorescein–labeled probes were used for PCR amplification: MMP-1, 5′-AAAGACAGATTCTACATGCGCACAA-3′; 18S rRNA, 5′-TGGAGGGCAAGTCTGGTGCCAGCAG-3′. The specific primers for MMP-1 and 18S rRNA were predicted to amplify 150-

and 120-bp DNA fragments, respectively. A total reaction volume of 25 μl contained 12.5 μl of 2 × TaqMan Universal Master Mix, No AmpErase UNG (Applied Biosystems), 3 μl cDNA (prepared as described above), 1.25 μl of 20 × Assays-on-Demand Gene Expression products (Applied Biosystems) for MMP-1, consisting of 20 × mix of unlabeled PCR primers (18 μmol/l) and 5 μmol/l TaqMan MGB probe (6-carboxy-fluorescein dye–labeled MMP-1). Forty PCR cycles of 95°C for 15 seconds and 60°C for 1 minute were run after an initial incubation at 95°C for 10 minutes.

The MMP-1 gene copy number in samples to be analyzed was quantified by simultaneously generating a standard curve for both MMP-1 and 18S rRNA as an endogenous control from serial dilutions of HT-29 cDNA (equivalent to a cDNA amount from 100 ng to 100 pg of initial total RNA). The target amounts of unknown samples were divided by the endogenous reference amount to obtain a normalized target value. Results were expressed as *n*-fold differences in MMP-1 mRNA relative to 18S rRNA. Data collection and analysis was performed with the SDS software version 1.0.1 (Applied Biosystems). Data were then exported and further processed using the Excel software (Microsoft, Redmond, WA).

Luciferase Reporter Gene Assay

Exponentially growing cells (7×10^5) of HT-29 and CoGa-1 derivatives were plated in six-well cluster plates (Greiner) in 2 ml RPMI 1640/10% FCS and grown to 80% to 90% confluency. The cells were washed, transferred into 1 ml/well fresh medium, and cotransfected with 1 μg of MMP-1 promoter/luciferase construct and 0.1 μg of the pRL-TK *Renilla* luciferase plasmid (Promega, Madison, WI) as an internal control for transfection efficiency by using PolyFect reagent (Qiagen, Hilden, Germany). Both DNAs were diluted with growth medium containing no serum, antibiotics, or proteins to a final volume of 100 μl. The solutions were mixed and 9 μl of PolyFect was added per well. The mixture was incubated at room temperature for 5 to 10 minutes to allow complex formation before 1 ml medium was added. After 14 hours incubation at 37°C, the cells were gently washed with RPMI 1640 and incubated with fresh RPMI, optionally containing IL-6 (20 ng/ml). The cells were harvested 8 hours later using reporter lysis buffer (Promega). Luciferase and *Renilla* activities were determined with the Dual-Luciferase Reporter Assay System kit from Promega and following the manufacturer's instructions. Luminescence was measured on a Micro Luminat LB 96 P Luminometer and reported as relative light units. Three independent transfections, each run in triplicate, were performed, and the results were normalized to the *Renilla* activity.

Determination of MMP-1 Activity in Cell Supernatants

Levels of enzymatically active MMP-1 were measured using an MMP-1 Fluorokine E ELISA kit (R&D Systems) according to the manufacturer's instructions. HT-29–derived cells were cultivated for 4 days in RPMI 1640/10% FCS in the presence or absence of 20 ng/ml IL-6. After centrifugation (4°C, 1000*g*, 5 minutes), 150 μl of culture supernatants from HT-29 cells was mixed with 100 μl of Assay diluent buffer (R&D Systems) in individual wells of 96-well ELISA plates. Simultaneously, standard samples containing known concentrations of active MMP-1 were treated in the same fashion. The plates were gently shaken for 3 hours at room temperature before unbound material was washed off. Subsequently, 200 μl of activation reagent (0.5 M APMA in DMSO, R&D systems) was added to each well for pro–MMP-1 activation. The plates were incubated for 2 hours at 37°C in a humidified environment. After washing, 200 μl of 1 mmol/l fluorogenic substrate in DMSO (R&D Systems) was added. After another 20 hours at 37°C, fluorescence was determined using a fluorescence plate reader set (SPECTROmax plus, Molecular Devices, Sunnyvale, CA) with an excitation wavelength set to 320 nm and emission wavelength set to 405 nm. Standard curves were generated by plotting the mean relative fluorescence units for each standard for active MMP-1 against the concentrations. Concentrations of active MMP-1 in the cell supernatant samples were determined from the standard curves.

Xenograft Experiments

A total of 10^5 cells of the HT-29 cell line was suspended in PBS and injected subcutaneously at a volume of 100 μl into the neck of 5- to 8-week-old male athymic Hsd:NMRI-nu/nu mice (Harlan, Indianapolis, IN). Mice were sacrificed after the tumors had reached a size of approximately 2000 mm^2. Tumor specimens were further treated similarly to the human biopsy samples (see above).

Statistical Analysis

Statistical analysis was performed using SPSS software version 11.0 (SPSS, Chicago, IL). To calculate significance levels, data sets were compared using the Wilcoxon test for paired samples and Mann–Whitney test for unpaired samples, respectively. Probability values of $P < .05$ were used as the generally accepted level of statistical significance.

Results

STAT3 Activity Enhances Anchorage-Independent Growth and Invasiveness of CRC Cells

We have shown that STAT3 is constitutively active in carcinoma cells from a majority of human CRC biopsies. It also drives proliferation of both the established CRC cell line HT-29 and the low passage number colon cancer cell line CoGa-1 [5]. To address the role of STAT3 in the development and maintenance of malignancy, we studied the influence of STAT3 activity on parameters of cell transformation in both cell lines.

First, the STAT3 expression–dependent formation of colonies in soft agar was determined as a measure of oncogenic cell transformation. For this purpose, we employed nontransfected HT-29 and CoGa-1 cells as well as derivatives stably overexpressing STAT3 or the mutant STAT3 c.a., respectively. STAT3 c.a. functions independently of cytokine

activation through dimerization via an artificial disulfide bridge. After confirmation of elevated STAT3 DNA-binding activity in the transfected cells compared with the parental cell lines [5] (data not shown) cells were seeded into soft agar, overlaid with medium, and incubated for 2 weeks before colonies were counted. As shown in Figure 1, in both cell lines an overexpression of wild type or, to a higher degree, of STAT3 c.a., resulted in a profoundly increased number of colonies, most notably in the absence of exogenous cytokines.

Next, we addressed the influence of STAT3 on the invasive cell properties of colon carcinoma cells as measured by their ability to cross an artificial ECM (Matrigel). Parental cells of HT-29 and CoGa-1 as well as derivatives overexpressing either STAT3 or STAT3 c.a. were seeded onto a layer of Matrigel and analyzed after 24 hours for the fraction of cells migrating through the gel and accumulating in the lower compartment of a transwell chamber (Figure 1*C*). In both cases, cells expressing STAT3 c.a. and overexpressing STAT3 had a much stronger invasive character than the parental CRC cell lines, indicating that STAT3 has an enhancing effect on invasiveness in colon carcinoma cells.

To support this notion, we measured the invasiveness of HT-29 cells dependent on STAT3 activation through IL-6 and/or reduction of STAT3 activity by means of a dominant-negative STAT3 mutant (STAT3 d.n.). As shown in Figure 1*D*, IL-6 evoked stronger cell invasiveness of HT-29 cells in addition to enhancing the invasion-promoting effect of overexpressed STAT3. On the other hand, expression of STAT3 d.n. with the critical Tyr705 mutated to Phe, which blocked receptor-mediated activation of endogenous STAT3, reduced the constitutive invasiveness of HT-29 cells and completely suppressed the effect of IL-6. These results are in good accordance with the tyrosine phosphorylation status of STAT3 in HT-29 cells under the respective conditions [5] and indicate a clear correlation of STAT3 activity with the potency of cells to grow in an invasive manner.

Elevated Expression of MMPs in Colorectal Tumor Biopsies Coincides with Constitutive Activity of STAT3

Our results initiated the question of the mode of action of STAT3 in enhancing the invasiveness of colon carcinoma cells. Proteinases, in particular collagenases, are known to be key lytic enzymes required for the invasion process because their inhibition totally prevented amnion or Matrigel invasion [45]. To explore the molecular mechanisms responsible for STAT3-mediated tumor invasion, we

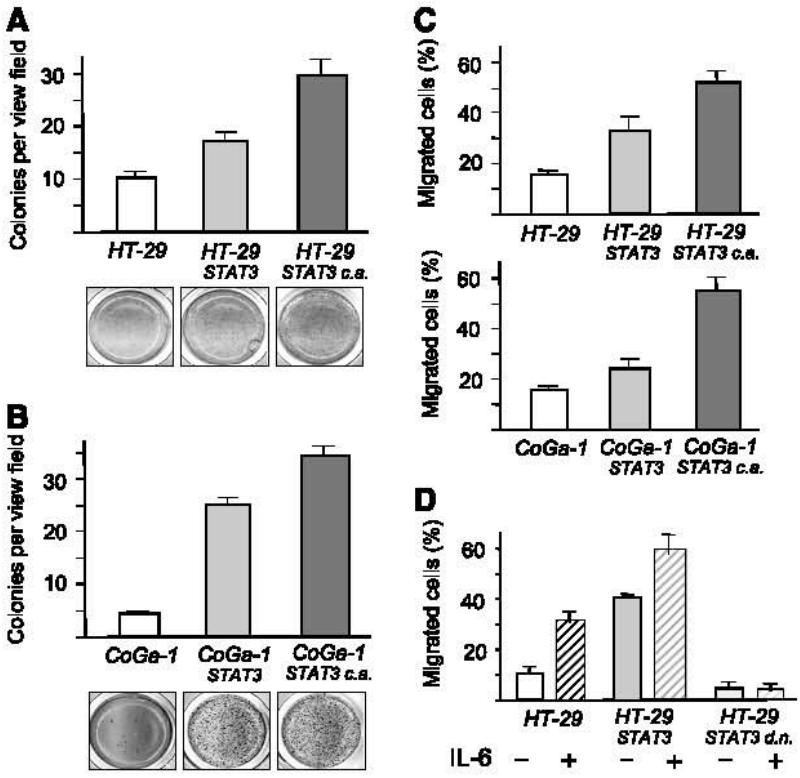

Figure 1. *Influence of STAT3 expression and activity on soft agar colony formation and invasiveness of colon carcinoma cells. (A and B) Dependence of colony formation of HT-29 and CoGa-1 cells on STAT3 expression and activity. Cell lines overexpressing STAT3 or STAT3 c.a. as well as nontransfected control cells were grown in soft agar for 2 weeks. Colonies formed were visualized by staining with MTT (500 μg/ml) (bottom) and counted (top). The values represent triplicate experiments. (C) STAT3 expression– and activity-dependent invasiveness* in vitro *of HT-29–derived cell lines. HT-29, HT-29-STAT3, and HT-29-STAT3 c.a. cells were incubated in invasion chambers containing Matrigel-coated membranes. After 24 hours, cells that had migrated through both Matrigel and membrane to the lower compartment of the system were counted. Invasiveness was expressed as the percentage of cells that had reached the lower chamber at the end of the experiment. The assay was repeated four times in triplicate. (D) IL-6–induced invasiveness of HT-29 cells and derivatives. HT-29, HT-29-STAT3, and HT-29-STAT3 d.n. were grown on Matrigel-coated membranes as in (C). IL-6 was optionally present in the medium (+; striped columns) at a concentration of 20 ng/ml 24 hours before the cell lines were tested and throughout the entire experiment. The experiment was repeated three times. All treatments were performed in triplicate.*

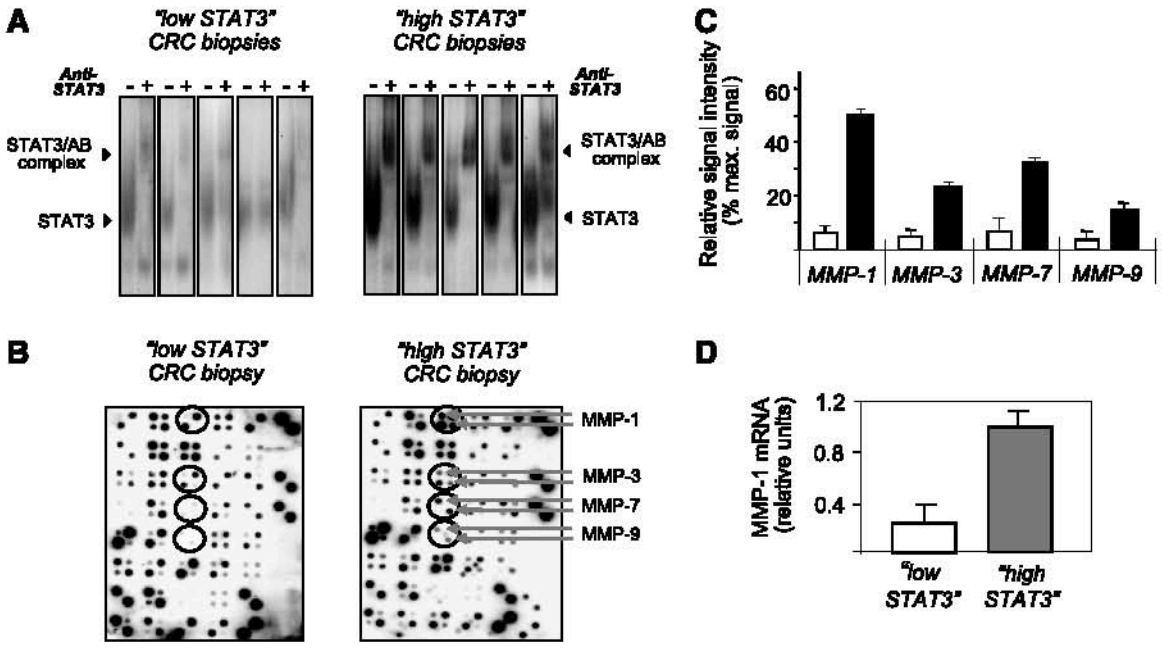

Figure 2. *Correlation of STAT3 activation and protease expression in CRC biopsies. (A) EMSA analysis of STAT3 activation in CRC biopsies scored as low STAT3 or high STAT3 according to previous determination of STAT3 tyrosine phosphorylation [5]. Extracts were incubated with the double-stranded ^{32}P-labelled SIE m67 STAT binding site. Complexes were resolved on 6% native polyacrylamide gels and visualized by autoradiography. The identity of STAT3-containing complexes was verified by including an antibody to STAT3 in the binding reactions as indicated. Positions of the specific STAT3-containing complexes are marked by arrows. (B) Comparative analysis of protease expression in a respective CRC sample with high and low STAT3 activity using protease cDNA macroarrays. Total RNA isolated from tumor samples was reverse transcribed into digoxigenin-labeled cDNA samples, which were hybridized to cDNA arrays covering probes for 50 different human proteases. (C) The relative expression levels of MMP-1, -3, -7, and -9 in 5 tumor samples of each group determined as in (B) were quantified by densitometry and normalized to four "housekeeping" mRNAs (GAPDH, β-actin, ubiquitin, and R-13a). (D) Quantification of MMP-1 mRNA expression levels in CRC biopsies of the high-STAT3 and low-STAT3 type. Three independent experiments, each run in triplicate, were performed; results were normalized to 18S rRNA expression and expressed as the means ± S.D. Relative MMP-1 expression was calculated by arbitrarily setting the expression level of high-STAT3 samples as 1.*

correlated STAT3 activation in colorectal tumors with protease expression.

First, we verified the previously determined status of 32 CRC biopsies with regard to STAT3 tyrosine phosphorylation [5] by electrophoretic mobility shift assay (EMSA) analysis of specific DNA-binding activity (data not shown) and categorized them into a "high STAT3" and a "low STAT3" group. A total of 13 samples with strikingly strong STAT3 activity in both assays were considered high STAT3, and 9 biopsy samples with very low STAT3 activity were considered low STAT3. Figure 2*A* shows five representative examples from each group. Seven samples with intermediate activity and three samples completely negative for STAT3 activity were excluded from further analysis. The remaining samples were tested in a comparative fashion for the respective abundance of protease mRNAs by subjecting them to the isolation of total RNA and the synthesis of digoxigenin-labeled cDNAs. cDNAs were hybridized to arrays covering 50 different human protease probes (arrangement of probes on the arrays is available upon request). Figure 2*B* shows in one representative biopsy for each group that in particular the mRNAs for MMP-1, MMP-3, MMP-7, and MMP-9 were much more abundant in colorectal tumor tissue with a high degree of STAT3 activity. Figure 2*C* summarizes expression data for the MMPs obtained from a larger population of tumors (22 patients in total) quantitated by densitometric determination of signal intensities of the arrays. MMP-1 was given special attention because its expression appeared to correlate with STAT3 activity in a particularly evident fashion and because of its important role in the invasiveness of colon carcinoma cells. As an independent criterion for MMP-1 expression, we determined MMP-1 mRNA in 13 specimens of high STAT3 and 9 specimens of low STAT3 colorectal tumor biopsies by real-time PCR. Figure 2*D* shows that the expression of MMP-1 was strikingly higher in tumors of strong STAT3 activity, confirming the results previously determined by using cDNA arrays.

MMP-1 Expression in CRC Is Colocalized with STAT3 Activity

Previously, we have shown that phosphorylated STAT3 in colorectal tumor tissue is predominantly localized to dedifferentiated epithelial cells [5]. To further elucidate possible functional connections between persistent STAT3 activity and elevated MMP expression, we studied the spatial distribution of MMP-1 expression in CRC tissue using immunohistochemical methods. Sections from biopsies, classified high or low STAT3 according to both biochemical and histological testing, were stained with an antibody to MMP-1. Figure 3 shows that no significant MMP-1 expression was detected in and around normal crypts of both high- and low-STAT3 specimens. In contrast, the two tumor types showed a strikingly diverse picture with regard to MMP-1 abundance in

tumor tissue. Whereas tumor cells in the STAT3 low sample were virtually negative for MMP-1 expression, tumorous epithelium in the high-STAT3 specimens displayed strong MMP-1 staining. There was no significant MMP-1 expression in stromal cells (i.e., fibroblasts, inflammatory cells) around the cancerous tissue.

These findings indicate that an abundance of MMP-1 mRNA in CRC specimens of the high-STAT3 type results in considerable levels of immunoreactive MMP-1 protein within the malignant areas of the tumors.

STAT3 Drives Expression of Active MMP-1 in CRC Cells

To investigate a possible causal link between STAT3 activity and expression of MMP-1 in colon carcinoma cells, we examined MMP-1 gene transcription upon experimental activation of STAT3 in the HT-29 colon carcinoma cell line. Previously, we have shown that although quiescent HT-29 cells are negative for STAT3 activity, STAT3 is activated by IL-6. In addition, we generated HT-29 derivatives that either overexpress STAT3 (HT-29 STAT3) or stably express a constitutively active (HT-29 STAT3 c.a.) or a dominant-negative STAT3 variant (HT-29 STAT3 d.n.), respectively [5].

STAT3 activity in HT-29 cells was manipulated via IL-6 stimulation or through protein expression of the variants, and the resulting changes in both MMP-1 mRNA and MMP-1 enzyme activity were determined (Figure 5). MMP-1 mRNA was quantified by real-time PCR, whereas MMP-1 activity was measured by the turnover of a fluorogenic substrate. Figure 4*A* shows that incubating HT-29 cells with 20 ng/ml IL-6 leads to a clear increase in MMP-1 mRNA. An overexpression of STAT3 in HT-29 STAT3 cells, which coincides with a threshold activity of STAT3 tyrosine phosphorylation [5], results in an increase of MMP-1 mRNA compared with parental HT-29 cells. IL-6 stimulation of HT-29 STAT3 cells evokes a further strong increase in the concentration of MMP-1 mRNA. A stable expression of the constitutively active STAT3 variant in HT-29 STAT3 c.a. cells resulted in a more than threefold increase of MMP-1 mRNA compared with nontransfected cells.

The analysis of MMP-1 enzyme activity in HT-29 cells under an experimentally altered status of STAT3 activation gave similar results (Figure 4*B*). Stable expression of STAT3 as well as acute IL-6 stimulation evoked a more than 10-fold induction of MMP-1 enzyme activity in HT-29 cells. Stimulation of both HT-29 cells and HT-29 STAT3 cells led to enhanced MMP-1 activity compared with nonstimulated cells. Notably, the expression of a dominant-negative STAT3 variant (STAT3 Y705F) completely suppressed both basal and IL-6–induced MMP-1 activity in HT-29 cells.

These results clearly suggest that STAT3 is essential for increased expression of MMP-1 in CRC. More importantly, tyrosine phosphorylation analysis shows that the respective degrees of MMP-1 induction in HT-29 observed under varied conditions mirror the respective levels of STAT3 activation [5].

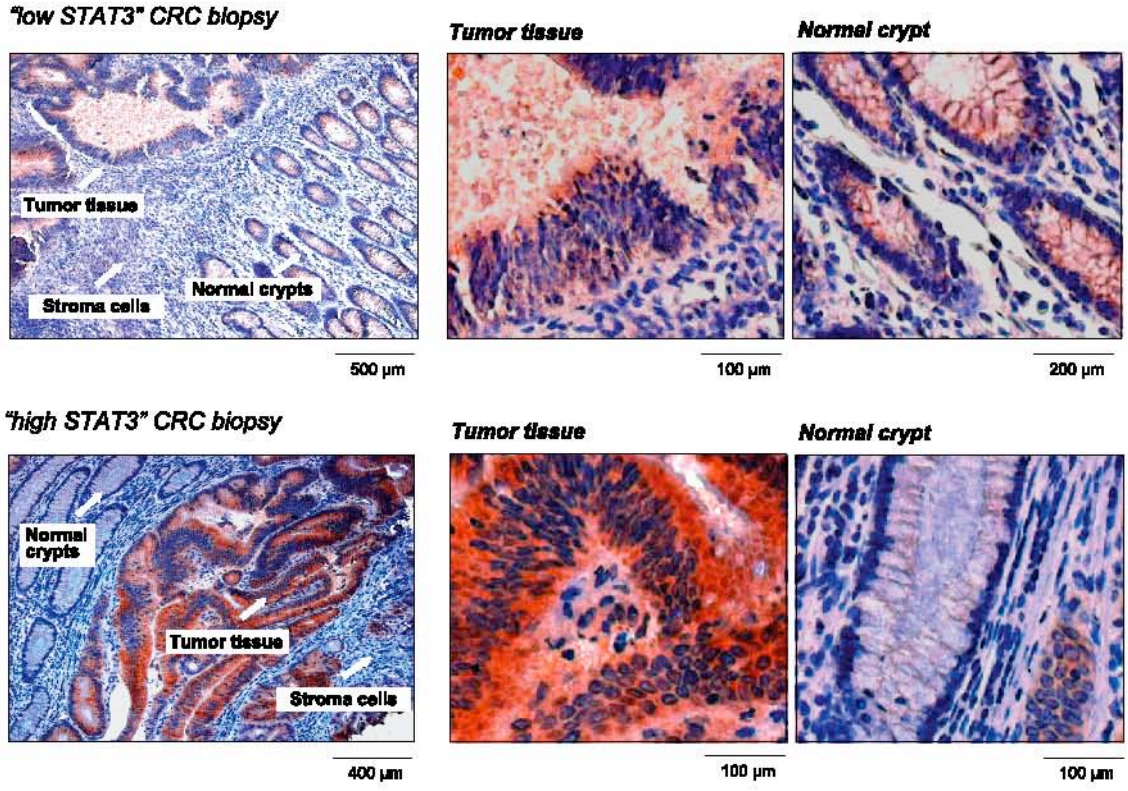

Figure 3. *Immunohistochemical staining for MMP-1 in paraffin-embedded specimens of high-STAT3 and low-STAT3 primary CRC biopsies. Sections from representative tumor samples positive (top) and negative (bottom) for tyrosine-phosphorylated STAT3, showing both differentiated normal cells in crypt structures and de-differentiated tumor tissue, were treated with an antibody specific for MMP-1. Sites of differentiated normal cells in crypt regions, of tumor tissue, and of stromal cells are indicated by arrows in the left-hand pictures, center, and right-hand pictures show enlargements of tumor tissue and normal crypt structures.*

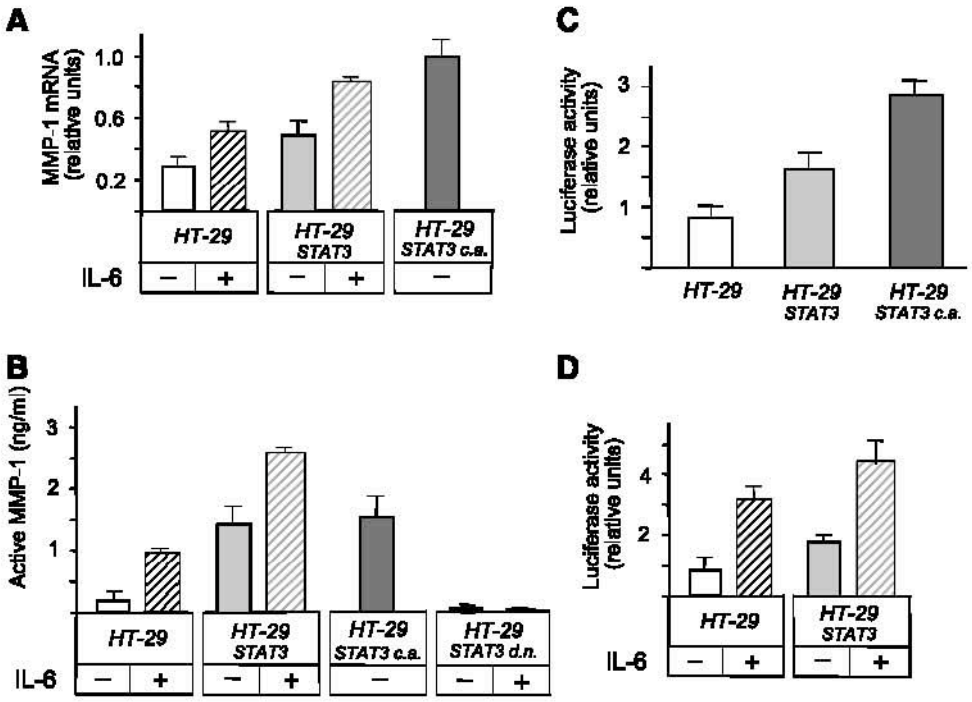

Figure 4. *Determination of MMP-1 expression in HT-29 colon carcinoma cells dependent on STAT3 activation. (A) Influence of STAT3 activation by cell stimulation with IL-6 and/or (over)expression of STAT3 variants. Parental HT-29 cells and derivatives stably expressing STAT3 or STAT3 c.a. were grown for 24 hours in the absence or presence of 20 ng/ml IL-6 as indicated. Total RNA was isolated, transcribed into cDNA, and subjected to quantitative RT-PCR with specific primers and probes for MMP-1 as described in Materials and Methods. Three independent experiments, each run in triplicate, were performed, and the results were normalized to 18S rRNA expression. Relative MMP-1 expression was calculated by arbitrarily setting the expressions from samples with STAT3 c.a. as 1 (100%). (B) Influence of STAT3 activation on enzymatic MMP-1 activity. HT-29 cells (over)expressing STAT3, the constitutively active variant STAT3 c.a. or the dominant-negative STAT3 mutant Y705F (STAT3 d.n.) were cultured for 4 days in the absence or presence of 20 ng/ml IL-6 as indicated. Culture supernatants were assayed for active MMP-1 by the turnover of a fluorogenic substrate as described in Materials and Methods. Data represent the means of three independent experiments. (C) Influence of STAT3 expression in HT-29 cells on MMP-1 promoter activity. HT-29 cells or HT-29 cells stably (over)expressing STAT3 or STAT3 c.a., respectively, were transiently transfected with 1 μg of the −4372 hMMP-luci plasmid together with 0.1 μg of* Renilla *plasmid as an internal control. After 14 hours, cells were harvested and protein lysates were assayed for luciferase and renilla luciferase activities as described in Materials and Methods. (D) Influence of IL-6–induced STAT3 activation on MMP-1 promoter activity in HT-29 cells. The experiment was performed as described in (C), but after 14 hours cells were washed and, before lysis, incubated for 8 hours with fresh medium with or without 20 ng/ml IL-6 as indicated. Results in (C) and (D) represent the means of three independent transfections, each run in triplicate.*

To determine whether activated STAT3 enhanced transcription from the MMP-1 promoter in colon carcinoma cells, we employed the reporter gene construct −4372 hMMP-luci in which the 4.3-kb human MMP-1 promoter was placed upstream of a luciferase reporter gene [39]. First, the reporter gene construct was transiently transfected into parental HT-29 cells and into HT-29 derivatives stably (over) expressing either STAT3 or STAT3 c.a. (Figure 4*C*). We observed that enhanced STAT3 expression and activity in both cell lines resulted in a two- to threefold increase in transcription driven by the MMP-1 promoter compared with nontransfected cells.

Figure 4*D* shows that IL-6 treatment strongly induced the activity of the MMP-1 promoter in HT-29 cells as well as in HT-29 cells overexpressing STAT3. In HT-29 STAT3 c.a. cells, IL-6 did not induce a further increase of MMP-1 transcription compared with nonstimulated cells (data not shown), probably due to a saturation of the respective mechanisms.

These data demonstrate that STAT3 activation promotes transcriptional activity of the MMP-1 promoter in HT-29 cells. They also point to a functional relation between STAT3 activity and expression of a protease with particular relevance for tumor cell malignancy by tissue invasion.

Xenografts of HT-29 Cells Develop STAT3 Activity and MMP-1 Expression Simultaneously and in a Colocalized Fashion

We have previously shown that HT-29 cells are negative for tyrosine-phosphorylated STAT3 activity in cell culture but develop STAT3 activity when growing out into tumors in nude mice [5]. Here, we demonstrated a transcriptional connection between STAT3 activation and induction of MMP-1 expression in colon carcinoma cells. We wanted to further substantiate these results by demonstrating that the development of STAT3 activation in HT-29 xenograft tumors is accompanied by an increase in MMP-1 abundance. First, by quantitative RT-PCR, we compared the levels of MMP-1 mRNA in cultured HT-29 cells with those in xenograft tumors arising 2 weeks after injection into nude mice. Figure 5*A* shows that the relative quantity of MMP-1 mRNA in HT-29–derived tumors was over fivefold higher compared with HT-29 cells cultivated *in vitro*.

Next, we studied the effect of altered STAT3 activity in HT-29 cells on MMP-1 expression upon development of xenograft tumors. Tumors grown from HT-29 cells as well as from HT-29 derivatives expressing constitutively active STAT3 (HT-29 STAT3 c.a.) or dominant-negative STAT3 Y705F

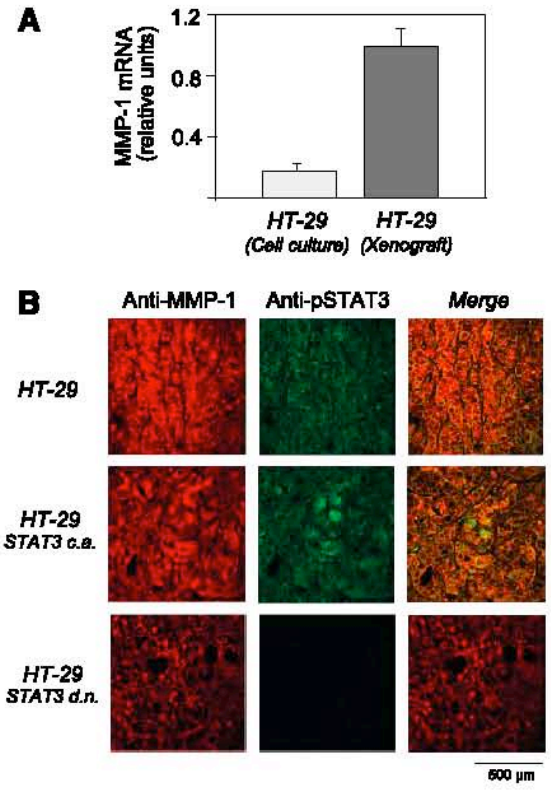

Figure 5. *Determination of MMP-1 expression in HT-29 xenograft tumors in correlation with STAT3 activity. (A) Comparative quantification of MMP-1 mRNA in cultured HT-29 cells and HT-29–derived xenograft tumors. Total RNA was isolated from confluent cultures of HT-29 cells or from a representative xenograft tumor explanted 2 weeks after subcutaneous injection of cells into a nude mouse. RNA was transcribed into cDNA, and quantitative RT-PCR with specific primers and probes for MMP-1 was performed as described in Materials and Methods. Results were normalized to 18S rRNA expression. Relative MMP-1 abundance was expressed as fraction of the value for the xenograft tumor, which was arbitrarily set 1. The figure represents the means of three independent experiments. (B) Immunohistochemical examination of HT-29–derived xenograft tumors for activated STAT3 and MMP-1. Representative sections from a tumor induced by injection of HT-29 (top), HT-29 STAT3 c.a. (center), and HT-29 STAT3 d.n. (bottom) into nude mice were reacted with an antibody specific for MMP-1 (left) or STAT3 pY705 (center) or with a combination of both antibodies (right).*

(HT-29 STAT3 d.n.) were subjected to immunohistochemical examination using antibodies to tyrosine-phosphorylated STAT3 and MMP-1 (Figure 5*B*). Both antibodies stained carcinoma cells in HT-29 tumors, and costaining with both antibodies revealed a colocalization of the two antigens. Levels of both p-Y-STAT3 and MMP-1 were clearly enhanced in tumors derived from HT-29 STAT3 c.a. cells and hugely diminished in tumors of HT-29 STAT3 d.n. cells.

These data further support our notion that STAT3 activation is directly involved in the control of expression and activity of MMP-1, and, thus, malignancy, of colon carcinoma cells.

High-Affinity Binding Sites for STAT Transcription Factors Exist within the Promoters for Human MMP-1 and MMP-3

Finally, we wished to demonstrate that STAT3 directly interacts with human MMP promoters and to identify relevant binding sites. To this end, the sequences of the human promoters for MMP-1 and MMP-3 were analyzed for DNA elements matching the known STAT-binding consensus sequence as given by Ehret et al. [46]. Using the MEME search blast algorithm [47], we identified six potential high-affinity STAT3 binding within the human MMP-1 promoter (GenBank accession no. AF023338) and four within the human MMP-3 promoter (GenBank accession no. U43511) and ordered them within the respective groups by decreasing similarity with the consensus STAT3 binding site defined by Ehret et al. (Figure 6*A*).

Oligonucleotide hybrids representing these sequences and a wild-type and a mutant (m67) STAT3-binding site from the human c-fos promoter [41] as positive controls were subjected to EMSA analysis for specific binding of activated STAT3. Upon expression in 293T cells, STAT3 was activated by IL-6 stimulation. Appearance of STAT3–DNA complexes was tested and verified by supershifting. As shown in Figure 6*B*, one site from each MMP-1 and MMP-3 promoter, notably the ones with the highest similarity to the consensus according to the MEME search blast, specifically interacted

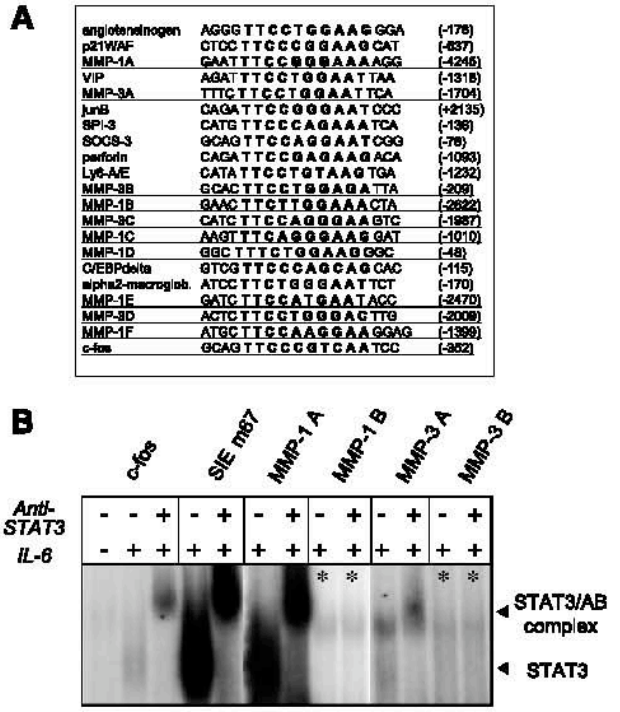

Figure 6. *Specific binding of STAT3 to cognate sequence elements within the human MMP-1 and MMP-3 promoters. (A) Sequences of potential STAT binding sites in the human MMP-1 and MMP-3 promoter as well as known STAT3 recognition elements employed as controls. Sites were identified using the MEME search blast algorithm [47] and ordered by decreasing similarity with the consensus STAT3 binding site defined by Ehret et al. [46]. Positions relative to the respective transcriptional start sites are given in brackets. (B) Analysis of STAT3 DNA binding to four potential STAT binding elements from the human promoters for MMP-1 and MMP-3 (sequences in A) and to two known STAT3 recognition sequences (wild-type and mutant SIE m67 STAT binding site from the human c-fos promoter). Extracts were either unstimulated or stimulated with IL-6 for 30 minutes as indicated before complex formation was assessed by EMSA. The specificity of STAT3 DNA binding was confirmed by supershifting using a STAT3-specific antibody. Positions of STAT3-containing DNA–protein complexes are marked by arrows. The asterisk (*) indicates background activity of unspecific DNA-binding complexes.*

with STAT3. MMP-1A represents the sequence element GAATTTCCGGGAAAAGG at position −4245 of the MMP-1 promoter, MMP-3A is the sequence element TTTCTTCCTGGAATTCA at position −1704 of the MMP-3 promoter. Neither the second best (MMP-1B and MMP-3B) nor any other putative STAT binding element from Figure 6*B* displayed significant complex formation with STAT3 in this assay (results not shown).

We infer from these results that activated STAT3 immediately interacts with the human MMP-1 and MMP-3 promoter.

Discussion

There is accumulating evidence for the importance of oncogenic signaling by STAT3 in the pathogenesis of various human cancers. Thus, we focused on the contribution of STAT3 to the onset and development of colorectal cancer. Our previous work shows that STAT3 may contribute to oncogenesis in the colon epithelium by exerting a promoting effect on cell proliferation [5], whereas this paper demonstrates its critical involvement in the enhancement of invasive cell behavior.

One of the prerequisites for the invasiveness of tumor cells is increased motility, and, of metastasis, a common feature of late-stage CRC. The pleiotropic protein STAT3 is known to exert control on cell motility in various settings. STAT3 is crucial, e.g., for cell motility during gastrulation [48], wound healing, and blood vessel formation [49]. We recently observed that the invasiveness of trophoblast cells in pregnancy is directly influenced through STAT3 activation [5,50].

More importantly, inadequate STAT3 activity was found correlated with cancer-associated motility of breast [27,51] and ovarian cancer [12] as well as of choriocarcinoma cells [44]. In mesenchymal-like and colon carcinoma cells, STAT3 plays a critical role in the transmission of invasiveness-promoting signaling by the c-Met receptor [52,53].

Altered invasiveness in transformed cells is a consequence of changes in the status of cell adhesion, the cytoskeleton, and gene expression. STAT3 has been shown to act on all these aspects: In addition to its well-established role as a transcription factor, STAT3 may also function as a signaling adaptor at focal adhesions and, presumably, as a persistent scaffold factor in cytokine/growth factor receptor assemblies [12]. As recently reported, STAT3 can signal in an as yet unknown way through Rho GTPases, thus regulating multiple cellular functions including actin cytoskeleton reorganization and cell migration [54].

Transcriptional regulation of target genes provides an obvious route through which STAT3 enhances cellular malignancy and, in particular, invasiveness. A central aspect of invasiveness is the expression of proteases that render the tumor cells capable of digesting constituents of the ECM. Various reports point to a role of STAT3 in promoting invasive cell behavior by exerting influence on the transcription of protease genes. In metastatic melanoma cells, a link was found between the expression of MMP-2, invasiveness, and constitutive STAT3 activity. More importantly, inhibition of STAT3 by a dominant-negative mutant reduced MMP-2 expression and invasiveness and blocked metastasis in nude mice [55]. In skin epithelial cells, STAT3 was shown to mediate the IL-6–provoked induction of MMP-1 and MMP-3 [56]. However, STAT3 is involved in controlling the expression of MMP-7 in prostate carcinoma cells [26] and of MMP-9 in cervix carcinoma cells [57].

We showed that STAT3 directly drives transcription from the MMP-1 promoter in colon carcinoma cells and also defined a binding site for STAT3 in the MMP-1 as well as in the MMP-3 promoter. However, the precise role of STAT factors in MMP gene regulation in colon cancer cells requires further elucidation. Despite the presence of various additional consensus sequences, we identified only one sequence element in both the MMP-1 and the MMP-3 promoter that specifically binds to activated STAT3. This finding leaves open the possibility that the other elements interact with STAT1 or STAT5, both of which are also frequently active in CRC biopsies [5]. Furthermore, those sequences showing no affinity for STAT3 in our assay may require additional binding sites for the interaction with STAT3 tetramers, as recently observed for other promoters [58,59].

Transcription of the MMP-1 gene is regulated in a complex manner. The process appears to be influenced by the orchestrated action of various transcription factors and seems also to depend on the type of cells involved. Apart from STAT cognate elements, other regulatory elements within the MMP-1 promoter region include various transcription factor binding sites for AP-1, GATA binding, and ETS proteins [60,61]. The cooperative contribution of AP-1 and ETS transcription factors toward control of MMP-1 expression was demonstrated by the observation that a single nucleotide polymorphism creating an additional ETS binding site close to the AP-1 recognition element at −1602 bp results in greater transcriptional activity [39]. However, we found that, starting from different "basal" levels, STAT3 activation profoundly enhanced transcription from both variants of the MMP-1 promoter in colon carcinoma cells (data not shown). The relative importance of AP-1– and STAT-related signaling pathways in the control of MMP-1 expression apparently depends on the cell type. For instance, a specific inhibitor of JAK3, a kinase operative in the activation of STATs, almost completely inhibited MMP-1 mRNA induction and protein abundance in human chondrocytes. In contrast, inhibition of ERK1/2 kinases signaling via AP-1 had little effect on the expression of MMP-1 in these cells [62]. We conclude that, along with its importance in CRC proliferation and transformation, the STAT3 pathway is one driving force responsible for overexpression and activity of MMP-1 in invasive colonic cancer cells. The prognostic significance of MMP-1 expression in colorectal cancer has already been reported. High levels of MMP-1 expression have been correlated with metastatic spread of tumors and poor prognosis of colorectal cancer [63–66]. Interestingly, MMP-1 inhibitors such as batimastat blocked peritoneal carcinomatosis and liver metastasis development in experimental colon carcinoma [67]. Of all the proteases addressed in study, MMP-1 is one whose expression level is particularly linked with STAT3 activation in colorectal cancer. There are, however, other

proteases whose expression level was also found to follow the degree of STAT3 phosphorylation during the course of this study. Induction of MMP-7 (matrilysin) expression in prostate carcinoma cells by fibroblast growth factor was shown to involve STAT3 through a probable interaction with STAT binding sites within the matrilysin promoter [26]. A recent study reported a correlation between tyrosine-phosphorylated STAT3 and expression of MMP-9 in breast carcinoma cells and demonstrated a direct influence of STAT3 on MMP-9 promoter activity [27].

The enzymatic activity of MMPs is specifically inhibited by TIMPs, and high levels of TIMP-1 and TIMP-2 are associated with aggressive cancers [62]. STAT3 has been described as contributing to the downregulation of TIMP-1 expression in synovial lining cells [22]. We recently found that STAT3 activation through leukemia inhibitory factor enhances invasiveness and coincides with a decrease of TIMP-1 expression in choriocarcinoma cells [44]. Interestingly, in the course of this study we observed that TIMP-1 mRNA was significantly less abundant in colorectal cancer biopsies with high STAT3 activity (data not shown).

In conclusion, STAT3 activation can contribute to the malignancy of many different types of cancer. One such contribution involves the promotion of cell invasiveness through (cell type specific) alteration in the pattern of protease activity. Our data suggest that STAT3-controlled proteolysis via MMPs is a major determinant of local tumor progression and metastasis of colorectal cancer and, thus, is an attractive potential target for therapeutic intervention. Moreover, p-Y-STAT3 and MMP-1 are likely to be of prognostic value or be of diagnostic importance with regard to CRC progression.

Recent reports point to an important role of aberrant STAT3 activity in metastasis of various malignant tumor entities such as cutaneous squamous cell carcinoma [68], melanoma [69], or hepatocellular carcinoma [70]. To investigate the underlying molecular mechanisms, our future work will include the analysis of patient CRC biopsy samples and will take advantage of mouse models that closely mimic stages of human CRC.

Acknowledgements

We thank Constanze E. Brinckerhoff for the MMP-1 reporter construct and Edith Pfitzner for the HT-29– and CoGa-1–derived cell lines.

References

[1] Buettner R, Mora LB, and Jove R (2002). Activated STAT signaling in human tumors provides novel molecular targets for therapeutic intervention. *Clin Cancer Res* **8**, 945–954.

[2] Levy DE and Lee CK (2002). What does Stat3 do? *J Clin Invest* **109**, 1143–1148.

[3] Bromberg J (2002). Stat proteins and oncogenesis. *J Clin Invest* **109**, 1139–1142.

[4] Bromberg JF, Wrzeszczynska MH, Devgan G, Zhao Y, Pestell RG, Albanese C, and Darnell JE Jr (1999). Stat3 as an oncogene. *Cell* **98**, 295–303.

[5] Corvinus FM, Orth C, Moriggl R, Tsareva SA, Wagner S, Pfitzner EB, Baus D, Kaufmann R, Huber LA, Zatloukal K, et al. (2005). Persistent STAT3 activation in colon cancer is associated with enhanced cell proliferation and tumor growth. *Neoplasia* **7**, 545–555.

[6] Niu G, Heller R, Catlett-Falcone R, Coppola D, Jaroszeski M, Dalton W, Jove R, and Yu H (1999). Gene therapy with dominant-negative Stat3 suppresses growth of the murine melanoma B16 tumor *in vivo*. *Cancer Res* **59**, 5059–5063.

[7] Garcia R, Bowman TL, Niu G, Yu H, Minton S, Muro-Cacho CA, Cox CE, Falcone R, Fairclough R, Parsons S, et al. (2001). Constitutive activation of Stat3 by the Src and JAK tyrosine kinases participates in growth regulation of human breast carcinoma cells. *Oncogene* **20**, 2499–2513.

[8] Masuda M, Suzui M, Yasumatu R, Nakashima T, Kuratomi Y, Azuma K, Tomita K, Komiyama S, and Weinstein IB (2002). Constitutive activation of signal transducers and activators of transcription 3 correlates with cyclin D1 overexpression and may provide a novel prognostic marker in head and neck squamous cell carcinoma. *Cancer Res* **62**, 3351–3355.

[9] Epling-Burnette PK, Liu JH, Catlett-Falcone R, Turkson J, Oshiro M, Kothapalli R, Li Y, Wang JM, Yang-Yen HF, Karras J, et al. (2001). Inhibition of STAT3 signaling leads to apoptosis of leukemic large granular lymphocytes and decreased Mcl-1 expression. *J Clin Invest* **107**, 351–362.

[10] Shen Y, Devgan G, Darnell JE Jr, and Bromberg JF (2001). Constitutively activated Stat3 protects fibroblasts from serum withdrawal and UV-induced apoptosis and antagonizes the proapoptotic effects of activated Stat1. *Proc Natl Acad Sci USA* **98**, 1543–1548.

[11] Kusaba T, Nakayama T, Yamazumi K, Yakata Y, Yoshizaki A, Inoue K, Nagayasu T, and Sekine I (2006). Activation of STAT3 is a marker of poor prognosis in human colorectal cancer. *Oncol Rep* **15**, 1445–1451.

[12] Silver DL, Naora H, Liu J, Cheng W, and Montell DJ (2004). Activated signal transducer and activator of transcription (STAT) 3: localization in focal adhesions and function in ovarian cancer cell motility. *Cancer Res* **64**, 3550–3558.

[13] Nagase H and Woessner JF Jr (1999). Matrix metalloproteinases. *J Biol Chem* **274**, 21491–21494.

[14] Airola K, Karonen T, Vaalamo M, Lehti K, Lohi J, Kariniemi AL, Keski-Oja J, and Saarialho-Kere UK (1999). Expression of collagenases-1 and -3 and their inhibitors TIMP-1 and -3 correlates with the level of invasion in malignant melanomas. *Br J Cancer* **80**, 733–743.

[15] Hofmann UB, Westphal JR, Van Muijen GN, and Ruiter DJ (2000). Matrix metalloproteinases in human melanoma. *J Invest Dermatol* **115**, 337–344.

[16] Nikkola J, Vihinen P, Vlaykova T, Hahka-Kemppinen M, Kahari VM, and Pyrhonen S (2002). High expression levels of collagenase-1 and stromelysin-1 correlate with shorter disease-free survival in human metastatic melanoma. *Int J Cancer* **97**, 432–438.

[17] Wilson CL, Heppner KJ, Labosky PA, Hogan BL, and Matrisian LM (1997). Intestinal tumorigenesis is suppressed in mice lacking the metalloproteinase matrilysin. *Proc Natl Acad Sci USA* **94**, 1402–1407.

[18] Itoh T, Tanioka M, Matsuda H, Nishimoto H, Yoshioka T, Suzuki R, and Uehira M (1999). Experimental metastasis is suppressed in MMP-9–deficient mice. *Clin Exp Metastasis* **1999**, 177–181.

[19] Masson R, Lefebvre O, Noel A, Fahime ME, Chenard MP, Wendling C, Kebers F, LeMeur M, Dierich A, Foidart JM, et al. (1998). *In vivo* evidence that the stromelysin-3 metalloproteinase contributes in a paracrine manner to epithelial cell malignancy. *J Cell Biol* **140**, 1535–1541.

[20] Lozonschi L, Sunamura M, Kobari M, Egawa S, Ding L, and Matsuno S (1999). Controlling tumor angiogenesis and metastasis of C26 murine colon adenocarcinoma by a new matrix metalloproteinase inhibitor, KB-R7785, in two tumor models. *Cancer Res* **59**, 1252–1258.

[21] Naglich JG, Jure-Kunkel M, Gupta E, Fargnoli J, Henderson AJ, Lewin AC, Talbott R, Baxter A, Bird J, Savopoulos R, et al. (2001). Inhibition of angiogenesis and metastasis in two murine models by the matrix metalloproteinase inhibitor, BMS-275291. *Cancer Res* **61**, 8480–8485.

[22] Gatsios P, Haubeck HD, Van de Leur E, Frisch W, Apte SS, Greiling H, Heinrich PC, and Graeve L (1996). Oncostatin M differentially regulates tissue inhibitors of metalloproteinases TIMP-1 and TIMP-3 gene expression in human synovial lining cells. *Eur J Biochem* **241**, 56–63.

[23] Korzus E, Nagase H, Rydell R, and Travis J (1997). The mitogen-activated protein kinase and JAK-STAT signaling pathways are required for an oncostatin M-responsive element–mediated activation of matrix metalloproteinase 1 gene expression. *J Biol Chem* **272**, 1188–1196.

[24] Vincenti MP, Schroen DJ, Coon CI, and Brinckerhoff CE (1998). v-src activation of the collagenase-1 (matrix metalloproteinase-1) promoter through PEA3 and STAT: requirement of extracellular signal–regulated kinases and inhibition by retinoic acid receptors. *Mol Carcinog* **21**, 194–204.

[25] Catterall JB, Carrere S, Koshy PJ, Degnan BA, Shingleton WD Brinckerhoff CE, Rutter J, Cawston TE, and Rowan AD (2001). Synergistic induction of matrix metalloproteinase 1 by interleukin-1alpha and oncostatin M in human chondrocytes involves signal transducer and activator of transcription and activator protein 1 transcription factors via a novel mechanism. *Arthritis Rheum* **44**, 2296–2310.

[26] Udayakumar TS, Stratton MS, Nagle RB, and Bowden GT (2001). Fibroblast growth factor-1 induced promatrilysin expression through the activation of extracellular-regulated kinases and Stat3. *Neoplasia* **1**, 60–67.

[27] Dechow TN, Pedranzini L, Leitch A, Leslie K, Gerald WL, Linkov I, and Bromberg JF (2004). Requirement of matrix metalloproteinase-9 for the transformation of human mammary epithelial cells by Stat3-C. *Proc Natl Acad Sci USA* **101**, 10602–10607.

[28] Lovejoy B, Welch AR, Carr S, Luong C, Broka C, Hendricks RT, Campbell JA, Walker KA, Martin R, Van Wart H, et al. (1999). Crystal structures of MMP-1 and -13 reveal the structural basis for selectivity of collagenase inhibitors. *Nat Struct Biol* **6**, 217–221.

[29] Ossowski L (1992). Invasion of connective tissue by human carcinoma cell lines: requirement for urokinase, urokinase receptor, and interstitial collagenase. *Cancer Res* **52**, 6754–6760.

[30] Murray GI, Duncan ME, O'Neil P, Melvin WT, and Fothergill JE (1996). Matrix metalloproteinase-1 is associated with poor prognosis in colorectal cancer. *Nat Med* **2**, 461–462.

[31] Bendardaf R, Lamlum H, Vihinen P, Ristamaki R, Laine J, and Pyrhonen S (2003). Low collagenase-1 (MMP-1) and MT1-MMP expression levels are favourable survival markers in advanced colorectal carcinoma. *Oncology* **65**, 337–346.

[32] Baba M, Itoh K, and Tatsuta M (2004). Glycine-extended gastrin induces matrix metalloproteinase-1– and -3–mediated invasion of human colon cancer cells through type I collagen gel and Matrigel. *Int J Cancer* **111**, 23–31.

[33] Westermarck J and Kahari VM (1999). Regulation of matrix metalloproteinase expression in tumor invasion. *FASEB J* **13**, 781–792.

[34] Simon C, Simon M, Vucelic G, Hicks MJ, Plinkert PK, Koitschev A, and Zenner HP (2001). The p38 SAPK pathway regulates the expression of the MMP-9 collagenase via AP-1–dependent promoter activation. *Exp Cell Res* **271**, 344–355.

[35] Crawford HC, Fingleton B, Gustavson MD, Kurpios N, Wagenaar RA, Hassell JA, and Matrisian LM (2001). The PEA3 subfamily of Ets transcription factors synergizes with beta-catenin–LEF-1 to activate matrilysin transcription in intestinal tumors. *Mol Cell Biol* **21**, 1370–1383.

[36] Esteve PO, Chicoine E, Robledo O, Aoudjit F, Descoteaux A, Potworowski EF, and St-Pierre Y (2002). Protein kinase C-zeta regulates transcription of the matrix metalloproteinase-9 gene induced by IL-1 and TNF-alpha in glioma cells via NF-kappa B. *J Biol Chem* **277**, 35150–35155.

[37] Hall MC, Young DA, Waters JG, Rowan AD, Chantry A, Edwards DR, and Clark IM (2003). The comparative role of activator protein 1 and Smad factors in the regulation of Timp-1 and MMP-1 gene expression by transforming growth factor-beta 1. *J Biol Chem* **278**, 10304–10313.

[38] Vécsey-Semjen B, Becker KF, Sinski A, Blennow E, Vietor I, Zatloukal K, Beug H, Wagner E, and Huber LA (2002). Novel colon cancer cell lines leading to better understanding of the diversity of respective primary cancers. *Oncogene* **21**, 4646–4662.

[39] Rutter JL, Mitchell TI, Buttice G, Meyers J, Gusella JF, Ozelius LJ, and Brinckerhoff CE (1998). A single nucleotide polymorphism in the matrix metalloproteinase-1 promoter creates an Ets binding site and augments transcription. *Cancer Res* **58**, 5321–5325.

[40] Kammer W, Lischke A, Moriggl R, Groner B, Ziemicki A, Gurniak CB, Berg LJ, and Friedrich K (1996). Homodimerization of interleukin-4 receptor α chain can induce intracellular signaling. *J Biol Chem* **271**, 23634–23637.

[41] Moriggl R, Gouilleux-Gruart V, Jahne R, Berchtold S, Gartmann C, Liu X, Hennighausen L, Sotiropoulos A, Groner B, and Gouilleux F (1996). Deletion of the carboxyl-terminal transactivation domain of MGF-Stat5 results in sustained DNA binding and a dominant negative phenotype. *Mol Cell Biol* **16**, 5691–5700.

[42] Schütz A, Schneidenbach D, Aust G, Tannapfel A, Steinert M, and Wittekind C (2002). Differential expression and activity status of MMP-1, MMP-2 and MMP-9 in tumor and stromal cells of squamous cell carcinomas of the lung. *Tumour Biol* **23**, 179–184.

[43] Huang RP, Peng A, and Golard A (2001). Hydrogen peroxide promotes transformation of rat liver non-neoplastic epithelial cells through activation of epidermal growth factor receptor. *Mol Carcinog* **30**, 209–217.

[44] Fitzgerald JS, Tsareva SA, Poehlmann TG, Berod L, Meissner A, Corvinus FM, Wiederanders B, Pfitzner E, Markert UR, and Friedrich K (2005). Leukemia inhibitory factor triggers activation of signal transducer and activator of transcription 3, proliferation, invasiveness, and altered protease expression in choriocarcinoma cells. *Int J Biochem Cell Biol* **37**, 2284–2296.

[45] Matrisian LM (1994). Matrix metalloproteinase gene expression. *Ann N Y Acad Sci* **732**, 42–50.

[46] Ehret GB, Reichenbach P, Schindler U, Horvath CM, Fritz S, Nabholz M, and Bucher P (2001). DNA binding specificity of different STAT proteins. Comparison of *in vitro* specificity with natural target sites. *J Biol Chem* **276**, 6675–6688.

[47] Bailey TL and Elkan C (1994). Fitting a mixture model by expectation maximization to discover motifs in biopolymers. *Proceedings of the Second International Conference on Intelligent Systems for Molecular Biology*, pp. 28–36. AAAI Press, Menlo Park, California.

[48] Yamashita S, Miyagi C, Carmany-Rampey A, Shimizu T, Fujii R, Schier AF, and Hirano T (2002). Stat3 controls cell movements during zebrafish gastrulation. *Dev Cell* **2**, 363–375.

[49] Sano S, Itami S, Takeda K, Tarutani M, Yamaguchi Y, Miura H, Yoshikawa K, Akira S, and Takeda J (1999). Keratinocyte-specific ablation of Stat3 exhibits impaired skin remodeling, but does not affect skin morphogenesis. *EMBO J* **18**, 4657–4668.

[50] Poehlmann TG, Fitzgerald JS, Meissner A, Wengenmayer T, Schleussner E, Friedrich K, and Markert UR (2005). Trophoblast invasion: tuning through LIF, signalling via Stat3. *Placenta* **Suppl A**, S37–S41.

[51] Badache A and Hynes NE (2001). Interleukin 6 inhibits proliferation and, in cooperation with an epidermal growth factor receptor autocrine loop, increases migration of T47D breast cancer cells. *Cancer Res* **61**, 383–391.

[52] Rivat C, Rodrigues S, Bruyneel E, Pietu G, Robert A, Redeuilh G, Bracke M, Gespach C, and Attoub S (2004). Disruption of STAT3 signaling leads to tumor cell invasion through alterations of homotypic cell–cell adhesion complexes. *Oncogene* **23**, 3317–3327.

[53] Cramer A, Kleiner S, Westermann M, Meissner A, Lange A, and Friedrich K (2005). Activation of the c-Met receptor complex in fibroblasts drives invasive cell behavior by signalling through transcription factor STAT3. *J Cell Biochem* **95**, 805–816.

[54] Debidda M, Wang L, Zang H, Poli V, and Zheng Y (2005). A role of STAT3 in Rho GTPase regulated cell migration and proliferation. *J Biol Chem* **280**, 17275–17285.

[55] Xie TX, Wei D, Liu M, Gao AC, Ali-Osman F, Sawaya R, and Huang S (2004). Stat3 activation regulates the expression of matrix metalloproteinase-2 and tumor invasion and metastasis. *Oncogene* **23**, 3550–3560.

[56] Yu CY, Wang L, Khaletskiy A, Farrar WL, Larner A, Colburn NH, and Li JJ (2002). STAT3 activation is required for interleukin-6 induced transformation in tumor-promotion sensitive mouse skin epithelial cells. *Oncogene* **21**, 3949–3960.

[57] Smola-Hess S, Schnitzler R, Hadaschik D, Smola H, Mauch C, Krieg T, and Pfister H (2001). CD40L induces matrix-metalloproteinase-9 but not tissue inhibitor of metalloproteinases-1 in cervical carcinoma cells: imbalance between NF-kappaB and STAT3 activation. *Exp Cell Res* **267**, 205–215.

[58] Lerner L, Henriksen MA, Zhang X, and Darnell JE (2003). STAT3-dependent enhanceosome assembly and disassembly: synergy with GR for full transcriptional increase of the alpha 2-macroglobulin gene. *Genes Dev* **17**, 2564–2577.

[59] Moriggl R, Sexl V, Kenner L, Duntsch C, Stangl K, Gingras S, Hoffmeyer A, Bauer A, Piekorz R, Wang D, et al. (2005). Stat5 tetramer formation is associated with leukemogenesis. *Cancer Cell* **7**, 87–99.

[60] Sato H, Kita M, and Seiki M (1993). v-Src activates the expression of 92-kDa type IV collagenase gene through the AP-1 site and the GT box homologous to retinoblastoma control elements. A mechanism regulating gene expression independent of that by inflammatory cytokines. *J Biol Chem* **268**, 23460–23468.

[61] Bidder M, Loewy AP, Latifi T, Newberry EP, Ferguson G, Willis DM, and Towler DA (2000). Ets domain transcription factor PE1 suppresses human interstitial collagenase promoter activity by antagonizing protein–DNA interactions at a critical AP1 element. *Biochemistry* **39**, 8917–8928.

[62] Behera AK, Thorpe CM, Kidder JM, Smith W, Hildebrand E, and Hu LT (2004). *Borrelia burgdorferi*–induced expression of matrix metalloproteinases from human chondrocytes requires mitogen-activated protein kinase and janus kinase/signal transducer and activator of transcription signaling pathways. *Infect Immun* **72**, 2864–2871.

[63] Curran S and Murray GI (1999). Matrix metalloproteinases in tumor invasion and metastasis. *J Pathol* **189**, 300–308.

[64] Shiozawa J, Ito M, Nakayama T, Nakashima M, Kohno S, and Sekine I

(2000). Expression of matrix metalloproteinase-1 in human colorectal carcinoma. *Mod Pathol* **13**, 925–933.

[65] Horiguchi A, Oya M, Shimada T, Uchida A, Marumo K, and Murai M (2002). Activation of signal transducer and activator of transcription 3 in renal cell carcinoma: a study of incidence and its association with pathological features and clinical outcome. *J Urol* **168**, 762–765.

[66] Zinzindohoue F, Lecomte T, Ferraz JM, Houllier AM, Cugnenc PH, Berger A, Blons H, and Laurent-Puig P (2005). Prognostic significance of MMP-1 and MMP-3 functional promoter polymorphisms in colorectal cancer. *Clin Cancer Res* **11**, 594–599.

[67] Aparicio T, Kermorgant S, Dessirier V, Lewin MJ, and Lehy T (1999). Matrix metalloproteinase inhibition prevents colon cancer peritoneal carcinomatosis development and prolongs survival in rats. *Carcinogenesis* **20**, 1445–1451.

[68] Suiqing C, Min Z, and Lirong C (2005). Overexpression of phosphorylated-STAT3 correlated with the invasion and metastasis of cutaneous squamous cell carcinoma. *J Dermatol* **32**, 354–360.

[69] Xie TX, Huang FJ, Aldape KD, Kang SH, Liu M, Gershenwald JE, Xie K, Sawaya R, and Huang S (2006). Activation of stat3 in human melanoma promotes brain metastasis. *Cancer Res* **66**, 3188–3196.

[70] Li WC, Ye SL, Sun RX, Liu YK, Tang ZY, Kim Y, Karras JG, and Zhang H (2006). Inhibition of growth and metastasis of human hepatocellular carcinoma by antisense oligonucleotide targeting signal transducer and activator of transcription 3. *Clin Cancer Res* **12**, 7140–7148.

3.2.4 Constitutive activation of Stat5 promotes its cytoplasmic localization and association with PI3-kinase in myeloid leukemias

Noria Harir[1], Christian Pecquet[1], Marc Kerenyi[2], Karoline Sonneck[3], Boris Kovacic[2], Remy Nyga[1], Marie Brevet[4], Isabelle Dhennin[1], Valerie Gouillex-Gruart[1], Hartmut Beug[2], Peter Valent[3], Kaiss Lassoued[1], Richard Moriggl[5] and Fabrice Gouillex[1]

[1]Institut Natioanl de la Sante et de la Recherche Medicale (EMI 351), Faculte de Medicine, Universite de Picardie J Verne, Amiens, France

[2]Institute of Molecular Pathology, Vienna, Austria

[3]Department of Intenal Medicine I, Division of Hematology, Medical University of Vienna, Austria

[4]Laboratory of Anatomo-Pathology, Centre Hospitalier Universitaire, Amiens, France

[5]Ludwig Boltzmann Institute for Cancer Research, Vienna, Austria

blood

2007 109: 1678-1686
Prepublished online Oct 12, 2006;
doi:10.1182/blood-2006-01-029918

Constitutive activation of Stat5 promotes its cytoplasmic localization and association with PI3-kinase in myeloid leukemias

Noria Harir, Christian Pecquet, Marc Kerenyi, Karoline Sonneck, Boris Kovacic, Remy Nyga, Marie Brevet, Isabelle Dhennin, Valerie Gouilleux-Gruart, Hartmut Beug, Peter Valent, Kaiss Lassoued, Richard Moriggl and Fabrice Gouilleux

Blood (print ISSN 0006-4971, online ISSN 1528-0020), is published semimonthly by the American Society of Hematology, 1900 M St, NW, Suite 200, Washington DC 20036.

Constitutive activation of Stat5 promotes its cytoplasmic localization and association with PI3-kinase in myeloid leukemias

Noria Harir,[1] Christian Pecquet,[1] Marc Kerenyi,[2] Karoline Sonneck,[3] Boris Kovacic,[2] Remy Nyga,[1] Marie Brevet,[4] Isabelle Dhennin,[1] Valerie Gouilleux-Gruart,[1] Hartmut Beug,[2] Peter Valent,[3] Kaiss Lassoued,[1] Richard Moriggl,[5] and Fabrice Gouilleux[1]

[1]Institut National de la Santé et de la Recherche Médicale (EMI 351), Faculté de Médecine, Université de Picardie J. Verne, Amiens, France; [2]Institute of Molecular Pathology, Vienna, Austria; [3]Department of Internal Medicine I, Division of Hematology, Medical University of Vienna, Austria; [4]Laboratory of Anatomo-Pathology, Centre Hospitalier Universitaire, Amiens, France; [5]Ludwig Boltzmann Institute for Cancer Research, Vienna, Austria

Persistent activation of Stat5 is frequently found in hematologic neoplasms. Studies conducted with constitutively active Stat5 mutants (Stat51*6 and cS5^F) have shown that deregulated Stat5 activity promotes leukemogenesis. To investigate the oncogenic properties of these mutants, we used cS5^F-expressing bone marrow cells which induce a multilineage leukemia when transplanted into recipient mice. Here, we show by immunocytochemistry that cS5^F is localized mainly in the cytoplasmic compartment of leukemic cells, suggesting that the transforming nature of cS5^F may be associated with a cytoplasmic function. In support of this hypothesis, we found that cS5^F forms a complex with the p85 subunit of the phosphatidylinositol 3-kinase (PI3-K) and the scaffolding adapter Gab2 in leukemic bone marrow cells, resulting in the activation of Akt/PKB, a crucial downstream target of PI3-K. By using transducible TAT-Gab2 or TAT-Akt recombinant proteins, we were able to demonstrate that activation of the PI3-kinase/Akt pathway by cS5^F molecules through Gab2 is essential for induction of cell growth. We also found that persistently phosphorylated Stat5 in primary cells from patients with myeloid leukemias has a cytoplasmic localization. These data suggest that oncogenic Stat5 proteins exert dual transforming capabilities not only as transcriptional activators but also as cytoplasmic signaling effectors. (Blood. 2007;109:1678-1686)

Introduction

Stat5A and Stat5B transcription factors are important mediators of cytokine-induced cell survival and proliferation.[1] There is a large body of evidence indicating that they play crucial roles in hematopoiesis in humans and mice. Stat5a/b$^{-/-}$ mice have multiple hematopoietic defects which affect the proliferation and/or survival of both lymphoid and myeloid lineages.[2-7] In addition, Stat5 proteins regulate the growth of hematopoietic progenitor cells, and a recent report has suggested that Stat5 might be involved in self-renewal of human CD34$^+$ progenitor cells.[8,9]

Deregulation of the Jak-Stat signaling pathway, particularly Stat3 and Stat5, was reported in many different types of cancer, including hematopoietic neoplasms.[10,11] Persistent activation of these transcription factors is frequently found in many tumor cells, most probably as a consequence of deregulated tyrosine kinase activity. Importantly, Stat5 is a common target for different oncoproteins with tyrosine kinase activity such as Tel-Jak2, Bcr-Abl, the mutated forms of Flt3 and c-Kit, and the Jak2V617F mutant which has been recently characterized in various myeloproliferative disorders.[12-16] Furthermore, it was shown that Stat5 plays a critical role in Bcr-Abl– and Tel-Jak2–induced leukemia.[17-19] The most direct evidence that constitutive activation of Stat5 is an important causative event in cell transformation came from the analysis of the Stat5 mutants, Stat5A1*6, Stat5B1*6, and cS5^F. These proteins with mutations at residues $H_{299}\rightarrow R$ and $S_{711/716}\rightarrow F$ (Stat5A1*6) or with the single mutation $S_{711}\rightarrow F$ (cS5^F) possess constitutive tyrosine phosphorylation and DNA binding activity and are capable of transforming cell lines to growth factor independence.[20] Stat5A1*6 can also induce a fatal myeloproliferative disease in mice, whereas cS5^F has been shown to induce a multilineage leukemia and to restore the defective phenotype of Stat5a/b-deficient mice, closely mimicking wt Stat5 function.[20,21]

Comprehensive analysis of gene-deleted mice as well as dominant-negative approaches shed light onto the mechanisms by which Stat5 controls cell growth and survival of hematopoietic cells. In particular, Stat5 has been shown to regulate expression of genes involved in cell survival and cell-cycle progression, such as *Bcl-x$_L$*, *A1* and D type cyclins, as well as genes encoding cytokines or growth factors, such as *Osm* or *Igf-1*, and the proto-oncogene *Pim-1*.[2,22-26] Thus, persistent transcriptional activation of these genes by Stat51*6 or cS5^F transcription factors may be the sole consequence for the oncogenic properties of these mutants, a hypothesis that awaits experimental evidence. Several studies suggested that Stat5 proteins may control cellular processes independently of their nuclear functions, through interactions with various signaling molecules. Accordingly, the tyrosine-phosphorylated forms of Stat5 were shown to interact with the SH2-SH3–containing adapter CrkL, the scaffolding adapter Gab, and the PI3-K.[27-29] We previously reported that activation of the PI3-K–signaling cascade plays an important role in Stat51*6-induced cell growth and survival via the scaffolding adapter Gab2.[30,31] It is well

Submitted January 19, 2006; accepted September 25, 2006. Prepublished online as *Blood* First Edition Paper, October 12, 2006; DOI 10.1182/blood-2006-01-029918.

The online version of this article contains a data supplement.

The publication costs of this article were defrayed in part by page charge payment. Therefore, and solely to indicate this fact, this article is hereby marked "advertisement" in accordance with 18 USC section 1734.

established that PI3-K function requires the activation of the serine threonine kinase Akt.[32] Akt regulates the activity of a number of substrates involved in cell apoptosis or proliferation such as Bad, Forkhead, NFκB, and GSk3β.[33,34] Akt is the cellular homologue of the v-akt oncogene, and there is strong evidence that inappropriate activation of the PI3-K/Akt pathway contributes to the development of cancers.[35] Altogether, these different data argue that oncogenic activation of Stat5 triggers its association with PI3-kinase and that activation of this pathway may be involved in the leukemic potential of constitutively active Stat5 molecules. By using bone marrow (BM) cells from mice that received a transplant of $cS5^F$-expressing cells, we demonstrated for the first time that $cS5^F$ is essentially localized in the cytoplasm of primary leukemic cells. We also found that $cS5^F$ forms a signaling complex with the PI3-K and the scaffolding adapter Gab2 which results in the activation of Akt in primary leukemic cells. We were able to show that Gab2 and Akt play a critical role in $cS5^F$-induced cell growth through the use of transducible TAT fusion proteins. In addition, we demonstrated that persistent Stat5 phosphorylation is detected mainly in the cytoplasm of primary cells from patients with chronic myeloid leukemia (CML) and patients with acute myeloid leukemia (AML). Collectively, these data indicate that oncogenic activation of Stat5 affects its cellular localization and function and that activation of the PI3-kinase/Akt pathway via an interaction with p85 and Gab2 is implicated in Stat5-induced leukemia.

Patients, materials, and methods

Animals, primary cell isolation, retroviral infection

Bone marrow (BM) was harvested from hind limbs of 6-week-old male mice (C57/B6 × Sv129j F1). Freshly isolated BM cells were preactivated for 48 hours in medium containing IL-3 (25 ng/mL), IL-6 (50 ng/mL), and SCF (10 ng/mL). Cells were then cocultured on irradiated (1.5 Gy) semiconfluent ecotropic producer cell lines for 48 hours in the presence of 6 μg/mL Polybrene. Generation of retroviral packaging cell lines carrying the $cS5^F$ mutant or the GFPv was described elsewhere.[2] Lethally irradiated wt female (1 Gy) recipients were then reconstituted with the transduced BM cells by tail vein injection (4×10^6 cells/mouse). Mice that received a transplant were checked for disease onset through blood analysis.

Patients

Four patients with acute myeloid leukemia (AML; FAB-subtype: M2, M3, M6, M7), 3 patients with chronic myeloid leukemia (CML; chronic phase, cp, n = 1; myeloid blast phase, pb, n = 1; megakaryoblast crisis, n = 1), and 1 control patient (no hematologic neoplasm, normal bone marrow) were examined. Diagnosis and classification of cases were performed according to established criteria.[36] This study was approved by the institutional review board (Medical University of Vienna) and conducted in accordance with the declaration of Helsinki. Informed consent was obtained before bone marrow biopsies were taken.

Cell culture, plasmids, and reagents

BM cells from mice that received a transplant of $cS5^F$ were grown for 24 hours in RPMI 1640 with 10% fetal calf serum (FCS) and SCF (10 ng/mL; Valbiotech, Paris, France), and GFPv BM cells were grown in the same medium supplemented with IL-3 (10 ng/mL). The next day, GFP^+ cells were sorted by flow cytometry and cultured in their respective medium for 6 weeks.

Ku-812 cells were grown in RPMI 1640 medium (Life Technologies, Cergy-Pontoise, France) containing 10% FCS, 2 mM L-glutamine (10 U/mL), and penicillin/streptomycin (10 μg/mL) at 37°C with 5% CO_2. The LY294002 PI3-K inhibitor and imatinib mesylate were purchased from Sigma (St Quentin Fallavier, France) and Novartis (Basel, Switzerland), respectively.

The coding regions of Akt and Akt (K_{179}→M), Gab2, and Gab2-3YF were amplified by polymerase chain reaction (PCR) and cloned at *Nco*I and *Eco*RI sites of the bacterial expression vector pTAT-HA (for the Akt cDNAs) or at the *Kpn*I-*Xho*I sites (for the Gab2 cDNAs).

Fluorescence-activated cell sorting (FACS) analysis

Cells were incubated 20 minutes with the following phycoerythrin-conjugated antibodies: CD117, CD34, Mac-1, Gr-1, Ter-119, Sca-1, CD19, and Thy1.2 (BD Biosciences, le Pont de Claix, France) and analyzed by flow cytometry (Elite; Becton Dickinson, Le Pont de Claix, France).

Immunohistochemistry and immunocytochemistry

Immunohistochemistry was performed on sections prepared from paraffin-embedded formalin-fixed BM specimens using the indirect immunoperoxidase staining technique as described.[37,38] Endogenous peroxidase was blocked by methanol/H_2O_2. Prior to staining with anti–P-Y-Stat5a/b antibody, sections were pretreated by microwave oven. Sections were stained with an anti–P-Y-Stat5a/b antibody AX-1 (Advantex Bioreagents, Conroe TX) (1.2 μg/mL) diluted in 0.05 M Tris-buffered saline (TBS, pH 7.5) plus 1% BSA for 20 hours. Then slides were washed and incubated with biotinylated goat anti–mouse IgG for 30 minutes, washed, and exposed to streptavidin-peroxidase complex. AEC was used as chromogen. Slides were counterstained in Mayer Hemalun. For immunocytochemical analysis, cells were spun on cytospin slides prior to staining with the AX1 antibody. DAB was used as chromogen. Slides were counterstained with Mayer Hemalun. Acquisition of micrographs was performed by an Olympus DP11 camera connected to an Olympus microscope equipped with 40×/0.85 (Figure 7A,C) and 100×/1.35 (Figure 3A) Uplan-Apo objective lenses (Olympus, Hamburg, Germany). Images were acquired with Photoshop CS2 software version 9.0 (Adobe Systems, San Jose, CA) and were processed with PowerPoint software (Microsoft, Redmond, WA).

Purification of TAT fusion proteins

Purification of TAT fusion proteins was performed as previously described[39] with the following modifications: BL21 (DE3) pLysS bacteria (Stratagene, Amsterdam, The Netherlands) expressing the TAT fusion proteins were cultured in LB broth medium containing 50 μg/mL ampicillin and 34 μg/mL chloramphenicol at 37°C. Protein expression was induced by addition of 1 mM IPTG at 37°C during 4 hours. Cells were harvested and sonicated in buffer A (8 M urea, 20 mM HEPES [pH = 8.0], and 500 mM NaCl). Lysates were clarified by centrifugation at 15 600*g* for 4 minutes at 4°C. The supernatants containing the recombinant TAT fusion proteins were equilibrated in 30 mM imidazole and then applied to Ni-NTa agarose columns (Qiagen, Courtabeuf, France). Columns were washed with 6 bed volumes of buffer B (4 M urea, 20 mM HEPES [pH 8.0], 500 mM NaCl, and 30 mM imidazole). After washing, bound proteins were eluted with buffer B containing 250 mM imidazole. Eluates containing the purified proteins were dialyzed against PBS or (0.9% NaCl) with 4 buffer changes overnight at 4°C. The purity and concentration of TAT fusion proteins was assessed by Coomassie blue–stained SDS–polyacrylamide gel electrophoresis (PAGE) using standard concentrations of BSA. Stability and biologic activity of TAT fusion proteins were determined in Ba/F3 cells expressing the constitutively active form Stat51*6 (See Figures S1-S6, available on the *Blood* website; see the Figure link at the top of the online article).

In vitro proliferation studies

Cells were incubated as triplicates in flat-bottom 24-well plates at a density of 2×10^4 cells/well in medium supplemented with the different TAT fusion proteins at the indicated concentration for 16, 24, or 48 hours. The percentage of living cells was evaluated using the trypan blue dye exclusion assay.

Subcellular fractionation

Cells were lysed in hypotonic buffer (20 mM HEPES, 10 mM KCl, 1 mM EDTA, 0.2% NP40, 10% glycerol, 5 μg/mL aprotinin, 5 μg/mL leupeptin, 1 mM phenylmethylsulfonide fluoril, and 1 mM Na_2VO_4) and centrifuged for 5 minutes at 800*g* (Eppendorf centrifuge). Supernatants (cytoplasmic fraction) were frozen at −70°C. Pelleted nuclei were resuspended in hypertonic buffer (Hypotonic buffer plus 350 mM NaCl), and proteins extracts were prepared by constant agitation during 30 minutes at 4°C. Debris was removed by centrifugation, and nuclear extracts were frozen at −70°C.

Immunoprecipitations, Western blotting, and antibodies

Cells were lysed in Laemmli buffer (62.5 mM Tris, pH 6.8, 2% SDS, 5% β-mercaptoethanol, 10% glycerol). Equal amounts of each protein sample were separated by electrophoresis on SDS-PAGE and blotted onto nitrocellulose membrane (Bio-Rad, Munich, Germany). Blots were incubated as indicated with antibodies raised against the following proteins: Actin, Akt, Gab2, Raf-1, and Lamin C (Santa Cruz Biotechnology, Santa Cruz, CA), $p27^{kip,1}$ Stat5 (Transduction Laboratories, Lexington, KY), Bim (Affinity BioReagents, Golden, CO), HA (Roche, Basel, Switzerland), P-Stat5 or P-Akt^{Ser473} (Cell Signaling Technology, Boston, MA), and topoisomerase I. The blots were developed with the enhanced chemiluminescence (ECL) system (Amersham Pharmacia Biotech, Orsay, France) using specific peroxidase-conjugated anti-IgG Abs. Immunoprecipitation experiments were performed as previously described.[27]

Results

Mice that received a transplant of cS5^F as a model to characterize the transforming properties of Stat5

Mice that received a transplant of cS5^F have been previously reported to develop a multilineage leukemia as a result of enhanced and sustained Stat5 tetramer DNA binding complexes.[21] It remained questionable how cS5^F proteins transduce signals to transform hematopoietic cells and if the predominant function can be attributed only to the transcriptional activity of the oncogenic mutant. In the present model, BM cells were infected with a retrovirus carrying the cS5^F mutant or the GFP vector (GFPv) alone, analyzed for infection efficiency by FACS and injected into lethally irradiated wt mice. Eight mice that received a transplant of cS5^F and 4 mice that received a transplant of GFPv were analyzed. All 8 cS5^F mice were fully reconstituted 4 weeks after transplantation. They developed multilineage leukemia after 4 weeks, whereas no disease was seen in the 4 control mice (Figure 1A). None of the cS5^F-expressing mice survived more than 8 weeks after transplantation, whereas all control mice remained disease free. Thus, in our experiments we chose to analyze diseased mice that received a transplant of cS5^F at 6 weeks after transplantation (Figure 1A). Blood from these animals always contained a remarkable increase in white blood cell counts as compared with controls that was associated with splenomegaly and mesenterial lymphadenopathy (Figure 1B-C). Persistent activation of Stat5 was demonstrated by Western blotting in extracts from cS5^F-transformed splenic (SP) and BM cells using anti–phospho-Y^{694}-Stat5 (P-Y-Stat5) antisera (Figure 1D, lanes 3, 4, 8, 9). Extracts from unstimulated or IL-3–stimulated Ba/F3 cells were also loaded as control (lanes 1 and 2). By contrast no phosphorylation was detected in the splenocytes or BM cells of control GFPv mice (lanes 5, 6, 7).

In vitro proliferation of cS5^F-expressing BM cells

Proliferation and survival of BM progenitors are influenced by various hematopoietic growth factors, including stem-cell factor

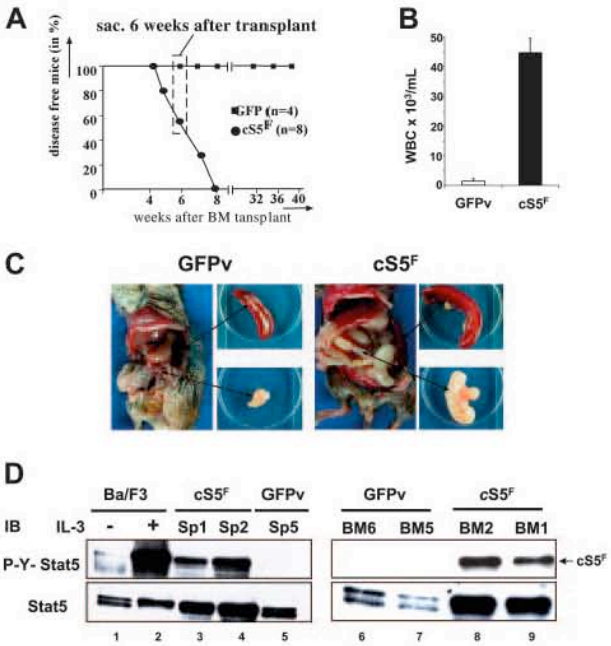

Figure 1. Leukemogenic mice that received a transplant of cS5^F as a model to characterize the transforming properties of Stat5. (A) Kaplan-Meier plot of mice that received a transplant of cS5^F (n = 8) versus mice that received a transplant of GFPv (n = 4). Mice that received a transplant of cS5^F died within 7 weeks after transplantation, while control GFPv mice remain disease free (followed for more then 10 months after transplantation). Thus, experimental mice that received a transplant of cS5^F were killed and analyzed 6 weeks after transplantation for all following experiments (dashed box). (B) White blood cell counts from mice that received a transplant of cS5^F (n = 8) and from GFPv mice (n = 4). Error bars represent SE. (C) Typical organic alterations of mice that received a transplant of cS5^F and control GFPv mice that were killed at 6 weeks after transplantation. Leukemic mice that received a transplant of cS5^F have a unique pathologic appearance with massively enlarged mesenterial lymph nodes (lymphadenopathy) and splenomegaly. (D) Splenic- and BM-cell extracts from 2 mice that received a transplant of cS5^F (Sp1, Sp2, BM1, BM2) or from control GFPv mice (Sp5, BM5, BM6) were analyzed by Western blotting with the indicated antibodies. Cell lysates from Ba/F3 cells unstimulated or stimulated with IL-3 for 30 minutes were also included as controls.

(SCF) and IL-3. Because persistent Stat5 signaling was shown to relieve the growth factor dependence of cell lines, we then analyzed the growth factor requirement of cS5^F-expressing BM cells. GFP$^+$ BM cells of 2 leukemic mice that received a transplant of cS5^F or of 2 control GFPv mice were isolated and cultured in a medium containing SCF. In these conditions, cS5^F-GFP$^+$ BM cells (BM1 and BM2) were able to grow, whereas control GFP$^+$ BM cells (BM5 and BM6) did not grow (Figure 2). Addition of IL-3 restored the proliferating capacities of control GFP$^+$ BM cells. However, we observed that the presence of SCF was absolutely required for the growth of these cS5^F-transformed primary cells, indicating that expression of this mutant partially relieved their cytokine (IL-3) dependence. Note, the growth rate of GFPv BM cells cultured in presence of SCF, and IL-3 was always higher than the growth rate of cS5F BM cells cultured in the presence of SCF alone (Table 1).

cS5^F promotes the growth of hematopoietic progenitor cells in vitro

Freshly isolated BM cells from animals that received a transplant of cS5^F (n = 4) were subjected to lineage markers and GFP expression by FACS analysis (Table 1). The lineage markers included Ter119 (erythroid); Gr-1/Mac-1 (myeloid); CD19 and Thy-1.2 (B and T lineages); and combinations of CD34, Sca-1, and CD117

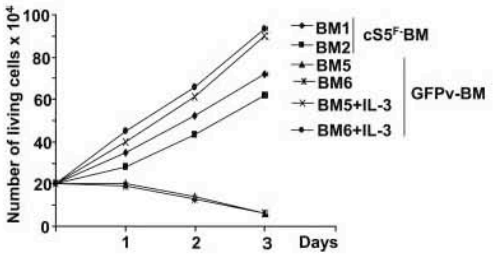

Figure 2. In vitro proliferation of cS5^F-transformed bone marrow cells. Sorted GFP$^+$ BM cells from 2 cS5^F-grafted mice (BM1 and BM2) or from 2 control GFPv mice (BM5 and BM6) were cultured in the presence of SCF (10 ng/mL). In addition to SCF, IL-3 (10 ng/mL) was added to BM5- and BM6-cell cultures. Cells were counted daily using the trypan blue dye exclusion method.

(c-Kit), typical markers for immature multipotent cells or hematopoetic stem cells (HSCs). The majority of cS5^F-GFP$^+$ BM cells was Gr-1– and Mac-1–positive myeloid cells and around 20% of GFP$^+$ BM cells were of B- or T-lymphoid origin. A fraction of cS5^F-GFP$^+$ BM cells also expressed markers typical for primitive multipotent cells. Following 1 week of culture, the myeloid- and lymphoid-specific markers disappeared from the cS5^F-GFP$^+$ BM cells. By contrast, GFP$^+$ cells expressing the immature markers CD34, Sca-1, and CD117 were amplified, indicating that cS5^F promotes the growth of immature progenitor cells. These data support the recent findings that the multilineage cell expansion observed in these mice arose from immature cells transformed by cS5^F.[21]

Cytoplasmic localization of cS5^F in transformed BM cells

It was previously shown that phosphorylated forms of Stat5 interact with various cytoplasmic signaling effectors.[27-29] We therefore addressed the question whether cS5^F may have a cytoplasmic function. We first determined the localization of cS5^F in transformed BM cells by immunocytochemistry with an anti–phospho-Y^{694}-Stat5 antibody before and after stimulation with IL-3. Results clearly showed (Figure 3A) that constitutively active cS5^F mutant is mainly localized in the cytoplasm of BM cells, whereas it is found in the nucleus after stimulation with IL-3. We also analyzed the localization of P-Y-Stat5 in control GFPv BM cells stimulated or not with IL-3. No phosphorylated Stat5 was detected in IL-3–deprived cells, whereas IL-3 treatment of GFPv cells induced the appearance of nuclear P-Y-Stat5. To confirm the specific cytoplasmic localization of cS5^F, we prepared cytoplasmic and nuclear extracts of cS5^F BM cells from 3 different leukemic mice, and the presence of P-Y-Stat5 in both fractions was analyzed by Western blotting with an anti–P-Y-Stat5 antibody (Figure 3B). P-Y-Stat5 was detected in the cytoplasmic fraction of cS5^F BM cells, whereas it was mainly found in the nucleus after stimulation with IL-3. The purity of the extracts was controlled by Western blot analysis for the cytoplasmic ser/thr kinase Raf-1 and the nuclear protein Lamin C. Altogether, these results support the idea that cS5^F has a cytoplasmic signaling function that might play an important role in cS5^F-induced leukemia.

Critical role of the Gab2/PI3-K/Akt pathway in cS5^F-mediated cell transformation

We have previously demonstrated that tyrosine-phosphorylated Stat5 is able to interact with both the PI3-K regulatory subunit p85 and the Gab2-scaffolding adapter in Ba/F3 cells.[30,31] We therefore determined whether cS5^F also interacts with PI3-K and Gab2 in the primary leukemic cells from diseased mice. For this purpose, cell lysates obtained from 2 different cS5^F-expressing BM cells (BM1 and BM2) were immunoprecipitated with anti-Stat5 or isotype-matched control antibodies. The coimmunoprecipitations of the p85 regulatory subunit of PI3-K and Gab2 were next evaluated by immunoblotting (Figure 4A). Results showed that both p85 and Gab2 were associated with cS5^F in primary leukemic-cell extracts. BM-cell lysates of mice that received a transplant with cS5^F or control GFPv mice were next analyzed by immunoblotting with anti–P^{ser473}-Akt and anti-Akt antibodies (Figure 4B, top). A weak phosphorylation of Akt was found in GFPv BM cells, whereas the level of phosphorylated Akt was much higher in cS5^F-expressing BM cells, indicating that Akt phosphorylation was significantly induced by cS5^F in these primary leukemic cells. IL-3 treatment of GFPv BM cells and cS5F BM cells did not further increase the level of phosphorylated Akt (Figure 4B, lower panel) but retained the capacity to activate Stat5 (see Figure S5A, available on the *Blood* website; click on the Supplemental Figures link at the top of the online article).

We next determined whether activation of the PI3-K is required for cS5^F-induced cell growth and survival. For this purpose, we used the pharmacologic PI3-K inhibitor LY294002. cS5^F BM cells cultured in the presence of SCF or control GFPv BM cells grown in the presence of SCF and IL-3 were treated with increasing concentrations (ranging from 1 to 10 μM) of LY294002 (Figure 4C). Growth arrest of the cS5^F-expressing BM cells was observed with 1 μM LY294002 after 48 hours of culture, whereas 10 μM was required to inhibit the growth of GFPv BM cells, indicating that cS5^F BM cells were more sensitive to the inhibition of PI3-K than were control cells. Collectively, our results suggest that cS5^F molecules form a signaling complex with Gab2 and PI3-K to promote the phosphorylation of Akt.

Recombinant TAT fusion proteins that interfere with PI3-K signaling block cS5^F-induced cell growth and Akt phosphorylation

To investigate the role of Gab2 and Akt in the transforming properties of cS5^F, we generated different recombinant TAT-Gab2 or TAT-Akt fusion proteins (Figure 5A). The use of TAT fusion proteins is an appealing approach to transduce cell lines or primary cells.[39,40] Adding them to the culture medium requires, however, biochemical testing for each individual fusion protein purification which had to be done freshly for each individual experiment. We first analyzed the role of Gab2 in cS5^F-induced cell growth, and, for this, we generated a TAT-wtGab2 and a TAT-Gab2-3YF deficient in PI3-kinase binding in which the 3 tyrosine residues (Y,^{452}, Y^{476}, and

Table 1. cS5^F promotes the growth of hematopoietic progenitor cells

cS5^F-BM*	Thy1.2	CD19	Mac-1	Gr-1	Ter119	CD117	CD34	Sca-1
Day 0	9.5 ± 1	12.25 ± 5.5	44.5 ± 8.4	44.25 ± 8.8	15.5 ± 1.9	15.75 ± 1.7	5.5 ± 1.3	9.25 ± 0.96
Day 7	0.375 ± 0.03	2.45 ± 0.07	0.9 ± 0.8	6.3 ± 1	5.9 ± 0.7	99.25 ± 0.7	43.6 ± 7.39	56.8 ± 4.1

Bone marrow cells from cS5^F leukemic mice (n = 4) were subjected to FACS analysis using indicated markers before (day 0) and after 1 week (day 7) of culture in medium containing SCF (10 ng/mL). Results are expressed as the percentage of positive cell markers among GFP-positive cells (mean ± SD).

*n = 4.

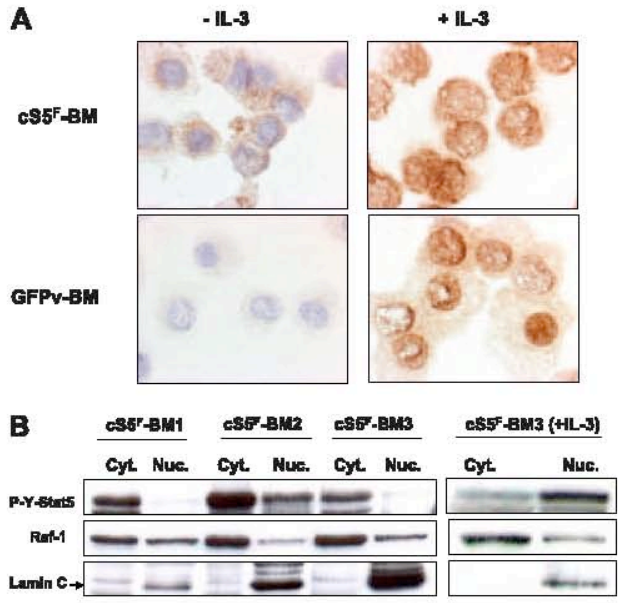

Figure 3. Cytoplasmic localization of cS5^F in bone marrow cells. (A) Immunocytochemical detection of phosphorylated Stat5 in cS5^F-expressing BM cells and control GFPv BM cells stimulated or not with IL-3. In each case, cells were spun on cytospin slides and analyzed by indirect immunocytochemistry using an anti–P-Y-Stat5 antibody (AX1). (B) The localization of cS5^F was also determined by Western blot analysis using cytoplasmic and nuclear extracts of unstimulated or IL-3–stimulated cS5^F BM cells from 3 different mice that received a transplant.

Y^{584}) were changed to phenylalanine (Figure 5A). It was shown that mutations of these 3 tyrosine residues inhibit activation of the PI3-K/Akt pathway in cytokine-stimulated cells.[41] TAT-wtGab2 and TAT-Gab2-3YF proteins were purified and quantified as described in "Patients, materials, and methods" (data not shown).

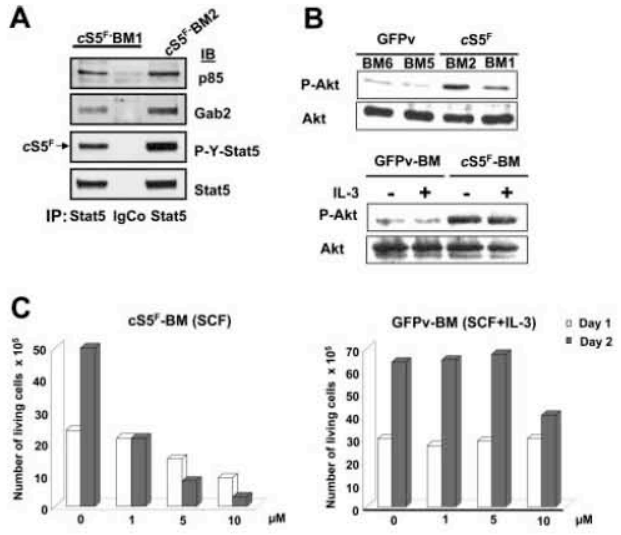

Figure 4. cS5^F interacts with Gab2 and PI3-K and induces Akt activation in transformed bone marrow cells. (A) Stat5 was immunoprecipitated from 2 cS5^F-expressing BM-cell lysates (BM1 and BM2). Subsequently, the content in p85 and Gab2 proteins was evaluated in the Stat5 immunoprecipitates by Western blotting using the indicated antisera. Cell lysates were also immunoprecipitated with an isotypic control IgG antibody. (B) BM-cell lysates from 2 mice that received a transplant of cS5^F or from 2 control GFPv mice (top) and lysates from GFPv BM and cS5^F BM cells stimulated or not with IL-3 (10 ng/mL) for 30 minutes (bottom) were analyzed by Western blotting with the indicated antibodies. (C) cS5^F-expressing BM and control GFPv BM cells cultured in the presence of SCF and SCF + IL-3, respectively, were incubated or not with different concentrations of LY294002 for 48 hours. The number of living cells was determined daily using the trypan blue dye exclusion method. Results are the mean of 3 independent experiments.

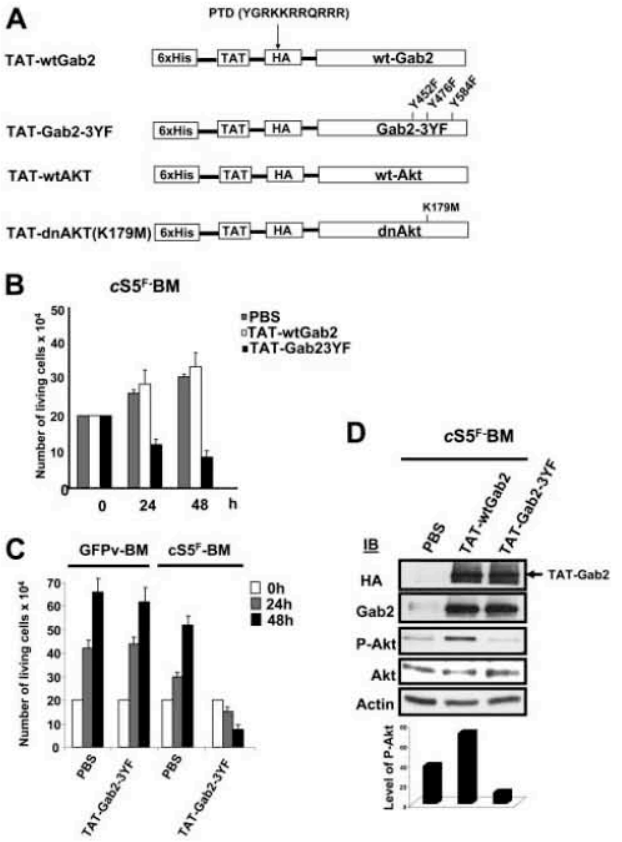

Figure 5. Effects of recombinant TAT-Gab2 fusion proteins on cS5^F-induced cell growth and Akt phosphorylation. (A) Schematic representation of TAT-Akt and TAT-Gab2 constructs. The different cDNAs were introduced into the bacterial expression vector pTAT-HA. Resulting recombinant Akt (wt and dn) and Gab2 (wt and Gab23YF) proteins were fused in their N-terminal part to a 6 ×His-Tag followed by the protein transduction domain (PTD) of the TAT protein and a HA tag sequence. (B) cS5^F BM cells were transduced or not with 100 nM of the different TAT-Gab2 proteins during 48 hours, and the number of living cells was determined daily using the trypan blue dye assay. Results are the mean of 3 independent experiments performed with 2 independent cS5^F BM-cell cultures. (C) GFPv BM cells and cS5^F BM cells were transduced with 100 nM TAT-Gab23YF fusion protein, and growth of the cells was determined daily. Results are the mean of 3 independent experiments. (D) After extensive washes, lysates from transduced cS5^F BM cells were prepared and analyzed by Western blotting with the indicated antibodies. Densitometric analysis was also performed to determine the ratio of P-Akt/Akt in the different samples (bottom).

cS5^F BM cells from 3 different mice that received a transplant were transduced or not with the TAT-Gab2 fusion proteins (100 nM) for 24 and 48 hours, and the number of living cells was estimated by the trypan blue dye exclusion method (Figure 5B). Transduction of TAT-Gab2-3YF protein abolished the growth of the cells, whereas transduction of TAT-wtGab2 slightly increased their proliferation. Transduction efficiency of the different TAT-Gab2 proteins was evaluated in cS5^F-expressing BM cells by Western blot analysis with anti-HA and anti-Gab2 antibodies (Figure 5D). Equal transduction of both proteins was observed. To verify the specific effect of the TAT-Gab2-3YF fusion protein, control GFPv BM cells grown in the presence of SCF and IL-3 or cS5^F BM cells were transduced with the TAT-Gab2-3YF protein (100 nM), and cell growth was determined next (Figure 5C). The TAT-Gab2-3YF protein clearly inhibited the proliferation of cS5^F BM cells, whereas control GFPv BM cells remained insensitive. Western blot analysis with anti-HA and anti-Gab2 antibodies showed that both types of cells were equally and efficiently transduced (data not shown). We also determined whether TAT-Gab2 proteins could alter the PI3-K activity in cS5^F BM cells by analyzing the phosphorylation level of

megakaryocytes and some immature myeloid cells, whereas mature granulocytes and mature erythrocytes did not contain substantial amounts of P-Y-Stat5. In chronic-phase CML (CML-cp), an increase in P-Y-Stat5–positive myeloid progenitors was found when compared with normal BM. Blast cells in patients with CML blast phase (CML-pb) were also found to react with the anti–P-Y-Stat5 antibody. In both cases, P-Y-Stat5 was predominantly detected in the cytoplasm of the leukemic cells. The most abundant staining reaction was seen in a patient with CML with megakaryoblast crisis. To confirm the cytoplasmic localization of P-Y-Stat5, cytoplasmic and nuclear fractions of cells from a patient with CML were analyzed by Western blotting using an anti–P-Y-Stat5 antibody. As shown Figure 7B, P-Y-Stat5 was exclusively localized in the cytoplasm of these leukemic cells. The purity of the cellular fractions was controlled by a Western analysis for the cytoplasmic Raf-1 kinase and the nuclear Topoisomerase I p97/p70 proteins. Bone marrow sections obtained from patients with AML-M2, -M3, -M6, and -M7 were also stained with anti–P-Y-Stat5 antibody (Figure 7C). A clear staining of blast cells was found in those with AML-M2 and AML-M3, and in the patient with AML-M7, in whom blasts cells contained huge amounts of P-Y-Stat5. By contrast, erythroid progenitors were found to be P-Y-Stat5-low cells in one patient (AML-M6) closely reflecting the situation in the normal BM. Collectively, these results suggested that oncogenic activation of Stat5 promotes the cytoplasmic localization of these transcription factors in myeloid leukemias.

Discussion

Beside their physiologic role in hematopoietic-cell development and function, deregulated Stat5 activities promote leukemogenesis.[10] Engineered Stat5 mutants with constitutive activities are a good model to mimic persistent tyrosine kinase activation and to investigate the role of deregulated Stat5 activity in cancers that are susceptible to tyrosine kinase oncogenes. Mutant tyrosine kinases activate distinct signaling pathways (eg, Ras/Map kinase, PI3-K/Akt, NFκB) that play a role in cell growth and survival.[44-47] It is therefore crucial to determine the precise contribution of Stat5 molecules in the transforming process. Here, we have started to analyze cytoplasmic functions of Stat5 that bridge to PI3-K signaling both in a murine transplantation system with oncogenic Stat5 or in cells from patients with CML and patients with AML associated with a constitutive Stat5 activity. To address signaling properties of activated cytoplasmic Stat5 proteins, we used mainly a murine transplantation model of Stat5-induced leukemia.[21] Mice that received a transplant with BM cells expressing $cS5^F$ exhibited a multilineage hematopoietic-cell expansion that lead to severe leukemia within 4 weeks after transplantation. We found that contrary to normal hematopoietic progenitors, the in vitro growth and survival of $cS5^F$-transformed BM cells did not require IL-3, but SCF was essential for self-renewal of immature cell populations. The possibility of an autocrine loop of IL-3 secretion was excluded by the lack of alteration of cell growth in the presence of neutralizing anti–IL-3 antibodies (data not shown). These findings are reminiscent of the loss of IL-3 dependence of Stat5A1*6-expressing Ba/F3 cells.[20]

The present study demonstrates for the first time that a major fraction of constitutively active Stat5 molecules is cytoplasmic under steady state culture conditions in the presence of growth factors such as SCF or in leukemic patient samples. The cytoplasmic localization of P-Y-Stat5 is not restricted to CML and is also found in AML. We lack a full understanding of the cytoplasmic localization of P-Y-Stat5 in leukemic cells, but active Stat5 proteins are rapidly shuttling between nucleus and cytoplasm.[48] It is therefore conceivable that persistent phosphorylation of Stat5 may affect its subcellular localization. Alternatively, it is possible that translocation signals provided by activated cytokine receptors or signals that induce activation of tyrosine phosphatases are lacking in $cS5^F$ BM cells, thereby inducing accumulation of $cS5^F$ in the cytoplasm. Studies with kinetic experiments of Stat5 protein shuttling in and out of the nucleus on cytokine action in normal versus transformed cell pairs would reveal important insights. Irrespective, persistent transcriptional activity of Stat5 seems not to be the dominant form of oncogenic Stat5 molecules in myeloid-cell types. Our results support the concept that a large part of oncogenic Stat5 activity might not only involve a nuclear function but also a cytoplasmic function. The data are consistent with previous work showing that phosphorylated forms of Stat5 act as signaling effectors by interacting with various signaling molecules such as Crkl, Gab2, and PI3-kinase.[27-31] Accordingly, we also found that expression of $cS5^F$ in BM cells induced activation of the PI3-K/Akt pathway via an interaction with the scaffolding adapter Gab2 and p85, the regulatory subunit of the PI3-K. It will be difficult in future experiments to create mutants of Stat5 that do not interact with PI3-K signaling, because tyrosine phosphorylation of Stat5 is absolutely required for Gab2 and p85 interaction.[31] Importantly, the PI3-K inhibitor LY294002 completely blocked the growth of $cS5^F$ BM cells, but PI3-K activation is also achieved efficiently through activation of the c-Kit receptor and SCF was always present in the primary murine-cell cultures. Thus, activation of the PI3-K/Akt pathway was required for $cS5^F$-mediated cell transformation. We also addressed in detail how activation of the Gab2/PI3-kinase/Akt pathway is involved in the $cS5^F$-induced cell transformation. Activation of the PI3-K by tyrosine kinases following activation by extracellular stimuli or after oncogenic challenge occurs via distinct mechanisms. One of them implies the binding of p85 to the scaffolding adapters Gab1/2.[49] In such a scenario, tyrosine phosphorylation of Gab proteins allows recruitment of the p85 subunit via its SH2 domain and this leads to the allosteric activation of the catalytic subunit. Data from our laboratory are in line with this model and we demonstrate here by means of a recombinant and transducible TAT-Gab2-3YF fusion protein, a deficient p85 binding mutant, that Gab2 is absolutely necessary for $cS5^F$-induced cell growth and Akt phosphorylation. We also analyzed the downstream effects of Akt on $cS5^F$-induced cell growth by using transducible recombinant TAT fusion proteins fused to a wt or a dominant-negative form of Akt. Akt has been shown to directly phosphorylate and inactivate members of the Forkhead family which includes AFX, FKHR, and FKHRL1.[33,34] Accordingly, we found that transduction of the mutant TAT-dnAkt protein inhibits the phosphorylation of FKHR and up-regulates expression of Bim and $p27^{kip1}$ proteins in transformed bone marrow cells inhibiting cell growth (see also Figure S3). In regard to the transformation process induced via $cS5^F$ activity, the overall increase in Akt phosphorylation contributes to growth and survival advantages in the absence of cytokines. Therefore, signaling via the Akt kinase is an essential step in Stat5-induced leukemogenesis.

Persistent Stat5 and PI3-K activation were observed in cells expressing various oncogenic tyrosine kinases such as Bcr-Abl, and it was shown that both pathways contribute to the transformation process controlled by this oncoprotein.[13,47] Interestingly enough, Bcr-Abl is unable to transform and to activate the PI3/Akt pathway in primary myeloid cells isolated from *gab2*$^{-/-}$ mice, indicating

that Gab2 signaling via the PI3-K is an important step in Bcr-Abl–induced leukemogenesis.[50] Collectively, these data support our novel findings that formation of a cytoplasmic signaling complex among Stat5, Gab2, and PI3-K might be one of the key steps in cS5^F-evoked multilineage leukemia. A recent report documented lentivirus-mediated RNA interference to inhibit Stat5 or Gab2 protein expression, leading to diminished in vitro colony formation of CML colony-forming units (CFUs) pinpointing to an essential role of both proteins for Bcr-Abl transformation in line with knock-out studies of both molecules.[17,51]

Immunohistochemistry or nuclear versus cytoplasmic fractionation proved that persistent Stat5 activity is mainly present in the cytoplasm of leukemic cells isolated from patients with CML or from primary cS5^F-transformed cells. In addition, we also found that phosphorylated Stat5 proteins interact with PI3-kinase and Gab2 in human Bcr-Abl–expressing cell lines such as K562[30] and Ku812 (data not shown). Thus, Stat5 proteins might also play an integral part as cytoplasmic signaling effectors via its association with Gab2 and PI3-K in the development of human CML. It is possible that oncogenic activation of Stat5 may affect the ratio of nonphosphorylated/phosphorylated forms of Stat5 in both cellular compartments which could enhance the capacity of these molecules to interact with other signaling pathways, most importantly the PI3-K/Akt pathway. However, the cytoplasmic function of Stat5 is not the sole mechanism by which these proteins promote leukemogenesis.

Some previously identified target genes of Stat5 have been shown to contribute to the development of cancer. DNA binding and transcriptional activities play an important role in the transforming properties of Stat5. We have shown that tetramer formation is required for cS5^F-induced leukemia.[21] Formation of Stat5 tetramers results in DNA binding to low-affinity Stat5 binding sites and putative Stat5 tetramer target genes include *CIS*, *SPI2.1*, *CD25*, D type cyclins, *OSM*, or *IGF-1*.[21,52-54] The transduction of persistently activated forms of Stat5 that are tetramerization deficient do not cause leukemia when transplanted in mice.[21] Nonetheless, we were able to stain for localization of tetramerization-deficient Stat5 mutants that are persistently active from transfected Ba/F3 cells followed by FACS sorting and immunocytochemistry. cS5^F and the tetramer-deficient mutants cS5^{F}W37A and cS5^{F}Δ136 proteins were found to have a predominant cytoplasmic localization under IL-3–deprived conditions in Ba/F3 cells, again IL-3 stimulation caused nuclear translocation and increased tyrosine phosphorylation of the mutants (see Figure S4; data not shown). Because the tetramer-deficient but constitutively active Stat5 mutants are not able to induce cell transformation, this would argue again that the cytoplasmic role of cS5^F is also not sufficient to transform cells. The data parallel the predominant cytoplasmic activation on persistent activation of mutant Stat5 in primary mouse cells and the findings from CML or AML patient samples. Our current hypothesis is that both cytoplasmic and nuclear functions are linked to the full transforming activity of cS5^F molecules or persistently active Stat5 proteins in leukemia.

In conclusion, both the transcriptional activity and the capacity to regulate the PI3-K/Akt activity are required for the full transforming properties through persistent Stat5 protein activation. Oncogenic activation of Stat5 revealed a surprising cytoplasmic localization and function. This report sheds light on the crucial role of the Gab2/PI3-K/Akt pathway to contribute to cancer progression through persistent Stat5 signaling.

Acknowledgments

We thank Dr Gu (Harvard Institutes of Medicine) and Dr Dowdy (University of California) for the kind gift of the Gab2 or pTAT-HA vectors and Aline Régnier for her excellent technical support.

This work was supported by Association de la Recherche contre le Cancer, Ligue contre le Cancer (Comité du Nord-Pas de Calais), Conseil Régional de Picardie, Fondation de France and Cent pour Sang la Vie, Fonds zur Förderung der Wissenschaftlichen Forschung in Österreich, FWF (grant P17205-B14) (P.V.) and (grant SFB F28) (R.M.), the French and Algerian Ministry for Research and Technology (N.H.), and ARERS Verre-Espoir (C.P.).

Authorship

Contribution: N.H., C.P., M.K., K.S., B.K., R.N., A.R., I.D., C.S., and M.B. designed and performed the research; V.G.-G. designed the research and wrote the paper; H.B. contributed analytical tools and analyzed the data; K.L. analyzed data and wrote the paper; P.V., R.M., and F.G. designed the research, analyzed data, and wrote the paper.

Conflict-of-interest disclosure: The authors declare no competing financial interests.

R.M. and F.G. contributed equally to this study.

Correspondence: Fabrice Gouilleux, Institut National de la Santé et de la Recherche Médicale (EMI 351), Faculté de Médecine, 3 rue des Louvels, 80036 Amiens, France; e-mail: fabrice.gouilleux@sa.u-picardie.fr.

References

1. Buitenhuis M, Coffer PJ, Koenderman L. Signal transducer and activator of transcription 5 (Stat5). Int J Biochem Cell Biol. 2004;36:2120-2124.
2. Moriggl R, Topham DJ, Teglund S, et al. Stat5 is required for IL-2-induced cell cycle progression of peripheral T cells. Immunity. 1999;10:249-259.
3. Sexl V, Piekorz R, Moriggl R, et al. Stat5a/b contribute to interleukin 7-induced B-cell precursor expansion, but abl- and bcr/abl-induced transformation are independent of stat5. Blood. 2000;96:2277-2283.
4. Kieslinger M, Woldman I, Moriggl R, et al. Antiapoptotic activity of Stat5 required during terminal stages of myeloid differentiation. Genes Dev. 2000;14:232-244.
5. Socolovsky M, Nam H, Fleming MD, Haase VH, Brugnara C, Lodish HF. Ineffective erythropoiesis in Stat5a(-/-)5b(-/-) mice due to decreased survival of early erythroblasts. Blood. 2001;98:3261-3273.
6. Bunting KD, Bradley HL, Hawley TS, et al. Reduced lymphomyeloid repopulating activity from adult bone marrow and fetal liver of mice lacking expression of STAT5. Blood. 2002;99:479-487.
7. Cui Y, Riedlinger G, Miyoshi K, et al. Inactivation of Stat5 in mouse mammary epithelium during pregnancy reveals distinct functions in cell proliferation, survival, and differentiation. Mol Cell Biol. 2004;24:8037-8047.
8. Schuringa JJ, Chung KY, Morrone G, Moore MAS. Constitutive activation of STAT5A promotes human hematopoietic stem cell self-renewal and erythroid differentiation. J Exp Med. 2004;200:623-635.
9. Kato Y, Iwama A, Tadokoro Y, et al. Selective activation of STAT5 unveils its role in stem cell self-renewal in normal and leukemic hematopoiesis. J Exp Med. 2005;202:169-179.
10. Benekli M, Baer MR, Baumann H, Wetzler M. Signal transducer and activator of transcription proteins in leukemias. Blood. 2003;101:2940-2954.
11. Bowman T, Garcia R, Turkson J, Jove R. STATs in oncogenesis. Oncogene. 2000;19:2474-2488.
12. Lacronique V, Boureux A, Monni R, et al. Transforming properties of chimeric TEL-JAK proteins in Ba/F3 cells. Blood. 2000;95:2076-2083.
13. Nieborowska-Skorska M, Wasik MA, Slupianek A, et al. Signal transducer and activator of transcription (STAT)5 activation by BCR/ABL is dependent on intact Src homology (SH)3 and SH2 domains of BCR/ABL and is required for leukemogenesis. J Exp Med. 1999;189:1229-1242.

14. Mizuki M, Fenski R, Halfter H. Flt3 mutations from patients with acute myeloid leukemia induce transformation of 32D cells mediated by the Ras and STAT5 pathways. Blood. 2000;96:3907-3914.
15. Growney JD, Clark JJ, Adelsperger J, et al. Activation mutations of human c-KIT resistant to imatinib are sensitive to the tyrosine kinase inhibitor PKC412. Blood. 2005;106:721-724.
16. Levine RL, Wadleigh M, Cools J, et al. Activating mutation in the tyrosine kinase JAK2 in polycythemia vera, essential thrombocythemia, and myeloid metaplasia with myelofibrosis. Cancer Cell. 2005;7:387-397.
17. Hölbl A, Kovacic B, Kerenyi M, et al. Clarifying the role of Stat5 in lymphoid development and Abelson induced transformation. Blood. 2006;107:4898-4906.
18. Ye D, Wolff N, Zhang S, Ilaria RL Jr. STAT5 signaling is required for the efficient induction and maintenance of CML in mice. Blood. 2006;107:4917-4925.
19. Schwaller J, Parganas E, Wang D, et al. Stat5 is essential for the myelo-and lymphoproliferative disease induced by TEL/JAK2. Mol Cell. 2000;6:693-704.
20. Onishi M, Nosaka T, Misawa K, et al. Identification and characterization of a constitutively active STAT5 mutant that promotes cell proliferation. Mol Cell Biol. 1998;18:3871-3879.
21. Moriggl R, Sexl V, Kenner L, et al. Stat5 tetramer association is associated with leukemogenesis. Cancer Cell. 2005;7:87-99.
22. Dumon S, Santos SC, Debierre-Grockiego F, et al. IL-3 dependent regulation of Bcl-x_L gene expression by STAT5 in a bone marrow derived cell line. Oncogene. 1999;18:4191-4199.
23. Feldman GM, Rosenthal LA, Liu X, et al. STAT5A-deficient mice demonstrate a defect in granulocyte-macrophage colony-stimulating factor-induced proliferation and gene expression. Blood. 1997;90:1768-1776.
24. Yoshimura A, Ichihara M, Kinjyo I, et al. Mouse oncostatin M: an immediate early gene induced by multiple cytokines through the JAK-STAT5 pathway. EMBO J. 1996;15:1055-1063.
25. Woelfle J, Billiard J, Rotwein P. Acute control of insulin-like growth factor-I gene transcription by growth hormone through Stat5b. J Biol Chem. 2003;278:22696-22702.
26. Nosaka T, Kawashima T, Misawa K, Ikuta K, Mui AL, Kitamura T. STAT5 as a molecular regulator of proliferation, differentiation and apoptosis in hematopoietic cells. EMBO J. 1999;18:4754-4765.
27. Oda A, Wakao H, Fujihara M, et al. Thrombopoietin and interleukin-2 induce association of CRK with STAT5. Biochem Biophys Res Commun. 2000;278:299-305.
28. Brockdorff JL, Gu H, Mustelin T, et al. Gab2 is phosphorylated on tyrosine upon interleukin-2/interleukin-15 stimulation in mycosis-fungoides-derived tumour T cells and associates inducibly with SHP-2 and Stat5. Exp Clin Immunogenet. 2001;18:86-95.
29. Rosa Santos SC, Dumon S, Mayeux P, Gisselbrecht S, Gouilleux F. Cooperation between STAT5 and phosphatidylinositol 3-kinase in the IL-3-dependent survival of a bone marrow derived cell line. Oncogene. 2000;19:1164-1172.
30. Santos SC, Lacronique V, Bouchaert I, et al. Constitutively active STAT5 variants induce growth and survival of hematopoietic cells through a PI 3K/Akt dependent pathway. Oncogene. 2001;20:2080-2090.
31. Nyga R, Pecquet C, Harir N, et al. Activated STAT5 proteins induce activation of the PI 3-kinase/Akt and Ras/Map kinase pathways via the Gab2 scaffolding adapter. Biochem J. 2005;390:359-366.
32. Burgering BM, Coffer PJ. Protein kinase B (c-Akt) in phosphatidylinositol-3-OH kinase signal transduction. Nature. 1995;376:599-602.
33. Brunet A, Bonni A, Zigmond MJ, et al. Akt promotes cell survival by phosphorylating and inhibiting a Forkhead transcription factor. Cell. 1999;96:857-868.
34. Datta SR, Brunet A, Greenberg ME. Cellular survival: a play in three Akts. Genes Dev. 1999;13:2905-2927.
35. Vivanco I, Sawyers CL. The phosphatidylinositol 3-Kinase AKT pathway in human cancer. Nat Rev Cancer. 2002;2:489-501.
36. Jaffe ES, Harris NL, Stein H, Vardiman JW, eds. World Health Organization (WHO) classification of tumours. Pathology and genetics. Tumours of haematopoietic and lymphoid tissues. Lyon, France: IARC Press, 2001.
37. Hsu SM, Raine L, Fanger H. Use of avidin-biotin-peroxidase complex (ABC) in immunoperoxidase techniques: a comparison between ABC and unlabeled antibody (PAP) procedures. J Histochem Cytochem. 1981; 29:577-580.
38. Jordan JH, Walchshofer S, Jurecka W, et al. Immunohistochemical properties of bone marrow mast cells in systemic mastocytosis: evidence for expression of CD2, CD117/Kit, and bcl-x(L). Hum Pathol. 2001;32:545-552.
39. Krosl J, Austin P, Beslu N, Kroon E, Humphries RK, Sauvageau G. In vitro expansion of hematopoietic stem cells by recombinant TAT-HOXB4 protein. Nat Med. 2003;9:1428-1432.
40. Vocero-Akbani A, Chellaiah MA, Hruska KA, Dowdy SF. Protein transduction: delivery of Tat-GTPase fusion proteins into mammalian cells. Methods Enzymol. 2001;332:36-49.
41. Gu H, Maeda H, Moon JJ, et al. New role for Shc in activation of the phosphatidylinositol 3-kinase/Akt pathway. Mol Cell Biol. 2000;20:7109-7120.
42. Dijkers PF, Medema RH, Pals C, et al. Forkhead transcription factor FKHR-L1 modulates cytokine-dependent transcriptional regulation of p27(KIP1). Mol Cell Biol. 2000;20:9138-9148.
43. Dijkers PF, Medema RH, Lammers JW, Koenderman L, Coffer PJ. Expression of the pro-apoptotic Bcl-2 family member Bim is regulated by the forkhead transcription factor FKHR-L1. Curr Biol. 2000;10:1201-1204.
44. Ho JM, Nguyen MH, Dierov JK, et al. TEL-JAK2 constitutively activates the extracellular signal-regulated kinase (ERK), stress-activated protein/Jun kinase (SAPK/JNK), and p38 signaling pathways. Blood. 2002;100:1438-1448.
45. Nguyen MH, Ho JM, Beattie BK, Barber DL. TEL-JAK2 mediates constitutive activation of the phosphatidylinositol 3′-kinase/protein kinase B signalling pathway. J Biol Chem. 2001;276:32704-32713.
46. Santos SCR, Monni R, Bouchaert I, et al. Involvement of the NF-κB pathway in the transforming properties of the TEL-Jak2 leukemogenic fusion protein. FEBS Lett. 2001;497:148-152.
47. Skorski T, Bellacosa A, Nieborowska-Skorska M, et al. Transformation of hematopoietic cells by BCR/ABL requires activation of a PI3-K /Akt-dependent pathway. EMBO J. 1997;16:6151-6161.
48. Vinkemeier U. Getting the message across, STAT! Design principles of a molecular signalling circuit. J Cell Biol. 2004;167:197-201.
49. Nishida K, Hirano T. The role of Gab family scaffolding adapter proteins in the signal transduction of cytokine and growth factor receptors. Cancer Sci. 2003;94:1029-1033.
50. Sattler M, Mohi MG, Pride YB, et al. Role for Gab2 in transformation by BCR/ABL. Cancer Cell. 2002;1:479-492.
51. Scherr M, Chaturvedi A, Battmer K, Dallmann I, et al. Enhanced sensitivity to inhibition of SHP2, STAT5, and Gab2 expression in chronic myeloid leukemia (CML). Blood. 2005;107:3279-3287.
52. Verdier F, Rabionet R, Gouilleux F, et al. A sequence of the CIS gene promoter interacts preferentially with two associated STAT5A dimers: a distinct biochemical difference between STAT5A and STAT5B. Mol Cell Biol. 1998;18:5852-8560.
53. John S, Vinkemeier U, Soldaini E, Darnell JE Jr, Leonard WJ. The significance of tetramerization in promoter recruitment by Stat5. Mol Cell Biol. 1999;19:1910-1918.
54. Meyer WK, Reichenbach P, Schindler U, Soldaini E, Nabholz M. Interaction of STAT5 dimers on two low affinity binding sites mediates interleukin 2 (IL-2) stimulation of IL-2 receptor alpha gene transcription. J Biol Chem. 1997;272:31821-31828.

3.2.5 STAT1 acts as a tumor promoter for leukemia development

Boris Kovacic[1,4], Dagmar Stoiber[1,2], Richard Moriggl[2], Eva Weisz[1], Rene G. Ott[1], Rita Kreibich[1], David E. Levy[3], Hartmut Beug[4], Michael Freissmuth[1] and Veronika Sexl[1]

[1]Department of Pharmacology, Medical University of Vienna (MUW), Vienna A-1090, Austria

[2]Ludwig Boltzmann Institute for Cancer Research (LBI-CR), Vienna A-1090, Austria

[3]Department of Pathology and Microbiology, New York University School of Medicine, New York 10016

[4]Institute of Molecular Pathology (IMP), Vienna A-1030, Austria

STAT1 acts as a tumor promoter for leukemia development

Boris Kovacic,[1,4] Dagmar Stoiber,[1,2] Richard Moriggl,[2] Eva Weisz,[1] René G. Ott,[1] Rita Kreibich,[1] David E. Levy,[3] Hartmut Beug,[4] Michael Freissmuth,[1] and Veronika Sexl[1,*]

[1] Department of Pharmacology, Medical University of Vienna (MUW), Vienna A-1090, Austria
[2] Ludwig Boltzmann Institute for Cancer Research (LBI-CR), Vienna A-1090, Austria
[3] Department of Pathology and Microbiology, New York University School of Medicine, New York 10016
[4] Institute of Molecular Pathology (IMP), Vienna A-1030, Austria
*Correspondence: veronika.sexl@meduniwien.ac.at

Summary

The tumor suppressor STAT1 is considered a key regulator of the surveillance of developing tumors. Here, we describe an unexpected tumor-promoting role for STAT1 in leukemia. *STAT1*$^{-/-}$ mice are partially protected from leukemia development, and *STAT1*$^{-/-}$ tumor cells induce leukemia in *RAG2*$^{-/-}$ and immunocompetent mice with increased latency. The low MHC class I protein levels of *STAT1*$^{-/-}$ tumor cells enable efficient NK cell lysis and account for the enhanced tumor clearance. Strikingly, *STAT1*$^{-/-}$ tumor cells acquire increased MHC class I expression upon leukemia progression. These findings define STAT1 as a tumor promoter in leukemia development. Furthermore, we describe the upregulation of MHC class I expression as a general mechanism that allows for the escape of hematopoietic malignancies from immune surveillance.

Introduction

The JAK (*Janus* kinase)-STAT (signal transducer and activator of transcription) signaling pathway mediates a variety of important cellular functions in the hematopoietic system. Ligand binding on the cognate receptor leads to activation of receptor-associated JAKs, which subsequently tyrosine-phosphorylate and activate STAT proteins. After formation of dimers, STAT proteins translocate to the nucleus, where they induce or modulate expression of target genes (Bromberg and Darnell, 2000; Levy and Darnell, 2002).

Targeted deletion was instrumental in clarifying the physiological role of STAT1 in vivo (Durbin et al., 1996; Meraz et al., 1996). *STAT1*$^{-/-}$ mice are viable and fertile but are more susceptible to viral and bacterial infections. This phenotype was attributed to a lack of IFN-γ signaling. Originally, the development and distribution of lymphocytes seemed unaffected in *STAT1*$^{-/-}$ animals. Later reports, however, revealed defects in the maturation of T lymphocytes (Fallarino and Gajewski, 1999; Lee et al., 2000b; Refaeli et al., 2002) and documented an impaired cytolytic capacity of NK cells (Lee et al., 2000a). *STAT1*$^{-/-}$ T cells proliferated faster and showed a reduced propensity to undergo apoptosis due to diminished expression levels of caspase 1, 8, and 11. Recently, an increased susceptibility to autoimmune disease was reported in *STAT1*$^{-/-}$ mice due to an impaired function of CD4$^+$/CD25$^+$ regulatory T suppressor cells (Nishibori et al., 2004).

STAT1$^{-/-}$ mice have also been shown to be tumor prone, and STAT1 was therefore classified as a tumor suppressor (Badgwell et al., 2004; Kaplan et al., 1998; Lesinski et al., 2003; Shankaran et al., 2001). One mechanism by which STAT1 suppresses tumor formation is its key role as a transcription factor downstream of type I and type II interferons (IFNs). IFN-α is widely used for the treatment of metastatic melanoma and for certain forms of leukemia, where it can induce disease regression. IFN-γ is a key component of tumor surveillance and protects the host against spontaneously arising tumors (Dalton et al., 1993; Sexl et al., 2003; Street et al., 2002). Accordingly, spontaneously arising and metylcholanthrene (MCA)-induced tumors evolve faster in mice deficient for components of IFN-γ signaling than in wild-type controls (Kaplan et al., 1998). Similarly, spontaneous tumor development is increased in IFN-γ- and perforin-deficient mice, which develop lymphomas and/or sarcomas with a higher frequency than wild-type animals (Smyth et al., 2000; Street et al., 2002). These findings support a model where IFN-γ tightly collaborates with lymphocytes to protect the host from tumor development; as predicted from this concept, tumors arising in immunocompromised *RAG2*$^{-/-}$ mice are easily rejected when transplanted into (syngenic) immunocompetent wild-type hosts (Dunn et al., 2002; Dunn et al., 2004; Ikeda et al., 2002; Shankaran et al., 2001).

Still, the mechanism of tumor editing is only poorly understood. A very recent report implies a so far underestimated

SIGNIFICANCE

So far, STAT1 was classified as a tumor suppressor, and *STAT1*$^{-/-}$ mice were shown to be prone to develop solid tumors. The tumor-suppressing effect of STAT1 was attributed to its role as a key transcription factor downstream of IFN signaling. We now show that STAT1 can accelerate the development of hematopoietic tumors independently of IFN signaling. Moreover, we demonstrate that the upregulation of MHC class I molecules represents a general mechanism to escape tumor surveillance and that low MHC class I expression might be beneficial for leukemia patients. Our study may therefore redirect immune-therapeutic considerations. The loss of STAT1 is observed in human malignancies, and anticancer drugs like fludarabine are known modulators of STAT1 protein expression.

role of the innate immune system for tumor surveillance (Street et al., 2004). Herein, it is shown that rejection of spontaneous B cell lymphoma arising in immunocompromised mice (β2-microglobulin- or perforin-deficient) was mediated by NK and γδ T cells. More importantly, depletion of either $CD4^+$, $CD8^+$, or both populations from wild-type mice did not prevent tumor rejection.

We explored the contribution of the innate immune system to tumor evolution by investigating two types of hematological cancers: B-lymphoid malignancies induced by the v-abl-oncogene and myeloproliferative disorders (MPDs) caused by the TEL/JAK2 oncogene. Both murine models are relevant to clinical disease in people because the oncogenes that drive tumor development have a human counterpart. The oncogenic properties of *v-abl* are based on a fusion of the retroviral *gag* gene with a C-terminal portion of the *c-abl* gene. The resulting fusion product codes for a constitutively active tyrosine kinase located in the cytoplasm (Rosenberg and Witte, 1988; Witte, 1986). Transformation with a replication-deficient retrovirus encoding v-abl transforms fibroblasts and B-lymphoid precursors in vitro and leads to development of primary B cell leukemia and lymphoma in vivo (Abelson and Rabstein, 1970; Palumbo et al., 1990). The inflicted disease develops slowly and allows the immune system to take corrective actions.

MPDs are clonal hematopoietic stem cell malignancies (Spivak, 2004). The TEL/JAK2 oncogene was initially isolated from T cell childhood leukemia and encodes an ETS transcription factor family member fused to the catalytic domain of JAK2 (Lacronique et al., 1997; Peeters et al., 1997). The fusion protein is a constitutively active tyrosine kinase. Transformed bone marrow cells that express TEL-JAK2 induce MPD and lymphoblastic lymphoma (LBL) after transplantation into lethally irradiated wild-type mice (Carron et al., 2000; Schwaller et al., 1998). Very recently, a single-nucleotide mutation in the pseudokinase domain of JAK2 (V617F) was found in ~75%–90% of polycythemia vera (PV) patients and in other MPDs (James et al., 2005; Kralovics et al., 2005; Levine et al., 2005). Again, this mutation leads to the constitutive activation of JAK2. These observations highlight the similarity between the murine model and the manifestation of the disease in people.

Here, we demonstrate, to our knowledge, a previously undescribed role of STAT1 for the development of hematopoietic malignancies. STAT1 promotes leukemia development by maintaining high MHC class I expression. Leukemic cells that express low MHC class I levels need to upregulate MHC class I levels to allow for development of leukemia in vivo. Our findings were recapitulated in two independent experimental systems, i.e., V-abl-induced and TEL-JAK2-induced tumors that arise from distinct progenitor cells. STAT1-mediated regulation of MHC class I is of general relevance to understand the mechanisms that underlie the evolution of tumor cells under the pressure of the immune system.

Results

STAT1$^{-/-}$ B cell precursors are susceptible to transformation with v-abl

The transforming activity of *v-abl* includes the ability to abrogate growth factor requirements of B cell progenitors (Palumbo et al., 1990). Lymphocytes from *STAT1*$^{-/-}$ mice have previously been shown to undergo increased proliferation and have prolonged survival in vitro (Lee et al., 2000b). We therefore assessed the consequences of STAT1 deficiency on growth factor-independent proliferation of fetal liver cells after oncogenic transformation. *STAT1*$^{-/-}$ fetal liver cells were transformed with *v-abl* more efficiently and gave rise to increased numbers of growth factor-independent $CD43^+/CD19^+/B220^+$ (pro-B) cell colonies (Figures S1A–S1C in the Supplemental Data available with this article online). The size of colonies in methylcellulose did not vary between *STAT1*$^{+/-}$ and *STAT1*$^{-/-}$ cells, indicating that transformed *STAT1*$^{-/-}$ cells did not have any proliferative advantage (Figure S1D). Because STAT1 has recently been implicated in apoptosis (Agrawal et al., 2002; Lee et al., 2000b), we analyzed cell death in response to serum starvation and UV irradiation. Three independently derived cell lines from *STAT1*$^{+/-}$ and *STAT1*$^{-/-}$ fetal liver cell suspensions were analyzed and displayed no significant differences ($p = 0.26$ in Figure S2A and $p = 0.6$ in Figure S2B). In some cell types, STAT1 was also shown to inhibit cell proliferation by increasing the levels of cyclin-dependent kinase inhibitors p21 and p27 (Lee et al., 2000b; Yu and Jove, 2004). As already indicated by the equal size of the transformed colonies, *v-abl*-transformed *STAT1*$^{+/-}$ and *STAT1*$^{-/-}$ pro-B cells did not vary in their proliferative capacity ($p = 0.49$; Figure S2C). Immunoblots for cell cycle components confirmed equal protein expression of cyclin D2, cyclin E, cyclin A, and the cell cycle inhibitors p53, p16, p19, p21, and p27 in *STAT1*$^{+/-}$ and *STAT1*$^{-/-}$ cell lines (Figures S2D and S2E). Taken together, our data lead us to conclude that STAT1 counteracts the initial transformation process but has no appreciable impact on cell proliferation or survival of transformed pro-B cells.

Lack of STAT1 decreases leukemia formation in immunodeficient mice

To address the role of STAT1 for the formation of B-lymphoid leukemia in vivo, six independently derived *v-abl*-transformed *STAT1*$^{+/-}$ and six *STAT1*$^{-/-}$ cell lines were injected intravenously into *RAG2*$^{-/-}$ mice. Three different concentrations of each transformed cell line were injected (10^6, 10^5, and 5×10^4 cells/mouse; Figures 1A–1C). All *RAG2*$^{-/-}$ mice that had received *STAT1*$^{+/-}$ leukemic cells succumbed to the disease and displayed the classical signs of leukemia: high numbers of B-lymphoid cells were detected in the peripheral blood, and leukemic cells infiltrated liver, spleen, and bone marrow (data not shown). The latency of disease correlated with the number of cells injected. Within 22 days, 10^6 cells induced leukemia; 10^5 cells induced leukemia within 34 days, and 5×10^4 cells induced leukemia within 46 days.

The correlation between injected cell number and disease latency was more evident when transformed *STAT1*$^{-/-}$ pro-B cells were injected. Whereas 10^6 *STAT1*$^{-/-}$ cells induced leukemia with the same latency as *STAT1*$^{+/-}$ cells ($p = 0.76$), differences emerged upon injection of 10^5 cells (Figure 1B). Most interestingly, some *RAG2*$^{-/-}$ mice even survived the challenge with *STAT1*$^{-/-}$ leukemic cells and remained disease-free for more than 12 months (Figures 1B and 1C). Injection of 10^5 *STAT1*$^{-/-}$ cells resulted in disease onset in 80% of the injected *RAG2*$^{-/-}$ mice with a disease latency of 47 days ($p = 0.04$). This difference was even more pronounced when cell numbers were lowered to 5×10^4 cells (Figure 1C). In this case, 40% of the injected *RAG2*$^{-/-}$ mice remained healthy for more than 10 months ($p = 0.03$). Mice that had developed leukemia upon injection of *STAT1*$^{-/-}$ cells showed a profound decrease in infiltration of

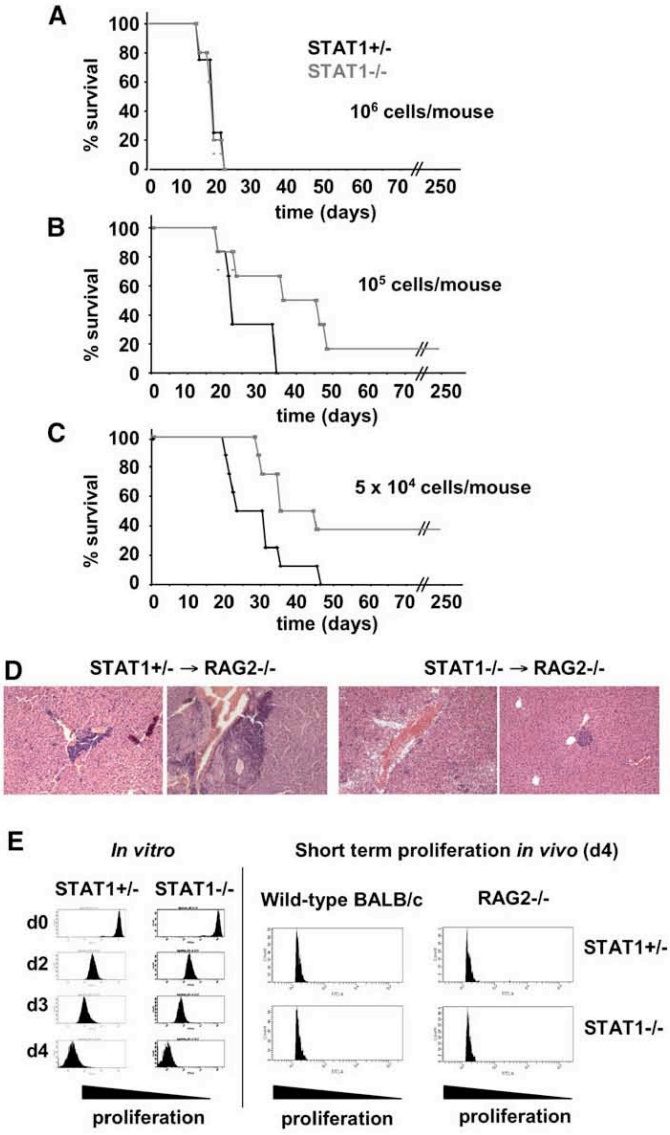

Figure 1. Lack of STAT1 decreases leukemia formation in *RAG2*$^{-/-}$ mice

A–C: In total, six individual cell lines (*STAT1*$^{+/-}$ and *STAT1*$^{-/-}$) were injected at different doses into *RAG2*$^{-/-}$ mice. Leukemia development was observed for more than 250 days. Three different cell numbers (10^6 cells [**A**], 10^5 cells [**B**], and 5×10^4 cells [**C**]) of each genotype were injected into *RAG2*$^{-/-}$ mice (n = 6 for each genotype/experiment in **A** and **B**; n = 8 for each genotype in **C**).

D: Hematoxylin/eosin-stained histological sections of infiltrated livers from *RAG2*$^{-/-}$ mice, which had received *STAT1*$^{+/-}$ (left panel) or *STAT1*$^{-/-}$ cell lines (right panel; magnification: ×100). Two representative examples are depicted for each genotype.

E: Short-term proliferation of CFSE-labeled *STAT1*$^{+/-}$ or *STAT1*$^{-/-}$ leukemic cells was assessed in vitro (left panel), and wild-type BALB/c and *RAG2*$^{-/-}$ mice were assessed 4 days after injection (right panel).

spleen and liver compared to mice that had received *STAT1*$^{+/-}$ cells (Figure 1D and data not shown). The bone marrow represents the initial site of disease development. To test whether *STAT1*$^{-/-}$ cells have difficulties in homing to the bone marrow, we labeled leukemic cells with the fluorescent dye CFSE and injected these into *RAG2*$^{-/-}$ as well as into wild-type recipient mice. The fluorescence intensity decreases with each cell division, since CFSE is equally distributed between the daughter cells. Four days after the injection of tumor cells, the bone marrow was analyzed for the presence of CFSE$^+$ cells. As depicted in Figure 1E, *STAT1*$^{+/-}$ and *STAT1*$^{-/-}$ cells were present at comparable numbers in *RAG2*$^{-/-}$ (0.099% ± 0.005% and 0.111% ± 0.006%; p = 0.8) and in wild-type mice (0.111% ± 0.019% and 0.104% ± 0.004%; p = 0.75). Importantly, the fluorescence intensity that was recorded ex vivo did not differ in *STAT1*$^{+/-}$ and *STAT1*$^{-/-}$ cells. This observation confirmed again that the proliferative capacity of *STAT1*$^{-/-}$ cells was not affected.

STAT1$^{-/-}$ tumor cells express low levels of MHC class I

Tumor development is a permanent battle of the evolving tumor and the immune system. It is evident that the injection of low numbers of tumor cells allows the immune system to take corrective action, whereas high cell numbers are likely to overrun the immunological defense mechanisms. Therefore, we reasoned that tumor surveillance accounted for the increase in survival of *RAG2*$^{-/-}$ mice. *RAG2*$^{-/-}$ mice lack functional T/B, NKT, and γδT cells and rely on NK cells for tumor surveillance (Shinkai et al., 1992). The presence of MHC class I molecules is one of the central mechanisms that allow NK cells to recognize their targets. Cells bearing low levels of MHC class I are readily recognized as "non-self" and eliminated by NK-mediated cytotoxicity (Cerwenka and Lanier, 2001; Colucci et al., 2003; Karre et al., 1986; Lee et al., 1999). Hence, we tested the expression levels of MHC class I (H-2D^d) on the surface of six individual *STAT1*$^{+/-}$ and six individual *STAT1*$^{-/-}$ cell lines. These in vitro-transformed *STAT1*$^{-/-}$ pro-B cells consistently showed drastically reduced MHC class I surface expression compared to in vitro-transformed *STAT1*$^{+/-}$ cells (Figure 2A). In contrast to transformed *STAT1*$^{-/-}$ cells, *v-abl*-transformed *IFN-γ*$^{-/-}$ pro-B cells did not show any alterations in MHC class I surface expression, indicating that the decreased expression is a cell-autonomous feature of transformed *STAT1*$^{-/-}$ B-lymphoid cells and independent of an autocrine IFN loop. In addition, we incubated freshly prepared fetal liver cells with high concentrations of v-abl retrovirus. Infection with the retrovirus did not enhance the MHC class I expression (Figure 2B).

Thus, the findings summarized are consistent with the interpretation that neither the retroviral infection nor an autocrine IFN-γ loop does per se elevate MHC class I expression and that changes in MHC class I expression reflected cell autonomous properties of the tumor cells. The regulation of MHC class I by STAT1 has also been documented by others (Kamiya et al., 2004; Lee et al., 1999; Lieberman et al., 2004). However, the experiments did not prove that the NK cell compartment was required to account for the differences in outcome observed in animals challenged with STAT1-expressing and STAT1-deficient cells (Figures 1A–1C). To address this issue, we injected *STAT1*$^{+/-}$ and *STAT1*$^{-/-}$ tumor cells at low numbers (5×10^4 cells each) into *RAG2*$^{-/-}\gamma c^{-/-}$ mice, which lack all effector cells of the immune system, including NK cells (Goldman et al., 1998). We did not observe any differences in latency, survival, or disease morphology in livers, spleens, lymph nodes, or bone marrow from mice bearing either *STAT1*$^{+/-}$ or *STAT1*$^{-/-}$ leukemia (Figure 2C; p = not significant and data not shown).

Raising MHC class I levels restores the leukemogenicity of *STAT1*$^{-/-}$ cells

We reasoned that the decreased incidence and increased latency of leukemia induced by *STAT1*$^{-/-}$ cells is a direct

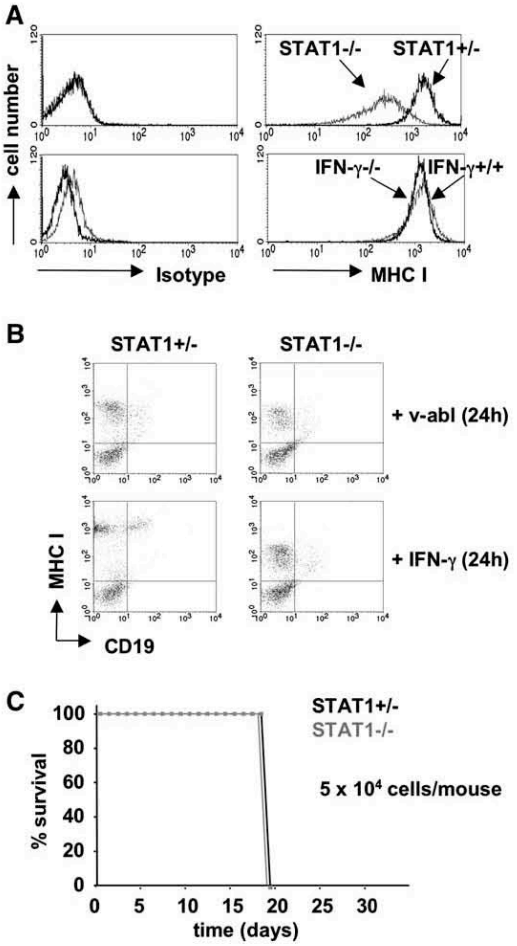

Figure 2. v-abl-transformed *STAT1*$^{-/-}$ cell lines express low levels of MHC class I

A: v-abl-transformed *STAT1*$^{+/-}$ and *STAT1*$^{-/-}$ as well as *IFN-γ*$^{+/+}$ and *IFN-γ*$^{-/-}$ cell lines were stained with isotype control (left panels) and α-H-2D^{d} (right panels).

B: *STAT1*$^{+/-}$ and *STAT1*$^{-/-}$ fetal liver cells were prepared and stained with antibodies against CD19 and MHC class I (H-2D^{d}). Prior to staining, the cells were infected with v-abl retrovirus (upper panel) or stimulated with IFN-γ (10 ng/ml, lower panel) for 24 hr.

C: Kaplan-Meier plot representing the survival of *RAG2*$^{-/-}$γc$^{-/-}$ mice (n = 5 each) injected with either *STAT1*$^{+/-}$ or *STAT1*$^{-/-}$ cells (v-abl-transformed, 5 × 10^{4} cells/mouse).

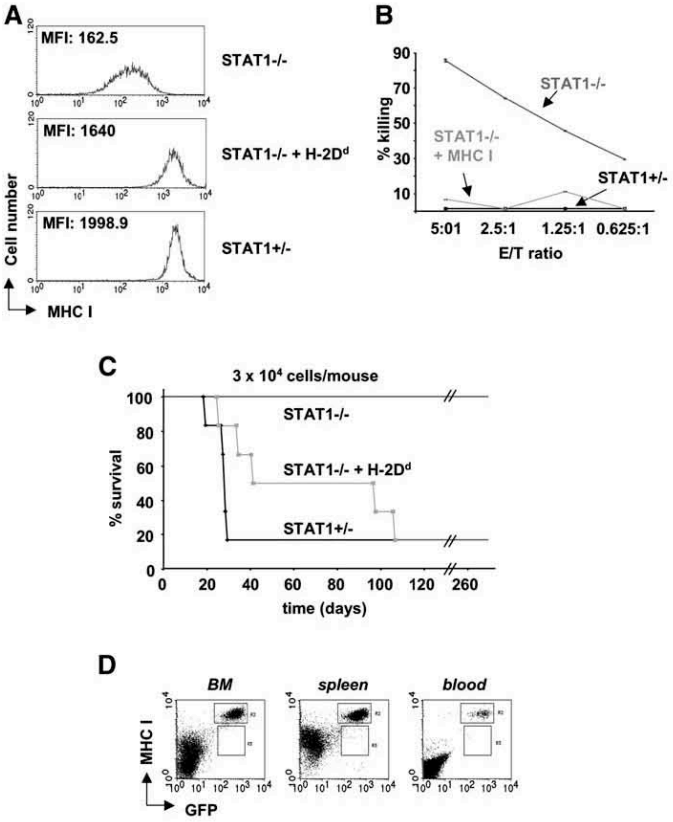

Figure 3. Overexpression of MHC class I in *STAT1*$^{-/-}$ cell lines increases the incidence and shortens the latency of leukemia

A: pMSCV-H-2D^{d}-IRESeGFP was transduced into a *STAT1*$^{-/-}$ cell line, and its expression was compared to the parental *STAT1*$^{-/-}$ and a *STAT1*$^{+/-}$ cell line infected with the empty retroviral construct by flow cytometry. The mean fluorescence intensity (MFI) of MHC class I is indicated in the panel. In parallel, cytotoxicity assays (**B**) were performed using wild-type NK cells as effectors. Data represent mean ± SD. Subsequently, cell lines were injected into *RAG2*$^{-/-}$ mice (n = 6 for each group), and leukemia development was observed over a time period of 300 days (**C**). Flow cytometry analysis of mice that had developed leukemia showed an infiltration of bone marrow (BM), spleen, and blood with tumor cells that were GFP^{+} and expressed high levels of MHC class I (**D**).

consequence of low expression of MHC class I, which allows for more efficient NK cell recognition. To test this, we overexpressed MHC class I (H-2D^{d}-IRES-GFP) in *STAT1*$^{-/-}$ leukemic cells (Figure 3A). As expected, *STAT1*$^{-/-}$ cells overexpressing H-2D^{d} could not be lysed efficiently by NK cells in an in vitro cytotoxicity assay (Figure 3B; $p < 0.001$ for *STAT1*$^{-/-}$ versus *STAT1*$^{+/-}$ and *STAT1*$^{-/-}$ versus *STAT1*$^{-/-}$ + MHC I; p = not significant for *STAT1*$^{+/-}$ versus *STAT1*$^{-/-}$ + MHC I). We selected one independently derived *STAT1*$^{-/-}$ cell line that expressed levels of H-2D^{d} comparable to *STAT1*$^{+/-}$ control cells. Forced expression of MHC class I did not alter cell proliferation or the response to proapoptotic stimuli (data not shown). Differences in survival are most readily detected if *RAG2*$^{-/-}$ mice are challenged with a low burden of tumor cells (Figure 1C). We therefore lowered the number of injected cells to 3 × 10^{4} cells/mouse. This burden of the parental *STAT1*$^{-/-}$ cell line was unable to inflict leukemia in *RAG2*$^{-/-}$ mice. In contrast, the cell line stably expressing MHC class I induced disease in 5/6 *RAG2*$^{-/-}$ mice, with a mean survival of 61.6 days. Transformed *STAT1*$^{+/-}$ cells were included as controls and also induced disease in 5/6 mice with a mean survival of 27.1 days (Figure 3C; p = 0.001). A second independently performed experiment using the same cell lines was repeated in *STAT1*$^{-/-}$ mice and confirmed this observation (Figure S3; p = 0.001). Analysis of the diseased animals revealed that the bone marrow, spleen, and blood were densely infiltrated with leukemic cells expressing high levels of H-2D^{d}, and these B cells were also positive for GFP (Figure 3D). These experiments define MHC class I expression on leukemic cells as a key determinant for the NK-mediated tumor surveillance.

Unrejected *STAT1*$^{-/-}$ leukemic cells have an "edited" phenotype

Tumor cells can evade the selective pressure of the adaptive immune system by downregulating MHC class I expression on their cell surface (Garcia-Lora et al., 2003; Karre et al., 1986;

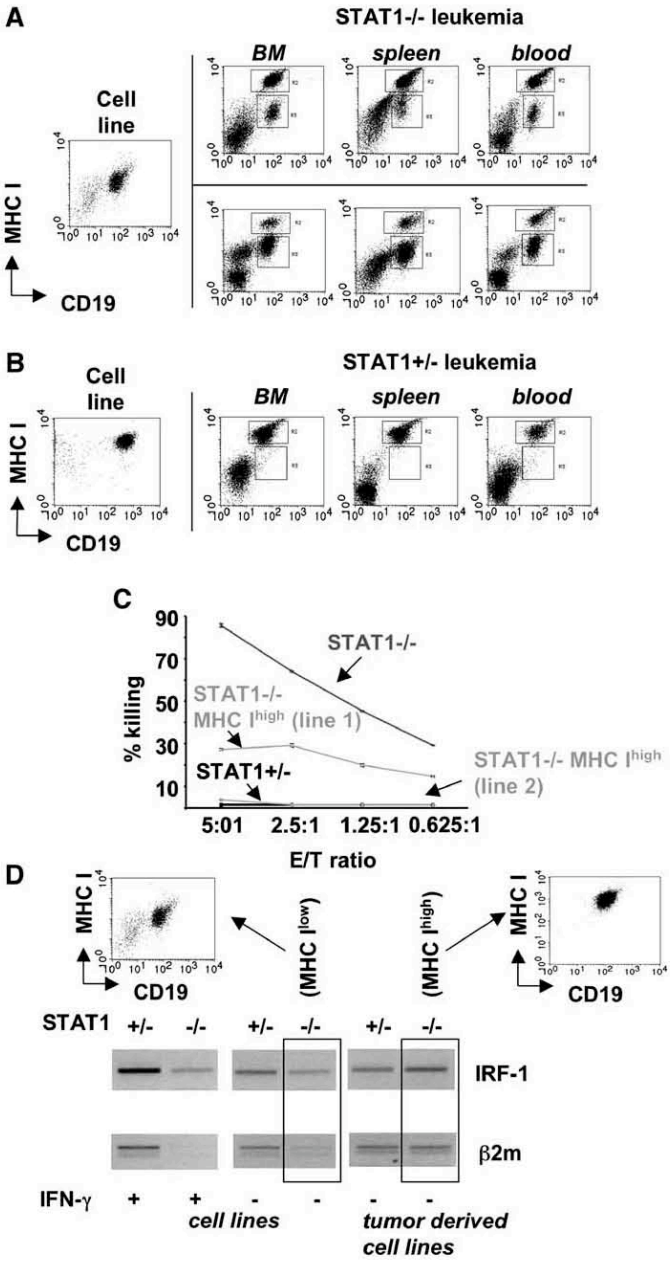

Figure 4. MHC class I upregulation in *STAT1*$^{-/-}$ tumor cells occurs as a consequence of immunoediting

A and B: V-abl-transformed *STAT1*$^{-/-}$ (**A**) and *STAT1*$^{+/-}$ (**B**) cell lines (5×10^4 cells/mouse) were injected into six *RAG2*$^{-/-}$ mice each. Tumor development was observed for 6 months. Expression of CD19 and MHC class I was assessed in the cell lines by flow cytometry prior to injection (left panels), as well as in bone marrow (BM), spleen, and blood of mice that had developed leukemia (right panels). Two representative examples for *STAT1*$^{-/-}$-induced leukemia (**A**) and one representative example for *STAT1*$^{+/-}$-induced leukemia (**B**) are depicted.

C: Cytotoxicity assays were performed using wild-type NK cells and two ex vivo derived *STAT1*$^{-/-}$ cell lines with high MHC class I expression, and *STAT1*$^{+/-}$ and *STAT1*$^{-/-}$ cell lines as control. Data represent mean ± SD.

D: Analysis of transcriptional expression of IRF-1 and β2-microglobulin (β2m) genes by semiquantitative RT-PCR. One representative *STAT1*$^{+/-}$ and *STAT1*$^{-/-}$ cell line and their corresponding tumor-derived cell lines were analyzed for the expression of IRF-1 and β2m mRNA (middle and right panel). As a control for expression of IRF-1 and β2m, cells were stimulated with 10 ng/ml IFN-γ for 2 hr (left panel). MHC class I^{low} corresponds to the in vitro derived *STAT1*$^{-/-}$ parental cell line, whereas MHC class I^{high} corresponds to the tumor-derived *STAT1*$^{-/-}$ cell line.

Mocikat et al., 2003; Smyth et al., 2002). We speculated that the opposite might occur in tumors that are predominantly eradicated by NK cells: tumors may escape the immune system by upregulating MHC class I molecules on their cell surface. This conjecture would also explain why, in *RAG2*$^{-/-}$ mice, *STAT1*$^{-/-}$ cells are not entirely cleared by the immune system and eventually succeed in inducing leukemia.

This hypothesis was verified by using the following approach: four individual *STAT1*$^{-/-}$ and three individual *STAT1*$^{+/-}$ cell lines (10^5 cells each) were injected into *RAG2*$^{-/-}$ mice (n = 12 each). The MHC class I expression of these cells was determined prior to injection and compared to the MHC class I levels on leukemic cells arising in bone marrow, spleen, and peripheral blood from diseased *RAG2*$^{-/-}$ mice.

As depicted in Figure 4A, in all mice (n = 12) that had received *STAT1*$^{-/-}$ transformed cells, a cell population emerged that was CD19^{+} and that expressed increased levels of MHC class I. This cell population was detected in peripheral blood, bone marrow, and spleen of the diseased *RAG2*$^{-/-}$ mice. In vitro cytotoxicity assays confirmed that the cells expressing high levels of MHC class I were either not killed or killed in fewer numbers by purified NK cells when compared to the parental cell line (Figure 4C, $p < 0.001$ for *STAT1*$^{-/-}$ versus *STAT1*$^{+/-}$, *STAT1*$^{-/-}$ versus *STAT1*$^{-/-}$ MHC I^{high} line 1, and *STAT1*$^{-/-}$ versus *STAT1*$^{-/-}$ MHC I^{high} line 2; $p = 0.01$ for *STAT1*$^{+/-}$ versus *STAT1*$^{-/-}$ MHC I^{high} line 1; p = not significant for *STAT1*$^{+/-}$ versus *STAT1*$^{-/-}$ MHC I^{high} line 2). In contrast, none of the transplanted *RAG2*$^{-/-}$ mice (n = 12) that had received *STAT1*$^{+/-}$ tumor cells displayed this phenomenon (Figure 4B). Most importantly, if the tumor-derived *STAT1*$^{-/-}$ cells were propagated in vitro, they retained the expression of high levels of MHC class I even after long cultivation periods (>2 months; Figure 4D). This allowed us to explore the underlying molecular mechanisms, which resulted in an increased MHC class I expression. We concentrated on the proposed regulatory factors implicated in the regulation of gene expression of the MHC class I protein complex and on the processing mechanism leading to their surface expression (Gobin et al., 2003; Hobart et al., 1997; Lee et al., 1999). When compared to their parental cell lines, MHC class I^{high} cells consistently expressed higher levels of the transcription factor IRF-1 and β_2-microglobulin (β2m) (Figure 4D). In contrast, we did not observe any alterations in the levels of LMP-2, LMP-7, TAP-1, CIITA, or SOCS-1 mRNAs (data not shown).

Taken together, these experiments prove that selective pressure of the innate immune system enables the upregulation of MHC class I expression by increasing the IRF-1 and β_2-microglobulin mRNA expression. The importance of this phenomenon is underlined by the fact that it occurred in all (12/12) *RAG2*$^{-/-}$ mice investigated.

STAT1$^{-/-}$ mice are partially protected from leukemia formation

Previous experiments revealed a reduced cytotoxic capacity of *STAT1*$^{-/-}$ NK cells (Lee et al., 2000a). It was therefore questionable whether the impaired cytotoxic ability of *STAT1*$^{-/-}$ NK cells

sufficed to kill leukemic cells and whether that sufficiently eradicated tumor cells arising in *STAT1*$^{-/-}$ mice (which bear *STAT1*$^{-/-}$ NK cells). These questions were addressed by the following experiments: we first confirmed that *STAT1*$^{-/-}$ cells have an impaired cytotoxic capacity by using purified and in vitro amplified NK cells as effectors and YAC-1 cells as target cells (data not shown). YAC-1 cells represent optimal target cells because of their low MHC class I levels. However, they may behave differently from transformed B-lymphoid cells. Therefore, we used v-abl-transformed cell lines as targets. *STAT1*$^{+/-}$ and *STAT1*$^{-/-}$ NK cells were tested for their ability to lyse *STAT1*$^{+/-}$ or *STAT1*$^{-/-}$ tumor cells in any possible combination. *STAT1*$^{+/-}$ tumor cells were not killed by NK cells, irrespective of their genotype (Figure 5A; $p < 0.001$ for *STAT1*$^{+/-}$ NK cells killing *STAT1*$^{-/-}$ versus *STAT1*$^{+/-}$ NK cells killing *STAT1*$^{+/-}$ targets and for *STAT1*$^{-/-}$ NK cells killing *STAT1*$^{-/-}$ versus *STAT1*$^{-/-}$ NK cells killing *STAT1*$^{+/-}$ targets; p = not significant for *STAT1*$^{+/-}$ targets versus *STAT1*$^{+/-}$ or *STAT1*$^{-/-}$ NK cells). In contrast, *STAT1*$^{-/-}$ tumor cells were efficiently recognized and lysed by NK cells of both genotypes. *STAT1*$^{+/-}$ NK cells efficiently eradicated *STAT1*$^{-/-}$ leukemic cells, but they were unable to eradicate leukemic cells of their own genotype. However, in spite of their reduced cytotoxic capacity, *STAT1*$^{-/-}$ NK cells were still able to recognize and eliminate *STAT1*$^{-/-}$ tumor cell targets (Figure 5A).

Infection of newborn BALB/c mice with a retrovirus encoding for v-abl results in onset of B-lymphoid leukemia/lymphoma within weeks. The inflicted disease is mono- or oligoclonal and evolves slowly, allowing the immune system to take corrective action. To ask whether the absence of STAT1 in the tumor or the absence of STAT1 in NK cells contributed to leukemia development in vivo, we performed infections in wild-type and *STAT1*$^{-/-}$ mice. To ensure appropriate littermate controls, *STAT1*$^{+/-}$ and *STAT1*$^{-/-}$ mice were intercrossed and the offspring injected with retrovirus within 24 hr after birth. All 11 *STAT1*$^{+/-}$ mice (100%) died from leukemia within 5 weeks, whereas 6/28 (21%) of the injected *STAT1*$^{-/-}$ mice remained healthy and disease-free for more than 8 months despite the oncogenic challenge (Figure 5B; $p < 0.001$). Twenty-two out of twenty-eight *STAT1*$^{-/-}$ animals developed leukemia, and in these animals the disease latency was increased and the signs of disease were mitigated (decreased white blood cell counts, reduced tumor cell infiltrations in liver, spleen, and bone marrow) compared to those in *STAT1*$^{+/-}$ littermate controls (Figure 5B).

Our model predicts that the leukemia that eventually arises in *STAT1*$^{-/-}$ mice is accompanied by an upregulation of MHC class I during the development of disease. As expected, MHC class I surface expression on leukemic cells infiltrating bone marrow, spleen, and forming tumors was highly increased compared to nonleukemic (CD19-negative) cells of the same tissue (Figure 5D).

STAT1$^{-/-}$ animals have been repeatedly used to study the effects of IFN-γ in tumor surveillance (Kaplan et al., 1998; Shankaran et al., 2001). However, transformed *IFN-γ*$^{-/-}$ and *STAT1*$^{-/-}$ B-lymphoid cells differ substantially in MHC class I expression. Thus, infection of newborn *IFN-γ*$^{-/-}$ mice with v-abl retrovirus is predicted to result in an opposite phenotype, that is, aggravated disease. As depicted in Figure 5E, 40% of the wild-type control C57BL/6 mice remained disease-free (this is the expected result for this genetic background), whereas

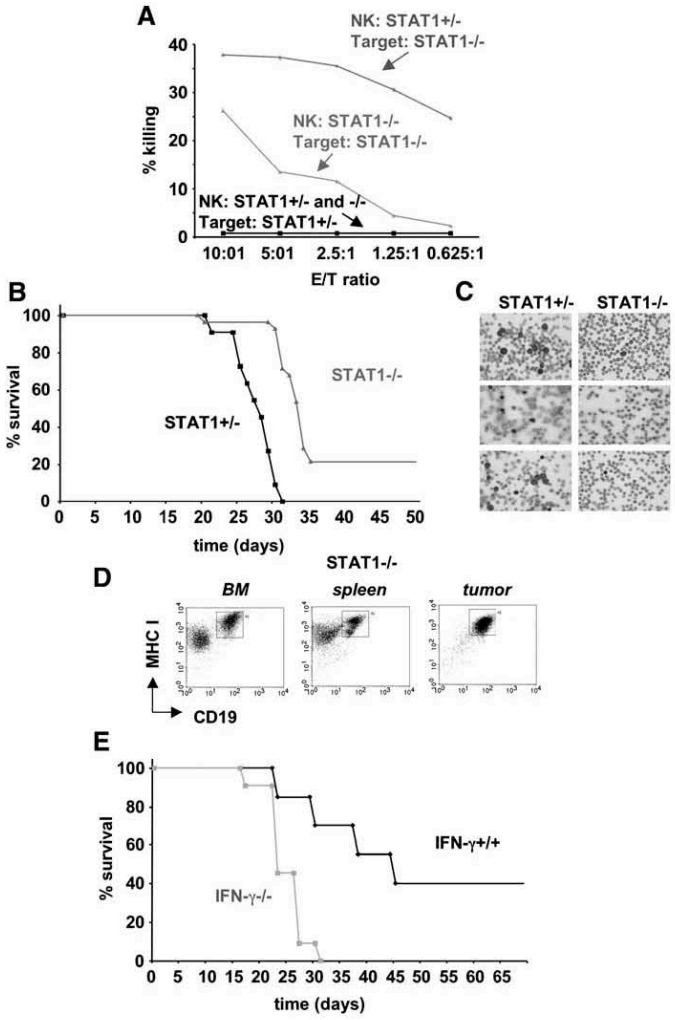

Figure 5. Decreased leukemia formation in *STAT1*$^{-/-}$ mice after V-abl challenge

A: Cytotoxicity assays were performed with purified NK cells from *STAT1*$^{+/-}$ and *STAT1*$^{-/-}$ mice as effector cells and *STAT1*$^{+/-}$ and *STAT1*$^{-/-}$ v-abl-transformed cell lines as target population. Data represent mean ± SD.

B: Kaplan-Meier plot indicating survival of the littermate progeny from a *STAT1*$^{+/-}$ × *STAT1*$^{-/-}$ intercross infected with v-abl retrovirus. Survivors were followed up over a period of 8 months for leukemia development (n = 11 for *STAT1*$^{+/-}$ and n = 28 for *STAT1*$^{-/-}$).

C: Representative hematoxylin/eosin-stained blood smears from three mice of each group are shown (magnification: ×100).

D: Expression of CD19 and MHC class I was assessed by flow cytometry in bone marrow (BM), spleen, and a tumor from one representative *STAT1*$^{-/-}$ mouse, which rapidly developed leukemia. An upregulation is observed for MHC class I in the leukemic cells compared to nonleukemic cells.

E: Kaplan-Meier plot of *IFN-γ*$^{+/+}$ and *IFN-γ*$^{-/-}$ mice after v-*abl* retrovirus challenge (n = 13 for *IFN-γ*$^{+/+}$ and n = 11 for *IFN-γ*$^{-/-}$).

100% of the *IFN-γ*$^{-/-}$ mice succumbed to a rapidly progressing leukemia within 4 weeks ($p < 0.0001$). We want to stress that the disease latency of *STAT1*$^{-/-}$ and *IFN-γ*$^{-/-}$ animals cannot be directly compared because the animals differ in their genetic background (see Experimental Procedures). These experiments confirm the important role of IFN-γ for tumor surveillance. More importantly, we stress that STAT1 and IFN-γ deficiency cannot be superimposed in the case of tumors predominantly eradicated by NK cells.

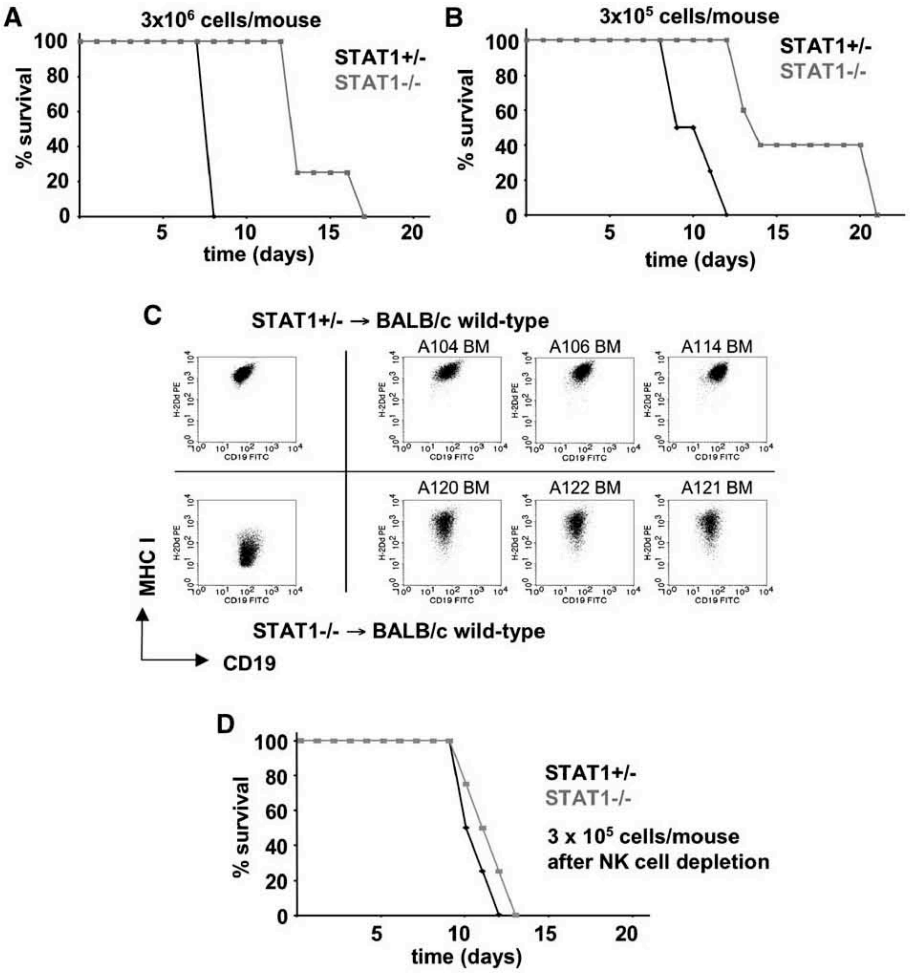

Figure 6. Low tumorigenicity of *STAT1*$^{-/-}$ leukemic cells in immunocompetent mice

A and B: Kaplan-Meier plots indicating survival of immunocompetent BALB/c mice bearing either *STAT1*$^{+/-}$ or *STAT1*$^{-/-}$ leukemia. Two different cell numbers (3×10^6 [**A**] cells and 3×10^5 [**B**] cells of each genotype) were injected into wild-type BALB/c mice (n = 10 per genotype and cell amount used).

C: Flow-cytometric analysis of CD19 and MHC class I expression in the cell lines used for injection (left panel) and in the bone marrow (BM) from three representative mice each that had developed leukemia upon injection of *STAT1*$^{+/-}$ and *STAT1*$^{-/-}$ cells (numbers on top of the scatter plot identify the individual mouse).

D: Kaplan-Meier plots of immunocompetent BALB/c mice injected with either *STAT1*$^{+/-}$ or *STAT1*$^{-/-}$ leukemic cells after depletion of NK cells with α-asialo GM1.

Loss of STAT1 delays disease progression in immunocompetent animals and in TEL-JAK2 leukemic mice

Our data show the central role of STAT1 during leukemia development in maintaining high expression levels of MHC class I. However, both *RAG2*$^{-/-}$ and *STAT1*$^{-/-}$ mice do have an impaired immune system. We therefore investigated disease progression inflicted by *STAT1*$^{-/-}$ and *STAT1*$^{+/-}$ leukemic cells in immunocompetent hosts (BALB/c animals). This experimental setup mimics the situation in human patients, where a loss of STAT1 can be found in leukemic cells (Irish et al., 2004; Landolfo et al., 2000; Sun et al., 1998).

We transplanted *STAT1*$^{+/+}$ or *STAT1*$^{-/-}$ v-abl-transformed cells at different numbers into syngeneic immunocompetent BALB/c (wild-type) mice. As depicted in Figures 6A and 6B, wild-type mice that had received *STAT1*$^{-/-}$ tumor cells showed an increased latency of disease—irrespective of the injected cell number ($p < 0.01$ and $p < 0.005$). *STAT1*$^{-/-}$ leukemic cells were isolated from the diseased mice and again showed a significant increase in MHC class I expression (Figure 6C). Depletion of NK cells by repeated injections of α-asialo GM1 antibody in wild-type mice abolished the differences in disease latency (Figure 6D; p = not significant). Together, these experiments prove that STAT1 also plays a crucial role as a tumor promoter in the context of an intact immune system by interfering with NK cell-mediated tumor lysis.

V-abl-induced B-lymphoid leukemia may represent a specific challenge to the immune system, and the observations summarized above may therefore be of limited importance. In order to document that they reflect a more general mechanism of tumor escape in hematopoietic malignancies, we chose MPD induced by constitutively active JAK2 as a second independent leukemia model. Bone marrow cells of wild-type and *STAT1*$^{-/-}$ BALB/c mice were infected with a retrovirus encoding the TEL/JAK2 fusion protein (Schwaller et al., 1998). Infection rates were controlled by FACS and were found to be comparable (around 5%) at the time point of injection. The cells were transplanted into five wild-type recipients each. All mice were analyzed 3 months after injection. At this time point, the first mice that had been injected with *STAT1*$^{+/-}$ bone marrow were obviously sick and displayed elevated red blood cell counts accompanied by thrombocytosis, granulocytosis, and splenomegaly (James et al., 2005; Kralovics et al., 2005; Levine et al., 2005). The hematocrit values as well as the numbers of granulocytes were significantly lower in mice that had been injected with STAT1-deficient cells than in those injected with STAT1-expressing cells (Figure 7A; $p < 0.001$ and data not shown). MPD is characterized by aberrations in early hematopoietic progenitors. As indicated in the upper panels of Figure 7B, erythroid precursor cell numbers (P2/P3/P4/P5 regions) were elevated 3-fold in mice that had been injected with TEL/JAK2-infected *STAT1*$^{+/-}$ bone marrow compared to TEL/JAK2-infected *STAT1*$^{-/-}$ bone marrow

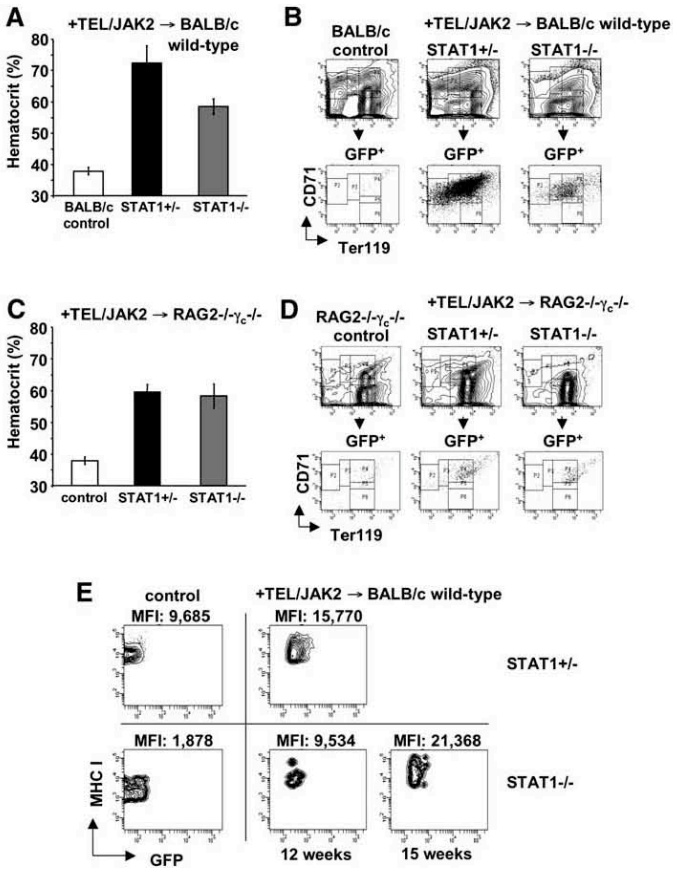

Figure 7. Low tumorigenicity of STAT1-deficient TEL/JAK2-induced MPD in immunocompetent mice

Mean hematocrit values from peripheral blood of immunocompetent (**A**) and immunodeficient (**C**) mice injected with TEL/JAK2-transduced *STAT1*$^{+/-}$ or *STAT1*$^{-/-}$ bone marrow cells and mice injected with PBS were analyzed after 3 months (n = 10/genotype/cell amount). Data represent mean ± SD. Flow-cytometric analysis of the erythroid compartment (CD71 and TER119) in the spleens from one representative PBS-injected, one *STAT1*$^{+/-}$-injected, and one *STAT1*$^{-/-}$-injected immunocompetent (**B**) and immunodeficient (**D**) mouse (upper panel). Distribution of GFP$^+$ cells in different stages of erythroid development is indicated in the lower panel. **E:** Flow-cytometric analysis of MHC class I expression and its mean fluorescence intensity (MFI). MHC class I expression in the spleen of wild-type mice prior to infection with the TEL/JAK2 oncogene (left panels). Representative examples of GFP$^+$ erythroid precursor cells were isolated from spleens 3 months after transplantation (right panels). Tumor editing is documented by the increase in MHC class I expression, which is confined to the *STAT1*$^{-/-}$ cells and progressive with time (bottom row, panels labeled 12 and 15 weeks).

(20.5% ± 1.1% versus 8.2% ± 0.4%, respectively; $p < 0.01$). This difference was even more pronounced with respect to the amount of GFP$^+$ cells. Whereas 31.4% ± 5.1% of erythroid precursor cells were GFP$^+$ in mice injected with wild-type TEL/JAK2-infected cells, only 3.7% ± 2.1% GFP$^+$ cells were observed in mice injected with *STAT1*$^{-/-}$ TEL/JAK2-infected cells ($p < 0.001$; Figure 7B, lower panels). This experiment was repeated using *RAG2*$^{-/-}\gamma c^{-/-}$ mice as recipients. In this setting, no differences in disease latency or hematocrit values were detected (Figure 7C), and the total amounts of erythroid precursors (20.2% ± 4.7% and 21.7% ± 7.0% in regions P2–P5 for *STAT1*$^{+/-}$ and *STAT1*$^{-/-}$ cells, respectively; p = not significant) and GFP$^+$ cells (8.95% ± 2.35% and 7.65% ± 3.65% in regions P2–P5 for *STAT1*$^{+/-}$ and *STAT1*$^{-/-}$ cells, respectively; p = not significant) in the spleens were comparable (Figure 7D). This experiment rules out that the lack of STAT1 within the tumor cells accounts for the differences observed in wild-type mice.

Again, in wild-type mice, the *STAT1*$^{-/-}$ GFP$^+$ erythroid precursor cells expressed significantly higher MHC class I levels compared to noninfected cells, indicating that the cells had undergone an "editing" process (Figure 7E) as observed for v-abl-induced B-lymphoid leukemia. The tumor editing of MHC class I was first observed 3 months after injection of *STAT1*$^{-/-}$ cells and was more pronounced 3 weeks thereafter (Figure 7E, middle and right panels). Thus, this experiment faithfully recapitulated the observations made in v-abl-induced B-lymphoid leukemia and confirms the hitherto unappreciated tumor-promoting role of STAT1 in hematopoietic malignancies.

Discussion

The absence of STAT1 is generally thought to be detrimental because it allows for more rapid tumor progression (Badgwell et al., 2004; Lee et al., 2000b; Lesinski et al., 2003; Nishibori et al., 2004; Refaeli et al., 2002). Thus, the presence of STAT1 protects against tumor development, and therefore the molecule is considered a tumor suppressor. The tumor-suppressing effect of STAT1 is consistent with the in vitro effects on v-abl-induced transformation; *STAT1*$^{-/-}$ cells gave rise to increased numbers of growth factor-independent colonies. This observation is in strong contrast with leukemia development in the mouse. We show here that the presence of STAT1 accelerates leukemia progression in vivo. This paradox can only be understood if immune surveillance is taken into account. Transformed *STAT1*$^{-/-}$ cells were efficiently eliminated in immunodeficient *RAG2*$^{-/-}$ mice by NK cells. The role for NK cell-mediated tumor surveillance was further substantiated in NK cell depletion studies that abolished the differences between *STAT1*$^{-/-}$ and *STAT1*$^{+/-}$ leukemic cells and accelerated disease onset. *STAT1*$^{-/-}$ mice were also more resistant to challenge with the v-abl oncogene, succumbed to the disease with a decreased incidence, and had an increased chance of survival. Moreover, using models for leukemia and MPD, we documented that the presence of STAT1 in a tumor was also detrimental in the context of an intact immune system.

Our observations demonstrate that tumor progression and tumor evolution can only be understood if the tumor is studied within the context of an intact organism. It has been recently appreciated that STAT1 supports expression of MHC class I molecules (Kamiya et al., 2004; Lee et al., 1999; Lieberman et al., 2004). Quite predictably, we observed that loss of STAT1 resulted in low expression of MHC class I molecules. Several arguments support the conclusion that there is a relation between MHC class I levels on the tumor cells and their ability to evade immunosurveillance by NK cells. (1) If MHC class I levels were raised using a viral promoter, STAT1-deficient tumor cells were rendered resistant to immunosurveillance. These cells were not cleared by the innate immune system of *RAG2*$^{-/-}$ mice and gave rise to a leukemic disease that progressed almost as rapidly as that induced by STAT1-expressing cells. This observation is consistent with the proposed model that B-lymphoid malignancies are predominantly under surveillance by NK cells (Cerwenka et al., 2000; Stoiber et al., 2004; Street et al., 2004). (2) The natural course of the disease allowed for escape of STAT1-deficient tumor cells from immunosurveillance.

This escape was consistently accompanied by the upregulation of MHC class I levels in all cases where injected *STAT1*$^{-/-}$ tumor cells eventually gave rise to B-lymphoid leukemia and MPD. (3) Finally, tumor evolution was associated with increased levels of β2-microglobulin, the dimeric partner of MHC class I (Gobin et al., 2003; Lee et al., 1999), and their common upstream regulator IRF-1 (Hobart et al., 1997). In all tumors that arose from transformed *STAT1*$^{-/-}$ cells, their MHC class I levels substantially exceeded those seen in the parental cell line and approached the levels observed in STAT1-expressing cells. Taken together, these data are consistent with a model where high MHC class I levels protect the tumor cells from elimination by NK cells (Cerwenka and Lanier, 2001; Colucci et al., 2003; Karre et al., 1986; Mocikat et al., 2003; Smyth et al., 2002).

When the concept of cancer immunoediting was originally introduced, the focus was placed on the evolutionary arms race between the tumor cell and the acquired immune system, that is, T and B cells (Shankaran et al., 2001). Very recently, the theoretical framework was expanded by the observation that lymphomas are subject to immunosurveillance by the innate immune system (Street et al., 2004). In the present work, we demonstrate that the evolutionary pressure exerted by NK cells sculpts and edits the leukemic tumor cells in a predictable manner. Under these conditions, upregulation of MHC class I molecules is the mechanism that allows for escape (Cerwenka and Lanier, 2001; Colucci et al., 2003; Karre et al., 1986; Mocikat et al., 2003; Smyth et al., 2002). Accordingly, in immunocompetent and immunodeficient mice, STAT1-expressing tumor cells gave rise to highly aggressive disease because they could not be cleared by NK cells. Likewise, the evolutionary arms race was readily evident, if STAT1-deficient tumor cells were injected: the tumor cells eventually overcame their defect by bypassing the STAT1-dependent regulation of MHC class I. This upregulation was stable—as seen by the fact that *STAT1*$^{-/-}$ tumors maintained high MHC class I levels after long cultivation periods (ex vivo)—and resulted in a concerted upregulation of β2-microglobulin and IRF-1. Thus, the mechanistic possibilities of a STAT1-independent regulation of MHC class I are diverse and may exceed a simple gain-of-function mutation.

Phenotypically, the disease inflicted by transplanting *STAT1*$^{-/-}$ v-abl-transformed cells into immunodeficient mice was similar to that induced in STAT1-deficient animals. The same effect was also observed in disease phenotypes caused by transplanting either *STAT1*$^{-/-}$ leukemia or *STAT1*$^{-/-}$ MPD in immunocompetent hosts. In other words, irrespective of the model system used, *STAT1*$^{-/-}$ transformed cells either were easily rejected, had increased latencies, developed more moderate forms of malignancies, or gave rise to tumors only after acquiring an "edited" phenotype, which manifested itself in an increase of MHC class I.

The concept of cancer immunoediting is based on the following predictions: the tumor can be eliminated by the immune system, and the tumor cells are sculpted by the immune system and may escape by Darwinian evolution. Our study verifies the predictions of this concept, supporting its general applicability. The role of IFN-γ and its signaling component STAT1, however, has to be reevaluated. While IFN-γ acts like a potent tumor suppressor, this role cannot be generally attributed to STAT1. In fact, the phenotypes observed in IFN-γ- and STAT1-deficient mice are diametrically opposed.

MHC class I-mediated killing by NK cells has been extensively investigated in various tumors. This concept is therefore well documented and understood in considerable detail. Hence, there is substantial circumstantial evidence from this earlier work that is in line with our model that STAT1 acts as a tumor promoter in leukemia and MPDs or, conversely, that a lack of STAT1 and low MHC class I expression protects the organism from hematopoietic malignancies. In light of this finding, our work may provide the basis for novel therapeutic approaches, using concerted inhibition of STAT1 and MHC class I.

Experimental procedures

Animals

BALB/cJ (BALB/c) *STAT1*$^{-/-}$ mice, C57BL/6J (C57BL/6) *IFN-γ*$^{-/-}$ mice, *RAG2*$^{-/-}$ mice, *RAG2*$^{-/-}$γc$^{-/-}$ mice, and wild-type BALB/c mice were maintained at the Biomedical Research Institute, Medical University of Vienna, Research Institute of Molecular Pathology, IMP, Vienna. All animal experiments were carried out in accordance with protocols approved by the Animal Welfare Committee and with the general regulations specified by the Good Scientific Practices guidelines of the Medical University of Vienna.

Mouse experiments

Each transplantation experiment was repeated at least in an additional independent experiment, and the observations were consistently reproducible. In detail, cells from six independently derived *STAT1*$^{+/-}$ and six *STAT1*$^{-/-}$ cell lines were injected into *RAG2*$^{-/-}$ mice (n = 40 in total) and *RAG2*$^{-/-}$γc$^{-/-}$ mice (n = 10 in total). For MHC class I (H-2D^{d}) reconstitution, *STAT1*$^{-/-}$ (parental cell line), *STAT1*$^{-/-}$ + H2D^{d}, and *STAT1*$^{+/-}$ (parental cell line) cells were injected into *RAG2*$^{-/-}$ mice (n = 18 in total), *STAT1*$^{-/-}$ mice (n = 18 in total), and wild-type BALB/c mice (n = 18 in total). For transplantation into immunocompetent mice, *STAT1*$^{+/-}$ and *STAT1*$^{-/-}$ leukemic cell lines were injected at different cell numbers (3×10^6 and 3×10^5) into syngeneic BALB/c recipients (n = 60 in total). For TEL/JAK2-induced experiments, bone marrow from *STAT1*$^{+/-}$ and *STAT1*$^{-/-}$ mice was transduced with pMSCV-TEL/JAK2-IRES-GFP-derived retrovirus and cultured as described earlier (Moriggl et al., 2005) prior to injection into syngeneic BALB/c mice (n = 20 in total) or *RAG2*$^{-/-}$γc$^{-/-}$ mice (n = 12 in total). For NK depletion experiments, wild-type BALB/c mice (n = 8 in total) were treated (i.p.) with α-asialo GM1 (WAKO, Japan) on days −4, 0, and 7 of tumor cell injection. For short-term homing experiments CFSE-labeled *STAT1*$^{+/-}$ and *STAT1*$^{-/-}$ cell lines were injected into wild-type (n = 8) or *RAG2*$^{-/-}$ mice (n = 8) and analyzed 4 days after injection. For newborn infection experiments, mice were injected intraperitoneally with 50 μl of replication incompetent ecotropic retrovirus encoding for v-abl.

Flow cytometry

Single-cell suspensions were preincubated with αCD16/CD32 antibodies (BD/Pharmingen) to prevent nonspecific Fc receptor-mediated binding. Cells (5×10^5) were stained with monoclonal antibodies conjugated with fluorescent markers and analyzed on FACScan and FACScanto (Beckton-Dickinson) with CellQuestPro and Facs Diva software. The antibodies used for lineage determination included the B cell lineage markers B220 (RA3-6B2), CD19 (1D3), and CD43 (1B11); the T cell marker CD3 (17A2); the pan-NK marker (DX5); and the erythroid lineage markers CD71 (C2) and TER119 (Ter119) (all BD/Pharmingen). In addition, an antibody against MHC class I (H-2Dd, clone 34-5-8S, BD/Pharmingen) was used. For cell cycle analysis, the cells were fixed in a buffer containing 0.05 mg/ml propidium iodide, 0.01% Triton X-100, and 0.1% sodium citrate.

Cytotoxicity assay

The YAC-1 cell line and fetal liver-derived *STAT1*$^{+/-}$, *STAT1*$^{-/-}$, and *STAT1*$^{-/-}$ + H-2D^{d} cell lines as well as tumor-derived *STAT1*$^{-/-}$ MHC I^{high} cells were used as target cells. DX5^{+} purified splenocytes were used as effector cells after 10 days of culture in h-IL-2 (5000 U/ml). Lactate dehydrogenase (LDH) release was measured as described using the CytoTox 96 Non-Radioactive Cytotoxicity Assay (Promega).

Statistical analysis

Statistics were carried out using Student's t test and the χ^2 test as appropriate. Kaplan-Meier plots were analyzed for statistical significance using the

log-rank test. Cytotoxicity assays were analyzed by the ANOVA test with Tukey's post hoc test for every E/T ratio.

Additional information regarding analysis of mice, RT-PCRs, tissue culture conditions, transformation, and proliferation assays is available within the Supplemental Data.

Supplemental data

The Supplemental Data include Supplemental Experimental Procedures and four supplemental figures and can be found with this article online at http://www.cancercell.org/cgi/content/full/10/1/77/DC1/.

Acknowledgments

This work was supported by grants P15033, P15865, and SFB 28 from FWF (Fonds zur Förderung der wissenschaftlichen Forschung). The authors thank Udo Losert and the staff of the Biomedical Research Institute, Medical University of Vienna (MUW) for taking care of mice. We are grateful to Peter Valent, Christian Sillaber, Mathias Müller, and Thomas Decker for helpful discussions in the course of this work. We also thank the staff of the Department of Neuro-Immunology, Center for Brain Research, MUW, for help with histopathology. We also thank the Austrian Academy of Sciences (OeAW) for the financial support to R.G.O. (DOC-Stipendium).

Received: September 27, 2005
Revised: March 11, 2006
Accepted: May 22, 2006
Published: July 17, 2006

References

Abelson, H.T., and Rabstein, L.S. (1970). Influence of prednisolone on Moloney leukemogenic virus in BALB-c mice. Cancer Res. *30*, 2208–2212.

Agrawal, S., Agarwal, M.L., Chatterjee-Kishore, M., Stark, G.R., and Chisolm, G.M. (2002). Stat1-dependent, p53-independent expression of p21(waf1) modulates oxysterol-induced apoptosis. Mol. Cell. Biol. *22*, 1981–1992.

Badgwell, B., Lesinski, G.B., Magro, C., Abood, G., Skaf, A., and Carson, W., III. (2004). The antitumor effects of interferon-alpha are maintained in mice challenged with a STAT1-deficient murine melanoma cell line. J. Surg. Res. *116*, 129–136.

Bromberg, J., and Darnell, J.E., Jr. (2000). The role of STATs in transcriptional control and their impact on cellular function. Oncogene *19*, 2468–2473.

Carron, C., Cormier, F., Janin, A., Lacronique, V., Giovannini, M., Daniel, M.T., Bernard, O., and Ghysdael, J. (2000). TEL-JAK2 transgenic mice develop T-cell leukemia. Blood *95*, 3891–3899.

Cerwenka, A., and Lanier, L.L. (2001). Natural killer cells, viruses and cancer. Nat. Rev. Immunol. *1*, 41–49.

Cerwenka, A., Bakker, A.B., McClanahan, T., Wagner, J., Wu, J., Phillips, J.H., and Lanier, L.L. (2000). Retinoic acid early inducible genes define a ligand family for the activating NKG2D receptor in mice. Immunity *12*, 721–727.

Colucci, F., Caligiuri, M.A., and Di Santo, J.P. (2003). What does it take to make a natural killer? Nat. Rev. Immunol. *3*, 413–425.

Dalton, D.K., Pitts-Meek, S., Keshav, S., Figari, I.S., Bradley, A., and Stewart, T.A. (1993). Multiple defects of immune cell function in mice with disrupted interferon-gamma genes. Science *259*, 1739–1742.

Dunn, G.P., Bruce, A.T., Ikeda, H., Old, L.J., and Schreiber, R.D. (2002). Cancer immunoediting: from immunosurveillance to tumor escape. Nat. Immunol. *3*, 991–998.

Dunn, G.P., Old, L.J., and Schreiber, R.D. (2004). The three Es of cancer immunoediting. Annu. Rev. Immunol. *22*, 329–360.

Durbin, J.E., Hackenmiller, R., Simon, M.C., and Levy, D.E. (1996). Targeted disruption of the mouse Stat1 gene results in compromised innate immunity to viral disease. Cell *84*, 443–450.

Fallarino, F., and Gajewski, T.F. (1999). Cutting edge: differentiation of antitumor CTL in vivo requires host expression of Stat1. J. Immunol. *163*, 4109–4113.

Garcia-Lora, A., Martinez, M., Algarra, I., Gaforio, J.J., and Garrido, F. (2003). MHC class I-deficient metastatic tumor variants immunoselected by T lymphocytes originate from the coordinated downregulation of APM components. Int. J. Cancer *106*, 521–527.

Gobin, S.J., Biesta, P., and Van den Elsen, P.J. (2003). Regulation of human beta 2-microglobulin transactivation in hematopoietic cells. Blood *101*, 3058–3064.

Goldman, J.P., Blundell, M.P., Lopes, L., Kinnon, C., Di Santo, J.P., and Thrasher, A.J. (1998). Enhanced human cell engraftment in mice deficient in RAG2 and the common cytokine receptor gamma chain. Br. J. Haematol. *103*, 335–342.

Hobart, M., Ramassar, V., Goes, N., Urmson, J., and Halloran, P.F. (1997). IFN regulatory factor-1 plays a central role in the regulation of the expression of class I and II MHC genes in vivo. J. Immunol. *158*, 4260–4269.

Ikeda, H., Old, L.J., and Schreiber, R.D. (2002). The roles of IFN gamma in protection against tumor development and cancer immunoediting. Cytokine Growth Factor Rev. *13*, 95–109.

Irish, J.M., Hovland, R., Krutzik, P.O., Perez, O.D., Bruserud, O., Gjertsen, B.T., and Nolan, G.P. (2004). Single cell profiling of potentiated phospho-protein networks in cancer cells. Cell *118*, 217–228.

James, C., Ugo, V., Le Couedic, J.P., Staerk, J., Delhommeau, F., Lacout, C., Garcon, L., Raslova, H., Berger, R., Bennaceur-Griscelli, A., et al. (2005). A unique clonal JAK2 mutation leading to constitutive signalling causes polycythaemia vera. Nature *434*, 1144–1148.

Kamiya, S., Owaki, T., Morishima, N., Fukai, F., Mizuguchi, J., and Yoshimoto, T. (2004). An indispensable role for STAT1 in IL-27-induced T-bet expression but not proliferation of naive CD4+ T cells. J. Immunol. *173*, 3871–3877.

Kaplan, D.H., Shankaran, V., Dighe, A.S., Stockert, E., Aguet, M., Old, L.J., and Schreiber, R.D. (1998). Demonstration of an interferon gamma-dependent tumor surveillance system in immunocompetent mice. Proc. Natl. Acad. Sci. USA *95*, 7556–7561.

Karre, K., Ljunggren, H.G., Piontek, G., and Kiessling, R. (1986). Selective rejection of H-2-deficient lymphoma variants suggests alternative immune defence strategy. Nature *319*, 675–678.

Kralovics, R., Passamonti, F., Buser, A.S., Teo, S.S., Tiedt, R., Passweg, J.R., Tichelli, A., Cazzola, M., and Skoda, R.C. (2005). A gain-of-function mutation of JAK2 in myeloproliferative disorders. N. Engl. J. Med. *352*, 1779–1790.

Lacronique, V., Boureux, A., Valle, V.D., Poirel, H., Quang, C.T., Mauchauffe, M., Berthou, C., Lessard, M., Berger, R., Ghysdael, J., and Bernard, O.A. (1997). A TEL-JAK2 fusion protein with constitutive kinase activity in human leukemia. Science *278*, 1309–1312.

Landolfo, S., Guarini, A., Riera, L., Gariglio, M., Gribaudo, G., Cignetti, A., Cordone, I., Montefusco, E., Mandelli, F., and Foa, R. (2000). Chronic myeloid leukemia cells resistant to interferon-alpha lack STAT1 expression. Hematol. J. *1*, 7–14.

Lee, C.K., Gimeno, R., and Levy, D.E. (1999). Differential regulation of constitutive major histocompatibility complex class I expression in T and B lymphocytes. J. Exp. Med. *190*, 1451–1464.

Lee, C.K., Rao, D.T., Gertner, R., Gimeno, R., Frey, A.B., and Levy, D.E. (2000a). Distinct requirements for IFNs and STAT1 in NK cell function. J. Immunol. *165*, 3571–3577.

Lee, C.K., Smith, E., Gimeno, R., Gertner, R., and Levy, D.E. (2000b). STAT1 affects lymphocyte survival and proliferation partially independent of its role downstream of IFN-gamma. J. Immunol. *164*, 1286–1292.

Lesinski, G.B., Anghelina, M., Zimmerer, J., Bakalakos, T., Badgwell, B., Parihar, R., Hu, Y., Becknell, B., Abood, G., Chaudhury, A.R., et al. (2003). The antitumor effects of IFN-alpha are abrogated in a STAT1-deficient mouse. J. Clin. Invest. *112*, 170–180.

Levine, R.L., Wadleigh, M., Cools, J., Ebert, B.L., Wernig, G., Huntly, B.J., Boggon, T.J., Wlodarska, I., Clark, J.J., Moore, S., et al. (2005). Activating

mutation in the tyrosine kinase JAK2 in polycythemia vera, essential thrombocythemia, and myeloid metaplasia with myelofibrosis. Cancer Cell *7*, 387–397.

Levy, D.E., and Darnell, J.E., Jr. (2002). Stats: transcriptional control and biological impact. Nat. Rev. Mol. Cell Biol. *3*, 651–662.

Lieberman, L.A., Banica, M., Reiner, S.L., and Hunter, C.A. (2004). STAT1 plays a critical role in the regulation of antimicrobial effector mechanisms, but not in the development of Th1-type responses during toxoplasmosis. J. Immunol. *172*, 457–463.

Meraz, M.A., White, J.M., Sheehan, K.C., Bach, E.A., Rodig, S.J., Dighe, A.S., Kaplan, D.H., Riley, J.K., Greenlund, A.C., Campbell, D., et al. (1996). Targeted disruption of the Stat1 gene in mice reveals unexpected physiologic specificity in the JAK-STAT signaling pathway. Cell *84*, 431–442.

Mocikat, R., Braumuller, H., Gumy, A., Egeter, O., Ziegler, H., Reusch, U., Bubeck, A., Louis, J., Mailhammer, R., Riethmuller, G., et al. (2003). Natural killer cells activated by MHC class I^{low} targets prime dendritic cells to induce protective CD8 T cell responses. Immunity *19*, 561–569.

Moriggl, R., Sexl, V., Kenner, L., Duntsch, C., Stangl, K., Gingras, S., Hoffmeyer, A., Bauer, A., Piekorz, R., Wang, D., et al. (2005). Stat5 tetramer formation is associated with leukemogenesis. Cancer Cell *7*, 87–99.

Nishibori, T., Tanabe, Y., Su, L., and David, M. (2004). Impaired development of CD4+ CD25+ regulatory T cells in the absence of STAT1: increased susceptibility to autoimmune disease. J. Exp. Med. *199*, 25–34.

Palumbo, G.J., Ozanne, B.W., and Kettman, J.R. (1990). Multistage progression of Abelson virus-infected murine pre-B-cells to the tumorigenic state. Cancer Res. *50*, 1917–1923.

Peeters, P., Raynaud, S.D., Cools, J., Wlodarska, I., Grosgeorge, J., Philip, P., Monpoux, F., Van Rompaey, L., Baens, M., Van den Berghe, H., and Marynen, P. (1997). Fusion of TEL, the ETS-variant gene 6 (ETV6), to the receptor-associated kinase JAK2 as a result of t(9;12) in a lymphoid and t(9;15;12) in a myeloid leukemia. Blood *90*, 2535–2540.

Refaeli, Y., Van Parijs, L., Alexander, S.I., and Abbas, A.K. (2002). Interferon gamma is required for activation-induced death of T lymphocytes. J. Exp. Med. *196*, 999–1005.

Rosenberg, N., and Witte, O.N. (1988). The viral and cellular forms of the Abelson (abl) oncogene. Adv. Virus Res. *35*, 39–81.

Schwaller, J., Frantsve, J., Aster, J., Williams, I.R., Tomasson, M.H., Ross, T.S., Peeters, P., Van Rompaey, L., Van Etten, R.A., Ilaria, R., Jr., et al. (1998). Transformation of hematopoietic cell lines to growth-factor independence and induction of a fatal myelo- and lymphoproliferative disease in mice by retrovirally transduced TEL/JAK2 fusion genes. EMBO J. *17*, 5321–5333.

Sexl, V., Kovacic, B., Piekorz, R., Moriggl, R., Stoiber, D., Hoffmeyer, A., Liebminger, R., Kudlacek, O., Weisz, E., Rothammer, K., and Ihle, J.N. (2003). Jak1 deficiency leads to enhanced Abelson-induced B-cell tumor formation. Blood *101*, 4937–4943.

Shankaran, V., Ikeda, H., Bruce, A.T., White, J.M., Swanson, P.E., Old, L.J., and Schreiber, R.D. (2001). IFNγ and lymphocytes prevent primary tumour development and shape tumour immunogenicity. Nature *410*, 1107–1111.

Shinkai, Y., Rathbun, G., Lam, K.P., Oltz, E.M., Stewart, V., Mendelsohn, M., Charron, J., Datta, M., Young, F., Stall, A.M., et al. (1992). RAG-2-deficient mice lack mature lymphocytes owing to inability to initiate V(D)J rearrangement. Cell *68*, 855–867.

Smyth, M.J., Thia, K.Y., Street, S.E., MacGregor, D., Godfrey, D.I., and Trapani, J.A. (2000). Perforin-mediated cytotoxicity is critical for surveillance of spontaneous lymphoma. J. Exp. Med. *192*, 755–760.

Smyth, M.J., Hayakawa, Y., Takeda, K., and Yagita, H. (2002). New aspects of natural-killer-cell surveillance and therapy of cancer. Nat. Rev. Cancer *2*, 850–861.

Spivak, J.L. (2004). The chronic myeloproliferative disorders: clonality and clinical heterogeneity. Semin. Hematol. *41*, 1–5.

Stoiber, D., Kovacic, B., Schuster, C., Schellack, C., Karaghiosoff, M., Kreibich, R., Weisz, E., Artwohl, M., Kleine, O.C., Muller, M., et al. (2004). TYK2 is a key regulator of the surveillance of B lymphoid tumors. J. Clin. Invest. *114*, 1650–1658.

Street, S.E., Trapani, J.A., MacGregor, D., and Smyth, M.J. (2002). Suppression of lymphoma and epithelial malignancies effected by interferon gamma. J. Exp. Med. *196*, 129–134.

Street, S.E., Hayakawa, Y., Zhan, Y., Lew, A.M., MacGregor, D., Jamieson, A.M., Diefenbach, A., Yagita, H., Godfrey, D.I., and Smyth, M.J. (2004). Innate immune surveillance of spontaneous B cell lymphomas by natural killer cells and $\gamma\delta$ T cells. J. Exp. Med. *199*, 879–884.

Sun, W.H., Pabon, C., Alsayed, Y., Huang, P.P., Jandeska, S., Uddin, S., Platanias, L.C., and Rosen, S.T. (1998). Interferon-alpha resistance in a cutaneous T-cell lymphoma cell line is associated with lack of STAT1 expression. Blood *91*, 570–576.

Witte, O.N. (1986). Functions of the abl oncogene. Cancer Surv. *5*, 183–197.

Yu, H., and Jove, R. (2004). The STATs of cancer—new molecular targets come of age. Nat. Rev. Cancer *4*, 97–105.

3.2.6 Clarifying the role of Stat5 in lymphoid development and Abelson-induced transformation

Andrea Hoelbl, Boris Kovacic, Marc A. Kerenyi, Olivia Simma, Wolfgang Warsch, Yongzhi Cui, Hartmut Beug, Lothar Hennighausen, Richard Moriggl and Veronika Sexl

From the
Institute of Pharmacology and Max F.Perutz Laborabories, Medical University of Vienna (MUW), Austria
Institute of Molecular Pathology (IMP), Vienna, Austria
Laboratory of Genetics and Physiology, National Institutes of Health (NIH), Bethesda, MD
Ludwig Boltzmann Institute for Cancer Research (LBI-CR), Vienna, Austria

blood

2006 107: 4898-4906
Prepublished online Feb 21, 2006;
doi:10.1182/blood-2005-09-3596

Clarifying the role of Stat5 in lymphoid development and Abelson-induced transformation

Andrea Hoelbl, Boris Kovacic, Marc A. Kerenyi, Olivia Simma, Wolfgang Warsch, Yongzhi Cui, Hartmut Beug, Lothar Hennighausen, Richard Moriggl and Veronika Sexl

Clarifying the role of Stat5 in lymphoid development and Abelson-induced transformation

Andrea Hoelbl, Boris Kovacic, Marc A. Kerenyi, Olivia Simma, Wolfgang Warsch, Yongzhi Cui, Hartmut Beug, Lothar Hennighausen, Richard Moriggl, and Veronika Sexl

The Stat5 transcription factors Stat5a and Stat5b have been implicated in lymphoid development and transformation. Most studies have employed Stat5a/b-deficient mice where gene targeting disrupted the first protein-coding exon, resulting in the expression of N-terminally truncated forms of Stat5a/b (*Stat5a/b*$^{\Delta N/\Delta N}$ mice). We have now reanalyzed lymphoid development in *Stat5a/b*$^{null/null}$ mice having a complete deletion of the *Stat5a/b* gene locus. The few surviving *Stat5a/b*$^{null/null}$ mice lacked CD8$^+$ T lymphocytes. A massive reduction of CD8$^+$ T cells was also found in *Stat5a/b*$^{fl/fl}$ *lck-cre* transgenic animals. While γδ T-cell receptor–positive (γδTCR$^+$) cells were expressed at normal levels in *Stat5a/b*$^{\Delta N/\Delta N}$ mice, they were completely absent in *Stat5a/b*$^{null/null}$ animals. Moreover, B-cell maturation was abrogated at the pre–pro-B-cell stage in *Stat5a/b*$^{null/null}$ mice, whereas *Stat5a/b*$^{\Delta N/\Delta N}$ B-lymphoid cells developed to the early pro-B-cell stage. In vitro assays using fetal liver-cell cultures confirmed this observation. Most strikingly, *Stat5a/b*$^{null/null}$ cells were resistant to transformation and leukemia development induced by Abelson oncogenes, whereas *Stat5a/b*$^{\Delta N/\Delta N}$-derived cells readily transformed. These findings show distinct lymphoid defects for *Stat5a/b*$^{\Delta N/\Delta N}$ and *Stat5a/b*$^{null/null}$ mice and define a novel functional role for the N-termini of Stat5a/b in B-lymphoid transformation. (Blood. 2006;107:4898-4906)

Introduction

Stat molecules are part of a highly conserved signaling pathway involved in cell-fate decisions like differentiation, proliferation, and apoptosis.[1-3] The cytokines interleukin-2, -4, and -7 (IL-2, IL-4, IL-7) regulate important aspects of lymphoid development and are strong activators of the transcription factors Stat5a and Stat5b.[4] The importance of Stat5a/b for lymphoid cells is also underlined by the fact that constitutively activated Stat5a/b are found in several forms of lymphoid leukemia in mice and humans.[5-10] Gene knockouts have greatly contributed to our knowledge about Stat transcription factors because they allowed exploration of their physiologic and pathophysiologic functions.[11] So far, all studies investigating the role of Stat5a/b in lymphopoiesis employed gene-targeted mice still expressing a residual protein corresponding to an N-terminal deletion mutant (Stat5a/bΔN).[4,12-14] *Stat5a/b*$^{\Delta N/\Delta N}$ mice revealed surprisingly mild phenotypes in B- and T-cell development and function.

Characterization of the lymphoid compartment in *Stat5a/b*$^{\Delta N/\Delta N}$ mice showed a modest reduction of B- and T-lymphoid–cell numbers accompanied by a complete lack of natural killer (NK) cells and CD4$^+$CD25$^+$ suppressor T cells.[4,13,15] CD8$^+$ T cells were present but failed to respond to α-CD3 and IL-2.[4] Mature B-cell numbers in the periphery were also reduced due to an incomplete block at the early pro-B-cell developmental stage (Hardy fraction B).[13,14]

Mice lacking IL-7 or the IL-7R have a block at the earliest step of B-cell development at Hardy fraction A and lack mature B-lymphoid cells in the periphery.[16,17] Notably, B-cell development can be rescued in these mice by forced expression of a constitutively active Stat5a/b mutant.[17] In addition, transgenic mice expressing a constitutively active Stat5b (Stat5b-CA) have increased numbers of pro-B cells.[14] As Stat5a/b are critical components in the signaling cascade downstream of IL-7R, abrogation of Stat5a/b was predicted to result in a dramatic phenotype. Thus, the observations in *Stat5a/b*$^{\Delta N/\Delta N}$ mice were difficult to reconcile with the current understanding of signaling pathways controlling B-cell development.

Moreover, Stat5a/b transcription factors have been shown to play an important role in various T-cell developmental decisions. Transgenic *Stat5b-CA* mice display increased numbers of CD8$^+$ but not CD4$^+$ T cells.[18] This implicates Stat5b as an important regulator of CD4$^+$/CD8$^+$ lineage decision. Moreover, Stat5a/b DNA binding sites were found in regulatory regions of the T-cell receptor γ (TCRγ) gene locus, and *Stat5b-CA* mice displayed a modest increase in γδ T-cell numbers.[18,19] In *Stat5a/b*$^{\Delta N/\Delta N}$ mice, embryonic γδ T-cell development was severely affected, but numbers were rapidly restored after birth.[20] Therefore, the relevance for Stat5a/b in adult γδ thymopoiesis remained elusive.

From the Institute of Pharmacology and Max F. Perutz Laboratories, Medical University of Vienna (MUW), Austria; Institute of Molecular Pathology (IMP), Vienna, Austria; Laboratory of Genetics and Physiology, National Institutes of Health (NIH), Bethesda, MD; and Ludwig Boltzmann Institute for Cancer Research (LBI-CR), Vienna, Austria.

Submitted September 7, 2005; accepted February 8, 2006. Prepublished online as *Blood* First Edition Paper, February 21, 2006; DOI 10.1182/blood-2005-09-3596.

Supported by grants of the Austrian Science Foundation (FWF; V.S.; P15865 and SFB F28) and by a grant of the Austrian National Bank (V.S.; 11132).

A.H., B.K., M.A.K., O.S., W.W., R.M., and V.S. designed and performed research; A.H., B.K., M.A.K., L.H., R.M., and V.S. analyzed data; H.B., Y.C., L.H., and R.M. provided vital new reagents and analytic tools; and A.H. and V.S. wrote the paper.

The online version of this article contains a data supplement.

Reprints: Veronika Sexl, Medical University of Vienna (MUW), Dept of Pharmacology, Währingerstrasse 13A A-1090 Vienna, Austria; e-mail: veronika.sexl@meduniwien.ac.at.

The publication costs of this article were defrayed in part by page charge payment. Therefore, and solely to indicate this fact, this article is hereby marked "advertisement" in accordance with 18 U.S.C. section 1734.

Another finding in *Stat5a/b*$^{\Delta N/\Delta N}$ mice was striking. Among many substrates that are phosphorylated downstream of the Abelson oncogene, Stat5a/b were originally described to be among the most strongly activated ones.[5,21-23] Therefore, Stat5a/b was considered potential critical factors in Ab-MuLV– and bcr/abl-mediated transformation. This hypothesis was substantiated by a plethora of in vitro data using various forms of dominant-negative Stat5a/b mutants.[24-27] Despite this evidence for an essential role for Stat5a/b in Abelson-induced transformation, *Stat5a/b*$^{\Delta N/\Delta N}$ mice were still susceptible to leukemia when challenged with Abelson oncogenes.[13]

Because of these inconsistencies and open questions, we set out to unveil the impact of Stat5a/b on lymphopoiesis and on Abelson-induced transformation using mice in which the entire Stat5a/b locus had been deleted (*Stat5a/b*$^{null/null}$ mice). Our experiments redefine the role of Stat5a/b in lymphoid development and we can clearly attribute a functional role to the truncated Stat5 proteins present in *Stat5a/b*$^{\Delta N/\Delta N}$ mice. We furthermore unravel the key role of Stat5a/b in Abelson-induced transformation.

Materials and methods

Mice

Stat5a/b$^{null/null}$, *Stat5a/b*$^{fl/fl}$, *lck-cre* (distal promoter) transgenic, *Stat5a/b*$^{\Delta N/\Delta N}$, and *Rag2*$^{-/-}$ mice were described previously[12,28-31] and were maintained at the Biomedical Research Institute, Medical University of Vienna, under specifically pathogen-free sterile conditions. The *Stat5a/b*$^{null/null}$, *Stat5a/b*$^{fl/fl}$, and *Stat5a/b*$^{\Delta N}$ mice were on a mixed 129/C57B/6 background. All animal experiments were carried out in accordance with protocols approved by Austrian law.

Flow cytometric analysis

Single-cell suspensions were preincubated with CD16/CD32 antibodies (BD Biosciences, San Jose, CA) to prevent nonspecific Fc-receptor–mediated binding. Subsequently, 5×10^5 cells were stained with monoclonal antibodies conjugated with fluorescent markers and analyzed by a FACScan flow cytometer using CellQuest Pro software (Becton Dickinson, Heidelberg, Germany). The antibodies used for determination of specific B-lineage maturation stages included the markers B220 (CD45R; RA3-6B2), CD43 (1B11), CD19 (1D3), BP-1 (6C3), IgM (R6-60.2), and IgD^b (IgH-5b; 217-170). For surface staining of T-lineage cells, antibodies directed against CD3 (ϵ chain; 145-2C11), CD4 (L3T4), CD8a (Ly-2; 53-6.7), TCRβ chain (H57-597), and γδ TCR (GL3) were used. Hematopoietic stem cell (HSC) staining was performed using a Mouse Lineage Panel kit and anti–sca-1 (Ly-6A/E; D7), anti–c-kit (CD117; 2B8), and anti-CD34 (RAM34) antibodies (all BD Pharmingen, Heidelberg, Germany).

Protein analysis and Western blotting

Splenic T cells were magnetic-activated cell sorted for Thy1.2$^+$ cells according to the manufacturer's instruction (Miltenyi Biotec, Bergisch Gladbach, Germany). Thy1.2$^+$ cells were separated using an autoMACS Instrument (Miltenyi Biotech). Cells were lysed in a buffer containing protease and phosphatase inhibitors (50 mM Hepes, pH 7.5; 0.1% Tween-20; 150 mM NaCl; 1 mM EDTA; 20 mM β-glycero-phosphate; 0.1 mM sodium vanadate; 1 mM sodium fluoride; 10 g/mL aprotinin; leupeptin; and 1 mM PMSF). Protein concentrations were determined using a BCA kit as recommended by the manufacturer (Pierce, Rockford, IL). Proteins (50-100 g) were separated on an 8% SDS polyacrylamide gel and transferred onto Immobilon membranes. Membranes were probed with anti-Stat5a/b (C-17; Santa Cruz Biotechnologies, Santa Cruz, CA) and anti–β-actin (clone Ac-54; Sigma, St Louis, MO) antibodies at dilutions of 1:500 and 1:2000, respectively.

T-cell stimulation

Splenic T cells were isolated from 3 12-week-old *Stat5a/b*$^{f/f}$, 3 *Stat5a/b*$^{f/f}$ *lck-cre*, and 4 *Stat5a/b*$^{\Delta N/\Delta N}$ mice. Splenic-cell solution was subjected to red blood cell lysis for 5 minutes using a lysis buffer containing 150 mM NH_4Cl, 1 mM $KHCO_3$, and 0.1 mM Na_2EDTA (pH 7.3) and cultured in T-cell culture medium (RPMI 1640 containing 10% FBS; 10 mM Hepes, pH 7.0; 2 mM L-glutamine; [1 ×] nonessential amino acids; 1 mM sodium pyruvate; and 50 μM 2-mercaptoethanol) in the presence of 1 μg/mL anti-CD3 monoclonal antibody 145.2C11 (Pharmingen) and 1000 units/mL recombinant human IL-2 (Boehringer Mannheim, Mannheim, Germany).[4] Pellets were prepared before and after 4 hours of stimulation and subjected to RNA isolation.

RNA isolation and semiquantitative RT-PCR analysis

First-strand cDNA synthesis and PCR amplification were performed using a reverse transcriptase–polymerase chain reaction (RT-PCR) kit (GeneAmp RNA PCR kit; Applied Biosystems, Weiterstadt, Germany) according to the manufacturer's instructions. The following primer sequences were used: pim-1, 5′-ACGTGGAGAAGGACCCGATTTCC-3′ and 5′-GATGTTTTCGTCCTTGATGTCGC-3′; cis, 5′-CTGCTGTGCATAGCCAAGACGTTC-3′ and 5′-CAGAGTTGGAAGGGGTACTGTCGG-3′; cyclin D2, 5′-AGAAGGGGCTAGCAGATGA-3′ and 5′-AGGATGATGAAGTGAACACA-3′; β-actin, 5′-CAGGTCCAGACCCAGGATGGC-3′ and 5′-ACTCCTATGTGGGTGACGAG-3′.

In vitro B-cell differentiation

Single-cell suspensions of fetal liver cells (embryonic day 14 [ED 14]) were prepared. The cells were maintained in RPMI medium containing 10% fetal calf serum (FCS), 100 U/mL penicillin/streptomycin, and 5 μM β-mercaptoethanol on an OP-9 fibroblast feeder layer. IL-7, Flt-3L, and SCF (each 10 ng/mL) were added every other day. Outgrowth of specific B-lineage cells was examined for 12 days by analyzing an aliquot of the suspension cells every other day by FACS.

Tissue culture conditions and virus preparation

Transformed fetal liver, bone marrow cells, and tumor-derived cell lines were maintained in RPMI medium containing 10% FCS, 100 U/mL penicillin/streptomycin, 5 μM β-mercaptoethanol, and 2 mM L-glutamine. GP+E86 cell lines (MSCV-*bcr/abl p185*-IRES-eGFP producer), A010 cells (Ab-MuLV producer), and mouse embryonic fibroblasts (MEFs) were maintained in DMEM medium containing 10% FCS, 100 U/mL penicillin/streptomycin, 5 μM β-mercaptoethanol, and 2 mM L-glutamine. A010 cells produce an ecotropic replication-deficient form of the Abelson virus and were a generous gift of Dr Naomi Rosenberg. For collection of the viral supernatant, A010 cells were plated in 100-mm dishes precoated with gelatin (1%) and grown to confluency. Supernatant was harvested every 8 hours for 40 hours, pooled, and filtered through a 0.45-μm filter, as described previously.[32]

Infections, in vitro transformation assays, and establishment of cell lines

For the preparation of fetal liver cells, *Stat5a/b*$^{null/+}$ animals were set up for breeding and vaginal plugs were checked daily. Fourteen days after conception, the pregnant animals were killed and fetal livers were prepared. The tail of the embryo was used for genotyping by PCR. Single-cell suspensions from fetal livers were infected for 1 hour with viral supernatant derived either from A010 cells or from GP+E86 bcr/abl p185-IRES-eGFP producer cell lines in the presence of 7 g/mL polybrene, as described previously.[13,32,33] Using the same procedure, single-cell suspensions of bone marrow of tibiae and femora of mice were infected. The cells were then maintained in complete RPMI medium or plated in cytokine-free methylcellulose at a density of 2.5×10^5 cells/mL in 35-mm dishes. After 10 days, cloning efficiency was evaluated by counting colonies by light microscopy (Leica Fluovert microscope, 4 × magnification; Heidelberg, Germany). Photographs of single colonies were taken using an Axiovert

200 microscope (ZEISS, Oberkochen, Germany; 40 ×/0.6 NA objective), a CoolSNAP fx camera (Visitron Systems, Puchheim, Germany), and MetaMorph software (Version 4.6; Molecular Devices, Downingtown, PA). The assays were performed in triplicates. Mock-infected cells did not result in growth factor–independent colonies. As a control, individual clones were picked and analyzed by flow cytometry for the expression of B-lineage markers (CD19, CD43). The ability to form cell lines was tested by transferring an aliquot of the infected cells (1×10^6) to growth factor–free medium. The medium was changed twice a week and the culture was observed for the outgrowth of stable cell lines.

Injection of Abelson-infected cells into Rag2$^{-/-}$ mice

For tail vein injections, 10^6 cells were resuspended in 200 μL of PBS and injected via tail vein into *Rag2*$^{-/-}$ mice. Prior to injection, the cells were infected with either Ab-MuLV or pMSCV-*bcr/abl p185*-IRES-eGFP retrovirus as described under "Infections, in vitro transformation assays, and establishment of cell lines." Sick mice were killed and analyzed for spleen weights, white blood cell counts, and the presence of leukemic cells in bone marrow, spleen, liver, and blood. The leukemic cells were also analyzed by flow cytometry and expressed the surface markers CD19 and CD43.

[^{3}H]thymidine incorporation

Cells were plated at a density of 2×10^5 cells in 96 round-bottom wells. [^{3}H]thymidine (0.1 μCi/well [0.0037 MBq/well]) was added 18 hours after plating, for another 12 hours.

Statistical analysis

Statistics were carried out using a paired *t* test, Mann-Whitney test, or a one-way analysis of variance (ANOVA) as appropriate. ANOVA was followed by a Tukey test. Differences in Kaplan-Meier plots were analyzed for statistical significance using the log-rank test.

Results

Stat5a/b are essential for CD8$^+$ and γδ T-cell development

Stat5a/b$^{\Delta N/\Delta N}$ mice on a mixed genetic background are viable and may survive up to 2 years in our mouse colony. However, about 40% of *Stat5a/b*$^{\Delta N/\Delta N}$ mice die due to an autoimmune phenotype caused by a significant reduction of CD4$^+$CD25$^+$ suppressor T cells within the first few months (Snow et al[15] and data not shown). In contrast, *Stat5a/b*$^{null/null}$ mice die perinatally[28] (Figure 1A). Although the cause of death is not known, severe anemia and reduced lung capacity are possibly contributing factors (Cui et al[28]; L.H., unpublished observation). Approximately 1% of the *Stat5a/b*$^{null/null}$ mice reach weaning age. These rare *Stat5a/b*$^{null/null}$ survivor mice are much smaller than their littermates, display a significantly reduced body weight, and die within the first 6 weeks after birth (Figure 1A). Stat5a/b$^{\Delta N/\Delta N}$ mice express N-terminally truncated Stat5a/b proteins that are found at significant levels in the lymphoid lineage (Figure S1, available on the *Blood* website; see the Supplemental Figures link at the top of the online article). We therefore monitored lymphoid development in the survivor mouse population. Five 4-week-old *Stat5a/b*$^{null/null}$ mice were killed and thymi and lymph nodes were subjected to flow cytometric analysis. Notably, thymi, spleen, and lymph nodes were smaller than would be expected from the body size of the mice. As depicted in Figure 1B, CD4$^-$CD8$^-$γδTCR$^+$ cells were present in wild-type, *Stat5a/b*$^{\Delta N/+}$, *Stat5a/b*$^{\Delta N/\Delta N}$, and *Stat5a/b*$^{null/+}$ mice but were completely absent in the thymic-cell suspension of *Stat5a/b*$^{null/null}$ mice. We stress that CD4$^-$CD8$^-$γδTCR$^+$ cells are present at significant levels in *Stat5a/b*$^{\Delta N/\Delta N}$ mice. Moreover, *Stat5a/b*$^{\Delta N/\Delta N}$ mice were reported to show a normal distribution of CD4$^+$ and CD8$^+$ T cells in the adult thymus, but *Stat5a/b*$^{\Delta N/\Delta N}$-derived CD8$^+$ cells show an inability to proliferate in response to IL-2.[4] Again, *Stat5a/b*$^{null/null}$ mice revealed a distinct phenotype. The thymus was reduced in size in relation to the body size and age of the mice. We found a significant reduction of CD8$^+$ T cells (2.5-fold). In the lymph nodes, the situation was even more pronounced; *Stat5a/b*$^{null/null}$ mice displayed a 12-fold reduction in CD8$^+$ T lymphocytes (Figure 1C).

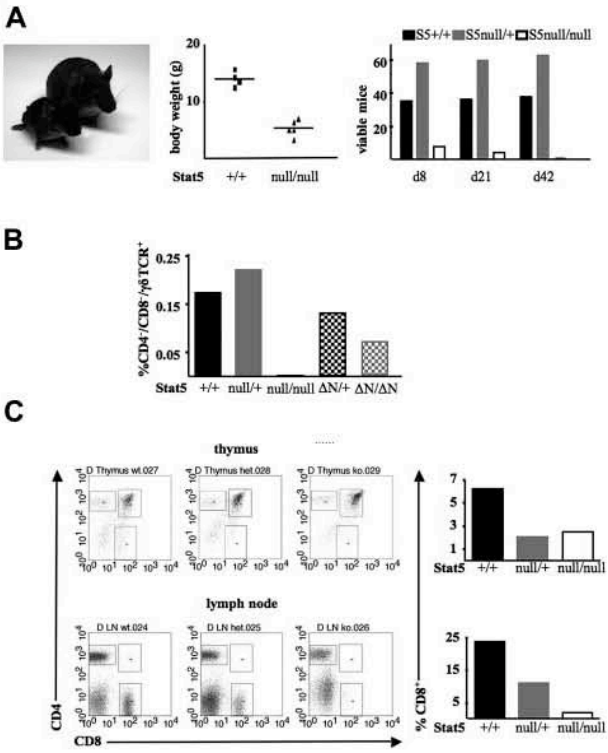

Figure 1. Impaired CD8$^+$ and γδ T-cell development in *Stat5a/b*$^{null/null}$ survivor mice. (A) Picture of a *Stat5a/b*$^{null/null}$ survivor mouse (left) compared with a *Stat5a/b*$^{+/+}$ littermate at the age of 4 weeks. Representative body weight values and numbers of *Stat5a/b*$^{null/null}$ mice and littermates surviving up to day 8, weaning (day 21), or day 42 are depicted. (B) Numbers of CD4$^-$/CD8$^-$/γδTCR$^+$ T lymphocytes in thymi of *Stat5a/b*$^{null/null}$, *Stat5a/b*$^{\Delta N/\Delta N}$, and respective littermate controls. (C) Flow cytometric analysis of CD4$^+$, CD8$^+$, and CD4$^+$/CD8$^+$ cells in thymi and lymph nodes of 5 *Stat5a/b*$^{null/null}$ survivors and 2 individual *Stat5a/b*$^{null/+}$ and 2 *Stat5a/b*$^{+/+}$ littermate controls. Data are summarized in bar graphs. Due to the small size of thymi and lymph nodes, cells were pooled and did therefore not allow generation of error bars (B-C).

To confirm cell autonomy of Stat5a/b in CD8$^+$ T-cell development, we generated *Stat5a/b*$^{f/f}$ *lck-cre* mice. These mice express the Cre-recombinase under the control of the distal promoter of the T-cell receptor–associated kinase Lck, which is first active at the double-negative (CD4$^-$CD8$^-$) stage.[30] T-cell lineage–specific deletion of Stat5a/b was confirmed by Western blot analysis of magnetic-activated cell separation (MACS)–sorted Thy1.2$^+$ splenic cells (Figure 2A). *Stat5a/b*$^{f/f}$ *lck-cre* mice displayed splenomegaly and lymphoid organ infiltration that was first detected at the age of 4 weeks. This phenotype is most probably due to the expected lack of suppressor T cells that was previously described as a consequence of Stat5a/b deficiency.[15] As observed in *Stat5a/b*$^{null/null}$ survivors, *Stat5a/b*$^{f/f}$ lck-cre mice showed a significant reduction of CD8$^+$ T cells in all organs analyzed (thymus, $P < .01$; peripheral blood, $P < .001$; spleen, $P < .01$; lymph node, $P < .05$; Figure 2B). The selective disappearance of CD8$^+$ cells is also indicated by the increased ratio of CD4$^+$ versus CD8$^+$ cells, as described in Table 1. In order to see whether a different induction of target genes might account for the differences in the phenotype of *Stat5a/b*$^{\Delta N/\Delta N}$

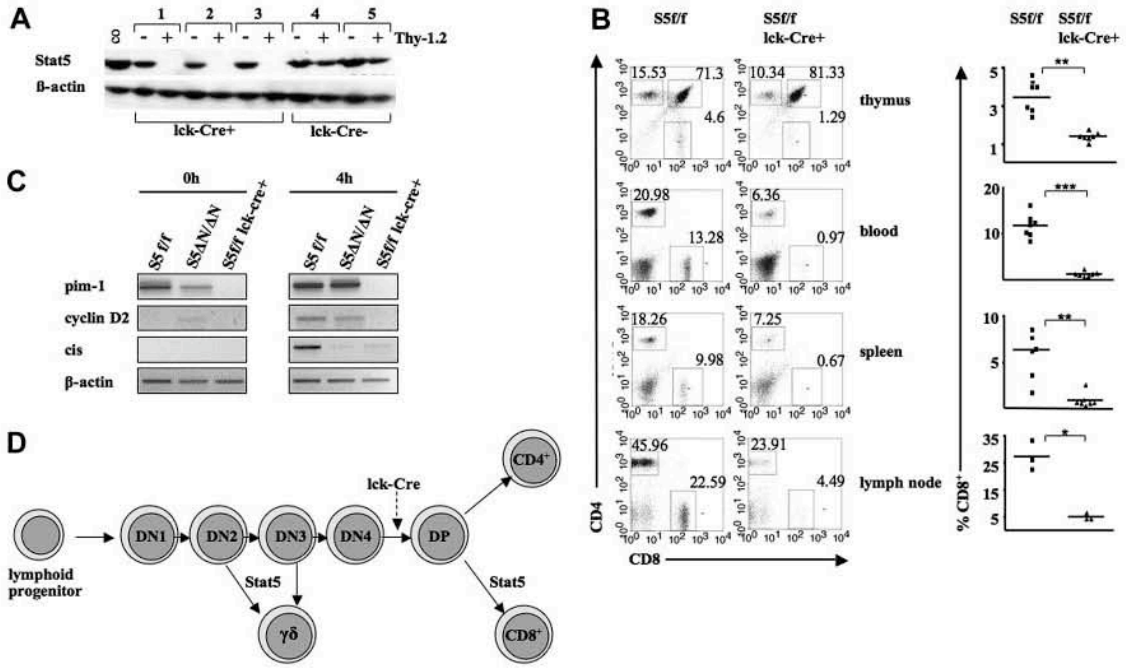

Figure 2. Impaired CD8⁺ T-cell development in *Stat5a/b*$^{f/f}$ *lck-cre* mice. (A) Splenic cells of 3 individual *Stat5a/b*$^{f/f}$ *lck-cre* (nos. 1-3) and 2 *Stat5a/b*$^{f/f}$ (nos. 4-5) mice were magnetically sorted for Thy1.2⁺ cells, and Stat5a/b expression was assessed by Western blot analysis. (B) Representative flow cytometric profile of CD4⁺, CD8⁺, and CD4⁺/CD8⁺ cells in thymus, blood, spleen, and lymph nodes of *Stat5a/b*$^{f/f}$ *lck-cre* mice and *Stat5a/b*$^{f/f}$ controls. Asterisks denote significant difference as determined by a paired *t* test. (C) Analysis of transcriptional expression of *pim-1*, *CIS*, and cyclin D2 genes by semiquantitative RT-PCR. Splenic T cells were stimulated for 4 hours with α-CD3 (1 μg/mL) and human IL-2 (hIL-2; 1000 U/mL) to induce Stat5a/b target gene transcription. (D) Schematic model for the role of Stat5a/b in T-cell developmental choices. Stages affected in *Stat5a/b*$^{null/null}$ survivor mice and/or *Stat5a/b*$^{f/f}$ *lck-cre* mice are indicated. The time point of Cre-recombinase activation under the control of the distal lck promoter is also depicted.

and *Stat5a/b*$^{null/null}$ mice, we stimulated splenic T cells with α-CD3 and IL-2, as depicted in Figure 2C. The Stat5a/b target genes *Pim1* and cyclin D2 were clearly expressed in *Stat5a/b*$^{f/f}$ and *Stat5a/b*$^{\Delta N/\Delta N}$ cells. Induction of these genes was not found in *Stat5a/b*$^{null/null}$ T cells, indicating that Stat5a/bΔN are still capable of inducing some target genes. In contrast, expression of the suppressor of cytokine signaling (SOCS) gene family member CIS was lacking in both *Stat5a/b*$^{\Delta N/\Delta N}$ and *Stat5a/b*$^{f/f}$ lck-cre cells. The development of γδ T cells was not altered in these mice (data not shown). This was to be expected because transcription from the distal *lck* promoter occurs after the junction of γδ TCR⁺ cells. Taken together, these findings provide evidence that Stat5a/b are indispensable for CD8⁺ T-cell and γδ TCR⁺-cell homeostasis (Figure 2D scheme).

Stat5a/b are essential for the pre–pro-B to early pro-B-cell stage transition in vivo

Specific B-cell developmental stages can be distinguished by differential cell-surface expression of B220, CD43, CD19, BP-1, IgM, and IgD (Figure 3C schematic overview). Single fractions can be classified according to the Hardy nomenclature in pre–pro-B (B220⁺/CD43^{hi}/CD19⁻/BP-1⁻; fraction A), early pro-B (B220⁺/CD43^{hi}/CD19⁺/BP-1⁻; fraction B), late pro-B (B220⁺/CD43^{hi}/CD19⁺/BP-1⁺; fraction C), pre-B (B220⁺/CD43^{lo}/IgM⁻/IgD⁻; fraction D), immature (B220⁺/CD43^{lo}/IgM⁺/IgD⁻; fraction E), and mature (B220⁺/CD43^{lo}/IgM⁺/IgD⁺; fraction F) B cells.[34,35]

Table 1. Mean ratio of CD4⁺ to CD8⁺ T cells in thymi, peripheral blood, spleen, and lymph nodes of *Stat5a/b*$^{f/f}$ and *Stat5a/b*$^{f/f}$ *lck-cre* mice

	Ratio of CD4⁺/CD8⁺ cells	
	S5f/f	S5f/f lck-cre
Thymus	4.1:1	11:1
Lymph node	1.9:1	5:1
Spleen	2.2:1	8:1
Peripheral blood	1.5:1	6:1

It had been shown in *Stat5a/b*$^{\Delta N/\Delta N}$ mice that Stat5a/b are required for the transition from the early pro-B (Hardy fraction B) to the late pro-B-cell stage (Hardy fraction C).[14] We prepared bone marrow, spleen, and lymph nodes of 5 *Stat5a/b*$^{null/null}$ survivor mice and their *Stat5a/b*$^{null/+}$ and wild-type littermates. The numbers of pre–pro-B cells were comparable in all 3 groups. However, we failed to detect early and late pro-B cells in *Stat5a/b*$^{null/null}$ mice in the bone marrow (22-fold and 40-fold reduction compared with *Stat5a/b*$^{+/+}$, respectively; Figure 3A). Accordingly, the numbers of mature B cells (Hardy fraction F) in spleen and lymph nodes were also significantly reduced compared with *Stat5a/b*$^{+/+}$ controls (6.4-fold and 2.2-fold, respectively; Figure 3B). We emphasize that these percentages cannot be directly compared, since the total size and the cellularity of hematopoietic organs differ in wild-type and *Stat5a/b*$^{null/null}$ animals. These data strongly argue for a role of Stat5a/b at the earliest steps of B-cell development (pre–pro-B cell to early pro-B-cell transition). However, the developmental block does not appear to be absolute, since few mature B-lymphoid cells are present in the periphery. Again, the phenotype in *Stat5a/b*$^{null/null}$ mice is aggravated and very distinct from *Stat5a/b*$^{\Delta N/\Delta N}$ mice, with a block occurring at an earlier B-cell developmental stage (as indicated in the scheme in Figure 3C).

In vitro B-cell differentiation of *Stat5a/b*$^{null/null}$ fetal liver–derived cells

To further investigate the role of Stat5a/b for early B-cell development, we established a protocol that allows following B-cell

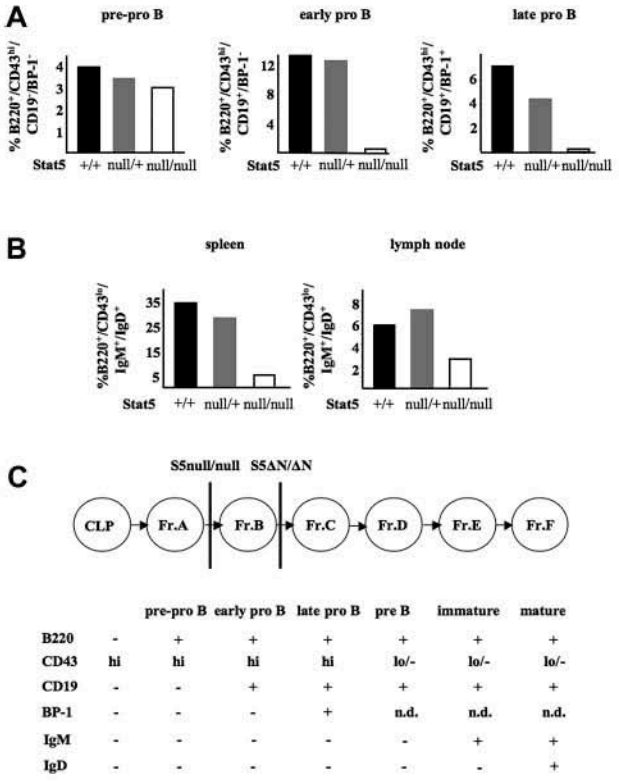

		pre-pro B	early pro B	late pro B	pre B	immature	mature
B220	-	+	+	+	+	+	+
CD43	hi	hi	hi	hi	lo/-	lo/-	lo/-
CD19	-	-	+	+	+	+	+
BP-1	-	-	-	+	n.d.	n.d.	n.d.
IgM	-	-	-	-	-	+	+
IgD	-	-	-	-	-	-	+

Figure 3. B-cell development is arrested at the pre–pro-B-cell stage in *Stat5a/b*$^{null/null}$ survivor mice. (A) Percentages of pre–pro-B, early pro-B, and late pro-B cells in bone marrow and (B) mature B cells in spleen and lymph node of 5 Stat5a/b$^{null/null}$ survivors compared with 2 *Stat5a/b*$^{null/+}$ and 2 *Stat5a/b*$^{+/+}$ controls. Due to the small body size, bone marrows were pooled and therefore did not allow generation of error bars. (C) Schematic model for maturation of B-cell developmental fractions A-F. As indicated, individual maturational stages were distinguished by differential surface expression of B220, CD43, CD19, BP-1, IgM, and IgD. The different blocks in *Stat5a/b*$^{\Delta N/\Delta N}$ and *Stat5a/b*$^{null/null}$ mice are indicated by vertical lines. CLP indicates common lymphoid progenitor.

differentiation of fetal liver–derived cells in vitro. First, we excluded that a reduction of *Stat5a/b*$^{null/null}$ HSCs causes any effects and determined the numbers of lin$^-$/c-kit$^+$/Sca-1$^+$ long term-HSCs (CD34$^-$) and short term-HSCs (CD34$^+$). Interestingly, *Stat5a/b*$^{null/null}$ fetal livers displayed comparable numbers of both populations (Figure S2A-S2B). We then cultured fetal liver cells (ED 14) of a *Stat5a/b*$^{null/+}$ intercross on an OP-9 fibroblast feeder layer in the continuous presence of IL-7, Flt-3L, and SCF (10 ng/mL each). Outgrowth of B-lineage cells was analyzed every second day by FACS analysis. Outgrowth kinetics of the single Hardy fractions reflected the observations made in the *Stat5a/b*$^{null/null}$ survivor mice (Figure 4). Fraction A was found comparable in cells of each genotype. Fraction B, C, E, and F cells were detectable in control cultures from day 6 on but were entirely missing in cultures derived from *Stat5a/b*$^{null/null}$ fetal livers. In these cultures, B-cell development was completely abrogated at fraction A and failed to proceed to any further maturation stages. We also performed an in vitro B-cell developmental assay only in the presence of IL-7 using an MEF feeder layer (10 ng/mL), confirming a critical role for Stat5a/b in the transition from Hardy fraction A to B (Figure S3).

Taken together, our data show that Stat5a/b are a critical transcription factor for the transition of pre–pro-B cells (fraction A) to the early pro-B-cell stage (fraction B) in adult and fetal hematopoiesis. Moreover, these findings indicate that the N-terminally truncated Stat5a/b proteins present in *Stat5a/b*$^{\Delta N/\Delta N}$ mice suffice to allow B-lymphoid cells to mature to the early pro-B-cell stage.

Stat5a/b are required for Ab-MuLV– and *bcr/abl p185*–induced transformation in vitro

A constitutive activation of Stat5a/b is found in a large variety of leukemias and lymphomas,[5,9,10,21,36] and constitutive activation of Stat5a/b suffice to induce a multi-lineage leukemia in mice.[36] Despite a broad experimental evidence for a role of Stat5a/b in lymphoid leukemia,[22,24,26,37,38] we have shown that *Stat5a/b*$^{\Delta N/\Delta N}$ mice developed Abelson-induced B-lymphoid leukemia with identical properties compared with wild-type littermate controls.[13] Bone marrow cells derived from *Stat5a/b*$^{\Delta N/\Delta N}$ mice were readily transformed by Abelson oncogenes and resulted in the outgrowth of stable cell lines.[13] We therefore repeated the transformation experiments with fetal livers and bone marrow from *Stat5a/b*$^{null/null}$ mice. Fetal liver cells (ED 14) were infected with Ab-MuLV and plated in growth factor–free methylcellulose. No colonies were detected in any of the *Stat5a/b*$^{null/null}$ fetal livers tested. A gene dosage effect was observed in *Stat5a/b*$^{null/+}$ fetal liver–derived cells, where we detected 50% to 60% of the growth factor–independent colonies compared with wild-type controls (Figure 5A-B). The retroviral constructs employed (Ab-MuLV and pMSCV-*bcr/abl p185*-IRES eGFP) result in the outgrowth of B-lymphoid colonies. This was confirmed by analyzing the colonies by flow cytometry for surface expression of CD43 and CD19. As expected, the transformed colonies were positive for both markers (Figure 5C).

A gene dosage effect was also observed regarding the proliferative capacity of *Stat5a/b*$^{+/+}$ and *Stat5a/b*$^{null/+}$ Abelson-transformed cell lines (Figure 5D). Transformation experiments were repeated with bone marrow of *Stat5a/b*$^{null/null}$ survivors and confirmed the lack of transformation ability: colony formation was completely

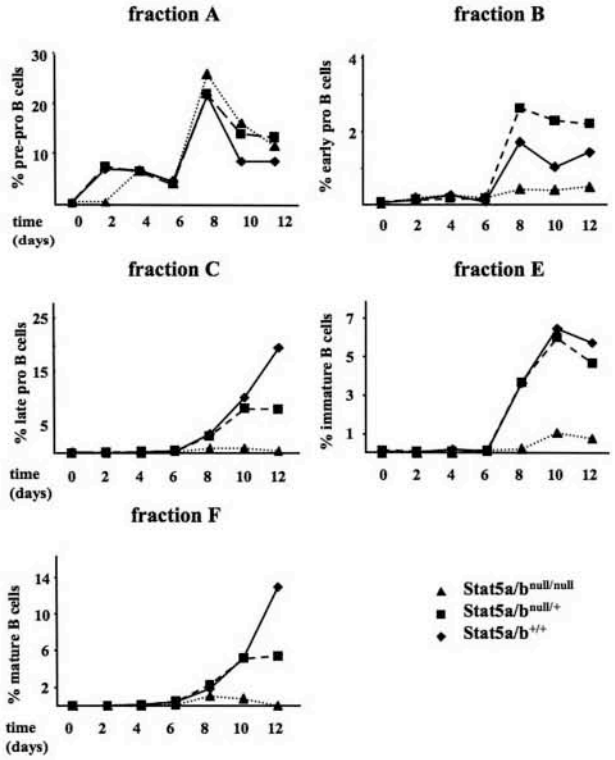

Figure 4. B-cell development is arrested at the pre–pro-B-cell stage in *Stat5a/b*$^{null/null}$ fetal liver–derived cultures. Fetal livers of 2 embryos of each genotype were pooled (ED 14) and cocultivated on an OP-9 fibroblast feeder layer in the presence of IL-7, Flt-3L, and SCF (10 ng/mL each). Outgrowth of pro-B-cell stages (fractions A-C), immature (fraction E), and mature (fraction F) B cells over a 12-day period is depicted.

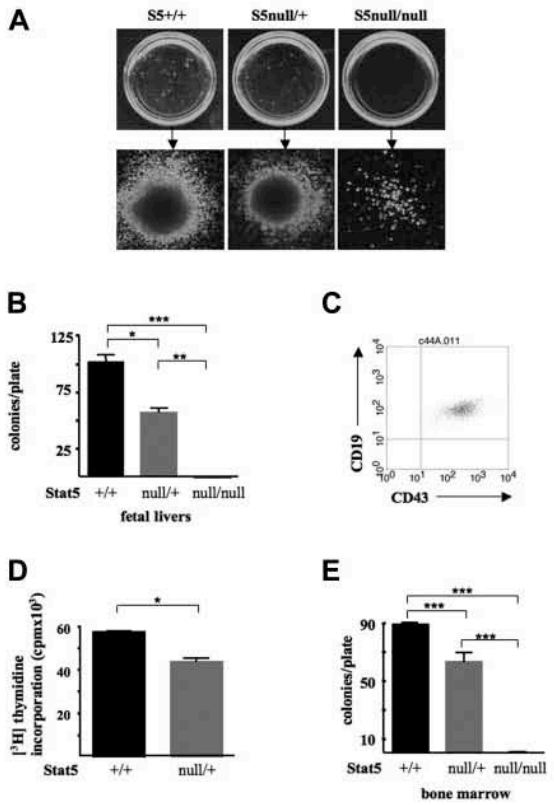

Figure 5. Abelson-induced transformation is dependent on Stat5a/b in vitro. (A) Ab-MuLV–induced colony formation of *Stat5a/b*$^{+/+}$, *Stat5a/b*$^{null/+}$, and *Stat5a/b*$^{null/null}$ fetal liver cells in methylcellulose. Single-colony pictures of each phenotype are depicted in the bottom panels. *Stat5a/b*$^{null/null}$ cells showed no ability to form growth factor–independent colonies. (B) Summary of data obtained from Ab-MuLV–induced colony formation assays represent means ± SEM of 4 embryos per genotype (each performed in triplicates). (C) Surface expression of B-lineage markers was verified by flow cytometric analysis (right; data of one representative CD19$^+$ CD43$^+$ colony is shown). (D) [^{3}H]thymidine incorporation of fetal liver–derived *Stat5a/b*$^{+/+}$ and *Stat5a/b*$^{null/+}$ Ab-MuLV–transformed cell lines. Stat5a/b-deficient fetal livers did not give rise to stable transformed cell lines. Data represent means ± SEM of 2 cell lines per genotype. cpm indicates counts per minute. (E) Ab-MuLV–induced colony formation of *Stat5a/b*$^{+/+}$ (n = 2), *Stat5a/b*$^{null/+}$ (n = 2), and *Stat5a/b*$^{null/null}$ (n = 5; pooled) survivor bone marrow cells in methylcellulose. *Stat5a/b*$^{null/null}$ survivor cells showed no ability to form growth factor–free colonies. Experiment was performed in triplicates. Asterisks denote significant differences as determined by a one-way ANOVA followed by a Tukey test (A,C) or a paired *t* test (B).

abrogated in *Stat5a/b*$^{null/null}$ cells (Figure 5E). Stable immortal Ab-MuLV–transformed cell lines were derived from wild-type and *Stat5a/b*$^{null/+}$ mice, but not a single cell line grew out from *Stat5a/b*$^{null/null}$ fetal livers or bone marrow (Table 2). These experiments indicate that Stat5a/b are required for Abelson-induced transformation but that Stat5a/bΔN suffice to support the transformation and immortalization process.

To control for this somewhat unusual observation, we performed several additional experiments that are summarized in Table 2. First, we repeated the transformation experiments side by side with bone marrow cells derived from *Stat5a/b*$^{\Delta N/\Delta N}$ and *Stat5a/b*$^{null/null}$ survivor mice. *Stat5a/b*$^{\Delta N/\Delta N}$ cells readily transformed, which resulted in the formation of growth factor–independent colonies and in the outgrowth of stable cell lines, but we failed to see signs of transformation when using *Stat5a/b*$^{null/null}$ cells.

We next reasoned that Ab-MuLV–induced transformation might target a distinct subset of B-cell precursors that were absent or present at low numbers in *Stat5a/b*$^{null/null}$ fetal liver cells or bone marrow. Hence, we employed a murine stem-cell virus encoding the *bcr/abl p185* retrovirus (pMSCV–*bcr/abl p185*-IRES-eGFP). MSCV infects murine hematopoietic stem cells, which are present at comparable numbers in *Stat5a/b*$^{null/null}$ fetal livers and controls (Figure S2). Cells derived from *Stat5a/b*$^{null/null}$ (fetal livers) or *Stat5a/b*$^{\Delta N/\Delta N}$ mice (bone marrow) were infected, the infection was controlled via FACS analysis, and the cells were subsequently plated in growth factor–free methylcellulose or transferred to growth factor–free medium. Again, cells derived from *Stat5a/b*$^{\Delta N/\Delta N}$ mice formed colonies and gave rise to cell lines, whereas *Stat5a/b*$^{null/null}$ cells failed to do so (Table 2).

Abelson-transformed *Stat5a/b*$^{null/null}$ cells fail to induce leukemia in vivo

One may speculate that the failure to transform *Stat5a/b*$^{null/null}$ cells might be compensated in vivo (eg, via cytokine-dependent activation of redundant signaling pathways). To test this, we first infected fetal livers with pMSCV–*bcr/abl p185*-IRES-eGFP and injected them via tail vein into 2 *Rag2*$^{-/-}$ mice each. Mice that had received wild-type bone marrow died from leukemia after 3 months, whereas the *Rag2*$^{-/-}$ mice that had received *Stat5a/b*$^{null/null}$ bone marrow survived in a disease-free state for at least 6 months (data not shown). Uninfected *Stat5a/b*$^{null/null}$ bone marrow was also injected into 2 *Rag2*$^{-/-}$ mice to verify that *Stat5a/b*$^{null/null}$ bone marrow did indeed have the capacity to reconstitute hematopoiesis, albeit to a lesser extent than control bone marrow (data not shown; J. O'Shea, NIH, Bethesda, MD, and L.H., oral communication). It is important to mention that *Stat5a/b*$^{null/null}$ fetal liver cells allowed the development of a few IgM$^+$ IgD$^+$ cells that were detected in the periphery. We next reasoned that the initial steps of transformation might be cytokine dependent or influenced by surrounding cells and that the environment within *Rag2*$^{-/-}$ mice only repopulated with *Stat5a/b*$^{null/null}$ marrow might prevent transformation in vivo.[39-41] To exclude this possibility we performed the following experiment. Bone marrow of 4 *Stat5a/b*$^{null/null}$ survivor mice was prepared and mixed with wild-type marrow derived from a littermate control at a ratio of 4:1. The cells were infected with Ab-MuLV retrovirus and again injected via tail vein into recipient *Rag2*$^{-/-}$ animals. As depicted in Figure 6A, mice that had received either *Stat5a/b*$^{+/+}$ or *Stat5a/b*$^{null/+}$ marrow succumbed to a B-lymphoid leukemia within 3 to 4 weeks. When administered mixed bone marrow that contained 80% of *Stat5a/b*$^{null/null}$ cells, *Rag2*$^{-/-}$ mice showed signs of a phenotypically identical disease with latency that was increased by 10 days ($P < .05$). The animals displayed splenomegaly and elevated white blood cell counts and

Table 2. Ability of fetal liver and bone marrow cells to form *bcr/abl p185*- or Ab-MuLV–induced colonies and stable cell lines

	Colony formation	Transformed cell lines
bcr/abl transformation		
S5$^{\Delta N/+}$, BM	Yes	Yes
S5$^{\Delta N/\Delta N}$, BM	Yes	Yes
S5$^{+/+}$, FL	Yes	Yes
S5$^{null/+}$, FL	Yes	Yes
S5$^{null/null}$, FL	No	No
Ab-MuLV transformation		
S5$^{\Delta N/+}$, BM	Yes	Yes
S5$^{\Delta N/\Delta N}$, BM	Yes	Yes
S5$^{+/+}$, FL	Yes	Yes
S5$^{null/+}$, FL	Yes	Yes
S5$^{null/null}$, FL	No	No
S5$^{+/+}$, BM	Yes	Yes
S5$^{null/+}$, BM	Yes	Yes
S5$^{null/null}$, BM	No	No

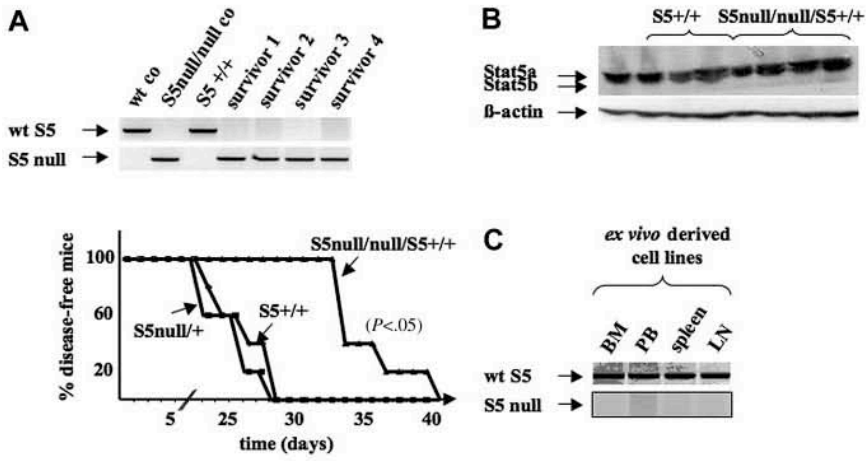

Figure 6. Abelson-induced transformation is dependent on Stat5 in vivo. (A) Kaplan-Meier plot of *Rag2*$^{-/-}$ mice that received a transplant of either *Stat5a/b*$^{+/+}$, *Stat5a/b*$^{null/+}$, or a 4:1 mixture of *Stat5a/b*$^{null/null}$ and *Stat5a/b*$^{+/+}$ freshly Ab-MuLV–transformed bone marrow cells (5 mice/group; 1 × 10^6 cells each mouse). Genotyping PCR analysis of mice used for 4:1 mixture is depicted. wt indicates wild type. (B) Immunoblotting for Stat5a/b of leukemic cells derived from bone marrow of *Rag2*$^{-/-}$ mice that received a transplant of either *Stat5a/b*$^{+/+}$ or a 4:1 mixture of *Stat5a/b*$^{null/null}$/*Stat5a/b*$^{+/+}$ bone marrow. (C) PCR analysis of ex vivo–derived cell lines. Representative data of bone marrow (BM)–, peripheral blood (PB)–, spleen-, and lymph node (LN)–derived leukemic cell lines of one *Rag2*$^{-/-}$ mouse that received a transplant of a 4:1 mixture of *Stat5a/b*$^{null/null}$/*Stat5a/b*$^{+/+}$ bone marrow cells, which was later killed. All cultures derived from *Rag2*$^{-/-}$ mice that received transplants of *Stat5a/b*$^{null/null}$/*Stat5a/b*$^{+/+}$ cells were *Stat5a/b*$^{+/+}$ as determined by PCR analysis.

spleen, bone marrow, and liver were infiltrated with CD19$^+$CD43$^+$ leukemic cells (Figure S4). Western blot analysis showed that all cells expressed Stat5a/b at comparable levels (Figure 6B). In addition, ex vivo–derived cell lines were established and analyzed by PCR (Figure 6C). All leukemic cells expressed Stat5a/b; no transformed cells derived from *Stat5a/b*$^{null/null}$ marrow were detectable. These experiments define Stat5a/b as essential transcription factors for Abelson-induced leukemia initiation and exclude the possibility that other signaling pathways compensate in vivo.

Discussion

The transcription factors Stat5a/b have been considered key regulators of immune functions and the lymphoid system.[10,12,14,15,42,43] Their relevance and importance are underlined by the fact that more than 1700 manuscripts have been published on Stat5a/b since their discovery. A major breakthrough was the generation of the first Stat5a/b knockout mouse in 1998 (*Stat5a/b*$^{\Delta N/\Delta N}$ mice) that served as a valuable tool for numerous studies and shed light on the multiple roles of Stat5a/b in the organism.[4,12,14,44] Despite the key role of IL-7–mediated Stat5a/b activation in lymphoid development, the phenotype of the *Stat5a/b*$^{\Delta N/\Delta N}$ mice in the lymphoid system is surprisingly moderate.[4,20] The most prominent effect is the complete absence of CD4$^+$CD25$^+$ suppressor T cells, leading to an autoimmune disease.[15]

Our present work provides compelling evidence that the function of Stat5a/b in lymphoid development and immune functions needs redefinition. Our findings prove that Stat5a/b are key regulators of early B-cell development and of CD8$^+$ and γδ T-lymphoid–cell generation. The difference between *Stat5a/b*$^{\Delta N/\Delta N}$ and *Stat5a/b*$^{null/null}$ mice implicitly defines separate roles for the N-terminally truncated Stat5a/b. Since deficiency in Stat5a/b was lethal,[28] one might also argue that disturbances at the locus occurred independently of the targeted deletion of *Stat5a/b*. We do exclude this possibility, since erythroid cells can be genetically complemented by wild-type Stat5a (M.A.K. and H.B., unpublished observations). Our attempts to complement *Stat5a/b*$^{null/null}$ HSCs with wild-type Stat5a to rescue lymphoid development continuously failed, most likely based on a severe defect of HSCs upon loss of Stat5a/b.[45-47] The vast majority of *Stat5a/b*$^{null/null}$ pups died rapidly after delivery. The rare survivors may have reflected outliers in the Gaussian distribution or a compensating adaptive change that occurred at low frequency. Regardless of the underlying basis, it is worth pointing out that the observations in these survivors were reproduced in the *Stat5a/b*$^{f/f}$ *lck-cre* mice. The analysis of T-cell development in *Stat5a/b*$^{f/f}$ lck-cre mice also excluded that *Stat5a/b*$^{null/null}$ thymic epithelial cells were responsible for the selective lack of CD8$^+$ cells. Finally, B-cell development was recapitulated in vitro by employing fetal hematopoietic progenitors. In this cell-culture system, the absence of Stat5a/b resulted in a complete block of B-cell development at that very stage predicted from the phenotype of the survivors (pre–pro-B-cell stage). Taken together, these data demonstrate that the observations obtained in the rare survivors are not confounded by an undefined adaptive escape phenomenon. They also provide formal proof for the interpretation that deficiency in Stat5a/b affects the lymphoid compartment by a cell-autonomous effect rather than an indirect effect mediated via abnormalities in stromal cells or thymic epithelium.

Hence, our observations fall in place with the predicted role of Stat5a/b in lymphopoiesis and are in perfect agreement with studies performed in other mouse models.[17,18,48] Goetz et al[49] recently showed that constitutively active Stat5b promotes B-cell development at the expense of early T-cell development in transgenic mice. The authors hypothesize that Stat5a/b serves as a switch, with Stat5a/b activation driving cells into the B-lymphoid lineage whereas a lack of Stat5a/b activation allows for the development of early T-lymphoid cells. Moreover, the block in B-cell development at the earliest step (Hardy fraction A) confirms the original concept that Stat5a/b are the relevant transcription factor downstream of IL-7 in early B-cell development.[17] It is also in line with an increased number of pro-B-cells in *Stat5b-CA* mice.[18]

Our experiments also lead to another important conclusion: the truncated proteins of Stat5a/b expressed in *Stat5a/b*$^{\Delta N/\Delta N}$ mice are able to partially rescue B-cell development and to allow for the development of γδTCR$^+$ and CD8$^+$ T cells. It is currently unclear how the truncated Stat5a/b operate but we know that the Stat5ΔN protein enters the nucleus and constitutively binds DNA (data not shown). We also know that, at least in T cells, the Stat5ΔN protein is able to induce some but not all Stat5a/b target genes (eg, cyclin D2, an important mediator of cell proliferation). Further analysis in different cell lineages will finally clarify which target genes can be activated or repressed by Stat5ΔN. In addition, Stat5a/b might act as a scaffold. It was recently shown that constitutively active Stat5a/b assemble in a complex with Gab2 to allow for activation of PI3K.[50,51] A potential protein docking function of Stat5a/b would be an alternative hypothesis to explain the differences observed in *Stat5a/b*$^{\Delta N/\Delta N}$ and *Stat5a/b*$^{null/null}$ cells.

Finally, we show that *Stat5a/b*$^{null/null}$ cells, in contrast to *Stat5a/b*$^{\Delta N/\Delta N}$ cells, fail to induce lymphoid leukemia in mice. The

truncated Stat5a/b proteins suffice to afford transformation as illustrated for Abelson oncogenes.[13] In each approach employed, growth factor–independent clones from *Stat5a/b*$^{\Delta N/\Delta N}$ cells grew out readily. In contrast, regardless of the experimental setup, we consistently failed to obtain a single colony or growth factor–independent clone from *Stat5a/b*$^{null/null}$ cells derived from either fetal livers or bone marrow. This key finding is of high clinical relevance because Stat proteins are potential candidates for drug targeting in the therapy of leukemia and other forms of cancer.[52,53] We have recently shown that constitutively active Stat5a/b induced a multi-lineage leukemia and that tetramer formation of Stat5a/b was crucial in this regard.[36] Apparently, N-terminally truncated Stat5a/b proteins that lack the tetramerization domain suffice to collaborate with at least some oncogenic tyrosine kinases, as proven here for the Abelson oncogenes. Therefore, a close definition of Stat5a/b functions in cancer progression is urgently needed. Our findings may therefore redirect therapeutic approaches that try to target Stat5a/b signaling in human leukemia. The importance of Stat5a/b in leukemia is further stressed by the fact that constitutively active mutations of Jak2 have recently been characterized as causative oncogenes in human leukemia.[54-57] Jak2 is a strong activator of Stat5a/b; hence, it is attractive to speculate that Stat5a/b are essential components in the signaling cascade underlying disease manifestation and progression in these patients. If this can be confirmed, Stat5a/b are likely to emerge as a potential target for therapeutic intervention.

Acknowledgments

The authors thank Udo Losert and the staff of the Biomedical Research Institute, Medical University of Vienna (MUW) for taking care of mice. We are grateful to Michael Freissmuth, Meinrad Busslinger, John O'Shea, Peter Valent, Christian Sillaber, and Kevin Bunting for helpful discussions in the course of this work.

References

1. Calo V, Migliavacca M, Bazan V, et al. STAT proteins: from normal control of cellular events to tumorigenesis. J Cell Physiol. 2003;197:157-168.
2. Levy DE, Darnell JE Jr. Stats: transcriptional control and biological impact. Nat Rev Mol Cell Biol. 2002;3:651-662.
3. Murray R. Physiologic roles of interleukin-2, interleukin-4, and interleukin-7. Curr Opin Hematol. 1996;3:230-234.
4. Moriggl R, Topham DJ, Teglund S, et al. Stat5 is required for IL-2-induced cell cycle progression of peripheral T cells. Immunity. 1999;10:249-259.
5. Gouilleux-Gruart V, Debierre-Grockiego F, Gouilleux F, et al. Activated Stat related transcription factors in acute leukemia. Leuk Lymphoma. 1997; 28:83-88.
6. Takemoto S, Mulloy JC, Cereseto A, et al. Proliferation of adult T cell leukemia/lymphoma cells is associated with the constitutive activation of JAK/STAT proteins. Proc Natl Acad Sci U S A. 1997; 94:13897-13902.
7. Bromberg J. Stat proteins and oncogenesis. J Clin Invest. 2002;109:1139-1142.
8. Mitchell TJ, John S. Signal transducer and activator of transcription (STAT) signalling and T-cell lymphomas. Immunology. 2005;114:301-312.
9. Schwaller J, Parganas E, Wang D, et al. Stat5 is essential for the myelo- and lymphoproliferative disease induced by TEL/JAK2. Mol Cell. 2000;6: 693-704.
10. Kelly JA, Spolski R, Kovanen PE, et al. Stat5 synergizes with T cell receptor/antigen stimulation in the development of lymphoblastic lymphoma. J Exp Med. 2003;198:79-89.
11. Levy DE. Physiological significance of STAT proteins: investigations through gene disruption in vivo. Cell Mol Life Sci. 1999;55:1559-1567.
12. Teglund S, McKay C, Schuetz E, et al. Stat5a and Stat5b proteins have essential and nonessential, or redundant, roles in cytokine responses. Cell. 1998;93:841-850.
13. Sexl V, Piekorz R, Moriggl R, et al. Stat5a/b contribute to interleukin 7-induced B-cell precursor expansion, but abl- and bcr/abl-induced transformation are independent of stat5. Blood. 2000;96: 2277-2283.
14. Goetz CA, Harmon IR, O'Neil JJ, Burchill MA, Farrar MA. STAT5 activation underlies IL7 receptor-dependent B cell development. J Immunol. 2004;172:4770-4778.
15. Snow JW, Abraham N, Ma MC, Herndier BG, Pastuszak AW, Goldsmith MA. Loss of tolerance and autoimmunity affecting multiple organs in STAT5A/5B-deficient mice. J Immunol. 2003;171: 5042-5050.
16. Peschon JJ, Morrissey PJ, Grabstein KH, et al. Early lymphocyte expansion is severely impaired in interleukin 7 receptor-deficient mice. J Exp Med. 1994;180:1955-1960.
17. Kikuchi K, Lai AY, Hsu CL, Kondo M. IL-7 receptor signaling is necessary for stage transition in adult B cell development through up-regulation of EBF. J Exp Med. 2005;201:1197-1203.
18. Burchill MA, Goetz CA, Prlic M, et al. Distinct effects of STAT5 activation on CD4+ and CD8+ T cell homeostasis: development of CD4+CD25+ regulatory T cells versus CD8+ memory T cells. J Immunol. 2003;171:5853-5864.
19. Baker JE, Kang J, Xiong N, Chen T, Cado D, Raulet DH. A novel element upstream of the Vgamma2 gene in the murine T cell receptor gamma locus cooperates with the 3' enhancer to act as a locus control region. J Exp Med. 1999; 190:669-679.
20. Kang J, DiBenedetto B, Narayan K, Zhao H, Der SD, Chambers CA. STAT5 is required for thymopoiesis in a development stage-specific manner. J Immunol. 2004;173:2307-2314.
21. Shuai K, Halpern J, ten Hoeve J, Rao X, Sawyers CL. Constitutive activation of STAT5 by the BCR-ABL oncogene in chronic myelogenous leukemia. Oncogene. 1996;13:247-254.
22. de Groot RP, Raaijmakers JA, Lammers JW, Jove R, Koenderman L. STAT5 activation by BCR-Abl contributes to transformation of K562 leukemia cells. Blood. 1999;94:1108-1112.
23. Carlesso N, Frank DA, Griffin JD. Tyrosyl phosphorylation and DNA binding activity of signal transducers and activators of transcription (STAT) proteins in hematopoietic cell lines transformed by Bcr/Abl. J Exp Med. 1996;183:811-820.
24. Nieborowska-Skorska M, Wasik MA, Slupianek A, et al. Signal transducer and activator of transcription (STAT)5 activation by BCR/ABL is dependent on intact Src homology (SH)3 and SH2 domains of BCR/ABL and is required for leukemogenesis. J Exp Med. 1999;189:1229-1242.
25. Sonoyama J, Matsumura I, Ezoe S, et al. Functional cooperation among Ras, STAT5, and phosphatidylinositol 3-kinase is required for full oncogenic activities of BCR/ABL in K562 cells. J Biol Chem. 2002;277:8076-8082.
26. Sillaber C, Gesbert F, Frank DA, Sattler M, Griffin JD. STAT5 activation contributes to growth and viability in Bcr/Abl-transformed cells. Blood. 2000; 95:2118-2125.
27. Huang M, Dorsey JF, Epling-Burnette PK, et al. Inhibition of Bcr-Abl kinase activity by PD180970 blocks constitutive activation of Stat5 and growth of CML cells. Oncogene. 2002;21:8804-8816.
28. Cui Y, Riedlinger G, Miyoshi K, et al. Inactivation of Stat5 in mouse mammary epithelium during pregnancy reveals distinct functions in cell proliferation, survival, and differentiation. Mol Cell Biol. 2004;24:8037-8047.
29. Wildin RS, Wang HU, Forbush KA, Perlmutter RM. Functional dissection of the murine lck distal promoter. J Immunol. 1995;155:1286-1295.
30. Wildin RS, Garvin AM, Pawar S, et al. Developmental regulation of lck gene expression in T lymphocytes. J Exp Med. 1991;173:383-393.
31. Shinkai Y, Rathbun G, Lam KP, et al. RAG-2-deficient mice lack mature lymphocytes owing to inability to initiate V(D)J rearrangement. Cell. 1992; 68:855-867.
32. Sexl V, Kovacic B, Piekorz R, et al. Jak1 deficiency leads to enhanced Abelson-induced B-cell tumor formation. Blood. 2003;101:4937-4943.
33. Stoiber D, Kovacic B, Schuster C, et al. TYK2 is a key regulator of the surveillance of B lymphoid tumors. J Clin Invest. 2004;114:1650-1658.
34. Hardy RR, Li YS, Allman D, Asano M, Gui M, Hayakawa K. B-cell commitment, development and selection. Immunol Rev. 2000;175:23-32.
35. Hardy RR. B-cell commitment: deciding on the players. Curr Opin Immunol. 2003;15:158-165.
36. Moriggl R, Sexl V, Kenner L, et al. Stat5 tetramer formation is associated with leukemogenesis. Cancer Cell. 2005;7:87-99.
37. Gesbert F, Griffin JD. Bcr/Abl activates transcription of the Bcl-X gene through STAT5. Blood. 2000;96:2269-2276.
38. de Groot RP, Raaijmakers JA, Lammers JW, Koenderman L. STAT5-dependent cyclinD1 and Bcl-xL expression in Bcr-Abl-transformed cells. Mol Cell Biol Res Commun. 2000;3:299-305.
39. Flamant S, Kortulewski T, Dugray A, et al. Osteopontin is upregulated by BCR-ABL. Biochem Biophys Res Commun. 2005;333:1378-1384.
40. Suda T, Arai F, Hirao A. Hematopoietic stem cells and their niche. Trends Immunol. 2005;26:426-433.
41. Heissig B, Ohki Y, Sato Y, Rafii S, Werb Z, Hattori K. A role for niches in hematopoietic cell development. Hematology. 2005;10:247-253.
42. Lin JX, Leonard WJ. The role of Stat5a and Stat5b in signaling by IL-2 family cytokines. Oncogene. 2000;19:2566-2576.
43. Kelly J, Spolski R, Imada K, Bollenbacher J, Lee

S, Leonard WJ. A role for Stat5 in CD8+ T cell homeostasis. J Immunol. 2003;170:210-217.

44. Moriggl R, Sexl V, Piekorz R, Topham D, Ihle JN. Stat5 activation is uniquely associated with cytokine signaling in peripheral T cells. Immunity. 1999;11:225-230.
45. Bradley HL, Hawley TS, Bunting KD. Cell intrinsic defects in cytokine responsiveness of STAT5-deficient hematopoietic stem cells. Blood. 2002; 100:3983-3989.
46. Bunting KD, Bradley HL, Hawley TS, Moriggl R, Sorrentino BP, Ihle JN. Reduced lymphomyeloid repopulating activity from adult bone marrow and fetal liver of mice lacking expression of STAT5. Blood. 2002;99:479-487.
47. Snow JW, Abraham N, Ma MC, Abbey NW, Herndier B, Goldsmith MA. STAT5 promotes multilineage hematolymphoid development in vivo through effects on early hematopoietic progenitor cells. Blood. 2002;99:95-101.
48. Ye SK, Agata Y, Lee HC, et al. The IL-7 receptor controls the accessibility of the TCRgamma locus by Stat5 and histone acetylation. Immunity. 2001; 15:813-823.
49. Goetz CA, Harmon IR, O'Neil JJ, Burchill MA, Johanns TM, Farrar MA. Restricted STAT5 activation dictates appropriate thymic B versus T cell lineage commitment. J Immunol. 2005;174:7753-7763.
50. Nyga R, Pecquet C, Harir N, et al. Activated STAT5 proteins induce activation of the PI 3-kinase/Akt and Ras/MAPK pathways via the Gab2 scaffolding adapter. Biochem J. 2005;390:359-366.
51. Santos SC, Lacronique V, Bouchaert I, et al. Constitutively active STAT5 variants induce growth and survival of hematopoietic cells through a PI 3-kinase/Akt dependent pathway. Oncogene. 2001;20:2080-2090.
52. Turkson J. STAT proteins as novel targets for cancer drug discovery. Expert Opin Ther Targets. 2004;8:409-422.
53. O'Shea JJ, Pesu M, Borie DC, Changelian PS. A new modality for immunosuppression: targeting the JAK/STAT pathway. Nat Rev Drug Discov. 2004;3:555-564.
54. Tefferi A, Gilliland DG. The JAK2V617F tyrosine kinase mutation in myeloproliferative disorders: status report and immediate implications for disease classification and diagnosis. Mayo Clin Proc. 2005;80:947-958.
55. Tefferi A, Gilliland DG. JAK2 in myeloproliferative disorders is not just another kinase. Cell Cycle. 2005;4:1053-1056.
56. James C, Ugo V, Le Couedic JP, et al. A unique clonal JAK2 mutation leading to constitutive signalling causes polycythaemia vera. Nature. 2005; 434:1144-1148.
57. Levine RL, Wadleigh M, Cools J, et al. Activating mutation in the tyrosine kinase JAK2 in polycythemia vera, essential thrombocythemia, and myeloid metaplasia with myelofibrosis. Cancer Cell. 2005;7:387-397.

References

Adams, G.B., and Scadden, D.T. (2006). The hematopoietic stem cell in its place. Nat Immunol *7*, 333-337.

Adams, J.M., and Strasser, A. (2008). Is tumor growth sustained by rare cancer stem cells or dominant clones? Cancer research *68*, 4018-4021.

Adolfsson, J., Mansson, R., Buza-Vidas, N., Hultquist, A., Liuba, K., Jensen, C.T., Bryder, D., Yang, L., Borge, O.J., Thoren, L.A.*, et al.* (2005). Identification of Flt3+ lympho-myeloid stem cells lacking erythro-megakaryocytic potential a revised road map for adult blood lineage commitment. Cell *121*, 295-306.

Akashi, K., Traver, D., Miyamoto, T., and Weissman, I.L. (2000). A clonogenic common myeloid progenitor that gives rise to all myeloid lineages. Nature *404*, 193-197.

Al-Hajj, M., Wicha, M.S., Benito-Hernandez, A., Morrison, S.J., and Clarke, M.F. (2003). Prospective identification of tumorigenic breast cancer cells. Proc Natl Acad Sci U S A *100*, 3983-3988.

Arinobu, Y., Mizuno, S., Chong, Y., Shigematsu, H., Iino, T., Iwasaki, H., Graf, T., Mayfield, R., Chan, S., Kastner, P.*, et al.* (2007). Reciprocal activation of GATA-1 and PU.1 marks initial specification of hematopoietic stem cells into myeloerythroid and myelolymphoid lineages. Cell Stem Cell *1*, 416-427.

Becker, S., Groner, B., and Muller, C.W. (1998). Three-dimensional structure of the Stat3beta homodimer bound to DNA. Nature *394*, 145-151.

Bennett, J.M., Catovsky, D., Daniel, M.T., Flandrin, G., Galton, D.A., Gralnick, H.R., and Sultan, C. (1976). Proposals for the classification of the acute leukaemias. French-American-British (FAB) co-operative group. Br J Haematol *33*, 451-458.

Boelens, J., Lust, S., Vanhoecke, B., and Offner, F. (2009). Chronic lymphocytic leukaemia. Anticancer research *29*, 605-615.

Bonnet, D., and Dick, J.E. (1997). Human acute myeloid leukemia is organized as a hierarchy that originates from a primitive hematopoietic cell. Nat Med *3*, 730-737.

Bowie, M.B., McKnight, K.D., Kent, D.G., McCaffrey, L., Hoodless, P.A., and Eaves, C.J. (2006). Hematopoietic stem cells proliferate until after birth and show a reversible phase-specific engraftment defect. J Clin Invest *116*, 2808-2816.

Bromberg, J.F., Wrzeszczynska, M.H., Devgan, G., Zhao, Y., Pestell, R.G., Albanese, C., and Darnell, J.E., Jr. (1999). Stat3 as an oncogene. Cell *98*, 295-303.

Burchill, M.A., Goetz, C.A., Prlic, M., O'Neil, J.J., Harmon, I.R., Bensinger, S.J., Turka, L.A., Brennan, P., Jameson, S.C., and Farrar, M.A. (2003). Distinct effects of STAT5 activation on CD4+ and CD8+ T cell homeostasis: development of CD4+CD25+ regulatory T cells versus CD8+ memory T cells. J Immunol *171*, 5853-5864.

Caligiuri, M.A., Strout, M.P., and Gilliland, D.G. (1997). Molecular biology of acute myeloid leukemia. Seminars in oncology *24*, 32-44.

Calo, V., Migliavacca, M., Bazan, V., Macaluso, M., Buscemi, M., Gebbia, N., and Russo, A. (2003). STAT proteins: from normal control of cellular events to tumorigenesis. Journal of cellular physiology *197*, 157-168.

Chen, X., Vinkemeier, U., Zhao, Y., Jeruzalmi, D., Darnell, J.E., Jr., and Kuriyan, J. (1998). Crystal structure of a tyrosine phosphorylated STAT-1 dimer bound to DNA. Cell *93*, 827-839.

Chiorazzi, N., Rai, K.R., and Ferrarini, M. (2005). Chronic lymphocytic leukemia. N Engl J Med *352*, 804-815.

Choi, K., Kennedy, M., Kazarov, A., Papadimitriou, J.C., and Keller, G. (1998). A common precursor for hematopoietic and endothelial cells. Development *125*, 725-732.

Clark, S.S., McLaughlin, J., Timmons, M., Pendergast, A.M., Ben-Neriah, Y., Dow, L.W., Crist, W., Rovera, G., Smith, S.D., and Witte, O.N. (1988). Expression of a distinctive BCR-ABL oncogene in Ph1-positive acute lymphocytic leukemia (ALL). Science *239*, 775-777.

Cumano, A., Dieterlen-Lievre, F., and Godin, I. (1996). Lymphoid potential, probed before circulation in mouse, is restricted to caudal intraembryonic splanchnopleura. Cell *86*, 907-916.

Druker, B.J. (2008). Translation of the Philadelphia chromosome into therapy for CML. Blood *112*, 4808-4817.

Druker, B.J., Sawyers, C.L., Kantarjian, H., Resta, D.J., Reese, S.F., Ford, J.M., Capdeville, R., and Talpaz, M. (2001a). Activity of a specific inhibitor of the BCR-ABL tyrosine kinase in the blast crisis of chronic myeloid leukemia and acute lymphoblastic leukemia with the Philadelphia chromosome. N Engl J Med *344*, 1038-1042.

Druker, B.J., Talpaz, M., Resta, D.J., Peng, B., Buchdunger, E., Ford, J.M., Lydon, N.B., Kantarjian, H., Capdeville, R., Ohno-Jones, S.*, et al.* (2001b). Efficacy and safety of a specific inhibitor of the BCR-ABL tyrosine kinase in chronic myeloid leukemia. N Engl J Med *344*, 1031-1037.

Durbin, J.E., Hackenmiller, R., Simon, M.C., and Levy, D.E. (1996). Targeted disruption of the mouse Stat1 gene results in compromised innate immunity to viral disease. Cell *84*, 443-450.

Dykstra, B., Kent, D., Bowie, M., McCaffrey, L., Hamilton, M., Lyons, K., Lee, S.J., Brinkman, R., and Eaves, C. (2007). Long-term propagation of distinct hematopoietic differentiation programs in vivo. Cell Stem Cell *1*, 218-229.

Faderl, S., Talpaz, M., Estrov, Z., O'Brien, S., Kurzrock, R., and Kantarjian, H.M. (1999). The biology of chronic myeloid leukemia. N Engl J Med *341*, 164-172.

Ferkowicz, M.J., and Yoder, M.C. (2005). Blood island formation: longstanding observations and modern interpretations. Exp Hematol *33*, 1041-1047.

Foon, K.A., Billing, R.J., Terasaki, P.I., and Cline, M.J. (1980). Immunologic classification of acute lymphoblastic leukemia. Implications for normal lymphoid differentiation. Blood *56*, 1120-1126.

Gekas, C., Dieterlen-Lievre, F., Orkin, S.H., and Mikkola, H.K. (2005). The placenta is a niche for hematopoietic stem cells. Dev Cell *8*, 365-375.

Grebien, F., Kerenyi, M.A., Kovacic, B., Kolbe, T., Becker, V., Dolznig, H., Pfeffer, K., Klingmuller, U., Muller, M., Beug, H.*, et al.* (2008). Stat5 activation enables erythropoiesis in the absence of EpoR and Jak2. Blood *111*, 4511-4522.

Groffen, J., Stephenson, J.R., Heisterkamp, N., de Klein, A., Bartram, C.R., and Grosveld, G. (1984). Philadelphia chromosomal breakpoints are clustered within a limited region, bcr, on chromosome 22. Cell *36*, 93-99.

Haar, J.L., and Ackerman, G.A. (1971). Ultrastructural changes in mouse yolk sac associated with the initiation of vitelline circulation. Anat Rec *170*, 437-455.

Hoelbl, A., Kovacic, B., Kerenyi, M.A., Simma, O., Warsch, W., Cui, Y., Beug, H., Hennighausen, L., Moriggl, R., and Sexl, V. (2006). Clarifying the role of Stat5 in lymphoid development and Abelson-induced transformation. Blood *107*, 4898-4906.

Holyoake, T., Jiang, X., Eaves, C., and Eaves, A. (1999). Isolation of a highly quiescent subpopulation of primitive leukemic cells in chronic myeloid leukemia. Blood *94*, 2056-2064.

Hu, Y., Liu, Y., Pelletier, S., Buchdunger, E., Warmuth, M., Fabbro, D., Hallek, M., Van Etten, R.A., and Li, S. (2004). Requirement of Src kinases Lyn, Hck and Fgr for BCR-ABL1-induced B-lymphoblastic leukemia but not chronic myeloid leukemia. Nat Genet *36*, 453-461.

Huber, T.L., Kouskoff, V., Fehling, H.J., Palis, J., and Keller, G. (2004). Haemangioblast commitment is initiated in the primitive streak of the mouse embryo. Nature *432*, 625-630.

Huntly, B.J., Shigematsu, H., Deguchi, K., Lee, B.H., Mizuno, S., Duclos, N., Rowan, R., Amaral, S., Curley, D., Williams, I.R.*, et al.* (2004). MOZ-TIF2, but not BCR-ABL, confers properties of leukemic stem cells to committed murine hematopoietic progenitors. Cancer Cell *6*, 587-596.

Ikuta, K., and Weissman, I.L. (1992). Evidence that hematopoietic stem cells express mouse c-kit but do not depend on steel factor for their generation. Proc Natl Acad Sci U S A *89*, 1502-1506.

James, C., Ugo, V., Le Couedic, J.P., Staerk, J., Delhommeau, F., Lacout, C., Garcon, L., Raslova, H., Berger, R., Bennaceur-Griscelli, A.*, et al.* (2005). A unique clonal JAK2 mutation leading to constitutive signalling causes polycythaemia vera. Nature *434*, 1144-1148.

Jamieson, C.H., Ailles, L.E., Dylla, S.J., Muijtjens, M., Jones, C., Zehnder, J.L., Gotlib, J., Li, K., Manz, M.G., Keating, A.*, et al.* (2004). Granulocyte-macrophage progenitors as candidate leukemic stem cells in blast-crisis CML. N Engl J Med *351*, 657-667.

Jordan, C.T. (2002). Unique molecular and cellular features of acute myelogenous leukemia stem cells. Leukemia *16*, 559-562.

Kantarjian, H., Sawyers, C., Hochhaus, A., Guilhot, F., Schiffer, C., Gambacorti-Passerini, C., Niederwieser, D., Resta, D., Capdeville, R., Zoellner, U*., et al.* (2002). Hematologic and cytogenetic responses to imatinib mesylate in chronic myelogenous leukemia. N Engl J Med *346*, 645-652.

Karaghiosoff, M., Neubauer, H., Lassnig, C., Kovarik, P., Schindler, H., Pircher, H., McCoy, B., Bogdan, C., Decker, T., Brem, G*., et al.* (2000). Partial impairment of cytokine responses in Tyk2-deficient mice. Immunity *13*, 549-560.

Karaghiosoff, M., Steinborn, R., Kovarik, P., Kriegshauser, G., Baccarini, M., Donabauer, B., Reichart, U., Kolbe, T., Bogdan, C., Leanderson, T*., et al.* (2003). Central role for type I interferons and Tyk2 in lipopolysaccharide-induced endotoxin shock. Nat Immunol *4*, 471-477.

Kelly, P.N., Dakic, A., Adams, J.M., Nutt, S.L., and Strasser, A. (2007). Tumor growth need not be driven by rare cancer stem cells. Science *317*, 337.

Kerenyi, M.A., Grebien, F., Gehart, H., Schifrer, M., Artaker, M., Kovacic, B., Beug, H., Moriggl, R., and Mullner, E.W. (2008). Stat5 regulates cellular iron uptake of erythroid cells via IRP-2 and TfR-1. Blood *112*, 3878-3888.

Kim, I., Saunders, T.L., and Morrison, S.J. (2007). Sox17 dependence distinguishes the transcriptional regulation of fetal from adult hematopoietic stem cells. Cell *130*, 470-483.

Kisseleva, T., Bhattacharya, S., Braunstein, J., and Schindler, C.W. (2002). Signaling through the JAK/STAT pathway, recent advances and future challenges. Gene *285*, 1-24.

Kondo, M., Weissman, I.L., and Akashi, K. (1997). Identification of clonogenic common lymphoid progenitors in mouse bone marrow. Cell *91*, 661-672.

Konopka, J.B., and Witte, O.N. (1985). Detection of c-abl tyrosine kinase activity in vitro permits direct comparison of normal and altered abl gene products. Mol Cell Biol *5*, 3116-3123.

Koushik, S.V., Wang, J., Rogers, R., Moskophidis, D., Lambert, N.A., Creazzo, T.L., and Conway, S.J. (2001). Targeted inactivation of the sodium-calcium exchanger (Ncx1) results in the lack of a heartbeat and abnormal myofibrillar organization. FASEB J *15*, 1209-1211.

Kovacic, B., Stoiber, D., Moriggl, R., Weisz, E., Ott, R.G., Kreibich, R., Levy, D.E., Beug, H., Freissmuth, M., and Sexl, V. (2006). STAT1 acts as a tumor promoter for leukemia development. Cancer Cell *10*, 77-87.

Kralovics, R., Passamonti, F., Buser, A.S., Teo, S.S., Tiedt, R., Passweg, J.R., Tichelli, A., Cazzola, M., and Skoda, R.C. (2005). A gain-of-function mutation of JAK2 in myeloproliferative disorders. N Engl J Med *352*, 1779-1790.

Krause, D.S., Lazarides, K., von Andrian, U.H., and Van Etten, R.A. (2006). Requirement for CD44 in homing and engraftment of BCR-ABL-expressing leukemic stem cells. Nat Med *12*, 1175-1180.

Krivtsov, A.V., Twomey, D., Feng, Z., Stubbs, M.C., Wang, Y., Faber, J., Levine, J.E., Wang, J., Hahn, W.C., Gilliland, D.G.*, et al.* (2006). Transformation from committed progenitor to leukaemia stem cell initiated by MLL-AF9. Nature *442*, 818-822.

Lapidot, T., Sirard, C., Vormoor, J., Murdoch, B., Hoang, T., Caceres-Cortes, J., Minden, M., Paterson, B., Caligiuri, M.A., and Dick, J.E. (1994). A cell initiating human acute myeloid leukaemia after transplantation into SCID mice. Nature *367*, 645-648.

Levine, R.L., and Gilliland, D.G. (2008). Myeloproliferative disorders. Blood *112*, 2190-2198.

Levine, R.L., Wadleigh, M., Cools, J., Ebert, B.L., Wernig, G., Huntly, B.J., Boggon, T.J., Wlodarska, I., Clark, J.J., Moore, S.*, et al.* (2005). Activating mutation in the tyrosine kinase JAK2 in polycythemia vera, essential thrombocythemia, and myeloid metaplasia with myelofibrosis. Cancer Cell *7*, 387-397.

Levy, D.E., and Darnell, J.E., Jr. (2002). Stats: transcriptional control and biological impact. Nat Rev Mol Cell Biol *3*, 651-662.

Medvinsky, A., and Dzierzak, E. (1996). Definitive hematopoiesis is autonomously initiated by the AGM region. Cell *86*, 897-906.

Meraz, M.A., White, J.M., Sheehan, K.C., Bach, E.A., Rodig, S.J., Dighe, A.S., Kaplan, D.H., Riley, J.K., Greenlund, A.C., Campbell, D.*, et al.* (1996). Targeted disruption of the Stat1 gene in mice reveals unexpected physiologic specificity in the JAK-STAT signaling pathway. Cell *84*, 431-442.

Minegishi, Y., Saito, M., Morio, T., Watanabe, K., Agematsu, K., Tsuchiya, S., Takada, H., Hara, T., Kawamura, N., Ariga, T.*, et al.* (2006). Human tyrosine kinase 2 deficiency reveals its requisite roles in multiple cytokine signals involved in innate and acquired immunity. Immunity *25*, 745-755.

Moore, M.A., and Metcalf, D. (1970). Ontogeny of the haemopoietic system: yolk sac origin of in vivo and in vitro colony forming cells in the developing mouse embryo. Br J Haematol *18*, 279-296.

Moriggl, R., Sexl, V., Kenner, L., Duntsch, C., Stangl, K., Gingras, S., Hoffmeyer, A., Bauer, A., Piekorz, R., Wang, D.*, et al.* (2005). Stat5 tetramer formation is associated with leukemogenesis. Cancer Cell *7*, 87-99.

Morrison, S.J., Wandycz, A.M., Hemmati, H.D., Wright, D.E., and Weissman, I.L. (1997). Identification of a lineage of multipotent hematopoietic progenitors. Development *124*, 1929-1939.

Morrison, S.J., and Weissman, I.L. (1994). The long-term repopulating subset of hematopoietic stem cells is deterministic and isolatable by phenotype. Immunity *1*, 661-673.

Muller, A.M., Medvinsky, A., Strouboulis, J., Grosveld, F., and Dzierzak, E. (1994). Development of hematopoietic stem cell activity in the mouse embryo. Immunity *1*, 291-301.
Murray, R. (1996). Physiologic roles of interleukin-2, interleukin-4, and interleukin-7. Curr Opin Hematol *3*, 230-234.

Murry, C.E., and Keller, G. (2008). Differentiation of embryonic stem cells to clinically relevant populations: lessons from embryonic development. Cell *132*, 661-680.

Neubauer, H., Cumano, A., Muller, M., Wu, H., Huffstadt, U., and Pfeffer, K. (1998). Jak2 deficiency defines an essential developmental checkpoint in definitive hematopoiesis. Cell *93*, 397-409.

North, T., Gu, T.L., Stacy, T., Wang, Q., Howard, L., Binder, M., Marin-Padilla, M., and Speck, N.A. (1999). Cbfa2 is required for the formation of intra-aortic hematopoietic clusters. Development *126*, 2563-2575.

North, T.E., de Bruijn, M.F., Stacy, T., Talebian, L., Lind, E., Robin, C., Binder, M., Dzierzak, E., and Speck, N.A. (2002). Runx1 expression marks long-term repopulating hematopoietic stem cells in the midgestation mouse embryo. Immunity *16*, 661-672.

Nosaka, T., van Deursen, J.M., Tripp, R.A., Thierfelder, W.E., Witthuhn, B.A., McMickle, A.P., Doherty, P.C., Grosveld, G.C., and Ihle, J.N. (1995). Defective lymphoid development in mice lacking Jak3. Science *270*, 800-802.

Notarangelo, L.D., Mella, P., Jones, A., de Saint Basile, G., Savoldi, G., Cranston, T., Vihinen, M., and Schumacher, R.F. (2001). Mutations in severe combined immune deficiency (SCID) due to JAK3 deficiency. Human mutation *18*, 255-263.

Nowell, P.C., and Hungerford, D.A. (1960). Chromosome studies on normal and leukemic human leukocytes. J Natl Cancer Inst *25*, 85-109.

O'Shea, J.J., Gadina, M., and Schreiber, R.D. (2002). Cytokine signaling in 2002: new surprises in the Jak/Stat pathway. Cell *109 Suppl*, S121-131.

Orkin, S.H., and Zon, L.I. (2008). Hematopoiesis: an evolving paradigm for stem cell biology. Cell *132*, 631-644.

Osawa, M., Hanada, K., Hamada, H., and Nakauchi, H. (1996). Long-term lymphohematopoietic reconstitution by a single CD34-low/negative hematopoietic stem cell. Science *273*, 242-245.

Ottmann, O.G., Druker, B.J., Sawyers, C.L., Goldman, J.M., Reiffers, J., Silver, R.T., Tura, S., Fischer, T., Deininger, M.W., Schiffer, C.A.*, et al.* (2002). A phase 2 study of imatinib in patients with relapsed or refractory Philadelphia chromosome-positive acute lymphoid leukemias. Blood *100*, 1965-1971.

Palis, J. (2008). Ontogeny of erythropoiesis. Curr Opin Hematol *15*, 155-161.

Palis, J., Robertson, S., Kennedy, M., Wall, C., and Keller, G. (1999). Development of erythroid and myeloid progenitors in the yolk sac and embryo proper of the mouse. Development *126*, 5073-5084.

Parganas, E., Wang, D., Stravopodis, D., Topham, D.J., Marine, J.C., Teglund, S., Vanin, E.F., Bodner, S., Colamonici, O.R., van Deursen, J.M.*, et al.* (1998). Jak2 is essential for signaling through a variety of cytokine receptors. Cell *93*, 385-395.

Park, C., Li, S., Cha, E., and Schindler, C. (2000). Immune response in Stat2 knockout mice. Immunity *13*, 795-804.

Passegue, E., Jamieson, C.H., Ailles, L.E., and Weissman, I.L. (2003). Normal and leukemic hematopoiesis: are leukemias a stem cell disorder or a reacquisition of stem cell characteristics? Proc Natl Acad Sci U S A *100 Suppl 1*, 11842-11849.

Passegue, E., Wagner, E.F., and Weissman, I.L. (2004). JunB deficiency leads to a myeloproliferative disorder arising from hematopoietic stem cells. Cell *119*, 431-443.

Piccaluga, P.P., Paolini, S., and Martinelli, G. (2007). Tyrosine kinase inhibitors for the treatment of Philadelphia chromosome-positive adult acute lymphoblastic leukemia. Cancer *110*, 1178-1186.

Pronk, C.J., Rossi, D.J., Mansson, R., Attema, J.L., Norddahl, G.L., Chan, C.K., Sigvardsson, M., Weissman, I.L., and Bryder, D. (2007). Elucidation of the phenotypic, functional, and molecular topography of a myeloerythroid progenitor cell hierarchy. Cell Stem Cell *1*, 428-442.

Quintana, E., Shackleton, M., Sabel, M.S., Fullen, D.R., Johnson, T.M., and Morrison, S.J. (2008). Efficient tumour formation by single human melanoma cells. Nature *456*, 593-598.

Randall, T.D., Lund, F.E., Howard, M.C., and Weissman, I.L. (1996). Expression of murine CD38 defines a population of long-term reconstituting hematopoietic stem cells. Blood *87*, 4057-4067.

Rhodes, K.E., Gekas, C., Wang, Y., Lux, C.T., Francis, C.S., Chan, D.N., Conway, S., Orkin, S.H., Yoder, M.C., and Mikkola, H.K. (2008). The emergence of hematopoietic stem cells is initiated in the placental vasculature in the absence of circulation. Cell Stem Cell *2*, 252-263.

Ricci-Vitiani, L., Lombardi, D.G., Pilozzi, E., Biffoni, M., Todaro, M., Peschle, C., and De Maria, R. (2007). Identification and expansion of human colon-cancer-initiating cells. Nature *445*, 111-115.

Rodig, S.J., Meraz, M.A., White, J.M., Lampe, P.A., Riley, J.K., Arthur, C.D., King, K.L., Sheehan, K.C., Yin, L., Pennica, D.*, et al.* (1998). Disruption of the Jak1 gene demonstrates obligatory and nonredundant roles of the Jaks in cytokine-induced biologic responses. Cell *93*, 373-383.

Rowley, J.D. (1973). Letter: A new consistent chromosomal abnormality in chronic myelogenous leukaemia identified by quinacrine fluorescence and Giemsa staining. Nature *243*, 290-293.

Samokhvalov, I.M., Samokhvalova, N.I., and Nishikawa, S. (2007). Cell tracing shows the contribution of the yolk sac to adult haematopoiesis. Nature *446*, 1056-1061.

Sawyers, C.L., Hochhaus, A., Feldman, E., Goldman, J.M., Miller, C.B., Ottmann, O.G., Schiffer, C.A., Talpaz, M., Guilhot, F., Deininger, M.W.*, et al.* (2002). Imatinib induces hematologic and cytogenetic responses in patients with chronic myelogenous leukemia in myeloid blast crisis: results of a phase II study. Blood *99*, 3530-3539.

Schindler, C., Levy, D.E., and Decker, T. (2007). JAK-STAT signaling: from interferons to cytokines. J Biol Chem *282*, 20059-20063.

Schwaller, J., Frantsve, J., Aster, J., Williams, I.R., Tomasson, M.H., Ross, T.S., Peeters, P., Van Rompaey, L., Van Etten, R.A., Ilaria, R., Jr.*, et al.* (1998). Transformation of hematopoietic cell lines to growth-factor independence and induction of a fatal myelo- and lymphoproliferative disease in mice by retrovirally transduced TEL/JAK2 fusion genes. The EMBO journal *17*, 5321-5333.

Sexl, V., Kovacic, B., Piekorz, R., Moriggl, R., Stoiber, D., Hoffmeyer, A., Liebminger, R., Kudlacek, O., Weisz, E., Rothammer, K.*, et al.* (2003). Jak1 deficiency leads to enhanced Abelson-induced B-cell tumor formation. Blood *101*, 4937-4943.

Sexl, V., Piekorz, R., Moriggl, R., Rohrer, J., Brown, M.P., Bunting, K.D., Rothammer, K., Roussel, M.F., and Ihle, J.N. (2000). Stat5a/b contribute to interleukin 7-induced B-cell precursor expansion, but abl- and bcr/abl-induced transformation are independent of stat5. Blood *96*, 2277-2283.

Shankaran, V., Ikeda, H., Bruce, A.T., White, J.M., Swanson, P.E., Old, L.J., and Schreiber, R.D. (2001). IFNgamma and lymphocytes prevent primary tumour development and shape tumour immunogenicity. Nature *410*, 1107-1111.

Singh, S.K., Hawkins, C., Clarke, I.D., Squire, J.A., Bayani, J., Hide, T., Henkelman, R.M., Cusimano, M.D., and Dirks, P.B. (2004). Identification of human brain tumour initiating cells. Nature *432*, 396-401.

Somervaille, T.C., and Cleary, M.L. (2006). Identification and characterization of leukemia stem cells in murine MLL-AF9 acute myeloid leukemia. Cancer Cell *10*, 257-268.

Spangrude, G.J., Heimfeld, S., and Weissman, I.L. (1988). Purification and characterization of mouse hematopoietic stem cells. Science *241*, 58-62.

Stoiber, D., Kovacic, B., Schuster, C., Schellack, C., Karaghiosoff, M., Kreibich, R., Weisz, E., Artwohl, M., Kleine, O.C., Muller, M.*, et al.* (2004). TYK2 is a key regulator of the surveillance of B lymphoid tumors. J Clin Invest *114*, 1650-1658.

Stubbs, M.C., and Armstrong, S.A. (2007). Therapeutic implications of leukemia stem cell development. Clin Cancer Res *13*, 3439-3442.

Takahashi, N., Miura, I., Saitoh, K., and Miura, A.B. (1998). Lineage involvement of stem cells bearing the philadelphia chromosome in chronic myeloid leukemia in the chronic phase as shown by a combination of fluorescence-activated cell sorting and fluorescence in situ hybridization. Blood *92*, 4758-4763.

Takeda, K., Noguchi, K., Shi, W., Tanaka, T., Matsumoto, M., Yoshida, N., Kishimoto, T., and Akira, S. (1997). Targeted disruption of the mouse Stat3 gene leads to early embryonic lethality. Proc Natl Acad Sci U S A *94*, 3801-3804.

Teglund, S., McKay, C., Schuetz, E., van Deursen, J.M., Stravopodis, D., Wang, D., Brown, M., Bodner, S., Grosveld, G., and Ihle, J.N. (1998). Stat5a and Stat5b proteins have essential and nonessential, or redundant, roles in cytokine responses. Cell *93*, 841-850.

Thomis, D.C., Gurniak, C.B., Tivol, E., Sharpe, A.H., and Berg, L.J. (1995). Defects in B lymphocyte maturation and T lymphocyte activation in mice lacking Jak3. Science *270*, 794-797.

Traver, D., Miyamoto, T., Christensen, J., Iwasaki-Arai, J., Akashi, K., and Weissman, I.L. (2001). Fetal liver myelopoiesis occurs through distinct, prospectively isolatable progenitor subsets. Blood *98*, 627-635.

Vainchenker, W., Dusa, A., and Constantinescu, S.N. (2008). JAKs in pathology: role of Janus kinases in hematopoietic malignancies and immunodeficiencies. Seminars in cell & developmental biology *19*, 385-393.

Vinkemeier, U., Moarefi, I., Darnell, J.E., Jr., and Kuriyan, J. (1998). Structure of the amino-terminal protein interaction domain of STAT-4. Science *279*, 1048-1052.

Ward, A.C., Touw, I., and Yoshimura, A. (2000). The Jak-Stat pathway in normal and perturbed hematopoiesis. Blood *95*, 19-29.

Weissman, I.L. (2000). Stem cells: units of development, units of regeneration, and units in evolution. Cell *100*, 157-168.

Williams, D.A., and Cancelas, J.A. (2006). Leukaemia: niche retreats for stem cells. Nature *444*, 827-828.

Wong, P.M., Chung, S.W., Chui, D.H., and Eaves, C.J. (1986). Properties of the earliest clonogenic hemopoietic precursors to appear in the developing murine yolk sac. Proc Natl Acad Sci U S A *83*, 3851-3854.

Wong, S., and Witte, O.N. (2001). Modeling Philadelphia chromosome positive leukemias. Oncogene *20*, 5644-5659.

Wurster, A.L., Tanaka, T., and Grusby, M.J. (2000). The biology of Stat4 and Stat6. Oncogene *19*, 2577-2584.

Yao, Z., Cui, Y., Watford, W.T., Bream, J.H., Yamaoka, K., Hissong, B.D., Li, D., Durum, S.K., Jiang, Q., Bhandoola, A.*, et al.* (2006). Stat5a/b are essential for normal lymphoid development and differentiation. Proc Natl Acad Sci U S A *103*, 1000-1005.

Yu, H., and Jove, R. (2004). The STATs of cancer--new molecular targets come of age. Nature reviews *4*, 97-105.

Zhu, J., Guo, L., Watson, C.J., Hu-Li, J., and Paul, W.E. (2001). Stat6 is necessary and sufficient for IL-4's role in Th2 differentiation and cell expansion. J Immunol *166*, 7276-7281.

Curriculum vitae

Boris Kovacic

Personal data

Date of Birth: 03.06.1978

Place of Birth: Mostar (BIH)

Citizenship: Austrian

Email: kovacic@imp.ac.at

Education & Career history

Oct.1997 - 03.08.2000	First Diploma in Biology (Microbiology) University of Vienna
Oct.2000 - 31.12.2003	Studies of Genetics and Microbiology
Sept.2002 - Dec.2003	Diploma thesis Department of Pharmacology, Medical University of Vienna (MUW), Vienna Laboratory of Veronika Sexl
01.01.2004 - 31.12.2004	Civil service
02.02.2005	Received Second Diploma (Magister rerum naturalium) in Genetics and Microbiology from the University of Vienna
01.05.2005 - until now	International PhD Program-student Institute of Molecular Pathology (IMP), Vienna Laboratory of Hartmut Beug

Publications 2003 – 2008 (peer-reviewed)

Kerenyi MA, Grebien F, Gehart H, Schifrer M, Artaker M, **Kovacic B**, Beug H, Moriggl R, Müllner EW. Stat5 regulates cellular iron uptake of erythroid cells via IRP-2 and TfR-1. *Blood*. 2008 Nov 1;112(9):3878-88. Epub 2008 Aug 11.

Kornfeld JW, Grebien F, Kerenyi MA, Friedbichler K, **Kovacic B**, Zankl B, Hoelbl A, Nivarti H, Beug H, Sexl V, Muller M, Kenner L, Mullner EW, Gouilleux F, Moriggl R. The different functions of Stat5 and chromatin alteration through Stat5 proteins. *Front Biosci.* 2008 May 1;13:6237-54. Review.

Grebien F, Kerenyi MA, **Kovacic B**, Kolbe T, Becker V, Dolznig H, Pfeffer K, Klingmüller U, Müller M, Beug H, Müllner EW, Moriggl R. Stat5 activation enables

erythropoiesis in the absence of EpoR and Jak2. *Blood*. 2008 May 1;111(9):4511-22. Epub 2008 Jan 31.

Tsareva SA, Moriggl R, Corvinus FM, Wiederanders B, Schütz A, **Kovacic B**, Friedrich K. Signal transducer and activator of transcription 3 activation promotes invasive growth of colon carcinomas through matrix metalloproteinase induction. *Neoplasia*. 2007 Apr;9(4):279-91

Harir N, Pecquet C, Kerenyi M, Sonneck K, **Kovacic B**, Nyga R, Brevet M, Dhennin I, Gouilleux-Gruart V, Beug H, Valent P, Lassoued K, Moriggl R, Gouilleux F. Constitutive activation of Stat5 promotes its cytoplasmic localization and association with PI3-kinase in myeloid leukemias. *Blood*. 2007 Feb 15;109(4):1678-86. Epub 2006 Oct 12.

Kovacic B, Stoiber D, Moriggl R, Weisz E, Ott RG, Kreibich R, Levy DE, Beug H, Freissmuth M, Sexl V. STAT1 acts as a tumor promoter for leukemia development. *Cancer Cell*. 2006 Jul;10(1):77-87.

Hoelbl A, **Kovacic B**, Kerenyi MA, Simma O, Warsch W, Cui Y, Beug H, Hennighausen L, Moriggl R, Sexl V. Clarifying the role of Stat5 in lymphoid development and Abelson-induced transformation. *Blood.* 2006 Jun 15;107(12):4898-906. Epub 2006 Feb 21.

Hoeller C, Pratscher B, Thallinger C, Winter D, Fink D, **Kovacic B**, Sexl V, Wacheck V, Gleave ME, Pehamberger H, Jansen B. Clusterin Regulates Drug-Resistance in Melanoma Cells. *J. Invest. Dermatol.* 124, 1300-7 (2005).

Stoiber D, **Kovacic B**, Schuster C,Schellack C, Karaghiosoff M, Kreibich R, Weisz E, Artwohl M, Kleine OC, Muller M, Baumgartner-Parzer S, Ghysdael J, Freissmuth M, Sexl V. TYK2 is a key regulator of the surveillance of B lymphoid tumors. *J. Clin. Inv* **114**, (2004).

Sexl V, **Kovacic B**, Piekorz R, Moriggl R, Stoiber D, Hoffmeyer A, Liebminger R, Kudlacek O, Weisz E, Rothammer K, Ihle JN. Jak1 deficiency leads to enhanced Abelson-induced B-cell tumor formation. *Blood* **101**, 4937-43 (2003).